The Taphonomy of a Carboniferous Lagerstätte: the Invertebrates of the Bear Gulch Limestone Member

A thesis submitted for the degree of

Doctor of Philosophy

at the University of Leicester

by

Natalie Thomas MSc. (Bristol)

Department of Geology

University of Leicester

2004

University *of* Leicester

ProQuest LLC
789 East Eisenhower Parkway
P.O. Box 1346
Ann Arbor, MI 48106-1346

This thesis is dedicated to my aunt

Mary Thomas

The Taphonomy of a Carboniferous Lagerstätte: the Invertebrates of the Bear Gulch Limestone Member

Natalie Thomas

Abstract

The Bear Gulch Limestone Member is proposed herein as the new name for the Bear Gulch Beds of central Montana, USA. This member contains articulated and exceptionally well preserved fossils.

Taphonomic investigation, employing scanning electron microscopy, electron dispersive x-ray analysis, element mapping, electron microprobe analysis and Raman spectroscopy reveals that original carbonate biominerals underwent early dissolution, whereas original apatite was converted to carbonate fluorapatite. Non-mineralised tissues were rapidly replaced by apatite and more rarely calcite, or are evident as tissue imprints. In some cases fossil morphology is preserved in organic carbon. The sediment is lacks both clay and iron and so previous models for carbon preservation cannot be invoked.

Bottom water conditions were periodically inimical to benthos. Reducing environments within the sediment and relatively rapid burial rates must have assisted in the preservation processes, including macroscavenger inhibition.

Geochemical analysis shows that calcite and quartz, which dominate the sediment, were derived from within the Bear Gulch bay.

Coiled cephalopods are found encrusted with *Sphenothallus*, 'microconchids', bryozoans and orbiculoid brachiopods. *Sphenothallus* demonstrates holoperipheral cover and preferred growth orientation on two cephalopods. This suggests that sphenothallids colonised the cephalopods *in vivo*.

Articulated polychaete jaw apparatuses, *Brochosogenys reidiae* and *Symmetrioprion* n. sp. are described. The latter is the first record of the genus from the Carboniferous and the first assemblage of Symmetrioprionidae found with the remains of its body.

Halicyne montanaensis n. sp., is recorded from the deposit. Several specimens with different styles of preservation have enabled its identification as a new species of cycloid.

ACKNOWLEDGEMENTS

I must first thank my supervisors, Sarah Gabbott and Mark Purnell, for their support, encouragement and for all the discussions we've had.

I'd also like to thank Prof. Schram and Arjan Boere for their discussions with the cycloid paper and for Prof. Schram's determination to email me the photos in time for me to print my thesis. Thanks also to Dick Lund and Eileen Grogan for all their help during the fieldwork, from information on the Bear Gulch to their advice on how to treat poison ivy.

I would also like to thank Al Koller of the Carnegie Museum for his enthusiasm and assistance with the project and also Janet Waddington and David Rudkin at the Royal Ontario Museum for all their help. Thanks also to Mindy Myers for her wonderful hospitality. I am also very grateful to George D. Stanley, from the University of Montana, for access to the collections at Missoula and making my stay there as hassle free as possible.

My thanks to Dr. Matt Bloomfield of Reinshaw plc. for his help and use of the Raman equipment, and his expertise in interpreting the data.

I am very grateful to all the people in the Geology Department in Leicester who have shown interest in the project and discussed it with me: Norry for advice on XRF data and Jan for his discussions on sedimentology. David Siveter for his advice on arthropods and John Hudson for his welcome advise on pyrite framboids. I'd also like to thank Rod Branson for his help with, and tweaking of, the SEM. I'd also like to thank Rob Wilson for his help with the electron microprobe and advice on various aspects of chemistry. Also Nick Marsh for XRF data and Kevin Sharkey for help with XRD data. And other Leicester people who have helped me with sample preparation: Colin, Lyn, Emma and Rob. Also a thank you to Graham in the engineering department for his support with their SEM.

Another big thank you must go to George Iliopoulos for his comments and the discussions we've had. And thanks must go to Pat for all her encouragement, and to writing up distracters James Howard, Marc Reichow, David Baines, Dave Gladwell, Matt Hooper and other postgrads around the department.

An enormous thank you to my family for their constant encouragement and understanding. Finally, I am indebted to Gary for helping me to put things in perspective as well as being my personal chauffer, financial supporter, destresser and drinking partner, I am very grateful for your support.

CONTENTS

LIST OF FIGURES

Polychaete jaw apparatuses (scolecodonts) from the Carboniferous Bear Gulch Limestone Member, central Montana

The taphonomy of the Bear Gulch Limestone Member

LIST OF TABLES

Sphenothallus and other epibionts on coiled cephalopods from the Carboniferous Bear Gulch Limestone Member of central Montana, USA

The taphonomy of the Bear Gulch Limestone Member

Figure 1. Locality map of Montana and surrounding region showing distribution of the Bear Gulch Limestone Member (BGLM) within the Big Snowy Trough and the position of the Williston Basin (redrawn from Maughan 1 984, figure 1).

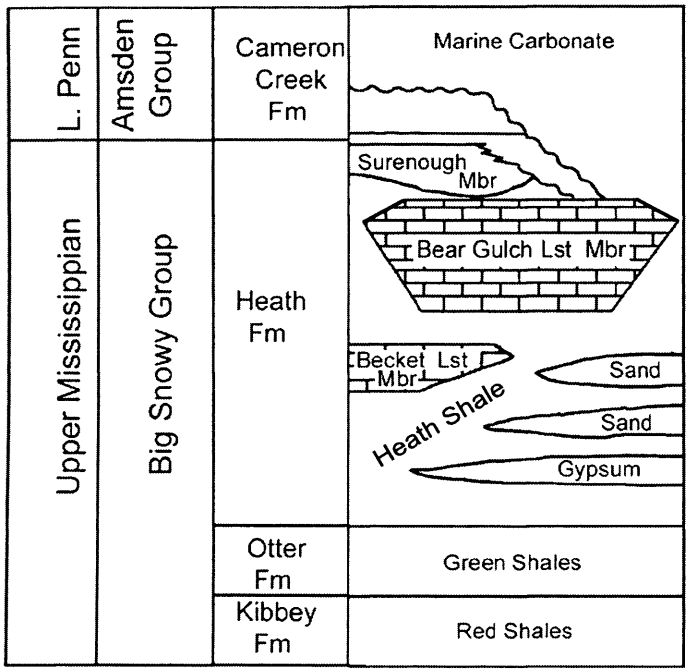

Figure 2. Stratigraphical position of the Bear Gulch Limestone Member (after Williams 1983).

SPECIAL NOTE

ITEM SCANNED AS SUPPLIED
PAGINATION IS AS SEEN

Geological context

During the Upper Mississippian, Pennsylvanian and Permian Pangea formed as a result of the collision of Gondwanaland and Laurentia (Torsvik and Cocks 2004).

This led to the onset of major continental glaciation at the palaeo-south pole and repeated advances and retreats of ice sheets, which resulted in multiple eustatic sea level changes (Saltzman 2003; see review in Shepard 1993). Consequently, throughout the Upper Mississippian the central Montana trough underwent alternate regression and transgression cycles (Williams 1983). The Kibbey Formation, an evaporitic and clastic sequence of the Big Snowy Group, was deposited during a marine transgression (Harris 1972)(fig. 2).

The Otter Formation overlies the Kibbey Formation and represents a starved basin sequence of intermixed clay, carbonate and evaporites (Harris 1972) (fig. 2). The Heath Formation, a black, petroliferous shale, with thin-bedded black limestones and thin gypsum deposits, overlies the Otter Formation (Harris 1972)(fig. 2). The Heath Formation may be representative of a rising sea level sequence as a result of glacial melting, and is considered a deeper water environment than both the Kibbey and Otter Formations (Williams 1981).

In the upper part of the Heath Formation, deltaic sandstones interfinger with black shales (Williams 1983). These sandstones, some of which contain intraconglomerates, reflect westward progressing pulses of uplift within the trough (Horner and Lund 1985). As a result a series of basins opened progressively from east to west, the Bear Gulch Limestone Member was deposited in the last of these basins to form (Williams 1983). Deposition of this limestone lens was thought to be in a shallow bay, with a maximum depth of 30-40m (Williams 1983). As east–west extension was underway there was regional uplift to the south and evidence for this uplift is perhaps seen in the Bear Gulch Limestone Member by the presence of large sedimentary slumps in the central basin facies that verge to the north-east (fig. 3) (Williams 1983).

Stratigraphy and sedimentology

The age of the Bear Gulch Limestone Member is Namurian and this was established using palynostratigraphy, bryozoa (Cox 1986), ammonites (Mapes 1987), conodont elements (Scott 1973; Norby 1976) and the fish assemblage (Feldman *et al.* 1994).

The Member is a limestone lens within the Heath Formation of Montana (fig. 2) and North Dakota. This limestone lens has also previously been termed the Bear Gulch Member (Williams 1983), the Bear Gulch Limestone (Lund *et al.* 1993) and the Bear

Figure 3. Large sedimentary slumps in the central basin facies that verge to the north-east. Scale bar represents 1 m.

Gulch Beds (Williams 1983; Horner and Lund 1985). These different names lead to a confusing situation and here it is suggested that the term Bear Gulch Limestone Member (Chapter 1) be used to conform to current stratigrapical nomenclature (c.f. Prothero 1990) (fig. 2). In addition the Surenough Beds and Becket Beds have been changed to the Surenough Member and the Becket Limestone Member (Thomas, Chapter 1) (fig. 2).

The Bear Gulch Limestone Member comprises a rhythmically alternating sequence of thicker (>30mm), nonfissile units with thinner (<30mm), argillaceous, fissile beds (Williams 1983). Williams (1983) suggested that this was similar to the Flinz and Fäule style of bedding found in the Mid-Jurassic Solnhofen lithographic limestone of Germany (Hemleben and Swinburne 1991).

Locality

The Bear Gulch Limestone Member has a visible outcrop area of 85km^2 (Grogan and Lund 2002) and a maximum thickness of 30m (Feldman *et al.*, 1994; Grogan and Lund, 2002). The thickest part of the Bear Gulch Limestone Member thins rapidly to the east; this led Williams (1983) to suggest that there was a structural lip at the mouth of the bay.

The Member is 15-30m thick in the central basin area of Sawmill, Blacktail, Atherton, Rose and Bear Canyons, and thins rapidly west, from 15–25m in Bear Canyon, to 5–10 m in Surenough canyon, to 0–2m in Tyler's Creek (fig. 4). To the north, east and south the Carboniferous section dips below ground (Williams, 1983). Upper and lower contacts are mostly covered, but where exposed the Bear Gulch Limestone Member grades downwards into dark, organic-rich platy shale (Williams 1983). The upper contact in Upper Sawmill Creek, upper Blacktail Creek, upper Atherton and Dickson Canyons and the eastern flank of Rose Canyon, grades upwards through increasing quantities of cherts to marls, rare stromatolites, and limestone conglomerates (Lund *et al.*, 1993). There is significant channelling of overlying Cameron Creek terrestrial deposits into the top of the Bear Gulch Limestone Member in the 'Blacktail drainage' (Lund *et al.* 1993). A geological map of the Bear Gulch Limestone Member and surrounding locations has not been published.

Previous palaeontological research on the Bear Gulch Limestone Member

The Bear Gulch Limestone Member was first described by Mundt (1956). Later, in 1968, finds of exceptionally preserved fish by local farmers led to the reinvestigation of the deposit by William G. Melton Jr. (1969). Melton excavated fish in the Bear Gulch Limestone Member during several field seasons. More recently, summer fossil collecting

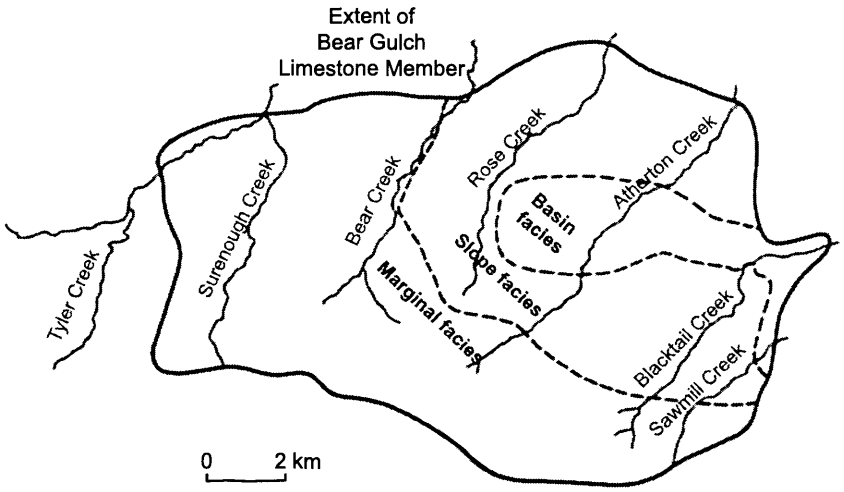

Figure 4. Locality map of the Bear Gulch Limestone Member showing the boundary of the marginal, slope and basin facies (redrawn from Williams 1983, figure 10b).

excavations have been led by Dr. Richard Lund (Prof. Emeritus, Adelphi University, New York) and Dr. Eileen Grogan (Associate Professor, St. Joseph's University, Philadelphia).

The Bear Gulch Limestone Member has three recognised facies; the margin, slope and basin facies, and fossils are known to occur in each of these (Williams 1983). Facies differentiation was based largely on changes in sedimentology, sedimentary structures and faunal distribution (Williams 1983). Detailed facies analyses have been hindered by poor outcrop exposure, which is limited to deeply incised canyons with minor lithological variation. However, Grogan and Lund (2002) have further redefined the marginal and basin facies, and added the 'arborispongia facies', 'filamentous algae facies' and a 'shallow facies', based upon their field evidence of the distribution of fossils, especially algae and sponges.

Literature on the Bear Gulch Limestone Member is extensive. Of the vertebrate fauna many species of fish have been documented, but there are many new species yet to be described (Richard Lund pers. comm.). Those fish from the Bear Gulch Limestone Member that have been investigated include chondrichthyans (Lund 1974, 1977a,b,c, 1980, 1982, 1983, 1984, 1985a,b, 1986a,b, 1988, 1989; Lund & Zangrel 1974) e.g. Euchondrocephali, Paraselachii, petalodontiforms, Holocephali, Cochliodontomorpha; Elasmobranchi; osteichthyans, acanthodians (Zidek, 1980), actinopterygians (Lund and Melton, 1982; Di Canzio 1985; Lowney, 1985; Lund and Poplin 1997, 2002; Poplin and Lund 2000, 2002) and sarcopterygians notably coelocanths (Lund & Lund 1984; Lund *et al.* 1985; Di Canzio 1985). Although conodont elements and apparatuses are present in the Bear Gulch Limestone Member (Scott 1973; Purnell 1993; Purnell and Donoghue 1998) no conodont animal soft tissues have yet been found.

Most of the vertebrate investigations centre on taxonomy and morphology, but some attention is paid to the state of preservation of the fish. In particular Grogan and Lund (2002) suggest that the remains of the liver, heart, spleen and venous systems are recognisable in some fossil fish. Grogan and Lund (1997, 2002) have compared the dark impressions within the fossil fish to the location of organs in modern fish and their argument for the impressions being the remains of internal organs is convincing. They have suggested that either haemoglobin or the iron within the haemoglobin is the now fossilized material delineating various organs (Grogan and Lund 1995).

The invertebrates from the Bear Gulch Limestone Member are diverse and have been documented by numerous authors. The crustaceans include concavicarids, phyllocarids, palaeostomatopods and eumalacostracans (Factor and Feldman 1985; Schram and Horner 1978; Schram 1979a, 1981; Schram and Schram 1979; Jenner, Schram and Hof (1998). Specimens of *Palaeolimulus* are rare and have been described by Schram (1979b).

Brachiopods from Bear Gulch Limestone Member are less diverse than other Carboniferous faunas from the USA (Lutz-Garihan, 1979). However, McRoberts and Stanley (1989) discovered more than 100 bivalves, including *Caneyella* sp. and ?*Ptychopteria* (*Actinopteria*) sp., attached in life position along 800 mm of brown algae. The assumption was that such assemblages existed in the water column indicating oxic conditions in the upper layers, and a normal, near shore marine salinity (McRoberts and Stanley 1989). Mapes (1987) and Landman and Davis (1988) both discussed the locally abundant cephalopods as indicative of open marine conditions.

Rigby (1979) reported on the sponge fauna from the Bear Gulch Limestone Member and Becket Limestone Member and the intervening shale within the Heath Formation. Rigby (1979) recorded that the Bear Gulch Limestone Member was dominated by lyssakid hexactinellids, although *Belemnospongia chorda* and a branching *Arborispongia delicatula* also occurred. A smoothly curved fragment of the skeletal net represented an additional dictyosponge, *Norfordia trypa,* of which there are only two specimens known (Rigby 1979).

Welch (1984) documented two species of the starfish *Lepidastella,* that had 35 arms, and ophiuroids, which are poorly preserved because of aragonite dissolution. Polychaete annelids with impressions of their scolecodonts preserved and other worms were described by Schram (1979b). However, the scolecodonts were not described in any detail.

Problematic fossils are common in the Bear Gulch Limestone Member. Conulariids and *Sphenothallus* have been described (Babcock and Feldmann, 1986; Van Iten, *et al.* 1992) and *Typhloesus wellsi* (Melton and Scott 1973), an enigmatic organism, was originally described as a conodont animal, because it is often found containing conodont elements (Melton and Scott 1973). However, Rhodes (1973) and Lindström (1974) discredited these claims and suggested the fossil represented an organism that preyed on conodonts. Conway Morris (1990) re-examined the putative conodont animal, but did not resolve its phylogenetic affinities and considered it a bizarre metazoan.

Fieldwork

From locality information and accounts by Horner and Lund (1985), Lund and Poplin (1999) and Williams (1983) it is evident that the basin facies has the highest diversity of fossils. For this reason sediment samples were collected from the basin facies, and all fossils considered in this study are from the basin facies.

Fieldwork was carried out in the summer of 2001, with Eileen Grogan and Dick Lund. I have been requested not to publish an exact location but it was within the central part of the basin facies. Most work was from one main location within the central basin

facies. The lithology was logged and each bed represented on the log was excavated to reveal a $4m^2$ bedding plane. Any fossil specimens that were found were recorded on the log and sediment samples were taken from each bed for analysis. Fossils were generally uncommon (see appendix 1).

Fossils were also studied and/or borrowed from the three museums that hold the main collections of Bear Gulch Limestone Member material. These are the Royal Ontario Museum, Canada (ROM), the Carnegie Museum, USA (CM) and the University of Montana, USA (UM).

Thesis layout

This thesis has been structured to present new data and interpretations in a format suitable for immediate publication. The chapters and their target journals are listed below:

Chapter 1, '*Sphenothallus* and other epibionts on cephalopods from the Carboniferous Bear Gulch Limestone Member of central Montana, USA' directed towards the journal *Palaeontology.*

Chapter 2, 'Polychaete jaw apparatuses (scolecodonts) from the Carboniferous Bear Gulch Limestone Member, central Montana' directed towards the *Journal of Paleontology.*

Chapter 3, 'The taphonomy of the Bear Gulch Limestone Member' directed towards the journal *Palaeontology.*

Appendix 8 contains a paper that has arisen from the result of this study and is in press. The paper entitled 'Cycloidea of the Mississippian Bear Gulch limestone of central Montana' is to be published in the *LA Museum Contributions in Science* and was written in collaboration with Arjan Boere and Prof. Frederick Schram (Institute for Biodiversity and Ecosystem Dynamics, University of Amsterdam). My contribution to this publication was to provide a description of a specimen (CM-45816) and discuss whether the cycloid specimens from the Bear Gulch Limestone Member represented a single new species of cycloid *Halicyne montanaensis.*

CHAPTER 1

SPHENOTHALLUS AND OTHER EPIBIONTS ON COILED CEPHALOPODS FROM THE CARBONIFEROUS BEAR GULCH LIMESTONE MEMBER OF CENTRAL MONTANA, USA.

ABSTRACT. The Bear Gulch Limestone Member, central Montana, USA, is proposed herein as the new name for the Bear Gulch Beds, which contain exceptionally well-preserved fossils. Coiled cephalopods (>70mm in diameter) from the member are encrusted with a variety of epibionts, including *Sphenothallus* Hall 1847, 'microconchids' (affinity uncertain), bryozoans and orbiculoid brachiopods. Specimens of the enigmatic organism *Sphenothallus* are well preserved in the Bear Gulch Limestone Member and exhibit previously unrecorded regularly spaced annulations on the thin film between their characteristic longitudinal thickenings. On two coiled cephalopods *Sphenothallus* demonstrates holoperipheral cover probably indicating colonization whilst the coiled cephalopods were in the water column. Furthermore, *Sphenothallus* show a strong, preferred, growth orientation towards and forward of the cephalopod aperture, suggesting that the cephalopod was alive, and swimming, rather than dead and adrift, when colonization occurred. 'Microconchids' grew over bryozoans, and show growth interference, with *Sphenothallus* basal attachment discs indicating that in addition to *Sphenothallus*, microconchids and bryozoans also attached during the cephalopod's life. That epibiont taxa are extremely rare in the Bear Gulch Limestone Member, other than when attached to coiled cephalopods, suggests that there were limited, readily available, benthic platforms onto which encrusters could colonise. Alternatively, the bottom water conditions may have been inimical to benthos.

EPIBIOSIS is a spatially close association between two or more organisms belonging to the same or different species (Wahl and Mark 1999). Through direct and indirect interactions, this association can often have major effects on the species involved and on community dynamics (Wahl and Mark 1999). Attachment of epibionts may occur on sessile benthonic, planktonic or nektonic organisms and is a very common life habit among modern benthic organisms, especially if the sediment is too soft to attach directly to, and they require a firm or hard substrate (Wahl and Mark 1999). When bottom water conditions are inimical, epibiosis may only occur on nektonic or planktonic organisms. In this paper we draw attention to the existence of coiled cephalopods from the Bear Gulch

Limestone Member, Upper Mississippian, of central Montana, USA, which are covered in epizoans of *Sphenothallus*, 'microconchids', bryozoans and orbiculoid brachiopods. Importantly, we argue that the enigmatic taxon *Sphenothallus* had the capacity of a commensal relationship with their coiled cephalopod hosts. This has implications for the palaeoecology of *Sphenothallus*, and corroborates the view that it was an opportunistic generalist and probably a filter feeder (Bodenbender *et al.* 1989; Van Iten *et al.* 1996; Neal and Hannibal 2000). Furthermore, evidence that epibionts preferentially attached to living cephalopods supports the view that the Bear Gulch Limestone Member had an inhospitable seabed and hence a very limited benthic fauna (Williams 1983; Grogan and Lund 2002).

STRATIGRAPHY

The Bear Gulch Limestone Member is proposed herein as the new name for the fossiliferous limestone lens within the Heath Formation of Montana (Text-fig. 1A) and North Dakota, which previously has been variously referred to. The Bear Gulch Limestone Member was first referred to as the Bear Gulch Member by Williams (1983) (Text-fig. 1B). Later, Horner and Lund (1985) assigned a more extensive portion of the upper part of the Heath Formation to the Bear Gulch Member (Text-fig 1B). Horner and Lund (1985) proposed that the Bear Gulch Member was composed of three isolated 'units' (the Becket Beds, the Bear Gulch Beds and the Surenough Beds), each of which represented a separate depositional basin (Text-fig. 1B). However, because the name Bear Gulch had been given to both the Bear Gulch Member and the Bear Gulch Beds, Feldman *et al.* (1994) believed that this could lead to confusion and abandoned the term Bear Gulch Member, but retained the term Bear Gulch Beds. The limestone lens referred to as the Bear Gulch Beds (Horner and Lund 1985, Feldman *et al.* 1994; Grogan and Lund 2002) contains exceptionally well preserved fossils and was considered by Williams (1983) to be a conservation Lagerstätte. This Lagerstätte has also traditionally been referred to as the Bear Gulch Limestone (Lund *et al.* 1993). Thus, I suggest that the terms Becket Beds, Bear Gulch Beds, and Surenough Beds be abandoned and replaced with, Becket Limestone Member, Bear Gulch Limestone Member and Surenough Members. The term 'Beds' is applied to the smallest lithological unit of sedimentary rock and should be limited to certain distinctive beds, whereas the term Member represents a particular part of a formation (Prothero 1999) (see text-fig. 1B). This is the terminology that will be employed herein. Due to the patchy nature of exposures boundary lithotypes have not been defined, but typical sections showing the lithological characteristics of the Becket Limestone Member, Bear Gulch Limestone Member and Surenough Members can

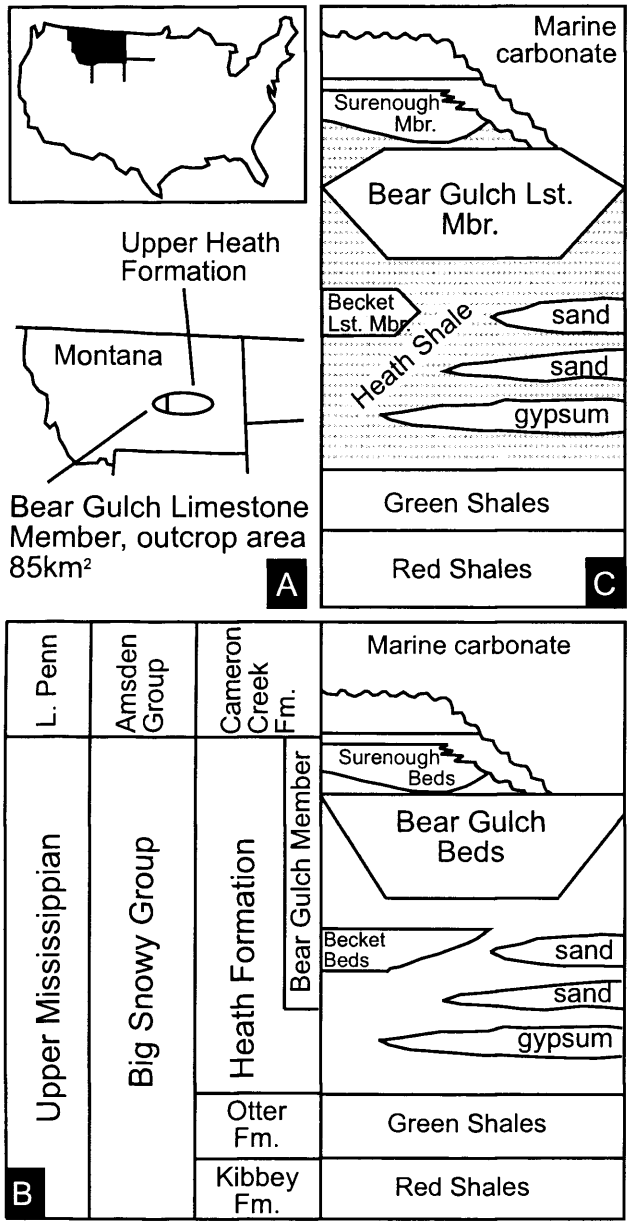

TEXT-FIG. 1. Location and stratigraphical position of the Bear Gulch Limestone Member. A, map of Montana, USA, with the location of the area outcrop indicated. B, stratigraphical section (after Williams 1983) showing the Bear Gulch Limestone Member (Horner and Lund 1985). C, revised nomenclature of the stratigraphy of the Heath Formation proposed herein; the Heath Formation comprises the Bear Gulch Limestone Member, the Becket Limestone Member, the Surenough Member and the Heath Shale.

be seen, respectively, at Rose Canyon, Atherton Creek and Surenough Canyon, Fergus County, Montana.

The Bear Gulch Limestone Member forms a carbonate mudstone lens approximately 15km in lateral extent and up to 24m thick in the eastern part of its outcrop (Feldman *et al.* 1994). It is Upper Mississippian (Upper Chesterian) in age (Text–fig. 1B), based upon a diverse spore assemblage and various acritarchs (Cox 1986), coiled cephalopods (Mapes 1987), conodonts (Scott 1973; Norby 1976) and fishes (Feldman *et al.* 1994). The Bear Gulch Limestone Member has been referred to as a lithographic limestone (plattenkalk) that shows a rhythmically alternating sequence of dark, fine grained massive to graded beds, and sets of lighter coloured laminar beds (Williams 1983; Grogan and Lund 2002). It was deposited in an isolated basin approximately 12 degrees north of the equator (Grogan and Lund 2002).

BIOTA

The Bear Gulch Limestone Member has been widely excavated because it contains a large assemblage of fossil marine soft-bodied invertebrate and vertebrate species (see review in Bottjer *et al.* 2002). Cephalopods from the Bear Gulch Limestone Member have been suggested to be locally abundant and indicators of open marine conditions (Mapes 1987; Landman and Davis 1988). Mapes (1987) recovered both isolated and in-situ mandibles in decalcified coiled cephalopod conchs. However, to date, no detailed morphological description of the coiled cephalopods has been published. Van Iten *et al.* (1992) noted evidence of *Sphenothallus* attached to nautiloids and other sphenothallids from the Bear Gulch Limestone Member, but did not discuss the palaeoecological significance of this association. Lund *et al.* (1993) briefly mentioned the presence of bryozoans in the Bear Gulch Limestone Member; prior to this it had been assumed that they were absent (Horner and Lund 1985). Orbiculoid brachiopods, although recorded from the Bear Gulch Limestone Member (Lund *et al.* 1993), have yet to be described in detail, whilst 'microconchids' have not previously been recorded from this deposit.

TIMING OF ATTACHMENT

Epibionts may have attached to a cephalopod whilst it was in the water column, in life or post-mortem, or when the cephalopod was lying on the seafloor. If we can distinguish between these possible scenarios we may be able to elucidate details of epibiont palaeoecology and may further our understanding of the substrate consistency and redox conditions of the seafloor environment. For example, in the Posidonia Shale (Jurassic,

Germany) the timing of colonisation of cephalopods was crucial to the argument proposed by Seilacher and Westphal (1971) that the bottom waters were inimical to life owing to anoxia. However, this is in conflict with the 'benthic island' model, also proposed for the Posidonia Shale, where the attachment of epibionts occurred whilst the cephalopods lay on the seabed (Kauffman 1978). Schmid-Rohl and Rohl (2003) confirmed that both scenarios were correct in the Posidonia Shale and that oxygen supply was the main factor that determined whether benthic colonisation occurred. It can be seen, therefore, that it is vital to accurately establish the timing of epibiont attachment onto a host in order to infer aspects of epibiont palaeoecology and the nature of the palaeoenvironment.

Below, examples of epibiont attachment to *Nautilus* are described, where the timing of colonisation can be well constrained owing to direct observation by ecologists (Landman *et al.* 1987). In addition, examples of the criteria that may be employed to determine the timing of epibiont colonisation on coiled cephalopods are explored.

In life colonisation of cephalopods. Many epizoans are found on live nautiloids. Serpulids, bryozoans, barnacles, foraminifers and scyphozoans occur on over half of the live *Nautilus* that inhabit steep fore-reef environments (Landman *et al.* 1987). It has also been shown that some juvenile nautiloids have fewer epibionts than the adults, and this is thought to be because the juveniles have a thicker periostracum, which is lost during ageing (Landman *et al.* 1987). A thicker periostracum may inhibit boring and encrustation (Bottjer 1981). However, there are notable exceptions such as the nautilid *Eutrephoceras dekayi* of the Late Cretaceous of the Western Interior of North America, which was encrusted during early growth with bryozoans and serpulids (Landman *et al.* 1987). For modern *Nautilus* the geographical and environmental settings affect the degree of encrustation and the percentage of shells encrusted by the different kinds of epizoan (Chamberlain *et al.* 1981). It is possible that this is also the case for ancient coiled cephalopods, but detailed investigation is necessary to determine whether there is a relationship between epibiont taxa and coiled cephalopod palaeogeographical distribution. Generally, it has been found that on modern living *Nautilus* epizoans on the shells are sparse, whereas on post mortem drift specimens epizoans are densely and randomly distributed (Landman *et al.* 1987).

In the fossil record it can be problematical to determine unequivocally whether colonisation by epibionts occurred whilst the host was alive or drifting post mortem. However, there is evidence for *in vivo* colonisation of fossil coiled cephalopods. For example, serpulids growing on the ventral margin of ammonites that were distally overgrown by later whorls provide indisputable evidence for in-life colonisation (Merkt 1966). In rare cases, ammonites have been recorded that have deviated from their

normal planispiral growth pattern due to the presence of oysters on one flank (Merkt 1966; Heptonstall 1970). Epibionts showing orientated growth, supposedly as a rheophilic response to the swimming motion of the host, may also indicate attachment to a live host. For example, Baird *et al.* (1989) described Ordovician orthoconic cephalopods encrusted by bryozoan zoaria, which displayed a consistent elongate growth orientation towards the orthocone's aperture. However, caution is required if using epibiont alignment as a signature for in life colonisation because it is also possible that epibionts colonizing a host on the seafloor may show a rheophilic response to a prevailing current direction. Alternatively, where a rheophilic response is not likely to be observed owing to the morphology of the epibionts, such as in bivalves and brachiopods, the size distribution of the epibionts on the host may be informative. The coiled cephalopod *Buchiceras bilobatum* from the Lower Senomanian of Otuscu, Peru, was believed to have been colonised in life by oysters (Seilacher 1960). The clinching evidence for *in vivo* colonisation in this example was the size of the oysters, because they required an extensive time to grow and were equally developed on both flanks (Seilacher 1960). Gabbott (1999) demonstrated that an orthocone from the Ordovician Soom Shale (South Africa) had been colonised in life as the size (and hence relative age) of epibiont orbiculoid brachiopods was correlated with the successive growth of the orthocone conch. Brachiopod shells were largest on the earliest formed part of the orthocone conch and became progressively smaller towards the youngest part, indicating that colonisation continued throughout the life of the orthocone (Gabbott 1999).

The inarticulate brachiopod *Discina papyracea*, recorded by Seilacher and Westphal (1971) on ammonite shells from the Posidonia shale, was interpreted as pseudoplanktonic on living, or drifting post-mortem, ammonites. However, Kauffman (1981) believed that these orbiculoids attached to the upper surface of dead ammonites resting horizontally on the seabed that acted as benthic islands (see below). Kaufman (1981) also remarked that no living discinid brachiopods are known to be pseudoplanktonic. However, pseudoplanktonic discinid brachiopods have been recorded from the Soom Shale by Gabbott (1999).

Colonisation on drifting post-mortem cephalopods. Studies assessing whether *Nautilus* sinks immediately upon death or drifts for some time have been used to infer the taphonomy of ancient coiled cephalopods. Buoyancy calculations by Chamberlain *et al.* (1981) showed that a modern *Nautilus* that dies in waters deeper than 200-300m will not rise to the surface. Maeda and Seilacher (1996) suggested that coiled cephalopods that lived and died in deep waters might never have surfaced, as the high ambient pressure would have caused the camerae to become waterlogged quickly, with the shell losing its

buoyancy and sinking rapidly to the bottom. However, many *Nautilus* shells are thought to surface post-mortem because their soft-tissue, which acts as ballast in life, drops out after a few hours or days (Chamberlain *et al.* 1981). Subsequent drifting in ocean currents may occur and has been demonstrated by Saunders and Spinosa (1979) who recorded a *Nautilus* drifting over 1000 km in 138 days, (a rate of 7.25 km per day). Drifting *Nautilus* shells have been found encrusted by oysters, serpulids, *Spirorbis* and barnacles (Hamada 1964).

It is possible that some ancient coiled cephalopods acted in a similar way post-mortem and were colonised by epibionts whilst dead and drifting. The Bear Gulch basin is reported to have been 30 and 40 meters in depth (see Williams 1983) suggests that the coiled cephalopods would have most likely floated post-mortem (cf. Chamberlain *et al.* 1981). Colonisation of dead coiled cephalopods floating in the water column cannot always be distinguished from *in vivo* colonisation. Epibionts within the body chamber would be a clear indication that colonisation occurred post-mortem. Similarly, a random distribution of epibionts, that might otherwise display orientated growth, may also be indicative of post-mortem colonisation. It is also difficult to distinguish between post-mortem colonisation in the water column and colonisation whilst the host is on the seafloor. Holoperipheral cover may suggest that epibiont attachment to the coiled cephalopod, dead or alive, occurred in the water column. However, Donovan (1989) suggested oyster growth on only one side of a Kimmeridgian *Pectinatites* implied that the shell of the dead coiled cephalopod was floating in a horizontal position at the surface, and that, consequently, only that side of the shell within the water was accessible for oyster colonisation.

Benthic island colonisation of cephalopods. Incursion of water into the chambers of *Nautilus* would ultimately lead to its sinking either onto its side, or more rarely, onto its ventral surface (Donovan and Baker 2003). Chambers may become infilled with sediment and the shell can become encrusted and bored (Donovan and Baker 2003). To date, benthic island style colonisation of modern *Nautilus* has not been recorded. The most compelling evidence for attachment to coiled cephalopods while on the seafloor would be colonisation restricted to its upper-side, indicating that it acted as a hardground or benthic island post deposition. Clearly, for this to be established the way-up of the specimen must be known.

Kauffman (1981) noted the presence of serpulid worms, byssate bivalves, boring polydorid (?) worms and inarticulate brachiopods on ammonites from the Posidonia Shale. Kauffman (1981) considered that the ammonites had sunk and had acted as benthic islands and that the order of epibiont attachment and placement on the coiled cephalopod

was a significant indicator of the position of the oxic/anoxic boundary. In addition it must be noted that holoperipheral colonisation of coiled cephalopod conchs on the seafloor may still take place if bottom currents overturn the coiled cephalopod.

MATERIAL and METHODS

The Bear Gulch Limestone Member specimens described here are from the Carnegie Museum, USA (CM) specimen CM-BG3 (Text-fig. 2A), the Royal Ontario Museum, Canada (ROM), specimens ROM-00-071802NC1/NC2 (Text-fig. 2B) ROM-88716 (Text-fig. 2C) ROM-91-70815, ROM-91-72404A and ROM-88-72819 and collections held in the University of Montana, USA (UM) specimen UM-7571014 (Text-fig. 2D). Epibiont-host and epibiont-epibiont relationships were investigated on four cephalopods that were selected because they are well preserved and display abundant epibiont taxa. All cephalopods were photographed using a Nikon Coolpix 995 digital camera.

DESCRIPTION OF MATERIAL

Cephalopods from the Bear Gulch Limestone Member

The coiled cephalopods from the Bear Gulch Limestone Member fall into two distinct categories: those, which are >70mm in diameter, four of which are the focus of this study, and those which are significantly smaller, approximately <50mm in diameter. The characteristic morphological features of the cephalopods investigated in this study are given in Table 1, along with an indication of their associated epibionts.

Larger coiled cephalopods (>70mm) from the Bear Gulch Limestone Member have relief, but lack sufficient morphological detail, such as septa, suture patterns or position of the siphuncle, to identify them further. They have undergone varying degrees of aragonite dissolution and subsequent compaction. Specimen CM-BG3 has a diameter of 156mm and has two and one-quarter whorls preserved (Text-fig. 2A), which retain sufficient relief to display an upper surface that has some periostracum preserved; the lower-most layer is mouldic. The aperture is present but broken (Text-fig. 2A) and keel fractures are present. Specimen ROM-00-071802NC1/NC2, is 72mm in diameter and has two whorls preserved (Text-fig. 2B). Although quite poorly preserved, the specimen retains some relief, and the aperture is present. Specimen ROM-88716 has a diameter of 160mm and has approximately two and one-quarter whorls (Text-fig. 2C). The coiled cephalopod has some relief, and the aperture is present but the surface is poorly preserved. Specimen

Specimen Number	Diameter (mm)	Number of Whorls	Growth Lines	Periostracum	Sphenothallus	Bryozoan	Microchonchids	Orbiculoids
CM-BG3	156	2 1/4	N	Y	Y	Y	Y	N
ROM-00-071802NC1/NC2	72	2	Y	Y	Y	N	N	N
ROM-88716	160	2 1/4	Y	N	Y	Y	N	Y
UM-7571014	212?	1/4	N	N	Y	Y	N	N

TABLE. 1.Summary of cephalopod morphology from the Bear Gulch Limestone Member, USA, and type of epibiont.

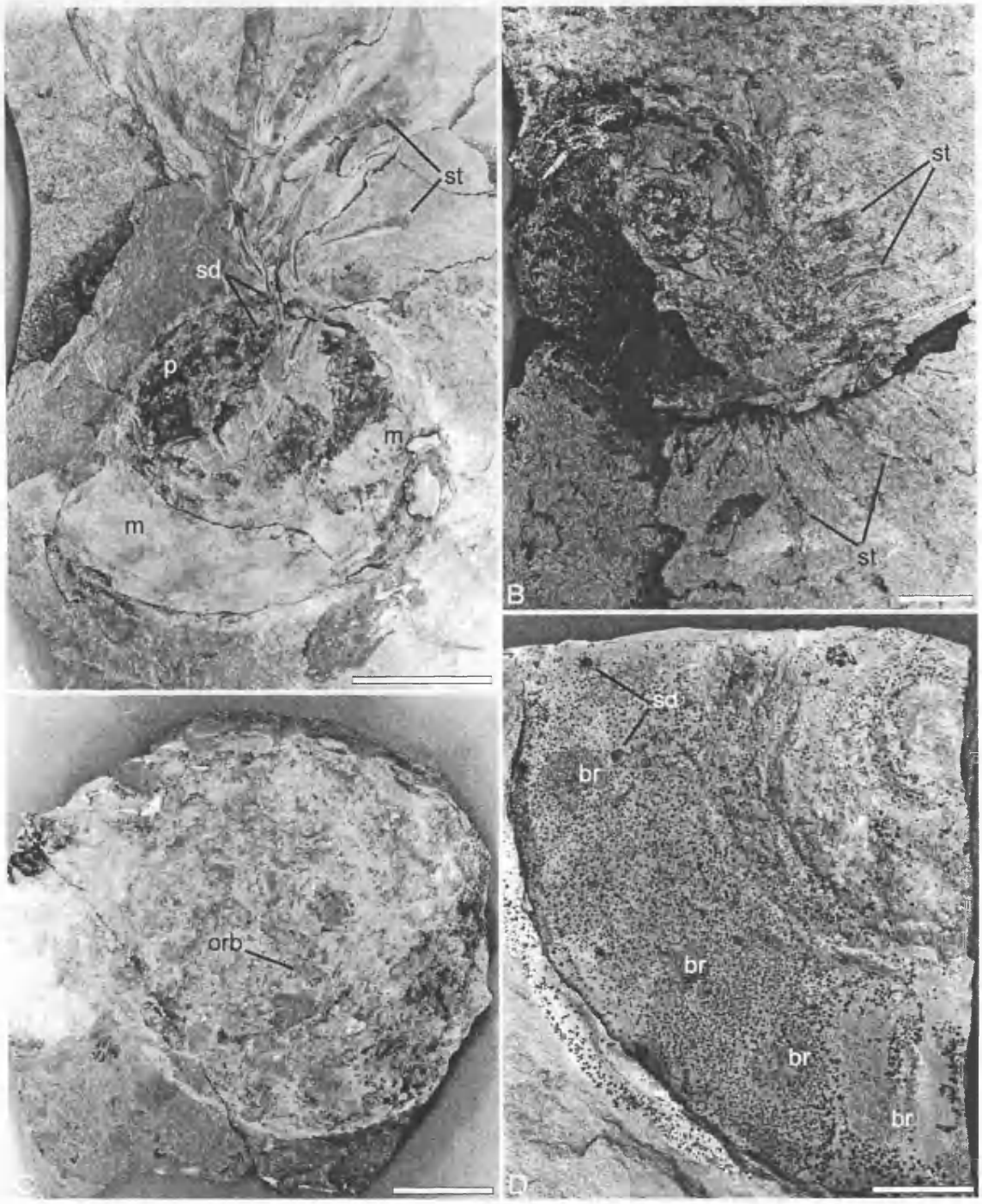
st
sd
p
m
m
st
st
B
orb
sd
br
br
br
br
D

TEXT-FIG. 2. Coiled cephalopods from the Bear Gulch Limestone Member (Upper Mississippian, USA). A, specimen CM-BG3 (clockwise coiling); a complete cephalopod with *Sphenothallus* longitudinal thickenings (st), *Sphenothallus* basal attachment discs (sd), a darker coloured periostracum (p) and mouldic area (m). The scale bar represents 25mm (see also text-fig. 6 for a camera lucida drawing). B, cephalopod ROM-00-071802NC1/NC2 (anticlockwise coiling) with *Sphenothallus* longitudinal thickenings visible close to the area of the aperture (st). The scale bar represents 15mm (See also text-fig. 7 for camera lucida drawing). C, cephalopod ROM-88716 (anticlockwise coiling) is poorly preserved; an orbiculoid brachiopod (orb) is indicated. The scale bar represents 50mm. D, cephalopod UM-7571014; one quarter of a whorl, which is mouldic, with bryozoan (br) occurring on the ribs of the cephalopod and *Sphenothallus* basal attachment discs (sd). Scale bar represents 25mm.

7571014 has an estimated diameter of 212mm, (only a quarter of a whorl is preserved) (Text-fig. 2D). The coiled cephalopod is mouldic and no aperture is preserved.

Smaller coiled cephalopods have few original features preserved. They have no relief and few fractures are evident, indicating dissolution, removal of the mineral component and perhaps a more flexible nature of the periostracum prior to compaction. A red-brown film is often associated with the smaller coiled cephalopods and this probably represents the remains of the periostracum. The smaller coiled cephalopods are often found as assemblages of several on a slab (specimen ROM-91-70815); epibionts are not known to be associated with these coiled cephalopods (Text-fig. 3).

EPIBIONTS

Epibionts are associated exclusively with the larger coiled cephalopods (>70mm) and include *Sphenothallus* (which are preserved as entire specimens or as the remnants of their basal attachment discs), bryozoans, 'microconchids' and rare orbiculoid brachiopods. The morphology of the well-preserved sphenothallids will be described in detail and compared with previous descriptions. Then the morphology of other epibionts will be described, followed by an examination of the host-epibiont relationships.

The morphology of Sphenothallus

General morphology. *Sphenothallus* consists of a ring like basal attachment disc, with a flat attachment surface at the posterior end, which develops into a ring like structure that extends into a single longitudinal thickening. The single longitudinal thickening gradually separates into 2 longitudinal thickenings. Between the longitudinal thickenings is a film with annulations each spaced at approximately a millimetre apart and positioned perpendicular to the length of the longitudinal thickenings. The convex nature of the annulations suggest that there were two films extending between the longitudinal thickenings and that the overall structure is cone-like. It is possible that soft tissues were housed between the films.

Basal attachment discs. Ruedemann (1896a, b) first described the anatomy of the *Sphenothallus* basal attachment disc and suggested that it resembled an inverted cup within a second inverted cup, with a closed tubule that connected both, and a thin membrane that joined the inverted rims of the cups. Bodenbender *et al.* (1989) suggested that this interpretation of the basal attachment disc was incorrect and that there was no internal structure, and Van Iten *et al.* (1992) later corroborated this based on their

G

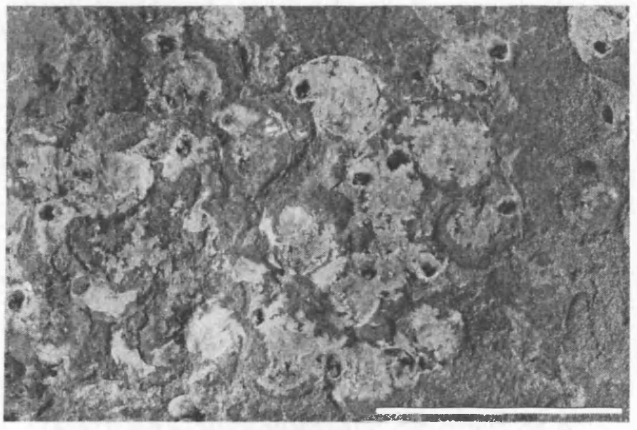

TEXT-FIG. 3. Specimen ROM-91-70815, approximately 30 small coiled cephalopods from the Bear Gulch Limestone Member (Upper Mississippian, USA) preserved as flattened compressions or moulds with no associated epibionts. Scale bar represents 50mm.

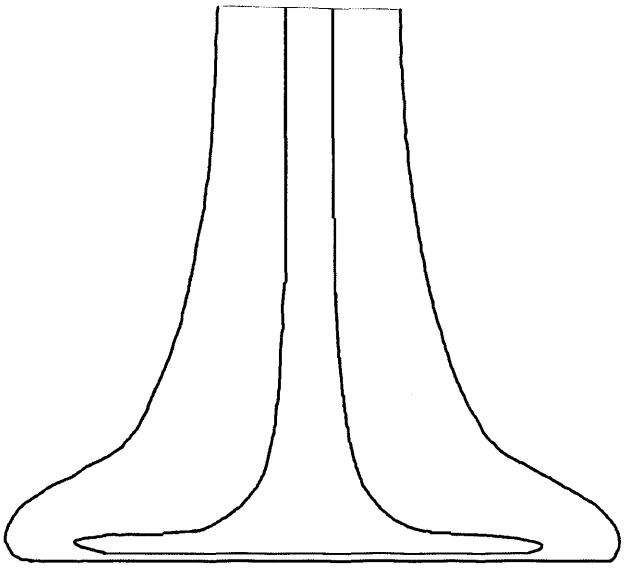

TEXT-FIG. 4. Schematic diagram of a *Sphenothallus* basal attachment disc forming a continuous structure with the tubule (after Van Iten *et al.* 1992).

investigation of *Sphenothallus* from the Bear Gulch Limestone Member. Van Iten *et al.* (1992) described the basal attachment disc as consisting of a single, thick, broadly conical expansion with a thin, flat, sub-circular membrane, and that the basal attachment disc and the tubule proper formed a single, continuous laminated structure (Text-fig. 4). The basal membrane, which is in direct contact with the substratum, is less than 10 µm thick in the specimens from the Bear Gulch Limestone Member (Van Iten *et al.* 1992). Bodenbender *et al.* (1989) discussed the central hollow of the basal attachment disc as being surrounded by a raised circular collar, which in specimens from the Dillsboro Formation (Upper Ordovician, USA) often exhibited circular depressions and cracks between the collar and the edge. From these observations Bodenbender *et al.* (1989) postulated that the basal attachment disc was hollow or balloon-like during life and had since collapsed.

The basal attachment discs of sphenothallids attached to coiled cephalopods from the Bear Gulch Limestone Member are often found in varying states of preservation and as a result of this different horizontal sections through the disc are seen. Well-preserved conical forms with hollow centres (Text-fig. 5A) to flat subcircular membranes (Text-fig. 5B). The poorest mode of preservation shows only the thickened circumference of the flat film (Text-fig. 5B), and this suggests that the circumference of the attachment disc is thicker than the flat subcircular basal membrane (specimens CM-BG3, ROM-88716, UM-7571014 and ROM-00-071802NC1/NC2). This investigation has shown that a flat, subcircular membrane forming the surface of the attachment site may be confirmed, and that the basal attachment disc is a continuous conical structure emanating from the basal membrane, as suggested by Bodenbender *et al.* (1989) and Van Iten *et al.* (1992). It is possible that the hollow area above the flat, basal membrane housed soft tissue.

Sphenothallus longitudinal thickenings. The surfaces of the *Sphenothallus* longitudinal thickenings have previously been described as being smooth (Hall, 1847; Mason and Yochelson 1985) and approximately crescentric in transverse cross-section (Schmidt and Teichmüller 1958). However, Van Iten *et al.* (1992) observed low, rounded, closely spaced, transverse ridges on specimens of *Sphenothallus* from the Collingwood Shale Formation (Upper Ordovician, Canada). Two coiled cephalopod specimens (CM-BG3 and ROM-00-071802NC1/NC2) (Text-figs. 2A-B; 6-7) and a bivalve shell fragment (specimen ROM-91-72404 Text-fig.8A), from the Bear Gulch Limestone Member have attached *Sphenothallus* with well preserved longitudinal thickenings. The longitudinal thickenings are crescentric in cross-section, but in each specimen one longitudinal thickening has a positive relief, whilst its partner longitudinal thickening has negative relief (Text-fig. 8A). Specimens from the Bear Gulch Limestone Member also have several low, rounded

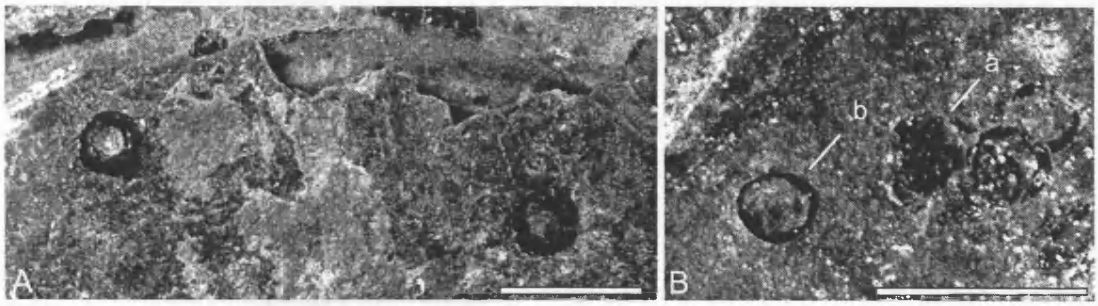

TEXT-FIG. 5. *Sphenothallus* attachment discs on ammonoid specimen CM-BG3 from the Bear Gulch Limestone Member (Upper Mississippian, USA). A, conical forms, scale bar represents 4mm. B, flat subcircular membranes (a) and thickened circumference of the rim of an attachment disc (b). Scale bar represents 6mm.

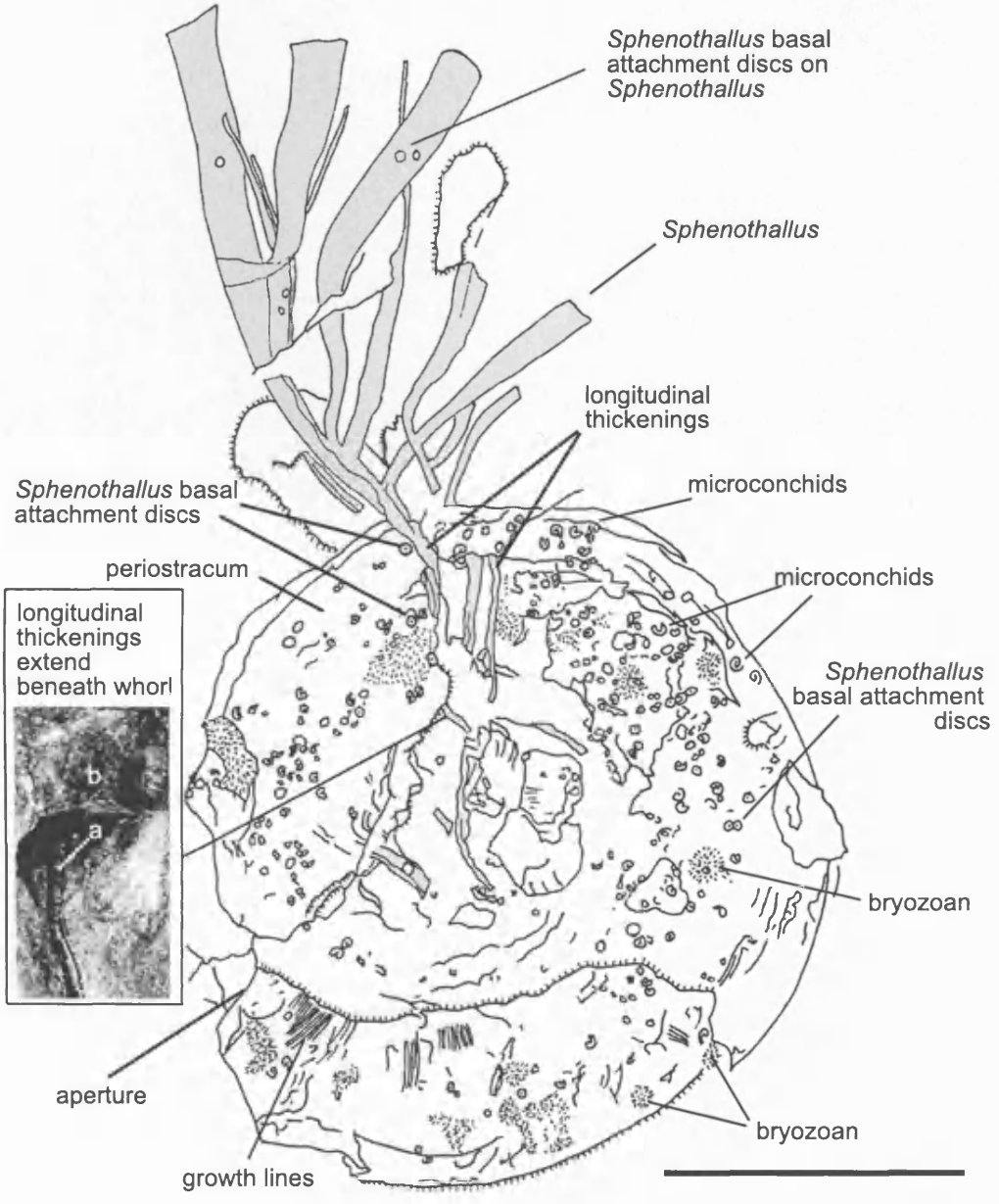
Sphenothallus basal attachment discs on *Sphenothallus*
Sphenothallus
longitudinal thickenings
microconchids
Sphenothallus basal attachment discs
periostracum
microconchids
longitudinal thickenings extend beneath whorl
b
a
Sphenothallus basal attachment discs
bryozoan
aperture
bryozoan
growth lines

TEXT-FIG. 6. Camera lucida drawing of specimen BG3 from the Bear Gulch Limestone Member (Upper Mississippian, USA). Scale bar represents 125 mm.

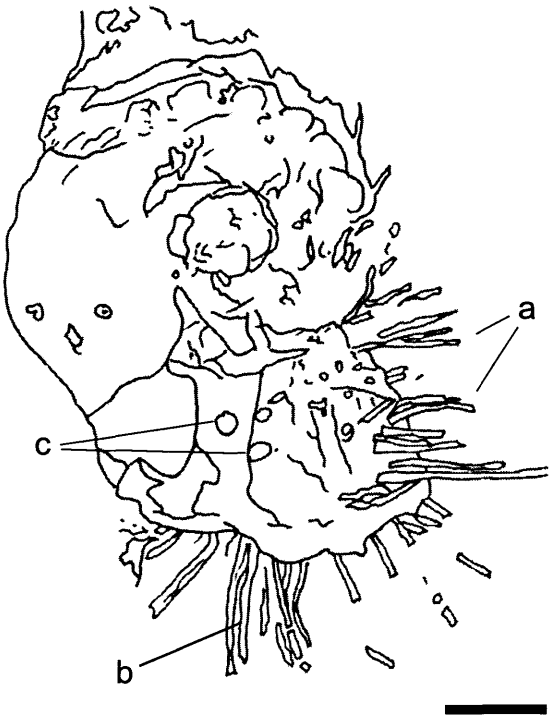

TEXT-FIG. 7. Camera lucida of coiled cephalopod specimen ROM-00-071802 NC1/NC2 from the Bear Gulch Limestone Member (Upper Mississipian, USA). The *Sphenothallus* longitudinal thickenings lie above the coiled cephalopod (a) and extend from below the coiled cephalopod (b). *Sphenothallus* basal attachment discs are present on the coiled cephalopod (c). Scale bar represents 15mm. See also text-fig. 2B.

ridges, which are aligned perpendicular to the length of the longitudinal thickenings (Text-fig. 8A). In both specimens CM-BG3 and ROM-00-071802NC1/NC2 the *Sphenothallus* longitudinal thickenings are directed towards the position of the cephalopod apertures (Text-figs. 2A-B; 6 -7)

The relationship between the Sphenothallus longitudinal thickenings and the attachment disc. The exact nature of the attachment between the basal attachment discs and the longitudinal thickenings of the sphenothallids has always been contentious. Specimens from the Dillsboro Formation (Ordovician, USA) indicate that no tube remains just above the attachment base and this led Bodenbender *et al.* (1989) to imply that there was a structural weakness in the organism just above the attachment base. Choi (1990) suggested that the sphenothallid longitudinal thickenings were flexible, so that presumably the part of the organism just above the attachment disc was also flexible.

This investigation has found basal attachment discs on coiled cephalopods with only one longitudinal thickening coming from them; unfortunately the nature of the divergence of this longitudinal thickening into the two longitudinal thickenings is not clear. However, a *Sphenothallus* attached to part of a bivalve shell (specimen ROM-91-72404) shows the connection between the basal attachment disc and the longitudinal thickenings (Text-fig. 8B). One longitudinal thickening extends from the basal attachment disc and gradually, beginning 10mm up from basal attachment disc, separates into two longitudinal thickenings (Text-fig. 8B). The presence of this proximal portion of the longitudinal thickening is extremely rare, even when the remainder of the *Sphenothallus* is very well preserved. This may be because it was brittle; or it may have been very delicate and easily damaged; or perhaps it was structurally supported *in vivo* by non-mineralised tissue which decayed rapidly post-mortem.

The film between the longitudinal thickenings. The *Sphenothallus* on coiled cephalopod CM-BG3 have a thin, red-brown film preserved between the two longitudinal thickenings, upon which are regularly spaced annulations, approximately 0.2mm in thickness and spaced 1mm apart. These annulations occur perpendicular to the longitudinal thickenings (Text-fig. 9). This is the first record of annulations occurring between the longitudinal thickenings on specimens of *Sphenothallus.* Van Iten *et al.* (2002) examined *Sphenothallus* from the Middle Cambrian of British Columbia, Canada, but these only had a smooth, thin wall (film) between the longitudinal thickenings. The annulations observed herein display a slight convex curvature toward the aperture and this is especially prominent at the distal end of the sphenothallids. Fauchald *et al.* (1986) described soft-bodied parts of a sphenothallid specimen from the Hunsrück Slate (Early Devonian,

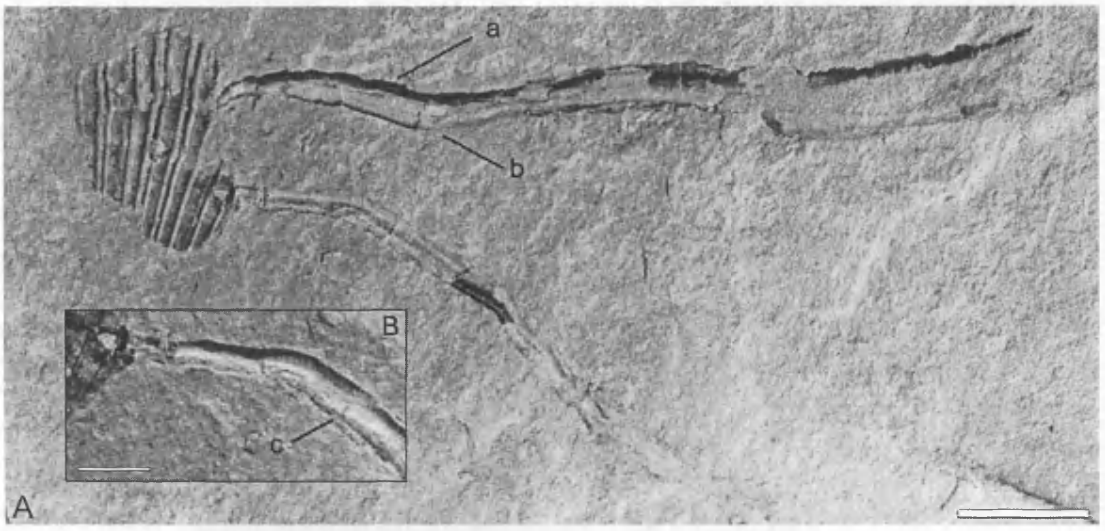

TEXT-FIG. 8. A, two specimens of *Sphenothallus* attached to part of a bivalve shell (specimen ROM-91-72404), from the Bear Gulch Limestone Member (Upper Mississippian, USA). One *Sphenothallus* clearly displays one longitudinal thickening with positive relief (a) and one longitudinal thickening with negative relief (b). Scale bar represents 10mm. B, enlargement of the lower *Sphenothallus,* which displays a connection between the longitudinal thickenings and the attachment disc and low round ridges (c). Scale bar represents 4mm.

TEXT-FIG. 9, *Sphenothallus* tubes on cephalopod specimen CM-BG3 of the Bear Gulch Limestone Member. Annulations (mm spacing) are present on the thin film perpendicular to the longitudinal thickenings (a); *Sphenohallus* basal attachment discs (b) also occur on the thin film. Scale bar represents 10 mm.

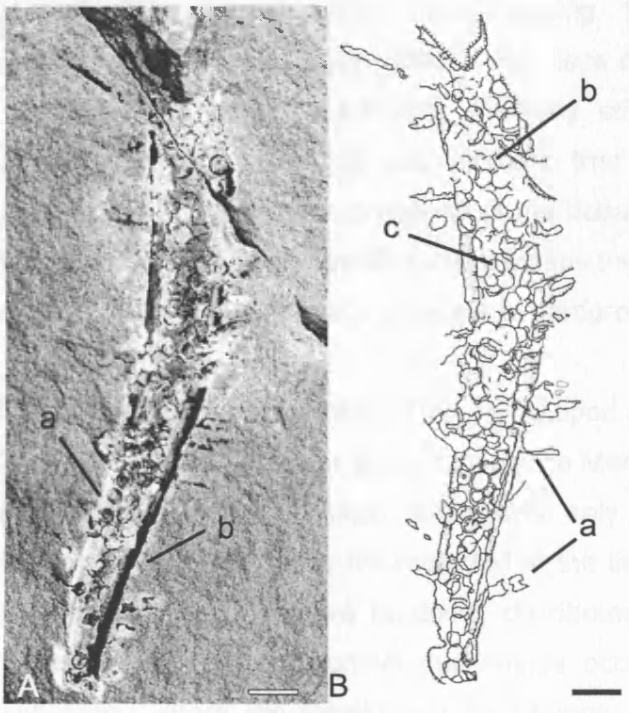

TEXT-FIG. 10, A. *Sphenothallus* (ROM 88-72819) from the Bear Gulch Limestone Member (Upper Mississippian, USA) found unassociated with cephalopods. The main *Sphenothallus* tube is covered in *Sphenothallus* basal attachment discs. Longitudinal thickening on the left show negative relief (a); on right the longitudinal thickening show positive relief (b). Scale bar represents 6mm, B, camera lucida drawing of the same *Sphenothallus* illustrating *Sphenothallus* longitudinal thickenings emanating from some of the basal attachment discs (a), basal attachment discs showing growth interference (b), and overgrowth (c). Scale bar represents 6mm.

Germany), in which the radiographs showed a two-tentacled, spool-like organism emerging from the aperture. This would suggest that the film of *Sphenothallus* is actually a tube-like structure and composed of two flattened sheets. One example of an isolated *Sphenothallus* (unassociated with cephalopods) from the Bear Gulch Limestone Member has a film, which is completely covered in other basal attachment discs, some of which have longitudinal thickenings extending from them (Text-fig. 10A-B). In this particular example growth interference between basal attachment discs on the *Sphenothallus* can be seen, and overgrowth of basal attachment discs by other *Sphenothallus* basal attachment discs has also occurred; this may indicate that competition for suitable substrates was intense. Furthermore, the presence of the basal attachment discs on the film between the longitudinal thickenings implies that perhaps this film was quite rigid, and not flexible, because *Sphenothallus* normally attaches to hardgrounds.

The Sphenothallus - cephalopod association. Two cephalopod specimens (CM-BG3 and ROM-00-071802-NC1/NC2) from the Bear Gulch Limestone Member have well-preserved *Sphenothallus* attached to them. In both specimens only one side of the coiled cephalopod is visible but the way-up was not recorded at the time of collection. Isolated *Sphenothallus* basal attachment discs are randomly distributed on specimen CM-BG3, and basal attachment discs with longitudinal thickenings occur towards the umbilical region of the cephalopod where the longitudinal thickenings are directed towards the aperture of the cephalopod (Text-fig. 2A). In the umbilical region of CM-BG3 the cephalopod shows a composite mould where the under side of the cephalopod is visible, and here longitudinal thickenings occur that extend below the last whorl with relief (Text-fig. 6). So sphenothallid tubes occur on both surfaces of the cephalopod, on top of and below a whorl. These two lines of evidence indicate that both surfaces were available for colonisation. Accordingly, colonisation may have occurred when the cephalopod was afloat in the water, or when the cephalopod was on the seafloor, but only if it was flipped over so that both surfaces were at some time available. In specimen ROM-00-071802NC1/NC2 sphenothallids also appear to be attached to both sides of the coiled cephalopod. In this case the longitudinal thickenings of the sphenothallids attached to the underside extend towards the venter whereas those attached to the upper side extend towards the aperture (Text-figs. 2B and 7).

'Microconchids'

'Microconchids' found on specimen CM-BG3, are mouldic and up to 5mm in diameter, and thus are of a similar size to the *Sphenothallus* basal attachment discs that also occur on

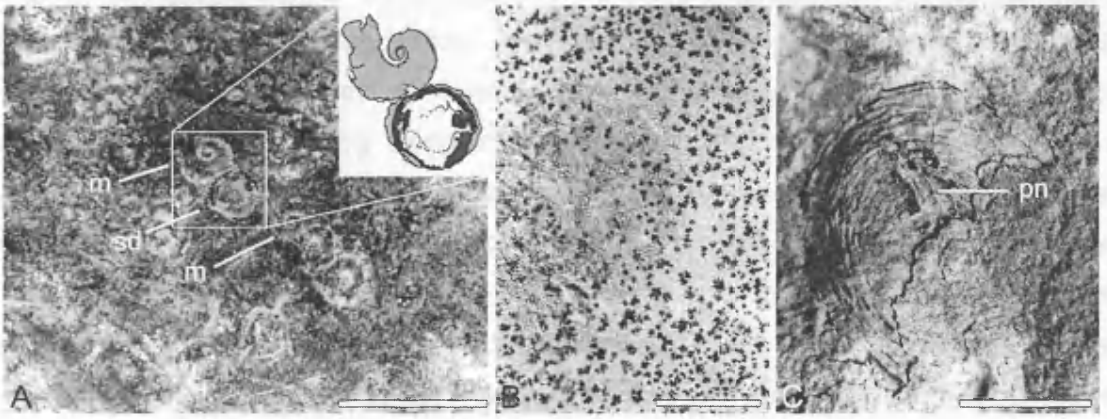

TEXT-FIG. 11. A, Specimen CM-BG3 from the Bear Gulch Limestone Member (Upper Mississippian, USA), microconchs display clockwise coiling (m) and lie in close association with *Sphenothallus* basal attachment discs (sd). Scale bar represents 8mm. Top inset. A camera lucida drawing of the microconch and the *Sphenothallus* basal attachment disc. B, ammonoid specimen UM-7571014 from the Bear Gulch Limestone Member (Upper Mississippian, USA), an example of a bryozoan which is covered by a thin layer of sediment and associated with manganese. Scale bar represents 10mm. C, specimen ROM-88716 of the Bear Gulch Limestone Member (Upper Mississippian, USA), orbiculoid brachiopod on ammonoid displaying a pedicle notch (pn). Scale bar represents 8mm.

the same specimen (Text-fig. 11A). The 'microconchids' generally have one full whorl; 80% of the 'microconchids' coil clockwise, and 20% anti-clockwise (n = 60). They are randomly distributed on the cephalopod shell, but are less common on the last quarter whorl of the coiled cephalopod, which may indicate either selective positioning by the microchonchs, a thicker periostracum on the newer shell, or perhaps, that the cephalopod could clean itself (presumably using tentacles) in this region. 'Microconchids' such as these have been assigned to vermiform gastropods (Burchette and Riding 1977), and spirorbids or serpulids (Beus 1980). Lower Carboniferous vermiform gastropods of less than 1.5mm diameter are distinguished from serpulids and spirorbids by the nature of the shell microstructure and the presence of imperforate septa and a protoconch structure (Burchette and Riding 1977; see Weedon 1990). However, these details are not preserved in the 'microconchid' specimens from the Bear Gulch Limestone Member and so their identity cannot be resolved further.

Bryozoans

Encrusting bryozoans occur on three large coiled cephalopods from the Bear Gulch Limestone Member (specimens CM-BG3, ROM-88716 and UM-7571014). However, their poor preservation means that it has not been possible to identify them further. Specimen CM-BG3 has approximately 17 colonies of encrusting bryozoan and these appear to have preferentially encrusted the raised ribs of the final cephalopod whorl (Text-fig. 6). Colony sizes vary from 1mm x 2mm to 4mm x 5mm and cover up to 20 % of the visible surface of the cephalopod shell. Specimen UM-7571014 (Text-fig. 11B), like specimen CM-BG3, has colonies of encrusting bryozoan on the raised ornament (Text-fig. 2D and 6), which may have been advantageous to the bryozoan for filter feeding, or perhaps the periostracum of the coiled cephalopod was thinner in these areas so that attachment was easier. On specimen UM-7571014 bryozoan colonies range in size from approximately 5mm x 5mm to 15mm x 15mm and cover approximately 35% of the visible surface of the cephalopod. Specimen ROM-88716 has six colonies of mouldic or brown coloured encrusting bryozoans towards the venter on the last quarter of the only preserved whorl (Text-fig. 2C). Colony sizes vary from 3mm x 5mm to 5mm x 5mm and cover approximately 60% of the visible surface of the cephalopod.

Orbiculoidea

Three flat, fragmented and demineralised orbiculoids are present on coiled cephalopod ROM-88716 (Text-fig. 11C). The diameters of the orbiculoids are approximately 10mm,

12mm and 13mm. The two smallest orbiculoids preserve the pedicle notch (Text-fig. 11C).

Relative order of epibiont attachment

It has only possible to determine the relative order of epibiont attachment on coiled cephalopod specimen CM-BG3, because it is only on this specimen that the epibiont taxa show any interaction. 'Microconchids' on coiled cephalopod specimen CM-BG3 have overgrown the bryozoans suggesting that, at least in some cases, bryozoans colonised before 'microconchids'. In at least one instance a microconch was already attached when a sphenothallid grew over it. However, some *Sphenothallus* basal attachment discs and the 'microconchids' show growth interference (Text-fig. 6) suggesting that they may well have colonised at the same time. A relationship between bryozoans and sphenothallids is not seen, but it may be speculated that the bryozoans colonised before sphenothallids.

Discussion of host epibiont relationships in the Bear Gulch Limestone Member

Distribution of the epibionts. Three-dimensional coiled cephalopods isolated from the sediment, or flattened coiled cephalopods where the way-up orientation is known, can reveal whether cover with epibionts is holoperipheral. However, only one surface of the coiled cephalopods from the Bear Gulch Limestone Member is visible and the way-up orientation is not known. Furthermore, the interiors of the body chambers, colonisation of which could only be post-mortem, are, when present. However, the distribution and orientation of the epibionts on the coiled cephalopod conchs from the Bear Gulch Limestone Member provide evidence for colonisation of the coiled cephalopods *in vivo*.

In specimen CM-BG3 attachment of *Sphenothallus* occurred to both sides of the cephalopod (Text-figs. 2A and 6). On the same specimen 'microconchids' occur infrequently on the last quarter whorl of the venter on one side (Text-fig. 6). However, it is not certain whether the microconchids also occur on the opposite side of the specimen, which is in the sediment and therefore unobservable. Specimen ROM-00-071802NC1/NC2 displays more relief in the region of the cephalopod aperture and here it is possible to see that the *Sphenothallus* longitudinal thickenings extend in front of the aperture and to what would have been the lowermost surface of the cephalopod in life (Text-fig. 7). On this upper surface, several *Sphenothallus* basal attachment discs are also present (Text-fig. 7). To the side of the aperture the cephalopod displays substantial relief and here the *Sphenothallus* longitudinal thickenings stop abruptly (Text-fig. 7); I consider that these longitudinal thickenings continue to the lower side of the cephalopod

and that the coiled cephalopod is colonised on both sides (Text-fig. 7). Therefore, two coiled cephalopod specimens (CM-BG3 and ROM-00-071802NC1/NC2) from the Bear Gulch Limestone Member have *Sphenothallus* on both sides of their compressed conchs. Epibionts may have attached to the cephalopod shells when they were on the seabed, but to account for this the cephalopods must have been colonised, flipped over, and then colonised again. There is no evidence for the strong currents or storms that would have been required in the Bear Gulch Limestone Member; there are no sedimentological indicators of currents or storm activity, nor tool marks, aligned fossils or other indications that other fossils moved once they had come to rest on the seabed (Lund *et al.* 1993). The evidence available implies that the epibionts attached to the cephalopod whilst in the water column. However, it is important to note that the orthocones and small coiled cephalopods from the Bear Gulch Limestone Member lack epibionts. There are several possibilities that may account for this. For example, this may be an ecological affect caused by the small coiled cephalopods and orthocones living at different depths in the basin from the large cephalopods. Alternatively, that the small coiled cephalopods lack epibionts may indicate that they are a different species from the large coiled cephalopods; perhaps the smaller coiled cephalopods and the orthocones were better able to defend themselves against epibiont attachment. Alternatively, Landman *et al.* (1987) suggested that thicker periostracal films occur on juvenile coiled cephalopods and this may deter epibiont attachment (see Bottjer 1981; Landman *et al.* 1987).

Orientation of the epibionts. Epibionts displaying a preferred growth orientation may indicate a rheophilic response to the swimming motion of the host. Wignall and Simms (1990) showed that such oriented growth is commonly directed towards the aperture of the cephalopod.

Coiled cephalopods CM-BG3 and ROM-00-071802NC1/NC2 (Text-figs 6 and 7) both have attached *Sphenothallus* with longitudinal thickenings that display a strong orientated growth. In specimen CM-BG3 (Text-fig. 2A; 6) the *Sphenothallus* tubes extend in front of the aperture (Text-fig. 12), whereas in specimen ROM-00-071802NC1/NC2 (Text-fig. 2B; 7) the *Sphenothallus* tubes radiate around the aperture of the coiled cephalopod.

Choi (1990) suggested that the longitudinal thickenings were flexible in life and, therefore, the final position of the longitudinal thickenings may have been a response to the way in which the coiled cephalopod shell sank and landed on the seabed. Alternatively, if the epibionts were flexible their orientation may have resulted from bottom water currents, which may have rotated the epibionts into what now appears to be a rheophilic position. Some organisms may have avoided growing towards the aperture

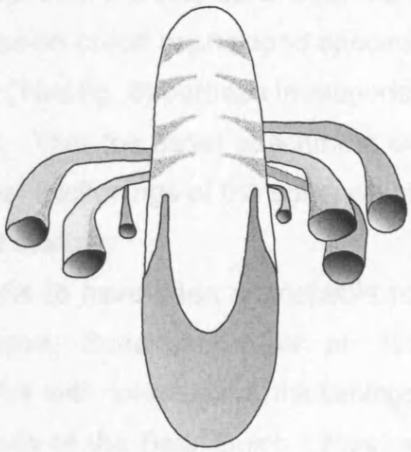

Text-fig. 12. 3d reconstruction of specimen CM-BG3

because of the coiled cephalopod's ability to actively cleanse itself using its tentacles (Wignall and Simms 1990). However, on specimen ROM-00-071802NC1/NC2 the density of the *Sphenothallus* longitudinal thickenings positioned around the aperture of the coiled cephalopod suggests that they preferentially grew there. If the *Sphenothallus* longitudinal thickenings were not flexible then it would be a clear indication of a rheophilic response. Indeed, *Sphenothallus* tubes on coiled cephalopod specimen CM-BG3 appear to display a change in growth direction (Text-fig. 6) perhaps in response to the growth and subsequent rotation of the cephalopod. That the basal attachment discs could colonise the thin film between the two longitudinal thickenings of the sphenothallid (Text-fig. 10A-B) also implies that *Sphenothallus* was not flexible.

Sphenothallus seems to have been susceptible to breaking just above the basal attachment disc (see above; Bodenbender *et al.* 1989). However, no detached specimens of *Sphenothallus* with longitudinal thickenings were found in the sediments surrounding the cephalopods of the Bear Gulch Limestone Member and, therefore, it is possible that they broke away from their basal attachment discs prior to the cephalopod coming to rest on the seabed. Consequently, many of the sphenothallid basal attachment discs could represent old attachment points, indicating colonisation in the water column during the early ontogeny of the cephalopod.

CONCLUSION

The Bear Gulch Limestone Member is proposed as the new name for the Bear Gulch Beds. Further, the Surenough Beds and Becket Beds are renamed the Surenough Member and Becket Limestone Members, respectively.

Epibionts only occur on the large coiled cephalopods (>70mm in diameter) from the Bear Gulch Limestone Member. The smaller coiled cephalopods (<50mm in diameter) may be a different species that was more able to remove epibionts, or they may be juvenile forms, which had a thicker periostracum, which deterred epibiont attachment. Alternatively, the smaller coiled cephalopods may have occupied a different depth of the water column, which was not suitable for epibiont attachment.

Epibionts are palaeobiologically and palaeoecologically very important. They provide an insight into the life history of the host and often they provide more palaeoenvironmental information than the fossil they are attached too.

The epibiont *Sphenothallus* displays holoperipheral cover and preferential growth towards and forwards of the apertures of two of the coiled cephalopods from the Bear Gulch Limestone Member (specimens CM-BG3, ROM-00-071802NC1/NC2). Bryozoans are rare in the Bear Gulch Limestone Member but do occur on the larger coiled

cephalopods, which implies either that no hard substrates were available elsewhere for colonisation, or that perhaps bottom water palaeoenvironmental conditions were inimical. Bryozoans show preferential attachment to the ribs of the larger cephalopods which may have been advantageous for filter feeding, or perhaps the periostracum of the cephalopod was thinner in these areas so that attachment was easier. 'Microconchids' are recorded for the first time from the Bear Gulch Limestone Member on the coiled cephalopod specimen CM-BG3. The implication is that they preferentially colonised the coiled cephalopod whilst it was alive in the water column, presumably because the substrate or bottom water conditions were inhospitable. The fact that 'microconchids' do not occur in the last third of the last whorl, towards the venter, on coiled cephalopod specimen CM-BG3 may be evidence of selective positioning by the 'microconchids', perhaps to aid their ability for effective filter feeding.

The most parsimonious conclusion for the timing of the attachment of *Sphenothallus*, 'microconchids' and bryozoans to the coiled cephalopod CM-BG3 would be that the epibionts attached to the cephalopod whilst it was alive.

This investigation has revealed new information on the morphology of the enigmatic organism *Sphenothallus*. Annulations occur on the thin film between the longitudinal thickenings. The connection between the basal attachment disc and the longitudinal thickenings was observed to comprise one longitudinal thickening that gradually separates into two longitudinal thickenings and the longitudinal thickenings themselves were observed to be crescentric in cross-section, but in each specimen one longitudinal thickening has a positive relief, whilst its partner longitudinal thickening has negative relief. Because *Sphenothallus* is encrusted by other sphenothallids it is thought to be inflexible.

CHAPTER 2

POLYCHAETE JAW APPARATUSES (SCOLECODONTS) FROM THE CARBONIFEROUS BEAR GULCH LIMESTONE MEMBER, CENTRAL MONTANA

ABSTRACT.—Articulated jaw apparatuses from two eunicid polychaetes are reported from the Bear Gulch Limestone Member, Fergus County, central Montana. One specimen is identified as *Symmetroprion* n. sp.; this is the first record of a member of the genus from the Carboniferous and the first assemblage of a member of Symmetrioprionidae found with the remains of the body. The other specimen is identified as *Brochosogenys reidiae*; this is the first record of this species from the Bear Gulch Limestone Member and only the second articulated assemblage of *B. reidiae* from the Carboniferous. Both jaw assemblages have suffered compaction and fracturing. Subsequently, after lithification of the sediment, most of the scolecodont material was lost leaving moulds of the jaws.

INTRODUCTION

SCOLECODONTS are jaw elements of fossil polychaetes (Eunicida and Glyceriformia). They range in size from approximately 0.1 mm to 2 mm in length and are thus commonly referred to as microfossils (Eriksson 2000). The first description of a scolecodont was of a single specimen in the Silurian of Saaremaa, Estonia (Eichwald 1854), however this was misinterpreted as a fish tooth. Although polychaetes are known from the Cambrian (Rouse and Pleijel 2001), the oldest unequivocal scolecodonts are from the Arenig (Szaniawski 1996); polychaetes with similar jaw apparatuses exist today (Szaniawski 1996; Eriksson 2000; Rouse and Pleijel 2001). The Ordovician had the greatest number of apparatus based families, the diversification within most of which continued until the end of the Devonian, followed by a decrease in the Carboniferous (Szaniawski 1996). Of the fifteen families present in the Permian only a possible five families continued into the Mesozoic (Szaniawski 1996). Morphological variation in scolecodont elements through time may permit major stratigraphic systems and series to be recognized; this is particularly the case for the Palaeozoic (Eriksson 2000). However, in strata older than the Ordovician there seems to be a lack of scolecodonts and this is also true for younger strata of the Mesozoic and Tertiary systems (Szaniawski 1996). This may be a consequence of poor preservation due to different compositions of the jaws (Mierzejawska

and Mierzejewski 1974) rather than low diversity, as variations in fossilisation potential, both between taxa and between different jaws of a single taxon are known (Szaniawski 1974; Brenchley 1979; Colbath 1986a). The relatively higher diversity of scolecodonts in the Palaeozoic, compared with younger systems, may also reflect increased research into faunas of this interval.

The majority of Palaeozoic polychaete jaws are traditionally placed in the order Eunicida (Ordovician to Recent) (Eriksson 2000). Most modern representatives of Eunicida live in shallow water sediments especially near shore, but some are pelagic (Szaniawski 1996). They are omnivorous and live largely on detritus; however, they have different systems of feeding and accordingly live in different types of environments, either in soft sediments, or on hard bottoms in reefs or lagoons. Suprageneric systematics of Recent Eunicida (and Phyllodocida) is based partly on their jaw morphology (Hartman 1954; Orensanz 1990, Rouse and Pleijel 2001). For example, Lumbrineridae Schmarda, 1861 externally resemble Oenonidae Kinberg, 1865 but these can be separated from one another on jaw structure (Rouse and Pleijel 2001). In the diagnosis of taxa of lower rank jaw morphology is rarely taken into account (Szaniawski 1996; Rouse and Pleijel 2001). However, Szaniawski (1996) suggested that the armature is sufficiently diversified and characteristic to distinguish not only Recent families and genera, but also most modern species.

Although scolecodonts are highly abundant in Palaeozoic sedimentary rocks (Eriksson 2000) the soft tissues of polychaetes are prone to rapid decay following death (Briggs and Kear 1993). Therefore, the body of the polychaete is usually lost and identification of fossils relies on the more decay resistant scolecodonts. Composite sets of jaws, however, generally disarticulate and become distributed through the sediment on decomposition of the polychaete (Eriksson 2000) or after being consumed by other organisms (Colbath 1986b, 1987a). This dispersal of scolecodont elements is the source of difficulty in recognising sets of polychaete jaw apparatuses from the fossil record and historically has caused isolated elements from the same apparatus to be given different names (Bergman 1989, Szaniawski 1996, Eriksson 2000). Therefore, articulated sets of jaw apparatuses are valuable for identification of the type, number and arrangement of the scolecodont elements (Bergman 1989). Articulated fossil polychaete jaws found in situ and preserved with the body are extremely rare and supply a second dimension to the identification of extinct polychaetes plus further morphological characters to compare with extant polychaetes.

Massalongo (1855) was the first to note impressions of polychaetes with intact jaws from Tertiary strata in Italy. Schram (1979) was the first to describe polychaetes from the Bear Gulch Limestone Member several of which had articulated jaw apparatuses,

which, however, were not described fully. Herein two genera, *Brochosogenys* and *Symmetroprion*, from the families Kielanoprionidae and Symmetroprionidae respectively are reported from the Bear Gulch Limestone Member. In both cases the composite sets of jaws are preserved as moulds and only *Symmetroprion* n. sp. has soft tissue remains of its body preserved.

Jaw morphology.--The jaws comprise a ventral proboscis, which is equipped with a complex dorsal jaw apparatus (Dales 1962; Kielan-Jaworowska 1966; Szaniawski 1996). In the majority of Recent eunicids the jaws are composed of one pair of ventral mandibles and a dorsal maxillary apparatus, the elements of which are identified using the notation of MI, MII MIII, MIV, MV (Szaniawski 1996).

The mandibles provide areas for muscle attachment and their anterior face may serve for chiselling hard substrates (Szaniawski 1996). In Recent eunicids MI elements are used to grasp prey, MII for cutting off parts of the prey and transporting them backwards, and MIII, MIV and MV are to cling to the prey tightly (Szaniawski 1996). The role of the carriers is for muscle attachment and support of the first maxillae. The mandibles and maxillary are connected by a muscle sack and cuticle, both of which may prevent disarticulation of the jaw apparatuses in the period immeadiately following death (Szaniawski 1996).

Most elements of the Eunicida are paired, but the pairs are usually not perfectly symmetrical (Kielan-Jaworowska 1966). Many apparatuses have one or two unpaired elements; normally these are the basal plate and the left MIII (Kielan-Jaworowska 1966). However, in some apparatuses both of these elements are paired or lacking (Szaniawski 1996). The two sets of jaws described here are of labidognath type, indicating that when the jaws are retracted the elements form a semicircle (Ehlers 1864-68).

The number and arrangement of elements and the shape of MI, MII, basal plates, carriers and mandibles are the most important diagnostic characters when identifying fossil eunicids at family and genus level (Szaniawski 1996). Fossil species are often differentiated on the basis of MI and MII element morphology (Eriksson and Bergman 1998), for example, the number and differentiation of denticles, metric proportions (length to width ratio) and the outline of the pulp cavity (Szaniawski 1996).

GEOLOGICAL SETTING

Symmetroprion n. sp and *B. reidiae* are from the Bear Gulch Limestone Member (fig. 1.1) one of a series of limestone lenses within the Heath Formation of Montana and North Dakota, first described by Mundt (1956). This limestone lens has also previously been termed the Bear Gulch Member (Williams 1983) the Bear Gulch Limestone (Lund *et al.* 1993) and the Bear Gulch Beds (Williams 1983; Horner and Lund 1985). These different names led to a confusing situation so that recently Thomas (Chapter 1) suggested that the term Bear Gulch Limestone Member be used to conform to current stratigrapical nomenclature (fig. 1.2). In addition the Surenough and Becket Beds were elevated to the status of Surenough and the Becket Limestone Members (Chapter 1) (fig. 1.2).

Only the Bear Gulch Limestone Member has been widely sampled for fossils. This unit comprises a carbonate mudstone lens approximately 15km in lateral extent and up to 24m thick near the eastern margin of the outcrop (Feldman *et al.* 1994). The Bear Gulch Limestone Member is Namurian in age, specifically Upper Chesterian; this is based upon palynostratigraphy of a diverse spore assemblage (Cox 1986), ammonoids (Mapes 1987) conodonts (Scott 1973; Norby 1976) and the fish assemblage (Feldman *et al.* 1994). The Bear Gulch Limestone Member was deposited about 12 degrees north of the equator as the last of a series of open-ended en-echelon basins that formed progressively from east to west by tectonic activity within the Big Snowy Trough (Williams 1983; Grogan and Lund 2002). The Big Snowy Trough was a narrow east-west trending embayment that connected the Big Snowy Basin to the east with the Cordilleran Miogeosyncline to the west (Mallory 1972; Williams 1981, 1983; Horner and Lund 1985; Witzke 1990). The Bear Gulch Limestone Member consists of finely laminated, massive beds (>30 mm thick), intercalated with fissile platy beds (<30 mm thick) (Williams 1983) and grades laterally and downwards into the black shales of the Heath Formation (Feldman *et al.* 1994) (fig. 1.2). The Bear Gulch Limestone Member contains large assemblages of fossil marine invertebrate and vertebrate species including soft-bodied forms. Variation in the degree of preservation of the fossils is considerable, ranging from complete organisms with excellent details of soft anatomy to completely disarticulated skeletal remains (Feldman *et al.* 1994).

MATERIALS AND METHODS

Three fossil eunicid polychaete jaw apparatuses are discussed herein. Two jaw apparatuses are from the Bear Gulch Limestone Member, these are *Symmetroprion* n. sp (ROM-49953a (part) (fig. 2.1), ROM-49953b (counter-part) (fig. 2.2) and *B. reidiae* (ROM-

1

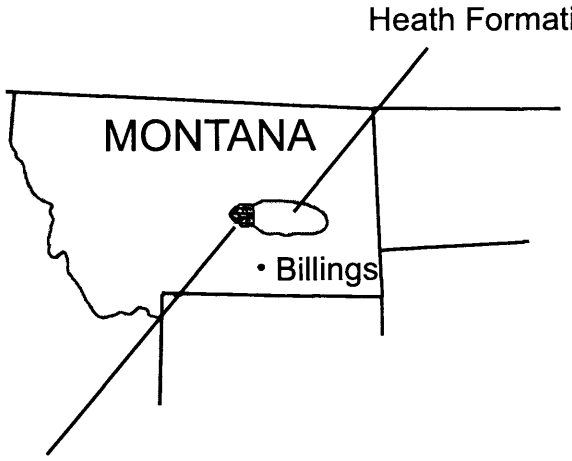

Bear Gulch Limestone Member,
visible outcrop area is 85km^2.

2

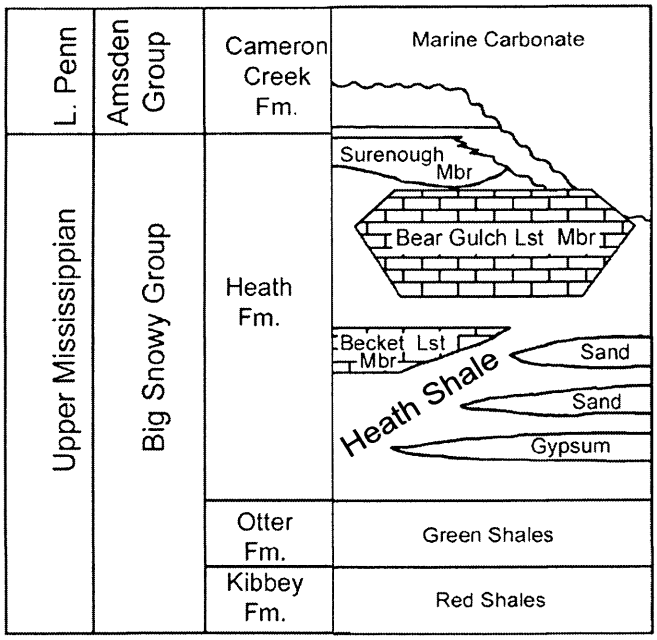

Figure 1-1-2. Location and stratigraphical position of the Bear Gulch Limestone Member. 1, map of Montana, USA, with the location of the outcrop area indicated. 2, stratigraphical position of the Bear Gulch Limestone Member (Thomas chapter 1, after Williams 1983).

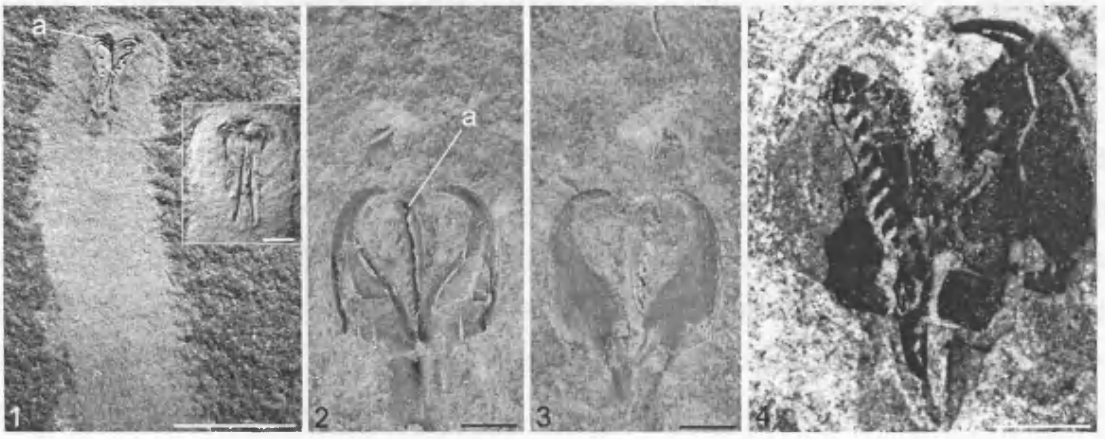

Figure 2-1-4. 1. *Symmetrioprion* n. sp. (specimen ROM-49953a part) from the Bear Gulch Limestone Member, body of the polychaete has mm scale annulations, scolecodonts are present as moulds with some organic material preserved in the tips (a), scale bar represents 7 mm. Inset of counterpart of fig. 2.1 *Symmetrioprion* n. sp. (specimen ROM-49953b), scale bar represents 2 mm. 2. *Brochosogenys reidiae* (specimen ROM-62602a) from the Bear Gulch Limestone Member, mouldic scloecodonts with some organic material preserved (a) but no evidence of soft tissue, scale bar represents 2 mm. 3. Counterpart of figure 2.2 *Brochosogenys reidiae* (specimen ROM-62602b), scale bar represents 2 mm. 4. *Brochosogenys reidiae* lectotype (specimen BGS-5303) from the Carboniferous Limestone Series (Visean and Tournasian, north Wales), scale bar represents 1 mm.

62602a (part) (fig. 2.3) and ROM-62602b (counter-part) (fig.2.4)). These Bear Gulch Limestone Member fossils are held in the collections at the Royal Ontario Museum, Canada. The third is *B. reidiae* (original specimens of Hinde 1882) (BGS-32160 (part) (fig. 2.5), BGS-5303 (counter-part) and BGS-32162 (fragment of part) together with specimens BGS-32161 and BGS-32162 (fragments of other specimens of *B. reidiae*) from North Wales (Carboniferous) which are held in the collections of the British Geological Survey.

Silicone rubber moulds of the fossils (ROM-62602a, ROM-62602b, ROM-49953a and BGS-5303) were made following the method of Purnell (2003). Cured rubber casts were coated in silver using a Polaron automatic sputter coater and photographed in a Hitachi S500 scanning electron microscope (SEM) (Department of Geology, University of Leicester). The images were scanned into Adobe Photoshop 5.0.2 and compiled to produce a photographic montage.

STYLE OF PRESERVATION AND MULTIELEMENT TAXONOMY

Polychaetes are preserved in a range of states from whole soft-bodied fossils to eventually just the scolecodonts (Briggs and Kear 1993). During decay the non-biomineralised soft tissue that binds the jaws decays rapidly and allows the elements to become dispersed (Eriksson 2000). Polychaetes have 4 main tissue types, from which a graded series, graded in terms of their resistance to decay, can be inferred (Briggs and Kear 1993). The order of decay is muscle (primarily protein), cuticle (collagen), setae (sclerotized chitin) and jaws (sclerotized collagen) (Briggs and Kear 1993). In decay experiments on the polychaete *Nereis* (Briggs and Kear 1993) it was found that in the absence of oxygen the preservation of more volatile tissues was greater than when oxygen was present. Therefore, death and burial in deoxygenated water was thought to favour fossilisation of soft tissue by providing more time for replication by early diagenetic minerals (Briggs and Kear 1993).

Specimen ROM-49953 (*Symmetroprion* n. sp) comprises the jaws plus the impression of the body of the eunicid polychaete (fig. 2.1); specimen ROM-62606 (*B. reidiae*) preserves a jaw apparatus but has no remains of the polychaete soft tissue (fig. 2.2-2.3). The presence of the body of the eunicid polychaete in ROM-49953 (*Symmetroprion* n. sp) implies rapid preservation whereas the lack of a body outline in ROM-62602 (*B. reidiae*) could imply more oxygenating conditions or a slower rate of burial than during the decay of *Symmetroprion* n. sp. Alternatively, it could reflect the two eunicid polychaetes having different original compositions implying that *Brochosogenys* was composed of recalcitrant tissues.

Specimen ROM-62602 (*B. reidiae*) has only one MII (fig. 2.2-2.3) whereas the lectotype of *B. reidiae* has a pair of MII elements. Paxton (1980) suggested that maxillae of most Eunicida, with the exception of Dorvilleidae, probably grow through life without replacement. Therefore, an MII element of specimen ROM-62602 (*B. reidiae*) lost prior to burial as a consequence of feeding would not have been replaced. However, in the area where the missing MII element of ROM-62602 (*B. reidiae*) should be located, there is a dark colouration, which may represent the remains of the MII element that did not form a mould.

Both jaw apparatuses from specimen ROM-49953 (*Symmetroprion* n. sp) and ROM-62602 (*B. reidiae*) are preserved as moulds. However, small amounts of organic material are present in both ROM-49953 (*Symmetroprion* n. sp) and ROM-62602 (*B. reidiae*). The location of the organic material is most obvious in the silicon rubber moulds where parts of the elements appear missing, for example some denticles in ROM-49953 (*Symmetroprion* n. sp) and part of the MII element in ROM-62602a (*B. reidiae*) (figs 2.1 and 2.3). Modern polychaete jaw apparatuses are composed of scleroprotein (Voss-Foucart *et al.* 1973) with highly variable compositions, including materials such as tanned protein, aromatic amino acids, glycine, hystidine, calcium carbonate and metals such as iron, zinc and copper. Schwab (1966) studied two fossil scolecodonts from the Upper Ordovician of Ohio and from the Independence Shale, Upper Devonian, Ohio. Spectrographic analysis from that study revealed that both specimens had large amounts of calcium, copper, silica and magnesium. Eriksson and Elfman (2000) noted that zinc, iron and copper were concentrated in the tips or delicate parts of jaws of fossil and extant polychaetes. They also suggested that the animal regulated the accumulation of those elements and that they had a functional significance. Lichtenegger *et al.* (2002) reported that the jaws of the extant marine bloodworm *Glycera dibranchiata* contained a protein mixture rich in glycine and histidine and the copper based biomineral atacamite [$Cu_2(OH)_3Cl$], enhancing hardness and resistance to abrasion and possibly mediating the activation of venom during injection. As there are organic remains in the jaw apparatuses of ROM-49953 (*Symmetroprion* n. sp) and ROM-62602 (*B. reidiae*) it is probable that these scolecodonts were originally composed of scleroprotein. Later burial would have caused these jaw apparatuses to be crushed and fractured. The presence of some of the original organic material of the jaws suggests that the moulds formed much later than lithification of the sediment and that the jaws were not lost through decomposition, but perhaps by later weathering or during collection.

SYSTEMATIC PALAEONTOLOGY

Order EUNICIDA Dales, 1963

Family SYMMETROPRIONIDAE Kielan-Jaworowska, 1966

Diagnosis.—See Kielan-Jaworowska (1966)

Type species.—*Symmetroprion spatiosus* (Hinde 1882, designated by Bergman 1995). *S. reduplicates* (Kielan-Jaworowska 1966) is a junior synonym of *S. spatiosus*

SYMMETROPRION NEW SPECIES (figures 2.1; 3.1—3.2).

Figure 3.1—3.2

Description.—Specimen ROM-49953 preserves a complete jaw apparatus of the genus *Symmetroprion* and the incomplete soft tissue remains of the eunicid polychaete that bore it (fig. 2.1). The body is elongate 33 mm in length, and, cut off abruptly at the posterior end, and 7 mm wide with regularly spaced 1 mm annulations. No eyes or setae are present and it lacks ventral palps fused to the prostomium and antennae. The jaws are of labidognath type, and contain both a basal and leobasal plates.

Carriers are sub rectangular, shorter than MIs. Lateral margins of carriers in anterior part have rounded and anterior lateral projections. Carriers appear flat and the posterior end is obscured. Basal and laeobasal plate present and appear symmetrical. Basal plate is crescent shaped. Anterior margin is directed postero-laterally and inner margin runs almost straight, curving very slightly posteriorly and curving anteriorly. Basal plate has a row of seven denticles present on the inner margin. First denticle is bigger than remainder and directed antero-laterally, remaining denticles decrease gradually in size posteriorly. Posterior denticles are very small, poorly developed as crenulations on the inner margin, which gradually becomes smooth and rounded, extending to the posterior end of the jaw. Denticulated inner edge is bent upwards in relation to jaw surface. There is no basal ridge. Laeobasal plate is in this articulated jaw slightly twisted but appears to be a mirror image of basal plate.

MI elements almost symmetrical with pulp cavities strongly enclosed. MIs crescent shaped with anterior denticles larger than posterior denticles. Right MI is a narrow long hooked jaw with its posterior end reaching undenticulated inner margin of basal plate. Inner margin is straight and directed posteriorly. Along the inner and anterior margins of right MI bears a row of approximately seven posteriorly directed denticles,

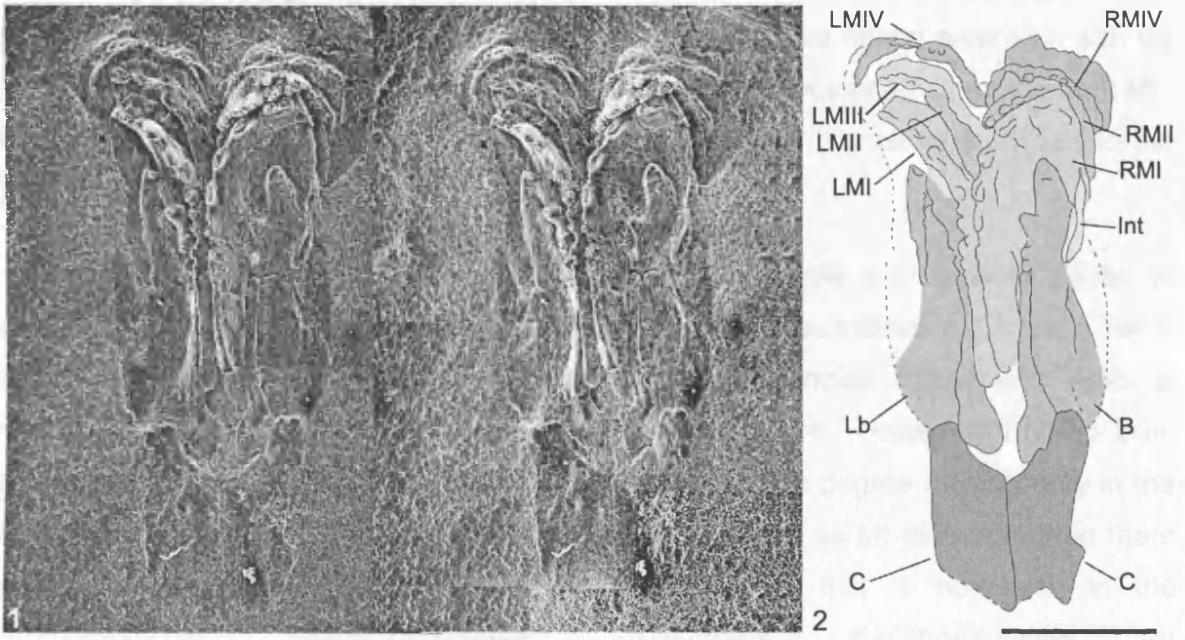

Figure 3-1-2 *Symmetroprion* n. sp. (ROM-49953a) from the Bear Gulch Limestone Member. 1, stereo pair of SEM images of *Symmetroprion* n. sp.; 2, camera lucida of the same specimen, carriers (C), leobasal plate (Lb), basal plate (B), left maxillae (LM), right maxillae (RM), intercalary tooth (int), scale bar represents 1 mm.

which decrease in size posteriorly. Left MI is almost a mirror image of right MI but has nine denticles that decrease in size posteriorly. This apparent difference in the number of denticles is probably an artefact of preservation.

Left MII is crescent shaped which profile that of the left MI. Anterior margin forms a lateral branch; the overlying MI obscures the longitudinal section of the MII element. Right MII resembles shape of right MI but is much smaller. Left MII and right MII have at least three denticles on each element. Left MIII is shorter laterally and posteriorly than the left MII, but denticles are unclear. Left MIV has a clearly visible lateral extension with six denticles poorly preserved. Right MIV is shorter laterally and posteriorly than the right MII, with approximately five denticles present. MVs are absent. Intercalary tooth lies to the right of the basal plate.

Discussion.—This jaw apparatus is of labidognath type and appears similar to members of Polychaetaspidae Kozlowski 1956, Paulinitidae Lange 1947, Ramphoprionidae Kielan-Jaworowska 1966 and Kielanoprionidae Szaniawski 1968, in terms of the length and shape of the MI elements and carriers. However, it differs from these groups in the presence of a laeobasal plate, and a high degree of symmetry in the jaw apparatus. Alternatively the basal plates are interpreted as MI elements then there appears to be a right MIII, which is very unlikely, as this is not seen in the Polychaetaspidae, Ramphoprionidae, Paulinitidae, Kielanoprionidae or Symmetrioprionidae. Two Eunicid families with laeobasal plates have been recorded in the fossil record, the Conjungaspidae (Hints 1999) (Ordovician) and Symmetroprionidae (Hinde 1882; Kielan-Jaworowska 1966 and Bergman 1995) (Silurian). Although Conjungaspidae has a basal and laeobasal plate the morphology of these elements together with the morphology of the carriers is very different from that of *Symmetroprion* n. sp. In Conjungaspidae the carriers are small distally rounded shafts with very long horns attached to the outer margins of the basal and laeobasal plates (Hints 1999).

The Silurian *S. spatiosus* more closely resembles *Symmetroprion* n. sp. but unfortunately only the carriers, basal plates and MIs have been found previously. *S. spatiosus* has a symmetrical jaw apparatus of labidognath type; both basal and laeobasal plates are present (Bergman 1995). These basal and laeobasal plates are subtriangular, with concave anterior margins, a description that fits *Symmetroprion* n. sp. The carriers of *S. spatiosus* are long, subtriangular and taper posteriorly. This differs from the rectangular carriers of *Symmetroprion* n. sp. The specimen of *Symmetroprion* n. sp. may also have a lateral right tooth, which is small and displaced lying over the right basal plate.

The main differences between *S. spatiosus* and *Symmetroprion* n. sp are the longer length of the basal plates and the rectangular shape of the carriers in *Symmetroprion* n. sp., These differences suggest that *Symmetroprion* n. sp is a different species from *S. spatiosus*. However, only one example of *Symmetroprion* n. sp is known, therefore more specimens are needed with the same distinguishing morphological features before *Symmetroprion* n. sp can be confidently described as a new species. This fossil eunicid polychaete represents the most complete jaw apparatus of Symmetroprionidae and the first specimen recorded from the Carboniferous, thus extending the range of this family from the Silurian (Hinde 1882 designated by Bergman 1995) to the Upper Mississippian. This specimen is also the first symmetroprionid found with the impression of its body.

In contrast to most modern Eunicida *Symmetroprion* n. sp lacks eyes and ventral palps fused to the prostomium and antennae. It is unlikely that these non-mineralized features were lost in this specimen through decay as the fine detail of the eunicid polychaete annulations along the body are preserved. The absence of these features may allow for a comparison with Recent Eunicida; indeed Lumbrineridae, a basal member of Eunicida, generally lacks eyes and all appendages (Rouse and Pleijel 2001). However, eyes are present in some taxa of Lumbrineridae (Rouse and Pleijel 2001), thus the lack of eyes may be the result of secondary loss. It is also possible that the presence of eyes is a more derived character of the family Eunicida. Indeed, other basal members of Eunicida are Hartmaniellidae, which has no eyes, and Oenonidae may which have eyes present (Rouse and Pleijel 2001).

Family KIELANOPRIONIDAE Szaniawski, 1968

Genus BROCHOSOGENYS Colbath,1987b

Type species.—Brochosogenys bipunctus Colbath 1987b

Included species.—*B. siciliensis and B. reidiae*

Diagnosis.—See Colbath 1987b

Description.—Asymmetrical apparatus, one side (commonly the left) has one more element than the other. Carriers are shorter than MIs and may be relatively broad, pointed or broadly rounded posteriorly. MI elements are falcate with the basal medial margin edentulate. Falcal arch may be edentulate or have one to several medially directed denticles. Posterior margin lies in narrow contact with carriers, and flares broadly to a lateral spur; a small clavus may be present on basal medial margin. Denticles on MII elements directed medially and aligned in a relatively straight row. MIII is relatively small

and arched with dorsally directed denticles on one side only. MIVs relatively large with dorsally directed denticles and MV elements absent.

BROCHOSOGENYS REIDIAE Hinde, 1896

Figures 2.2—2.3; 4.1— 4.4; 5.1—5.2

Synonymy.—*Eunicites reidiae* Hinde 1896. *Brochosogenys reidiae* (Hinde 1896) COLBATH 1987b, pp.448-450, pl.22, figs. 2-5.

Diagnosis.—A species of *Brochosogenys* with no prominent denticles on the falcal arch of the MI elements.

General Morphology. — The jaws consist of two sub rectangular carriers, which lie to the posterior of the two falcate MIs. The MIs both display small denticles and a small lateral spur, MII elements lie centrally, between the MIs and have well defined denticles. The single MIII element is small and denticulated and lies to the anterior of the MII elements. The two MIV elements are also small and well denticulated and are positioned to the anterior of the MIII element.

Type specimen.—In describing this species Hinde (1896) did not designate a holotype and illustrated and discussed more than one specimen under the heading *E. reidiae*. However, his description is clearly based on specimen BGS-5303 (part) BGS-32160 (counter-part) and BGS-32162 (fragment of part). Under the heading *E. reidiae*, Hinde also discussed specimens BGS-32161 and BGS-32162 (fragments of other specimens of *B. reidiae*). BGS-5303 (part) and BGS-32160 (counter-part) is hereby designated as the lectotype.

Description.—Carriers are shorter than MIs and sub rectangular. Carriers are in narrow contact with posterior margin of MIs and shorter than the MIs. MI elements are falcate, and the posterior margin flares broadly to a small lateral spur. A deep clavus on the ventral surface of the MI element is present. Posterior margins of the MIs have a small lateral spur. Primary denticles are present on the left basal medial margin of the left MI element. Fractures around the myoceol openings on both MI elements are the result of post-mortem crushing. Right MI has denticles that reduce in size towards the posterior margin. Right MII has denticles aligned on the right of the element in a straight row and directed posteriorly. Left MII is almost a mirror image of right MII, with denticles aligned on left of the element in a straight row directed posteriorly. MIII is arched with dorsally directed denticles in a straight row and present on one side only. MIVs are quadrate in outline with denticles present on one side only; anterior-most denticle is largest.

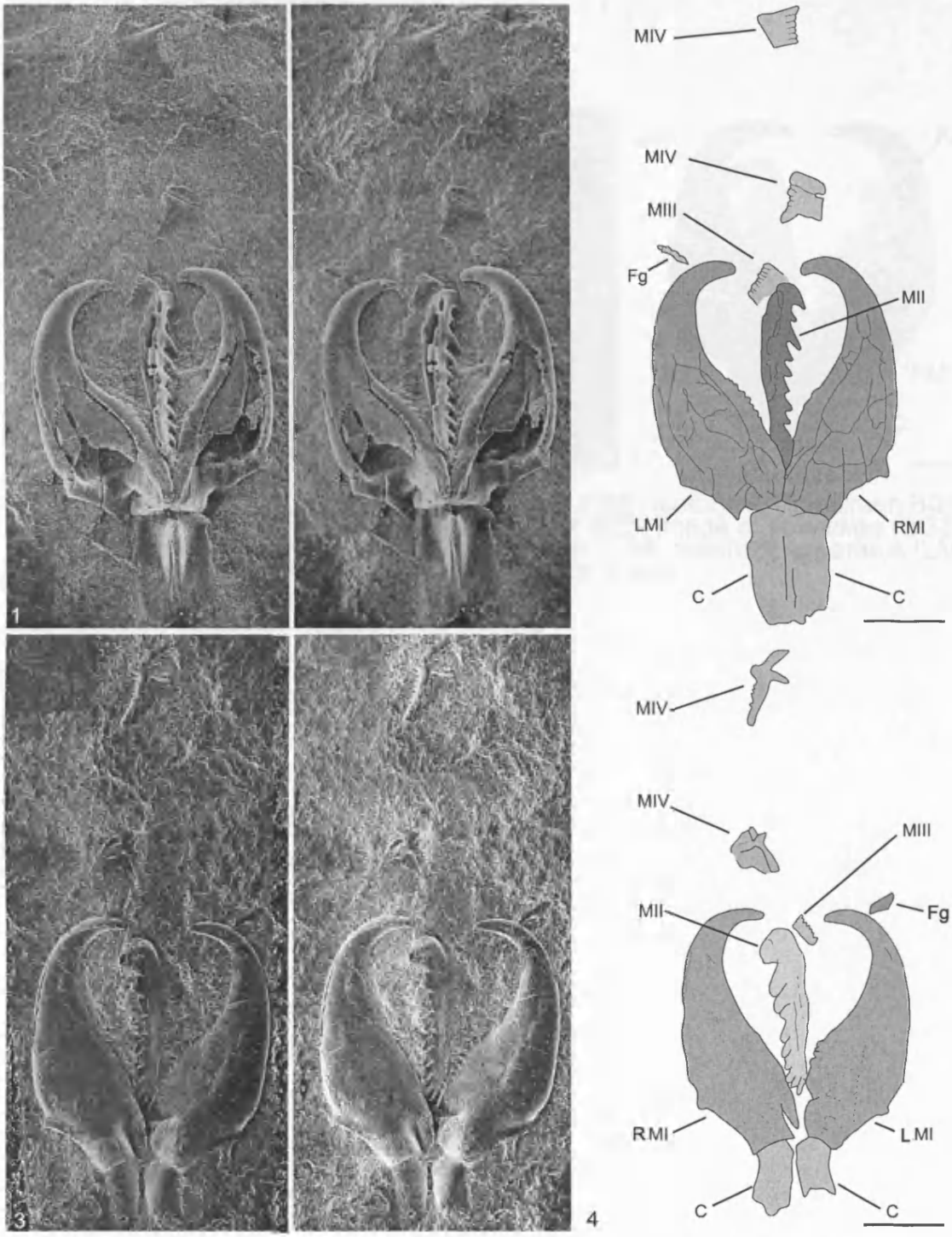

Figure 4-1-4 Brochosogenys reidiae (ROM-62602a, part and ROM-62602b, counter-part) from the Bear Gulch Limestone Member (Upper Mississippian, USA). 1, stereo pair of SEM images of (ROM-62602a) B. reidiae; 2, camera lucida of the same specimen, carriers (C), left maxillary apparatus (LM), right maxillary apperatus (RM), fragment (Fg), scale bar represents 2 mm. 3, stereo pair of SEM images of (ROM-62602b) B. reidiae; 4, camera lucida of the same specimen, carriers (C), right maxillary apparatus (RM), left maxillary apperatus (LM), fragment (Fg), scale bar represents 2 mm.

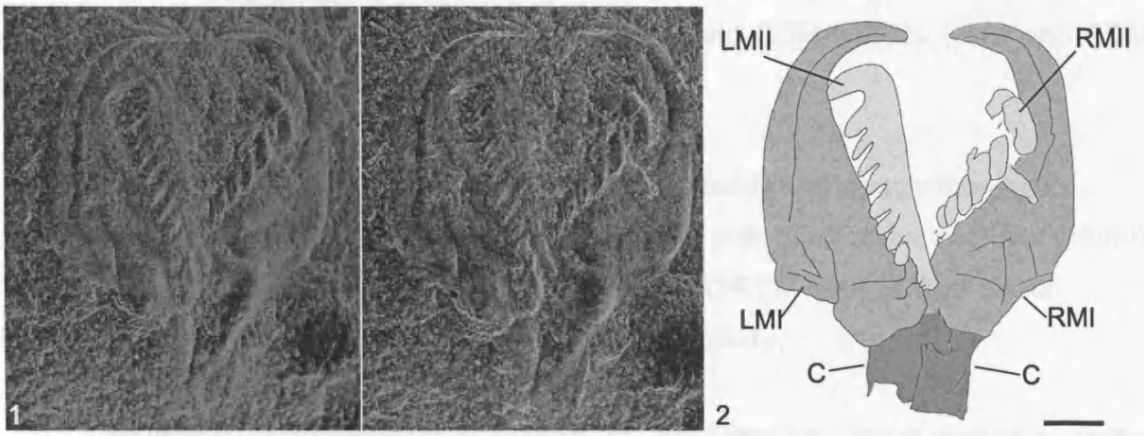

Figure-5-1-2. *Brochosogenys reidiae* (Hinde 1896) lectotype, (specimen BGS-5303 part) (Carboniferous, Wales), 1, Stereo pair of SEM image of *B. reidiae* (BGS-5303); 2, camera lucida of same specimen, carriers (C), left maxillary apparatus (LM), right maxillary apperatus (RM), scale bar represents 1 mm.

Posterior most MIV element has denticles that lie to left. Anterior most MIV element has straight denticles present that lie to right. MV elements absent.

Material.—Type material of Hinde (1896) BGS-32160 (part), BGS-5303 (counter-part) and BGS-32162 (fragment of part) (fig.5.1-5.2) and ROM-62602a (part) and ROM-62602b (counter-part).

Occurrence.— BGS-32160, BGS-5303 and BGS-32162 probably the Leete Limestone Formation (Carboniferous Limestone Series previously given by Hinde (1896)), Filntshire, North Wales (Hinde 1896). ROM-62602a and ROM-62602b Bear Gulch Limestone Member (Upper Chesterian, Upper Mississippian).

Discussion.—ROM-62602 is placed in the species *Brochosogenys reidiae* because the MI elements do not have the prominent second denticle that characterises *B. bipunctus* Colbath 1987b nor the small secondary denticles along the falcal arch that are characteristic of *B. siciliensis* Corradini and Olivieri 1974. In both the lectotype and ROM-62602 carriers and MIs are articulated. The lectotype carriers are 1.1 mm long and 0.7 mm wide, shorter than those of ROM-62602 (2 mm long and 1.1 mm wide); however, all of the carriers appear to have been broken to a different extent. MI elements of the lectotype are 4 mm long and 1.5 mm wide at the base. MI elements of ROM-62602 are also 4 mm long but are wider at the base (1.9 mm) than the lectotype.

There is only one MII present in ROM-62602 and *B. bipunctus.* However, both MII elements are present in the lectotype. It is likely this lack of an MII element is either an artefact of preservation or else it was lost prior to the death of the organisms. The MII element present in ROM-62602 has 11 denticles and is 3mm long whereas those of the lectotype are 3 mm long and there are 10 denticles on each. Hinde noted the presence of a paragnath in the specimen and although I have been unable to recognise this element in his material, his illustration (Hinde 1896, figure 2e) shows an element of very similar shape and relative size to the MIII of specimen ROM-62602. The MIII in ROM-62602 has eight dorsally directed denticles and is 0.6 mm long and 0.4 mm wide. MIVs are not present in the lectotype, however, and MIVs are present in ROM-62602 but are displaced. The MIV lying posteriorly has nine denticles and is 0.9 mm long and 0.9 mm wide, whereas the MIV lying to the anterior has seven denticles and is 1 mm long and 0.5 mm wide. MVs are not present in the lectotype, or in ROM-62602.

The main difference between the lectotype (fig.5.1-5.2) and ROM-62602 (fig.4.1-4.4) is that the lectotype has both MII elements present each with 10 denticles, whereas the single MII element of ROM-62602 has 11 denticles. The carriers in ROM-62602 are

slightly longer than those of the lectotype and the (clavus) posterior margin is less concave in appearance. Differences are minor and may be the result of ontogenetic or intraspecific variation. Indeed, the number of dental plates and element shape in Recent polychaete species has been shown to vary e.g. *Aglaurides fulgida* (Fauvel 1919, 1953; Hartman 1954) and *Arabella iricolor* (Kielan-Jaworowska 1966). Therefore, with so few specimens, ontogenetic variation cannot be excluded.

The relationship of *Brochosogenys* to Recent polychaetes is difficult to determine. Organic remains of the scolecodont jaws are present in both specimens of *B. reidiae* known (ROM-62602 and BGS-5303); therefore, it is clear that these jaws did not originally contain internal aragonite (c.f. Colbath 1986a). If the apomorphy for the clade comprising the Eunicidae and Onuphidae is jaws composed of aragonite (see Fauchald 1992) then *B. reidiae* is more basal than this clade. Therefore *B. reidiae* would be more closely related to the most basal members of the extant Eunicida, which are Lumbrineridae, Oenonidae and Hartmaniellidae.

Brochosogenys is included in the family Kielanoprionidae (Devonian to Triassic (Szaniawski 1996)) and is regarded by Szaniawski (1996) to be related to Hartmaniellidae Imajima 1977. Szaniawski and Imajima (1996) suggested that Hartmaniellidae originated in the Triassic and was also closely related to the to the extinct Paulinitidae. However, Orensanz (1990) suggested that Hartmaniellidae has a sister group relationship to *Synclinophora* and *Delosites*-like scolecodonts and that Hartmaniellidae originated in the Silurian. If Hartmaniellidae originated in the Silurian and Kielanoprionidae is more basal than Hartmaniellidae the family Kielanoprionidae may have originated in or before the Silurian.

CHAPTER 3

THE TAPHONOMY OF THE BEAR GULCH LIMESTONE MEMBER

ABSTRACT. The Bear Gulch Limestone Member (Upper Mississippian) of central Montana, USA, contains exceptionally preserved vertebrate and invertebrate fossils. Skeletons are often fully articulated and nonmineralized tissues are common. Analytical investigation using electron dispersive x-ray analysis, element mapping, electron microprobe analysis and Raman spectroscopy revealed a complex taphonomic history. Carbonate biominerals frequently underwent early dissolution whereas apatite was converted during diagenesis to carbonate fluorapatite. Non-mineralized tissues display four broad styles of preservation, being either rapidly replaced by apatite and more rarely calcite, or evident as imprints in the sediment, or present as carbonized refractory or carbonized volatile tissues. The survival of organic carbon indicates that processes must have occurred to inhibit carbon recycling.

Geochemical and mineralogical analysis demonstrates that bottom water conditions were episodically inimical to benthos, and at times excluded macroscavengers from destroying carcasses on the sea floor. Rapid burial rates and a reducing sediment protected the carcass from scavengers and bioturbators. In some instances, rapid authigenic mineralization of soft-tissues prevented their destruction through bacterial decay. The sediment is extremely clay poor, so that previous models to account for organic preservation, such as clay-bacteria interactions, cannot be invoked for the Bear Gulch Limestone Member fossils. Sediment from the Bear Gulch Limestone Member is dominated by calcite and quartz.

THE Bear Gulch Limestone Member of central Montana (Text-fig. 1A) constitutes a fossil conservation Lagerstätte, because it contains the articulated remains and non-mineralized tissues of many vertebrate and invertebrate taxa. Fossil Lagerstätten are important because they provide more comprehensive information on the diversity and palaeoecology of ancient communities than the normal fossil record. However, it is vital to assess, and as far as possible understand, the taphonomic history of fossils within conservation Lagerstätten to gauge preservational bias, and to determine how much of the original, living community is represented in the fossil assemblage. In addition, understanding the processes of preservation of the organisms from such deposits can aid

A

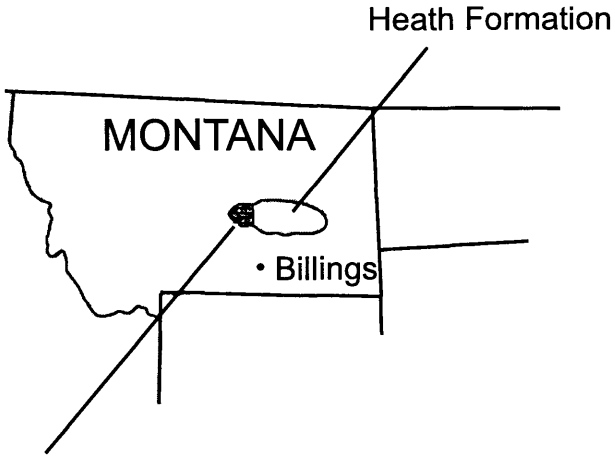

Bear Gulch Limestone Member, visible outcrop area is 85km^2.

B

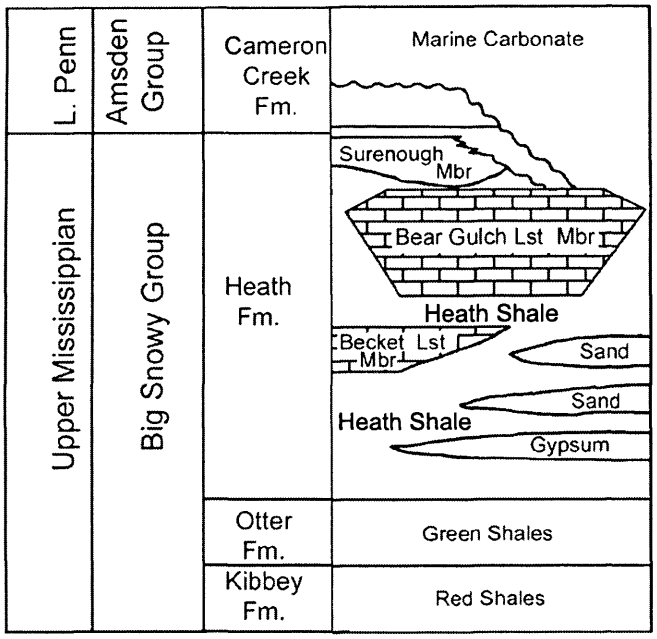

TEXT-FIG. 1. Location and stratigraphical position of the Bear Gulch Limestone Member. A, map of Montana, USA, with the location of the outcrop area indicated. B, stratigraphical position of the Bear Gulch Limestone Member (Thomas chapter 1, after Williams 1983).

in the interpretation of the morphology of soft-bodied fossils and determine the conditions under which the fossils were preserved.

The processes that led to the exceptional preservation of fossils in the Bear Gulch Limestone Member have not previously been described in detail. This investigation documents the mode of preservation of both biomineralized (hard parts) and non-biomineralized (soft parts) of organisms. The geochemistry of the Bear Gulch Limestone Member sediments is also analysed in detail for the first time providing an indication of the geochemical environment in which the organisms lived, died and were fossilized.

PREVIOUS WORK ON THE BEAR GULCH LIMESTONE MEMBER

Locality and Stratigraphy

The Bear Gulch Limestone Member is situated north of Billings in central Montana, USA (Text-fig.1A). The Member has a visible outcrop area of 85km^2 and a maximum thickness of 30m (Grogan and Lund 2002).

The Bear Gulch Limestone Member is a limestone lens within the Heath Formation of Montana (Text-fig. 1A) and North Dakota, which was first described by Mundt (1956). This limestone lens has also previously been termed the Bear Gulch Member (Williams 1983), the Bear Gulch Beds (Williams 1983; Horner and Lund 1985) and the Bear Gulch Limestone (Lund *et al.* 1993). These different names led to a confusing situation so that recently Thomas (Chapter 1) suggested that the term Bear Gulch Limestone Member be used to conform to current stratigrapical nomenclature (Text-fig. 1B). In addition the Surenough and Becket Beds renamed to the Surenough and the Becket Limestone Members (Thomas, Chapter 1) (Text-fig. 1B).

The Bear Gulch Limestone Member grades laterally and downwards into the black shales of the Heath Formation (Feldman *et al.* 1994). The Bear Gulch Limestone Member is Upper Mississippian (Upper Chesterian) in age (Text-fig. 1B), based upon palynostratigraphy (Cox 1986), ammonoids (Mapes 1987), conodonts (Scott 1973; Norby 1976) and fishes (Feldman *et al.* 1994).

Sedimentology

The Bear Gulch Limestone Member was deposited as part of an Upper Mississippian transgressive sequence in a series of open-ended, en-echelon basins that formed within the Big Snowy Trough (Williams 1981, 1983). This trough was a narrow east-west trending embayment that connected the Big Snowy Basin to the east with the Cordilleran Miogeosyncline to the west (Mallory 1972; Williams 1981; Horner and Lund 1985; Witzke

1990). During deposition the latitude of the bay was approximately 12 degrees north of the palaeoequator (Grogan and Lund 1997). The climate of the region was probably tropical to arid and this is corroborated by the presence of evaporite deposits in the adjacent Heath shale (Horner and Lund 1985), as well as abundant stromatolites towards the top of the section, exposed in eastern and northern margins of the Bear Gulch Limestone Member (Lund *et al.* 1993).

The Bear Gulch Limestone Member has three recognised facies; the margin, slope and basin facies, and fossils are known to occur in each of these (Williams 1983). Facies differentiation was based largely on changes in sedimentology, sedimentary structures and faunal distribution (Williams 1983). Detailed facies analyses have been hindered by poor outcrop exposure, which is limited to deeply incised canyons with minor lithological variation. However, Grogan and Lund (2002) have further redefined the marginal and basin facies, and added the 'arborispongia facies', 'filamentous algae facies' and a 'shallow facies', based upon their field evidence of the distribution of fossils, especially algae and sponges. The preserved fauna is most abundant and diverse in the basin facies (Williams 1983), and for this reason sediment samples and all fossils considered in this study are from the basin facies.

The basin facies. In outcrop basin facies beds may be traced over several meters and vary in thickness from several millimetres to several centimetres (Feldman *et al.* 1994). There is no macro-bioturbation and peloids and microscopic cyanobacteria seen in other facies are absent (Williams 1983). The basin facies sediments show a rhythmically alternating sequence of thick, hard, non-fissile beds and sets of thinner fissile beds (Williams 1983; Grogan and Lund 2002; and personal observation). Williams (1983) reported that the sediment of Bear Gulch Limestone Member basin facies had 79 wt% $CaCO_3$ and 8 wt% SiO_2.

Proposed models for deposition. The rhythmic alternating style of the thicker, nonfissile units with the thinner, argillaceous, fissile beds has been compared by Williams (1983) to the Flinz and Fäule style of bedding famous in the Mid-Jurassic Solnhofen lithographic limestone (Germany) (Hemleben and Swinburne 1991). The massive (Flinz) style bedding in the Bear Gulch Limestone Member has been described as dolomitic, micritic limestone (Williams 1983) characterised by normally graded laminations with sharp bottoms (Lund *et al.* 1993). The platy (Fäule) style beds are more clay rich and not obviously graded (Feldman *et al.* 1994). Williams (1983) based her model for the deposition for the Bear Gulch Limestone Member on Hemleben's (1977) model for the formation of the Solnhofen Flinz and Fäulen. Williams (1983) suggested that the massive

beds (Flinz) (>30mm) may reflect periods of deposition from frequently flowing, sediment-laden, turbidity currents. These currents were inferred based on the presence of slumps that are common in the slope facies, and also occur in the basin facies (Williams 1983). Grogan and Lund (2002) expanded Williams (1983) idea and suggested that the turbidity currents responsible for Flinz deposition were generated during summer monsoonal storms, and that they carried sheetwash-eroded and/or resuspended sediments into the bay from the surrounding land. Thus, the quartz in the Bear Gulch Limestone Member beds was thought to be land-derived clastic material. The sediment-laden flow would have travelled along a pycnocline until its momentum matched that of the surrounding water and then deposition would have occurred (Grogan and Lund 2002). The thinner platy beds (Fäule) (<30mm) were thought to have represented deposition during quieter periods (Williams 1983).

Williams (1983) suggested that the carbonate portion of the sediment in the Bear Gulch Limestone Member was formed from either a chemical precipitation from seawater, or from biochemical precipitation by noncalcareous algae and micro-organisms (e.g. cyanobacteria), which inhabited the basin margin.

Fauna

The bay in which the Bear Gulch Limestone Member was deposited has been interpreted as having been a highly productive, shallow marine water body with a diverse assemblage of fishes and a moderate to diverse invertebrate fauna (Lund *et al.* 1993; Feldman *et al.* 1994). The most common fossils are cephalopods and, in order of decreasing abundance shrimp, fish and non-mineralized organisms (Horner and Lund 1985). A low proportion of beds contain benthic fossils such as brachiopods, sponges, bivalves and conulariids (Lund *et al.* 1993). Bryozoan and crinoids are rare, whilst blastoids, corals, foraminifera and ostracods are absent (Feldman *et al.* 1994; Lund *et al.* 1993).

Physical Taphonomy

Fossils are typically flattened and are usually found parallel to bedding (Feldman 1994). However, *Arborispongia*, the branching sponge, is often found extending through several layers, and large fish (1000mm to 2700mm), and large cephalopods (70 to 400mm in diameter) project through the laminations (Feldman *et al.* 1994). Fossils are found in a range of preservational states from complete and articulated with preserved non-mineralized tissues through to disarticulated, isolated hard parts.

Spiny productid brachiopods have been reported fully articulated with ornamentation intact (Lutz-Garihan 1985), and this suggested to Lund *et al.* (1993) that organisms experienced little transport and abrasion post-mortem. Several 'in life' associations corroborate the concept of minimal transportation of organisms; examples of buried arborescent sponge communities with attached bivalves and associated shrimp and worms (Rigby 1985), and kelp-like algal fronds covered by dense associations of epibiont bivalves and brachiopods have been reported (McRoberts and Stanley 1989).

The physical taphonomy of fossils may help with the interpretation of the environmental conditions at the time of death of the organisms. In the Bear Gulch Limestone Member several fossils indicate what may have killed them, or the conditions that occurred directly after death. Time from death to burial probably varied greatly in the Bear Gulch Limestone Member. At times it must have been very rapid as indicated by the presence of preserved fully articulated fish, and buried arborescent sponge communities (Lund *et al.* 1993). Results of experiments on freshly killed mantis shrimp (Hof and Briggs 1997) may be useful to determine the time that elapsed between death and burial. Hof and Briggs (1997) recorded that in experiments on freshly killed stomatopods (Malacostraca) the raptorial thoracopods were originally folded underneath the carapace but they unfolded within three days as a result of decay. It was suggested by Hof and Briggs (1997) that fossil specimens that showed folded thoracopods were presumably buried alive, or at least undisturbed unless the specimen was orientated with the dorsal surface parallel to bedding, so that the limbs could not unfold. In the Bear Gulch Limestone Member malacostracan limbs are often poorly preserved and the flattened carapaces indicate a degree of decomposition prior to mineralization of the carapace. Specimens of the archaeostomatopod *Tyrannophontes theridion* (Schram and Horner 1978) are found lying on their sides, and frequently the second thoracopod is folded beneath the carapace, and, thus I conclude that these archaeostomatopods were likely to have been buried rapidly, i.e. within about three days post-mortem. Disarticulated fish and shrimp carcasses probably reflect periods when sedimentation was slow or not occurring, because there is no indication of currents that might have disturbed them in the Bear Gulch Limestone Member (Lund *et al.* 1993).

Asteroid arms are attached to the body disc of the organisms and are outstretched but not curled or twisted, which suggests burial and smothering of the asteroids occurred whilst in life position (Welch 1984). Welch (1984) suggested that the starfish died by gradual poisoning either by a decrease in oxygen, or a change in salinity or pH, because they had made no attempt to dig their way out. Williams (1983) considered that high sedimentation rates and low oxygen content in the sediment, and at the sediment-water

interface, were the most important factors in fossil preservation in the Bear Gulch Limestone Member.

Many fish specimens from the Bear Gulch Limestone Member exhibit only minor disarticulation resulting from gut rupture or minor scavenging (Lund *et al.* 1993). Remarkable, high fidelity, preservation has been reported where fish skin outlines, eye pigments, livers, spleen and gills are present, and frequently intestinal contents are undisturbed and undistorted (Horner and Lund 1985). However, muscles are rarely phosphatised (Lund *et al.* 1993). Grogan and Lund (1995, 1997, 2002) suggested that the fine preservation of venous systems and fish gill structures suggested death by asphyxiation and rapid burial. They noted that the Bear Gulch Limestone Member paraselachian fish often showed distended gills and raised operculums, necrolytic features that in recent fish are indicative of death by asphyxiation. Grogan and Lund (2002) further suggested that the presence of blood pigments, which requires the oxidation of haemoglobin or other oxygen sensitive molecules, would imply that the bottom waters were not consistently anoxic. Preferential preservation of the superficial vascular structures, and distended gill covers, was believed by Grogan and Lund (1997) to be a physiological response to asphyxia-induced stresses. Comparison between Bear Gulch Limestone Member fish and modern fish led Grogan and Lund (1997) to conclude that post-mortem diffusion of blood pigments was greatly limited in the fish of the Bear Gulch Limestone Member, a condition that would be expected only if minimal time existed between death and burial. Certain actinopterygian taxa, and the chondrichthyans *Falcatus falcatus* Lund 1985a and *Damocles serratus* Lund 1986a, are frequently found curled up, and Grogan and Lund (2002) proposed that this might indicate asphyxiation as the cause of death. Conversely, curled up fish in the Solnhofen Limestone were believed to have resulted owing to desiccation in hypersaline bottom waters (Mayr 1967).

Lund *et al.* (1993) inferred that turbidity currents would have induced a temporary asphyxiating environment causing rapid death and simultaneous burial, but they ruled out persistent anoxia on the evidence of a ubiquitous bottom-dwelling component of the fish fauna, and possibly some burrowing fish that occurred throughout the basin.

Grogan and Lund (2002) reported that seasonal climate variation was the main cause of exceptional fossil preservation. Grogan and Lund (2002) invoked the idea of a well-populated bay during the dry season, which during a monsoon season would be subject to mixing of resuspended sediments and organic matter from the marginal facies. This resuspended material would become anoxic and subsequently cascade from the upper water column to the lower water column (Grogan and Lund 2002). Under these circumstances higher water temperatures and oxygen depletion could have generated lethal asphyxiating conditions for organisms, and the descending sediment could have

immediately buried and trapped organisms (Grogan and Lund 2002). The absence of mass kill horizons led Grogan and Lund (2002) to suggest that a rise in water temperature was not a factor contributing to death.

In summary cause of death has been attributed to asphyxiation (Lund *et al.* 1993; Grogan and Lund 1995, 1997, 2002), and/or smothering and rapid burial by turbidity currents (Williams 1983; Lund *et al.* 1993; Grogan and Lund 2002), with associated anoxic waters (Grogan and Lund 2002). Published models account for exceptional preservation by death and burial of taxa in massive beds deposited by monsoonally triggered turbidity currents (Grogan and Lund, 2002). Whilst rapid burial may explain articulated fossils it does not account for the preservation of soft tissues. Furthermore, it does not explain why exceptionally preserved fossils are also found at the junction between laminated and massive beds throughout the member. Therefore, interpreting death and exceptional fossil preservation solely as a consequence of seasonal monsoons causing turbidity currents to rapidly bury carcasses does not seem appropriate. Further exploration of the causes of death and subsequent exceptional preservation are required to help understand the relationship between depositional environment and preservation. To date an investigation of taphonomic pathways of biominerals (hard parts) and non-biomineralised (soft parts) has not been reported, nor has the sediment geochemistry been analysed. This study aims to readdress this and to use data obtained as a guide to preservational bias within the Bear Gulch Limestone Member.

MATERIAL AND METHODS

Fossils investigated are from the University of Missoula (UM), the Carnegie Museum, Pittsburgh (CM) and the Royal Ontario Museum, Toronto (ROM). Other fossils and sediment were collected during fieldwork (F) in the Bear Gulch Limestone Member during 2001 (Table 1).

Sediment analysis

Observational analyses. A sedimentary log (300mm vertical section) was prepared (see appendix 1) from part of the basin facies of the Bear Gulch Limestone Member. Each bed represented on the log was excavated to reveal a $4m^2$ bedding plane, any fossil specimens found between were recorded on the log and sediment samples were taken from each bed. Thin sections were prepared from sediment samples for analysis by petrographic and scanning electron microscopy (Hitachi S-500 with Link AN10, 000

Fossil	Reference number	Original composition	Fossil Composition	Mode of Preservation	Type of Analysis
cephalopod	ROM-91-70815	Calcium carbonate	Calcium carbonate/imprint	Imprints/replacement	EDX
starfish	78-72412/22988	Calcite and organics	Carbon/imprint	Imprints/original	Element Mapping and Raman
fish	F-89-62401A	Calcium phosphate and organics	CARFAP	Remineralization	Quantative EDX and EM
lingulid brachiopod	ROM-00-123	Chitinophosphatic	CARFAP	Remineralization	Quantative EDX and EM
shrimp	UM-5996	Chitinous	CARFAP	Replacement	Quantative EDX and EM
	ROM-45841	Chitinous	CARFAP	Replacement	Quantative EDX and EM
Bristle worm	ROM-88-71712NC	chitin, organics	Calcium phosphate	Replacement	EDX and EM
Black worm	UM-87070704A	Collagen, chitin, organics	Calcium carbonate	Replacement	EDX
	UM-7106	Collagen, chitin, organics	Calcium carbonate	Replacement	EDX
Red worm/ gut tract	UM-87-8-10-B1/B2	Collagen, organics	Calcium Phosphate	Replacement	EDX
	UM-87-70907A	Collagen, organics	Calcium Phosphate	Replacement	EDX
	UM-87-810/45859	Collagen, organics	Calcium Phosphate	Replacement	EDX
Polychaete with scolecodonts	UM-84-71603NC	Scleroprotein	Carbon	Preservation	Raman
	ROM-49953	Collagen, organics	Imprint	Preservation	EDX
Fish with soft tissue	ROM 91-70803A	Collagen /organics/melanin	Carbon	Preservation?	EDX and EM
	ROM-29784	Collagen/organics/melanin	Carbon	Preservation?	EDX and EM
Conulariid	ROM-99-71805A	Unknown	CARFAP	Replacement	Quantative EDX and EM
	ROM-87-730NC	Unknown	CARFAP	Replacement	Quantative EDX and EM
Sphenothallus	ROM-88-72819	Unknown	CARFAP	Replacement	Quantative EDX and EM
	ROM-96-71715	Unknown	CARFAP	Replacement	Quantative EDX and EM
Square objects	CM-88-80310	Unknown	Carbon	Preservation?	Raman
Typhloesus	UM-7106 UM-6029	Unknown	Carbon and apatite	Replacement?	Element Mapping and Raman

TABLE 1. Fossils from the Bear Gulch Limestone Member with their original compositions, fossil compositions and mode of preservation indicated. Most effective mode of analyse found in this study is denoted. Abbreviations: Royal Ontario Museum (ROM) University of Montana (UM), Carnegie Museum (CM), field (F) Carbonate fluorapatite (CARFAP), electron dispersive x-ray (EDX) and electron microprobe (EM).

energy dispersive x-ray analysis capability and chemical analyses, Department of Geology, University of Leicester).

X-ray diffraction. X-ray diffraction (XRD) was carried out on both whole rock and <2μm fractions using a Phillips PW1730 x-ray generator with a PW1716 diffractometer and a PW1050/25 detector (Department of Geology, University of Leicester). A copper element was used to detect K α radiation and the current operating conditions were 40 kV, 30mA. The <2μm fractions were obtained by centrifuging the whole rock sample. The samples were air-dried, glycolated and heat-treated (330 and 550 °C).

X-ray fluorescence spectroscopy. Concentrations of major and trace elements were analysed using a Phillips PW 1400 wavelength dispersive X-ray fluorescence mass spectrometer, with a 3kw-anode x-ray tube (Department of Geology, University of Leicester). The method employed for major element analysis was described by Pickering *et al.* (1993). Trace element analysis was performed on powdered pellets using the method described by Tarney and Marsh (1991).

Fossil analysis

Observation of fossil material (Table 1) was undertaken to study the mode of preservation, degree of compaction, the presence or absence of soft or hard part structural tissue, and the fidelity of that tissue. The same SEM was used for fossil analysis as for sedimentary thin section work, but in addition a variable pressure SEM (Phillips XL30SEM 520: Department of Engineering, University of Leicester) and an optical binocular microscope were employed.

Scanning electron microscopy (SEM) and energy dispersive x-ray (EDX) analysis. Fossil bearing hand specimens were secured to a SEM stub with (UHU) glue and investigated uncoated using a Hitachi S-500 SEM. Uncoated specimens were prone to a high degree of charging because the point of impact of the electron beam was not earthed effectively by the natural conductivity of the specimen. To reduce the effects of charging the specimen was wrapped in aluminium foil (see Allison 1988) so that only the fossil or part of the fossil to be analysed was visible. In order to improve conductivity the aluminium foil was in contact with the stage so that the electrical charge was earthed. In backscattered electron images elements with higher mean atomic numbers appear brighter than those of a lower mean atomic number (see Orr *et al.* 2002). The backscatter electron image is

sensitive to surface topography, because the angle of the surface affects the fraction of the electrons backscattered; also the detector 'views' the specimen only from one direction and this causes shadowing effects (Reed 1993). Atomic number contrast proved useful in locating many of the fossils on the rock slabs in the SEM. In some cases fossil material was carefully dissected from the specimen, ensuring that no sediment was included, glued on to a SEM stub and coated in silver, which acted as a conductor, using a Polaron sputter coater. Specimens too large for the Hitachi S-500 SEM were analysed uncoated in the variable pressure Phillips XL30 SEM.

When element mapping is undertaken the depth to which the electron beam penetrates depends on the composition of the material being analysed and the accelerating voltage that has been applied to the electron beam (Orr *et al.* 2002). This has been used to good effect by Orr *et al.* (2002) where an ostracod specimen, from the Castlecomer Fauna (Upper Carboniferous, South eastern Ireland) was analysed. The higher the accelerating voltage applied, the further the electron beam penetrated allowing appendages concealed by the overlying ostracod carapace to be revealed (Orr *et al.* 2002). However, because the higher voltage beams penetrate further into the substrate this may cause problems when attempting to analyse very thin fossil material. So very thin fossil films from the Bear Gulch Limestone Member were analysed with a low accelerating voltage applied to the beam to try to confine analyses to near the surface. Unfortunately, this has the effect of widening the electron beam and results in an analysis of a wider area, but this is preferable to analysing through the fossil film to the sediment below.

Analysis using the electron microprobe. Specimens for electron microprobe analysis (Electron microprobe JEOL 8600 S, Department of Geology, University of Leicester) were prepared by carefully embedding small pieces of fossil into transparent polyester resin (Struers Ltd) sectioning and polishing the cut surface. Owing to an extremely low viscosity this resin can effectively impregnate pore spaces, consoidating the sample so that a well-polished surface may be achieved. Polished sections were carbon coated.

Raman spectroscopy. Fossil specimens that were preserved as thin films could not be accurately analysed by EDX, element mapping or in the electron microprobe; these were analysed using Raman spectroscopy. This constitutes a new technique for the analysis of fossil composition and has the advantage of being non-destructive. Raman spectroscopy detects elements by analysing the different vibrating frequencies of scattered light rays reflected from the specimen. The use of Raman spectroscopy on sediments and poorly mineralised surfaces often causes a high fluorescence so that the signals emitted are not

detectable. However, in some instances a clear Raman peak can be seen but careful observation is needed to determine whether the fluorescence masks any other elements present. Fossils were analysed using a Renishaw inVia Reflex Raman microscope with 514nm excitation. Analysis times were between 10 seconds and 60 seconds.

RESULTS

Sediment

Physical characteristics. Basin facies sediments did not show evidence of macro-bioturbation. The beds did not show any erosional features, tool marks, channels, or current-orientated skeletal debris.

The basin facies (Text-fig. 2A-B) contained both well-laminated beds (greater than 30mm in thickness) that were frequently graded, and poorly laminated beds (less than 30mm in thickness). In thin section three distinct types of lamina (Text-fig. 2A) are easily differentiated in the well-laminated sediments; lamina A is an extremely thin, brown layer, composed of sub–rounded quartz grains (3-40μm) and clay; lamina B is light brown and composed mainly of calcite with sub-rounded quartz grains of approximately 10-40μm in size; and, lamina C is very pale and consists of calcite crystals 10-50μm in size set in a mudstone matrix. Dolomite rhombs (5μm–60μm across) are present throughout the sediment and in all laminae; that they always demonstrate euhedral morphology and overgrow fossils suggests they probably grew diagenetically. This diagenetic growth of dolomite rhombi may be the cause of some minor disruption of laminae. XRD revealed both Ca-rich, ($CaMg(CO_3)_2$) and Fe rich ($CaFe(CO_3)_2$) dolomite present in the Bear Gulch basin facies.

Bedding parallel thin section analysis of the basin facies sediments revealed strands of mineralised algae or fungal hyphae which were greater than 100μm long and 4μm wide (Text-fig. 3A); there were also strands of modern algal or fungal hyphae, 3μm wide and up to 120μm in length, running across the fossils and sediments (Text-fig. 3B). Modern hyphae are easily distinguished from fossil ones owing to their pristine, non-fractured, morphology and non-mineralized organic composition. Mineralised hyphae were previously observed in the marginal facies and interpreted as being cyanobacteria, but none had been documented in the basin facies (Williams 1983; Williams and Reimers 1983). Williams (1983) suggested that this cyanobacterium might have been partially responsible for the production of the calcium carbonate portion of the sediment in the Bear Gulch basin.

Pyrite framboids occur disseminated throughout the sediment and are occasionally concentrated along laminae (as shown in Text-fig. 4A). Framboids are composed of

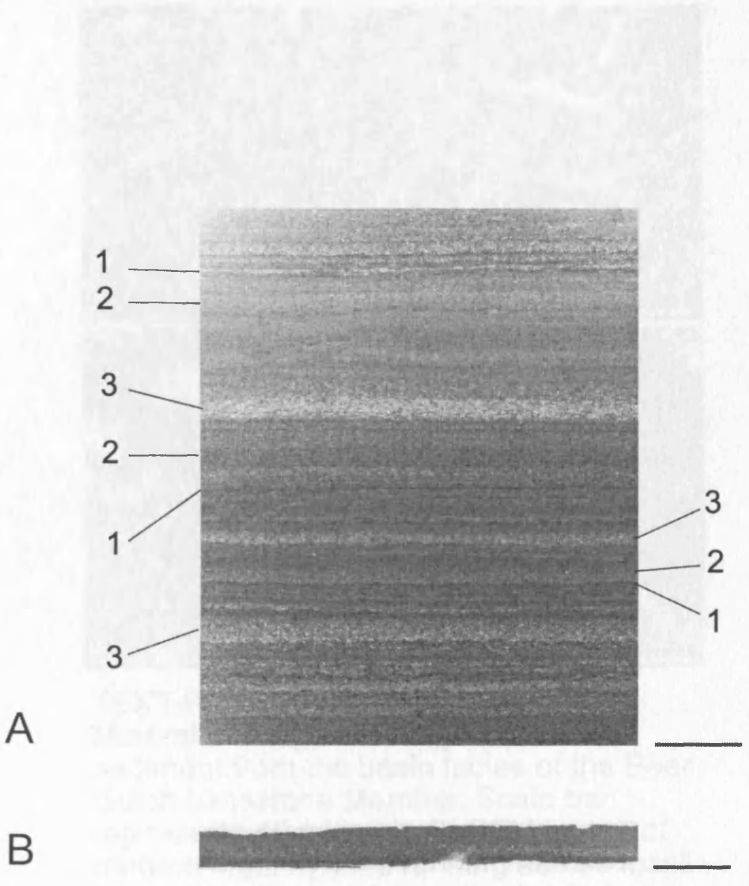

TEXT-FIG. 2. A, a typical bed >30mm thick from the Bear Gulch Limestone Member basin facies (Upper Mississippian, USA), clay rich dark laminae (1), calcite and quartz rich laminae (2) and calcite rich laminae (3), scale bar represents 10mm. B, a typical bed <30mm thick, scale bar represents 10mm.

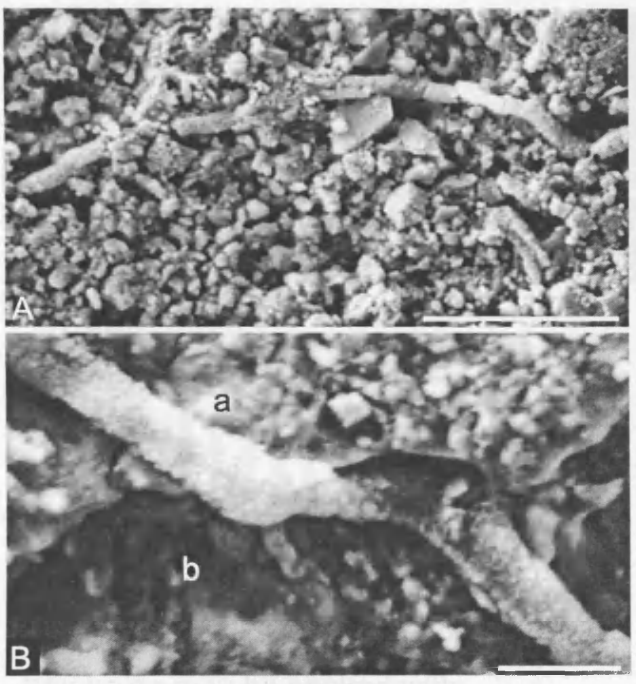

TEXT-FIG. 3. A, SEM image of Mineralized algae or fungal hyphae in sediment from the basin facies of the Bear Gulch Limestone Member. Scale bar represents 48 microns. B, SEM image of modern algal hyphae running across fossil (a) and sediment (b) from the basin facies of the Bear Gulch Limestone Member. Scale bar represents 6 microns.

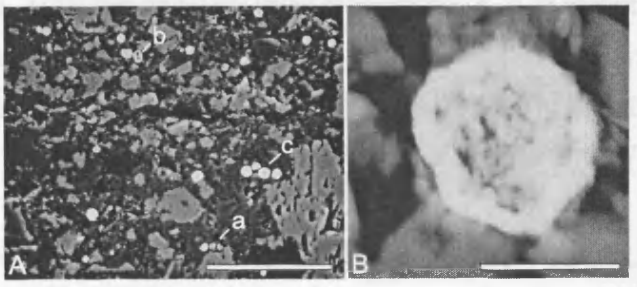

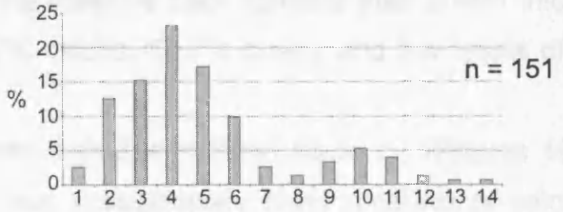

C

TEXT-FIG. 4. A, framboids occur along laminae in the Bear Gulch Limestone Member basin facies sediments these framboids may be packed with microcrystals (a) or are annular (b) or have faint microcrystals in the centre of a more pronounced ring of microcrystals (c). Scale bar represents 38 microns. B, a typical framboid from the Bear Gulch Limestone Member (Upper Mississippian, USA), with faint microcrystals in the centre. Scale bar represents 3 microns. C, Pyrite framboid size distribution from the basin facies sediments of the Bear Gulch Limestone Member. The majority of the framboids formed in euxinic to dysoxic conditions. Larger framboids with a maximum framboid diameter of 14 microns indicates that part of the framboid population grew within the sediment during oxygenation events.

subhedral, closely-packed microcrystals between 0.5 and 1μm in diameter. Often the small framboids (<5μm) appear as a ring in section with no microcrystals in the centre. Kosacz and Sawlowicz (1983) proposed the term 'annular framboids' to describe such hollow framboids, or framboids with faint microcrystals in the centre of a more pronounced ring of microcrystals (Text-fig. 4B). Nearly 81 percent (80.75%, n = 151) of the framboids have a mean diameter less than 6μm (Text-fig. 4C). Whilst less than 20 percent (19.25%, n = 151) of the framboids have a mean diameter of greater than 7μm.

Geochemical characteristics. XRD analysis of the Bear Gulch Limestone Member basin facies revealed that the massive beds (greater than 30mm thick, flinz cf. Williams 1983) have a mean of 67.7% calcite, 20.7% quartz and low levels of clay 2.3%, and dolomite 3.3% (see table 2)

Platy beds (less than 30mm thick) (fäule cf. Williams 1983) from the Bear Gulch Limestone Member have proportionally lower amounts of calcite (mean 41.8%), higher amounts of quartz, (mean 36.8%) and slightly more clay, (mean 5.3%), than the massive beds. The percentage dolomite and ankerite are slightly higher in the smaller beds, 7.8% and 4.1% respectively (see table 2).

XRD of the <2μm fraction of the sediment showed that in both massive and platey beds the dominant clay minerals are illite/mica with subordinate Na smectite, and kaolinite occurred in two sample (Table 3). The massive and platy beds could not be distinguished based on the composition of this fine-grained fraction, indicating perhaps that the source for the clay fraction of the sediment was the same during deposition of massive and platy beds.

XRF analyses. All XRF analyses on sediment from the Bear Gulch Limestone Member were compared to Post Archean Average Shale (PAAS) (Taylor and McLennan 1985). PAAS was chosen for elemental comparisons for two reasons; firstly, no averaged carbonate equivalent exists and secondly, normalizing the data to PAAS and alumina removes the dilution effect of the carbonate component. The amount of CaO, Mg, Sr, and Mn in the Bear Gulch Limestone Member sediment is considerably higher than in PAAS (see text-fig. 5A-B and table 4A-B). The higher abundance of these elements is expected for a limestone and reflects calcite's ability to incorporate them into its structure (see appendix 2). The high abundance of Mg is a reflection of the presence of secondary dolomite rhombs in the basin facies sediment and, perhaps an indication that the sediment originally contained high Mg-calcite. XRF data also reveals that Si in the Bear Gulch Limestone Member is higher than in PAAS (Text-fig. 5A-B) and this reflects the high abundance of quartz (see table 2).

	Bear Gulch Limestone Member				Solnhofen	
	Massive		Platey		Flinz	Fäule
	Mean	SD	Mean	SD		
Calcite	67.70%	2.1	41.80%	6.5	95-98%	77-87%
Quartz	20.70%	1.5	36.80%	4.7	0.40%	3%
Clay	2.30%	0.6	5.30%	1.2	3%	10-20%
Dolomite	3.30%	0.6	7.80%	1.5		
Ankerite	2%	1	4.50%	1.1		

Table 2. A summary of XRD data from the Bear Gulch Limestone Member basin facies of 3 massive beds (>30mm) and 16 platey beds (<30mm). And a summary of the mineralogical composition of Flinz and Fäule from the Solnhofen (from Barthel *et al.* 1990; Kemp and Trueman 2002).

Bed	Mineral	Weight of <2µm fraction	Proportion of <2µm fraction
1	Illite/Mica	17.00	100.00
2	Illite/Mica	17.00	100.00
3	Illite/Mica	16.00	66.25
	Smectite		33.75
4	Illite/Mica	21.00	100.00
5	Illite/Mica	27.00	100.00
6	Kaolinite	21.00	15.36
	Illite/Mica		84.64
8	Illite/Mica	21.00	100.00
9	Illite/Mica	16.00	100.00
10a	Illite/Mica	11.00	100.00
10b	Illite/Mica	7.00	100.00
11	Kaolinite	14.00	9.85
	Illite/Mica		43.88
	Smectite		46.27
12	Illite/Mica	18.00	47.80
	Smectite		52.20
13	Illite/Mica	18.00	100.00
14	Illite/Mica	13.00	100.00
15	Illite/Mica	13.00	100.00
17	Illite/Mica	18.00	100.00
18	Illite/Mica	13.00	100.00
19	Illite/Mica	14.00	55.70
	Smectite		44.30
20	Illite/Mica	20.00	100.00

Table 3. XRD analyses of sediment weight and portion of the sediments > 2µm and indication of the clay mineralogy of those beds.

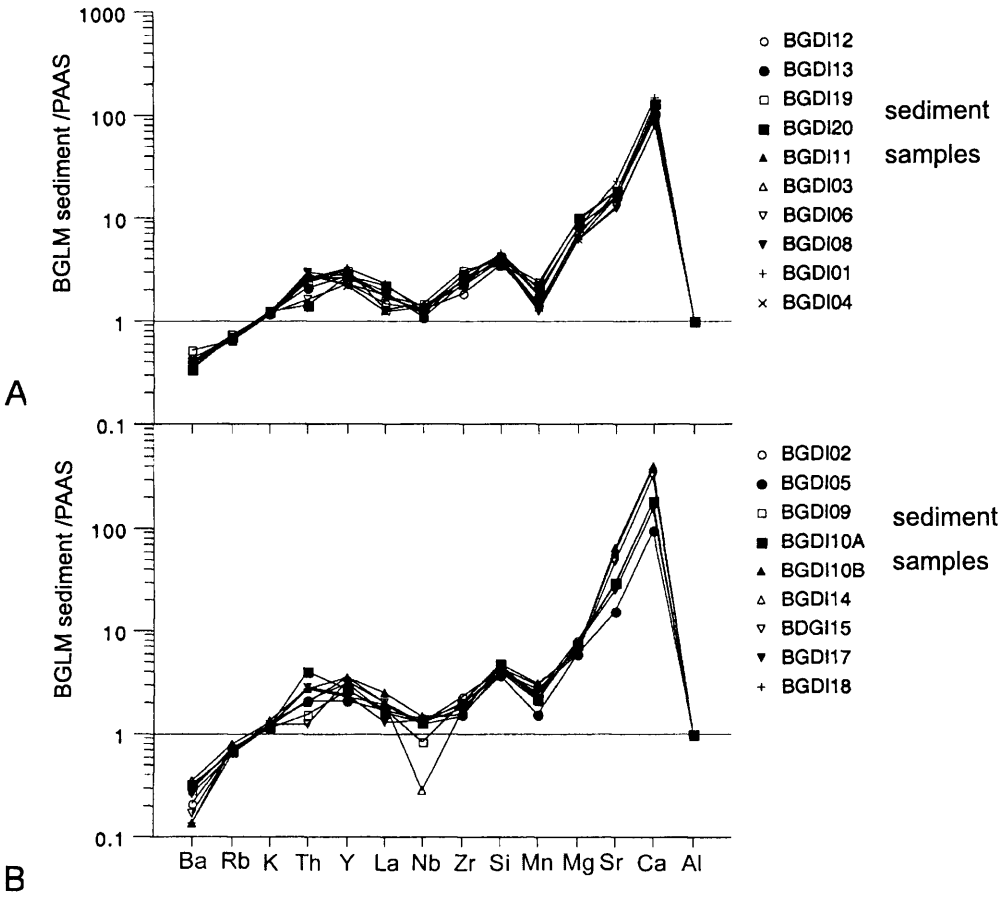

TEXT-FIG. 5. A and B elemental data from XRF of Bear Gulch Limestone Member basin facies sediment normalised to PAAS and Al_2O_3.

	Bear Gulch Limestone Member		PAAS	Burgess Shale			
(Wt.%)	Mean	SD		Walcott 1	Walcott 2	Raymond	Tuzoia
SiO_2	37.26	8.10	62.8	53.71	50.34	50.10	50.63
TiO_2	0.19	0.06	1.00	0.68	0.76	0.65	0.75
Al_2O_3	2.74	0.69	18.90	24.11	23.32	21.25	24.54
FeO	1.45	0.51	6.50	2.74	3.87	7.17	5.56
MnO	0.03	0.00	0.11	0.01	0.02	0.07	0.03
MgO	2.35	0.69	2.20	1.69	1.89	2.56	2.03
CaO	27.52	6.12	1.30	3.43	4.55	5.62	2.58
Na_2O	0.17	0.02	1.20	0.34	0.34	0.63	0.67
K_2O	0.65	0.16	3.70	6.75	7.07	4.15	6.15
P_2O_5	0.36	0.08	0.16	0.11	0.15	0.20	0.14
SO_3	0.14	0.06					
LOI	26.93			6.08	7.22	6.72	6.18

Table 4A. Mean XRF bulk chemistry analyses and standard deviation for 19 samples from the Bear Gulch Limestone Member, in comparison with bulk rock chemistry of the average shale composition (PAAS; Taylor and McLennan 1985) and low carbonate metamudstones from fossil quarries (Walcott Quarry, Raymond Quarry, Tuzoia Beds) on Fossil Ridge, Burgess Shale, Canada (from Powell 2003).

	Bear Gulch Limestone Member		PAAS
(ppm)	Mean	SD	
Ba	32.34	15.23	*580.0*
Ce	10.54	6.16	*50.0*
Co	2.36	1.67	*20.0*
Cr	38.35	20.27	*100.0*
Cs	1.57	2.72	*5.0*
Cu	3.90	1.27	*57.0*
Ga	4.59	0.95	*19.0*
La	9.57	2.56	*40.0*
Mo	2.52	0.59	*2.0*
Nb	3.48	1.16	*20.0*
Nd	12.11	2.36	*23.0*
Ni	10.61	4.93	*95.0*
Pb	4.18	1.40	*20.0*
Rb	16.02	4.03	*140.0*
Sn	8.02	1.48	
Sr	658.51	141.74	*450.0*
Th	5.03	1.83	*11.0*
U	2.00	1.20	*3.2*
V	26.21	6.17	*130.0*
Y	10.44	1.98	*30.0*
Zn	10.16	6.27	*80.0*
Zr	67.63	25.45	*200.0*

Table 4B. Mean XRF trace element analyses and standard deviation for 19 samples from the Bear Gulch Limestone Member, in comparison with bulk rock chemistry of the average shale composition (PAAS; Taylor and McLennan, 1985).

Fossil Biomineral preservation

The fate of each of the original biominerals that were present is discussed in turn.

Aragonite. Small coiled cephalopods (less than 60mm in diameter) and orthocone conchs, which were originally composed of aragonite, are now mouldic with no trace of mineral remaining. Large cephalopods (greater than 60mm in diameter) do retain mineralized tissues and, EDX spot analysis revealed that the mineral is $CaCO_3$, which is almost certainly calcite, after aragonite.

Calcite. Echinoderms have tests composed of calcite (Chia and Koss 1994). In the Bear Gulch Limestone Member the articulated starfish *Lepidasterella* Welch 1984, which has as many as 35 arms and clearly visible madreporites, is rare (n = 14) (Williams 1983). 4 have been found as moulds, whilst 3 are found as thin films with a dark brown to black colouration, and 3 show both modes of preservation, where the dark colour occurs particularly towards the centre of the starfish. This dark colouration is shown by element mapping on an SEM to contain a slightly elevated abundance of carbon relative to the mouldic starfish and the matrix. Raman spectroscopy revealed that this carbon was amorphous.

Apatite. SEM images of a small fish (specimen F-89-62401) from the Bear Gulch Limestone Member showed well-preserved fin spines, composed of a granular textured apatite with dolomite rhombs (3µm in length) protruding from the fossil material (Text-fig. 6A). In backscatter view it was possible to pick out very small bright spherical objects (0.5µm across) confined to the fossil and not seen in the surrounding matrix; EDX spot analyses of the fins and body of the fish revealed high levels of iron and some sulphur, indicating that these are pyrite (FeS_2) crystals that formed on the surface of the fossilising fish (Text-fig. 6A). In modern fish (actinopterygii) the chemical compositions of fins and skin are poorly studied; the chief minerals are phosphorous, potassium and calcium (Van Oosten 1957). Modern fish scales (actinopterygii) are composed of between 41% and 84% organic protein, mostly albuminoids such as collagen (24%) and ichthylepidin (76%), and up to 59% bone, mostly $Ca_3(PO_4)_2$ and $CaCO_3$ (Helfman *et al.* 1997). Quantitative EDX analysis (Table 5) revealed that the bones and scales of the Bear Gulch Member fish investigated are composed of fluorapatite (mean CaO = 53.33 wt%, sd = 0.53; mean P_2O_5 = 36.47 wt%, sd = 0.64; F = 6.26 wt%, sd = 0.79) with some sulphur (mean S = 2.74 wt%, sd = 0.62) and minor amounts of sodium (mean Na = 0.76 wt%, sd = 0.62) and magnesium (mean Mg = 0.1 wt%, sd = 0.08, n = 7 for all analyses). Electron microprobe

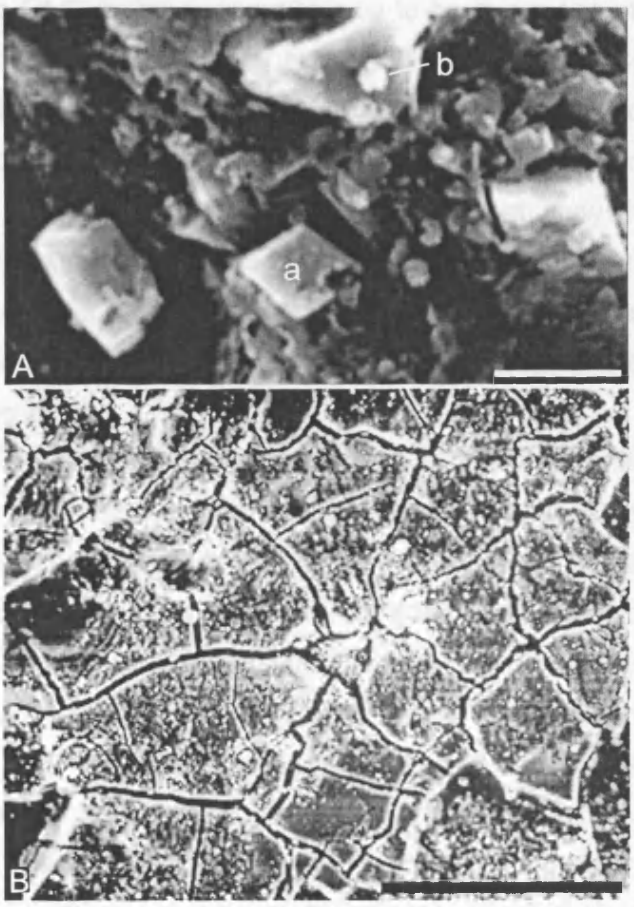

TEXT-FIG. 6. A, dolomite rhombs (a) that have grown into the fossil fish (specimen F-89-62401) from the Bear Gulch Limestone Member and pyrite crystals (b) occurring on the surface. Scale bar represents 3 microns. B, polygonal cracks in the cuticle of a shrimp (specimen ROM-45841). Scale bar represents 86 microns.

data revealed that the scales have a mean F content of 2.87 % (n = 31, sd = 0.55) (Table 6). If the F in the apatite compound is greater than 1% then the apatite is a fluorapatite (Hubert *et al.* 1996; Wilson *et al.* 1999). The molecular weight ratio of Ca/P in apatite should be 2.15 (Deer *et al.* 1995); a value above this implies that substitution has occurred, so that either Ca^{2+} has been added, or that P has been lost. In the Bear Gulch Limestone Member electron microprobe analysis of the biomineralized tissues of a fossil fish revealed the Ca/P molecular weight ratio to have a mean of 2.51, (sd = 0.1, n = 31). This ratio may be accounted for by substitution of PO_4^{3-} by CO_3^{2-} and/or SO_4^{2-}; in this instance CO_3^{2-} is probably the ion responsible because the surrounding sediment is a limestone providing a ready supply of carbonate ions. However, it is not known whether high carbonate ion concentrations in the sediment may have allowed for either replacement of PO_4^{3-} on the surface of the original apatite crystals, or for the authigenesis of apatite with a higher than usual concentration of CO_3^{2-}. This substitution of PO_4^{3-} by CO_3^{2-} may be balanced with excess F (Deer *et al.* 1995), and therefore, the apatite is a carbonate fluorapatite.

Modern lingulid brachiopods secrete two valves in stratiform, alternating layers of organic material and a fluorine-bearing carbonate-hydroxyapatite, previously described as francolite or dahllite (Watabe and Pan 1984, Puura and Nemliher 2001). Bear Gulch Limestone Member lingulid brachiopods are compressed, but otherwise well preserved. Quantitative EDX analyses (Table 5) produced peaks of CaO, (mean CaO = 52.61 wt%, sd = 0.3), P_2O_5 (mean P_2O_5 = 36.36 wt%, sd = 0.28) and additional F_2O (mean F_2O = 6.62 wt%, sd = 0.19), SO_3 (SO_3 = 2.12 wt%, sd = 0.2) and traces of Na_2O (mean Na_2O = 1.26 wt%, sd = 0.11) and MgO (mean MgO = 0.69 wt%, sd = 0.16, n = 5 for all analyses). Electron microprobe data (Table 6) confirmed that F was greater than 1% (mean F = 3.03 wt%, sd = 0.22, n = 32) and that the Ca/P ratio was above 2.15 (mean = 2.43, sd = 0.07, n = 32), and hence, lingulid brachiopods are composed of carbonate fluorapatite.

Non-mineralized tissues

The biomolecular composition of fossil organisms is difficult to determine. Most assumptions of the original composition of fossil taxa are based upon their extant relatives. Below I have divided non-mineralized tissues into recalcitrant and labile tissue (see table 1) and further subdivided these into the most likely composition of the organism prior to fossilization. Enigmatic organisms have original tissue types that are entirely unknown and are discussed last.

	Fish		Lingulid brachiopod		Shrimp		Conulariid	
	Average	SD	Average	SD	Average	SD	Average	SD
SiO_2	0.00	0.01	0.04	0.09	0.13	0.20	0.03	0.04
Al_2O_3	0.08	0.05	0.13	0.02	0.22	0.05	0.13	0.04
FeO	0.06	0.07	0.09	0.10	0.05	0.04	0.05	0.07
MnO	0.01	0.02	0.00	0.00	0.00	0.00	0.06	0.08
MgO	0.10	0.08	0.69	0.16	0.32	0.06	0.37	0.13
CaO	53.33	0.53	52.62	0.30	54.16	0.47	51.22	1.16
Na_2O	0.76	0.23	1.26	0.12	0.86	0.06	1.06	0.14
K_2O	0.04	0.03	0.02	0.04	0.08	0.04	0.13	0.03
P_2O_5	36.47	0.64	36.36	0.28	34.89	0.25	36.32	0.27
SO_3	2.74	0.62	2.13	0.20	1.99	0.08	1.74	0.15
F_2O	6.26	0.79	6.62	0.19	6.80	0.37	8.76	0.87
Cl_2O	0.05	0.06	0.03	0.03	0.07	0.04	0.12	0.05

Table 5. Mean quantitative EDX analyses and standard deviations for fossils with an apatite composition. Where values were lower than the detection limits of the EDX values of zero were recorded, therefore the standard deviation appears greater than the mean for several analyses.

A

	Shrimp		*Sphenothallus*		Fish		Lingulid brachiopod		Conulariid	
	Mean	**SD**	**Mean**	**SD**	**Mean**	**SD**	**Mean**	**SD**	**Mean**	**SD**
SiO_2	0.35	0.76	0.00	0.00	0.06	0.25	0.00	0.02	0.01	0.03
FeO	0.03	0.03	0.02	0.02	0.05	0.11	0.01	0.01	0.02	0.02
MnO	0.01	0.01	0.01	0.01	0.01	0.01	0.01	0.01	0.01	0.01
MgO	0.32	0.28	0.41	0.03	0.12	0.11	0.57	0.05	0.29	0.04
CaO	42.59	2.98	49.76	1.79	50.81	4.19	49.31	2.57	40.82	3.18
Na_2O	0.72	0.11	1.01	0.04	0.90	0.81	1.15	0.09	0.76	0.06
SrO	0.38	0.06	0.27	0.04	0.23	0.16	0.41	0.10	0.24	0.04
La_2O_3	0.03	0.04	0.04	0.06	0.03	0.04	0.04	0.05	0.03	0.04
Ce_2O_3	0.03	0.02	0.06	0.05	0.04	0.05	0.06	0.06	0.09	0.06
Y_2O_3	0.02	0.02	0.02	0.02	0.03	0.02	0.03	0.03	0.04	0.02
P_2O_5	27.18	1.85	30.39	1.27	33.15	3.23	33.26	1.30	26.89	2.24
F	3.07	0.85	4.12	0.22	2.87	0.55	3.03	0.22	3.14	0.29
-O=F	1.29	0.36	1.74	0.09	1.21	0.23	1.27	0.09	1.32	0.12
Cl	0.04	0.01	0.04	0.01	0.17	0.43	0.02	0.01	0.05	0.02
-O=Cl	0.01	0.00	0.01	0.00	0.04	0.10	0.00	0.00	0.01	0.00
SO_3	1.60	0.12	1.63	0.09	2.22	0.60	1.73	0.17	1.00	0.08
Total	75.06	4.71	86.05	3.08	89.44	7.02	88.35	3.77	72.07	4.94
O	10.00	0.00	10.00	0.00	10.00	0.00	10.00	0.00	10.00	0.00
Si	0.03	0.08	0.00	0.00	0.00	0.02	0.00	0.00	0.00	0.00
Fe^2	0.00	0.00	0.00	0.00	0.00	0.01	0.00	0.00	0.00	0.00
Mn	0.00	0.00	0.00	0.00	0.00	0.00	0.00	0.00	0.00	0.00
Mg	0.05	0.04	0.05	0.00	0.01	0.01	0.07	0.01	0.04	0.01
Ca	4.38	0.11	4.57	0.03	4.31	0.11	4.24	0.07	4.40	0.18
Na	0.13	0.02	0.17	0.01	0.14	0.14	0.18	0.02	0.15	0.02
Sr	0.02	0.00	0.01	0.00	0.01	0.01	0.02	0.01	0.01	0.00
La	0.00	0.00	0.00	0.00	0.00	0.00	0.00	0.00	0.00	0.00
Ce	0.00	0.00	0.00	0.00	0.00	0.00	0.00	0.00	0.00	0.00
Y	0.00	0.00	0.00	0.00	0.00	0.00	0.00	0.00	0.00	0.00
P	2.21	0.07	2.21	0.02	2.22	0.05	2.26	0.03	2.29	0.08
F	0.93	0.22	1.12	0.05	0.72	0.14	0.77	0.08	1.01	0.13
Cl	0.01	0.00	0.01	0.00	0.02	0.06	0.00	0.00	0.01	0.00
S	0.12	0.01	0.11	0.01	0.13	0.04	0.10	0.01	0.08	0.00
Total	6.95	0.10	7.13	0.03	6.84	0.13	6.88	0.05	6.99	0.12

B

Ca	30.42	35.54	36.29	35.22	29.16
P	11.86	13.26	14.47	14.52	11.73
Ca/P	2.56	2.68	2.51	2.43	2.48

Table 6. A, mean electron microprobe analyses, standard deviations and cation proportions for fossils composed of apatite. B, molecular weight ratio of Ca/P in apatite.

Recalcitrant non-mineralized tissues

Chitin. Recent shrimp carapaces are composed of chitin (Baas *et al.* 1995). In the Bear Gulch Limestone Member the remains of shrimp (Malacostraca) cuticles including the limbs are common, whereas the antennae are rare. Shrimp are generally dark red/brown to pale brown in colour, almost translucent and most show minor relief.

SEM imaging revealed that the fossil cuticle surface texture is cracked, producing a polygonal texture (Text-fig. 6B). At higher magnification, (x2.5K) a granular texture was evident, with individual granules being approximately 2µm in diameter. A similar granular texture was reported in the Santana Formation (Cretaceous, Brazil) fish muscle and was interpreted to comprise mineralized bacteria (Wilby 1993). However, preservation was not of sufficient fidelity in the Bear Gulch Limestone Member to suggest that individual granules represented autolithified bacteria. Analyses of the shrimp cuticle by EDX spot analyses indicate it is composed of calcium and phosphorous and quantitative EDX spot analyses (Table 5) have revealed this to be fluorapatite (mean CaO = 54.16 wt%, sd = 0.47; mean P_2O_5 = 34.89 wt%, sd = 0.25; mean F_2O = 6.78 wt%, sd = 0.37) with some sulphur (mean SO_3 = 1.99 wt%, sd = 0.08) and minor amounts of sodium (mean Na_2O = 0.86 wt%, sd = 0.06) and magnesium (mean MgO = 0.32 wt%, sd = 0.06, n = 5 for all analyses). Electron microprobe analyses of polished cuticle sections confirmed a carbonate fluorapatite composition for the shrimp cuticle (mean F = 1.91 wt%, sd = 1.3; mean Ca/P = 2.45, sd = 2.47, n = 7 for all) (Table 6). No crystals of calcium carbonate have been found associated with the shrimp analysed.

Setae of Recent polychaete worms are chitinous and are composed of tanned β-chitin and inorganics (Briggs and Kear 1993). Bear Gulch Limestone Member polychaete specimen ROM-88-71712 has only the marginal outline of the worm and the setae preserved (Text-fig. 7). In hand specimen the setae appear iridescent with some relief. SEM examination revealed that setae comprise euhedral, elongate crystals, 600µm in length and 150-200µm wide, with their long axis parallel to the long axis of the setae (Text-fig. 7A-B). EDX spot analyses of these crystals gave strong Ca and P peaks and elemental mapping confirmed that Ca and P were elevated in the setae relative to the sediment (Text-fig. 7C-D), indicating that their fossil composition is apatite.

Scleroprotein. Modern jaws of polychaetes (scolecodonts) are composed of scleroprotein (Voss-Foucart *et al.*, 1973). Raman spectroscopy of scolecodonts (e.g. specimen UM-84-71603) from the Bear Gulch Limestone Member revealed that the jaws were composed of amorphous carbon.

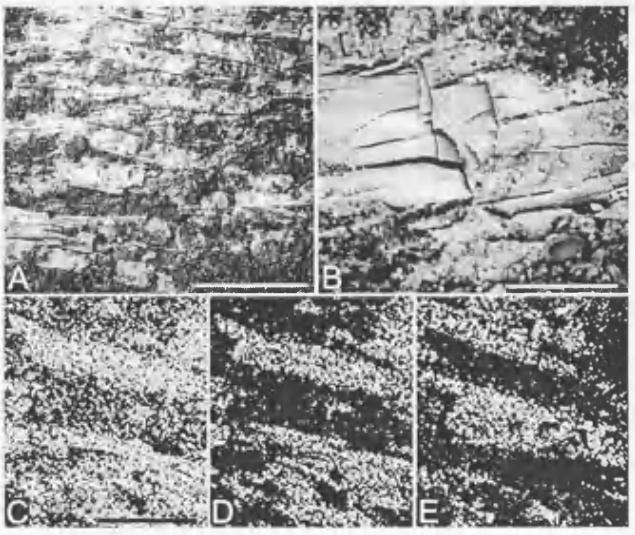

TEXT-FIG. 7. A, setae of a polychaete worm (ROM 88-71712) from the Bear Gulch Limestone Member. Scale bar represents 380 microns. B, setae are preserved as euhedral elongate crystals of apatite. Scale bar represents 43 microns. C, element map of Ca, bristles appear slightly brighter than the surrounding sediment. Scale bar represents 300 microns. D, element map of P, bristles appear very bright and surrounding sediment is black. Scale bar represents 300 microns. E, element map of Si, bristles appear very dark whilst the sediment appears bright. Scale bar represents 300 microns.

Collagen. Modern polychaete bodies are collagenous (Briggs and Kear 1993). Many polychaete fossils from the Bear Gulch Limestone Member are preserved as imprints where no chemical compositional difference between the body of the polychaete and the sediment was detected, for example *Symmetroprion* n. sp. (specimen ROM-49953, see chapter 2). Two small polychaete worms from the Bear Gulch Limestone Member (UM-87070704A and UM-MI7106) preserving the body and scolecodont jaw apparatuses were seen to be composed of a mesh of highly reflective, almost glassy, black material (Text-fig. 8A). When viewed using a SEM, at approximately x500 magnification, the black reflective material was seen to have two different forms, both of which were composed of $CaCO_3$. The most commonly occurring crystal form consisted of large (30-40µm in length), elongate crystals radiating outwards from the margins of the body of the worm and the scolecodonts (Text-fig. 8B-C); the morphology is suggestive of crystal growth within a void space. The second crystal form was a much finer, microcrystalline texture that occurred between the large radiating crystals (Text-fig. 8C).

Element mapping of three Bear Gulch Limestone Member polychaetes (specimens UM-87810b1/b2, 87810/45859 and 8770907), all approximately 20mm in length and a maximum of 3mm wide, which were red/brown in colour, showed that the area of the worm surrounding the gut tract had greater abundances of Si and C than the surrounding carbonate sediment and that the gut had high abundances of P (Text-fig. 9A-B). High magnification revealed that the preserved gut tract contained bright areas with a flat and fractured texture, and darker areas with a clay-like platy texture (Text-fig. 9C-D). EDX spot analyses determined that the bright areas were abundant in Ca and P, whilst the dark areas had a high abundance of Si (Text-fig. 9E-F).

In summary collagen biomolecules are represented in the Bear Gulch Limestone Member by tissue imprints, $CaCO_3$ mineralisation and apatite mineralisation of worm cuticles.

Labile tissue. Fish specimen ROM-91-70803A showed a circular dark coloured eyespot, and a second dark and circular area, which, when compared to modern actinopterygii, possibly represents the position of the heart or liver, and possibly the remains of one of these organ. Fish specimen ROM-29784 (Text-fig. 10A) had a dark eye spot which was highly fractured and showed slight relief (Text-fig. 10B). EDX spot analyses of the eye area (specimen ROM-91-70803A) revealed peaks of C, O, Mg, Al, Si, P, and Ca, although because the eye spot was very thin it was not certain which elements were occurring in the eye, and which in the underlying sediment. Therefore, element mapping was undertaken and this revealed a slightly higher abundance of C coincident with the eye spot than the surrounding area, and elevated Ca and P around its rim. Elemental

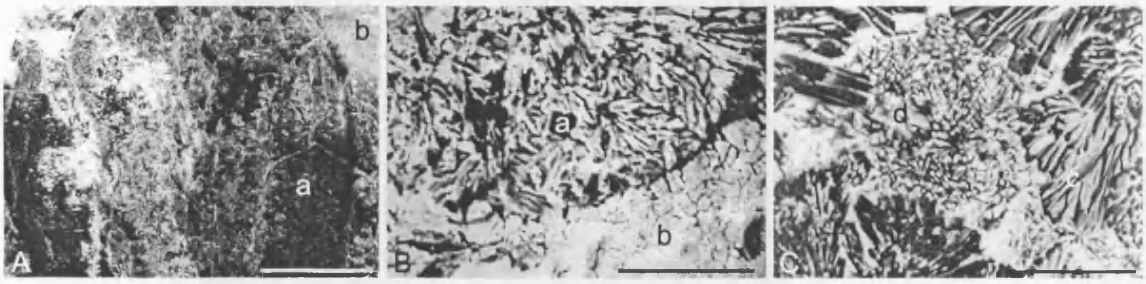

TEXT-FIG. 8, a small black coloured polychaete worm (UM-87070704A) from the Bear Gulch Limestone Member (Upper Mississippian, USA). A, the jaw of the polychaete (a) and (b) the sediment. Scale bar represents 1200 microns. B, crystals of $CaCO_3$ radiating from the body of the worm (a) and the sediment (b). Scale bar represents 60 microns. C, two distinct crystal forms are present, large euhedral crystals (c) and a fine microcrystalline texture that occurs between the larger crystals (d). Scale bar represents 30 microns.

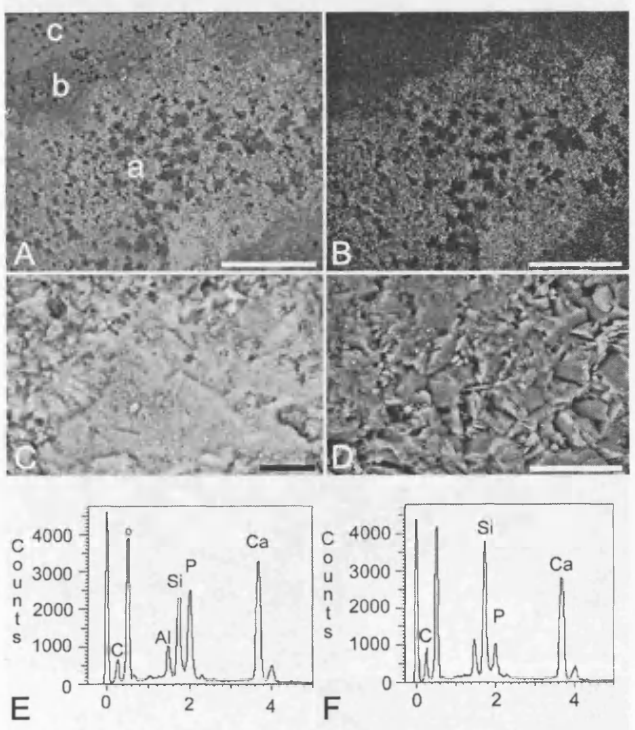

TEXT-FIG. 9. A, SEM image of part of a polychaete worm (specimen ROM-87-70907) from the Bear Gulch Limestone Member the gut (a), the exterior body of the polychaete (b) and the sediment (c). Scale bar represents 1 mm. B, corresponding element map of P of text-figure 9A, the bright area indicates elevated levels of P. Scale bar represents 1 mm. C, Phosphate rich region of gut tract of polychaete. Scale bar represents 10 microns. D, Si rich region of gut tract of polychaete. Scale bar represents 10 microns E, EDX of phosphate rich region of gut tract. F. EDX of Si rich region of gut tract.

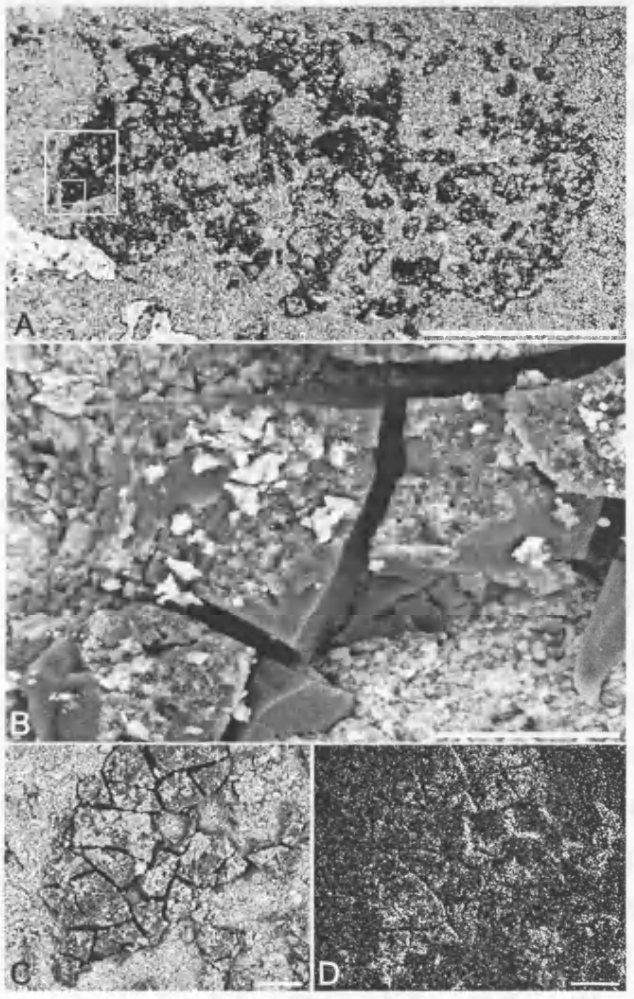

TEXT-FIG. 10. A. Eye of a small fish from the Bear Gulch Limestone Member (specimen ROM-29784). Scale bar represents 500 microns. B, the eye is composed of carbon and has some relief, a thin layer of Si-Al rich sediment covers the carbon (image of small boxed area in text-figure 11A). Scale represents 20 microns. C,SEM image of part of the eye (large boxed area in text-fig11A). Scale represents 50 microns. D, corresponding element map of carbon. Scale bar represents 50 microns.

mapping of the eye spot in specimen ROM-29784 revealed a strong concentration of C coincident with the eye (Text-fig. 10C-D). Interestingly, the C was often encrusted by what appears to be a thin layer of sediment, which gave EDX peaks for Si and Al, indicating that it is a clay mineral (see text-fig. 10B). This clay mineral may be associated with fossil preservation, or could also be a clay rich lamination, which was part of the overlying sediment. The area, that may represent the heart or liver (specimen ROM-91-70803A) also showed a highly fractured surface and EDX spot analyses revealed C, O, Mg, Al, a large Si peak, some P, S, K, Ca and minor traces of iron; other spot analyses revealed similar results but only C, O, Al, Si, P and Ca appeared in all analyses. No fossilized bacteria were associated with the eye spot or the remains of the heart or the liver; therefore, it is unlikely that these areas represent microbial films pseudomorphing the organic soft parts as observed by Martill (1987).

Unknown original composition

Conulariids and Sphenothallus. The original composition of extinct conulariids and *Sphenothallus* is not known; however, fossils of both taxa are found often preserved in apatite (Babcock and Feldman 1986; Van Iten et al. 1992, 1996, 2002). All Bear Gulch Limestone Member conulariids consist of dark red/brown ribs, which are laterally compressed (Text-fig. 11A). The preserved, but probably not complete, length of conulariids in the Bear Gulch Limestone Member ranges from approximately 10mm up to 200mm. Quantitative EDX (Table 5) revealed they are composed of fluorapatite (mean CaO = 51.22 wt%, sd = 1.6; mean P_2O_5 = 36.32 wt%, sd = 0.27; F_2O = 8.76 wt%, sd = 0.87) with small amounts of sulphur (mean SO_3 = 1.74 wt%, sd = 0.15, n = 5 for all). Microprobe data (Table 6) revealed that conulariid composition is carbonate fluorapatite with sulphur (mean Ca/P = 2.49, sd = 0.2, mean F = 3.14 wt%, sd = 0.3, n = 11 for all).

Sphenothallus is very common in the Bear Gulch Limestone Member (Van Iten *et al.* 1992; Thomas see chapter 1), and consists of circular attachment discs (approximately 5mm in diameter) and two longitudinal thickenings up to 200mm in length. Both discs and longitudinal thickenings are a deep red/brown colour. EDX spot analysis revealed that the Bear Gulch Limestone Member sphenothallids had a high concentration of Ca and P. Electron microprobe data on polished sections (Table 6) showed that their composition was almost certainly carbonate fluorapatite because F was higher than 1% and the Ca/P molecular weight ratio was greater than 2.15 (mean F = 2.78 wt%, sd = 0.84, mean Ca/P ratio = 2.46, sd = 2.31, n = 35 for all).

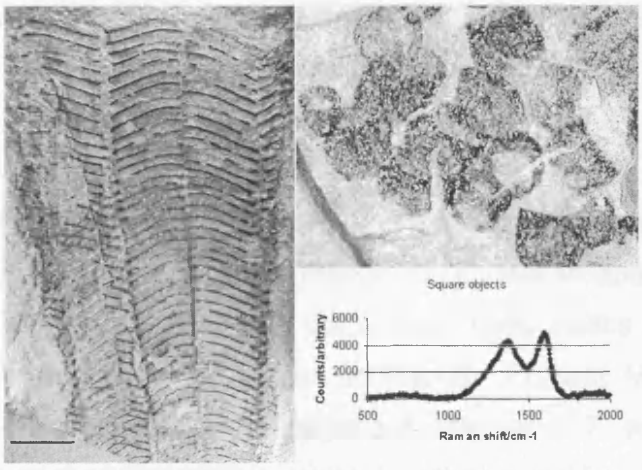

TEXT-FIG. 11. A, conulariid (specimen ROM-45849) from the Bear Gulch Limestone Member. Scale bar represents 10mm. B, square objects (specimen CM-I-83-71204)of the Bear Gulch Limestone Member. C, Raman graph displays two peaks that are indicative of amorphous carbon.

Square objects. These enigmatic organisms, or parts of organisms, colloquially referred to as square objects, appear square in outline. However, examination of different flattening orientations reveals that they originally were tubular shaped and possibly closed at one end (Text-fig. 11B). They vary in colour and style of preservation and they may be partly preserved as tissue imprints or a brown to pale brown colouration; all display a mottled texture. No fossilized bacteria were found associated with the square objects. EDX spot analysis and element mapping revealed no compositional change between the fossil and the sediment. However, when the square objects were analysed with Raman spectroscopy it was found that they were composed of an amorphous carbon film (Text-fig. 11C).

Typhloesus wellsi (Melton and Scott 1973). This is an enigmatic organism once thought to be a conodont (Richardson 1969; Melton 1972; Melton and Scott 1973). However, Rhodes (1973) and Lindström (1974) discredited these claims and suggested the fossil represented an organism that preyed on conodonts. Conway Morris (1990) re-examined *T. wellsi* but did not resolve its phylogenetic affinities. *T. wellsi* is preserved as an extremely thin, flattened impression, which is either a red-brown colour, or occasionally black. The area called the ferrodiscus was so named because of the presence of iron detected by Melton and Scott (1973). Analysis of the ferrodiscus (specimen UM-6029 analysed by Melton and Scott (1973) and specimen UM-7106) (Text-fig. 12A-B) by EDX spot analyses, element mapping and Raman spectroscopy (Text-fig. 12C) revealed that this area is in fact composed of carbon. There is also a thin layer of Si and Al associated with the carbon (Text-fig. 12B). The light area surrounding the ferrodiscus is composed of calcium and phosphorous suggesting an apatite composition. No iron was detected in association with the ferrodiscus and no fossilized bacteria were found. Elsewhere on *T. wellsi* the same elements were detected, so that the remains of the animal appear to have the same elemental composition as the ferrodiscus.

Summary of fossil analyses

Table 1 shows the original and fossil composition of various taxa in the Bear Gulch Limestone Member. A summary of quantitative EDX is shown in table 5 and a summary of electron microprobe results is shown in table 6. Biomineralized areas of organisms underwent dissolution if originally composed of aragonite or calcite, but occasionally large cephalopods are still a carbonate composition, this is presumably calcite after aragonite. Originally organic tissues where preserved, have been mineralised by apatite or calcite or have retained an organic composition, often associated with clay minerals. In addition, impressions of labile tissues have been left in the sediment prior to decaying completely.

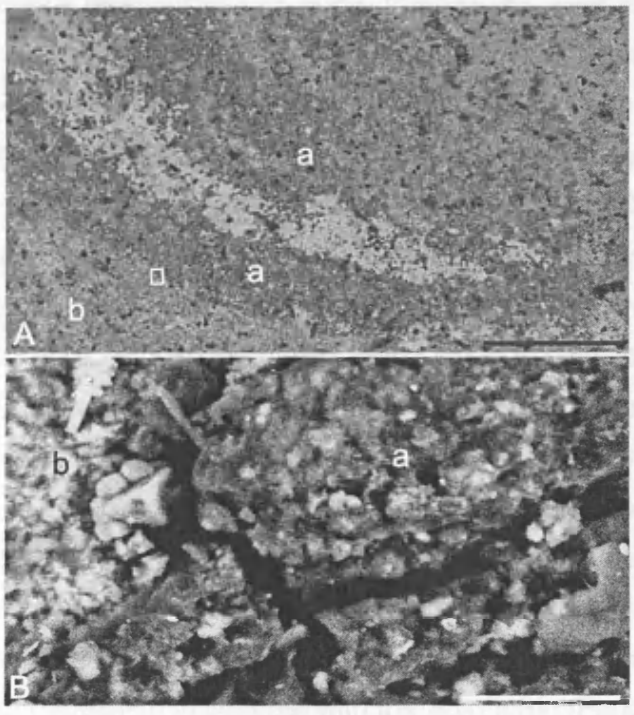

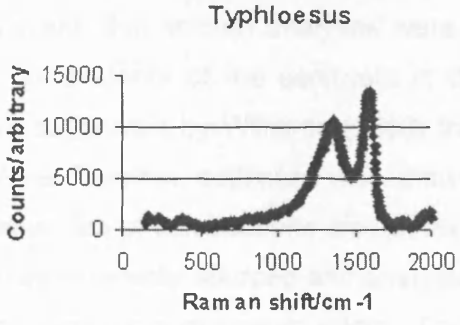

C

TEXT-FIG. 12. A, rim of ferrodiscus of *T. wellsi* Conway-Morris 1990 (specimen UM-7106) (a) and area outside of the ferrodiscus (b). Scale bar represents 500 microns. B, ferrodiscus, high magification (from boxed location on text-figure 12A) carbon with sediment coating (a) sediment (b). Scale bar represents 5 microns. C, Raman graph showing two peaks indicating amorphous carbon.

Discussion of Sediment Composition

The differences between the larger, massive (Flinz) beds and the thinner platy (Fäule) beds have previously been attributed to result from seasonal climatic variations altering mineralogy (Grogan and Lund 2002). The mineralogical distinction between Flinz and Fäulen in the Solnhofen is clearly defined; the Flinz (large) beds are pure micritic limestones which have 95-98% $CaCO_3$, up to 0.4% quartz and up to 3% clay, whereas the Fäulen (thinner) beds are fissile platy beds which have 77-87% $CaCO_3$, 3% quartz and 10-20% clay (Barthel *et al.* 1990; Kemp and Trueman 2002). Mineralogical comparison with the Bear Gulch Limestone Member basin facies sediments shows that the massive (Flinz) beds are not as pure as the Solnhofen Flinz beds having less $CaCO_3$, more quartz abundances, and comparable clay abundances. The platy beds (Fäulen) of the Bear Gulch Limestone Member have slightly less calcite, less clay, and more quartz than Fäulen beds of the Solnhofen Limestone (see table 2). Based on the mineralogical differences the Bear Gulch Limestone Member beds should not be referred to as Flinz and Fäulen but as massive and platy beds. There is also no evidence of cyclicity in the beds of the Bear Gulch Limestone Member (Grogan and Lund 2002) and hence no obvious pattern of deposition in contrast with the Solnhofen (Park and Fürsich 2001).

Geochemistry and thin section analyses were undertaken to try to determine the source of different components of the sediment in the Bear Gulch Limestone Member basin facies. It was suggested by Williams (1983) that the carbonate component of the Bear Gulch Limestone Member sediment was derived from within the basin. In this investigation SEM analyses of thin sections did not reveal any obvious features to suggest that the carbonate was externally sourced and analysis was unable to resolve whether the carbonate was of biogenic or nonbiogenic origin. Certainly, the low latitude (12 degrees north of the equator (Grogan and Lund 2002) and shallow, restricted nature of the basin would have led to seasonal high evaporation rates. Where water is warm, and where CO_2 is being lost through evaporation or photosynthesis, precipitation of calcium carbonate directly from seawater is favoured; $Ca^{2+} + 2HCO_3^- \leftrightarrow CaCO_3 + CO_{2\,(aq)} + H_2O$ (Krauskopf and Bird 1995). Therefore, with every molecule of $CaCO_3$ formed, a molecule of CO_2 is released. However, even in modern sediments fine-grained carbonate precipitated indirectly by organisms is difficult to distinguish from inorganic precipitation (Riding 2000), because both processes give rise to very small grains of calcium carbonate.

Pyrite. Thin section analysis has revealed pyrite framboids in the Bear Gulch Limestone Member basin facies sediments. Pyrite is commonly pervasive authigenic mineral found in sediments and sedimentary rocks (Berner 1970). Variations in the size of pyrite

framboids have been related to redox conditions in modern and ancient aquatic environments (Wilkin *et al.* 1996; Wignall and Newton 2001). Mean framboid diameters of 5.0 +/- 1.7µm have been reported from modern euxinic environments (Wilkin *et al.* 1996), and the dominance of framboids less than 5µm in diameter is typical of these environments (e.g. Suits and Wilkin 1998). However, framboids from oxic and dysoxic environments have larger diameters 7.7 +/- 4.1µm (Wilkin *et al.* 1996). This relationship appears to be true in ancient sediments. Framboids in three sections from the black shales of the Boulonnais (Upper Jurassic, Northern France) have mean diameters of 4.97µm, 3.95µm and 5.88µm, which indicated periods of water column anoxia (Wignall and Newton 2001). However, Wignall and Newton (2001) also found rare, large framboids up to 19µm in diameter. These large framboids were assumed to have been too large to have grown in the water column, and therefore, Wignall and Newton (2001) attributed their presence to oxygenated conditions in the water column so that the zone of framboid formation occurred solely within the sediment.

In the Bear Gulch Limestone Member (Text-fig. 4C) the small size (80.75% with diameters <6µm; mean = 7.14µm, mean increased because of several large framboids, sd = 7.2, n = 151) of many of the framboids in the beds is consistent with their formation under predominantly anoxic conditions in the water column. However, the presence of larger framboids (maximum framboid diameter = 14µm) in some parts of the section would suggest brief periods of oxic bottom water conditions, and this is supported by the presence of benthic invertebrates in the Bear Gulch Limestone Beds. Many of the small framboids (<6µm) from the Bear Gulch Limestone Member have hollow or faint centres; Kizilshtien and Minaeva (1972) have shown that annular framboids can be the first step in the development of complete framboids. The hollow interiors of the annular framboids may be the result of low availability of iron or sulphur (Papunen 1966; Love 1967), or the differential dissolution properties of the core (Sawlowicz 1992, 1993). Therefore, the low percentage of Fe in the Bear Gulch Limestone Member sediment (PAAS FeO = 6.5 wt%; Bear Gulch Limestone Member mean FeO = 1.45 wt%, sd = 0.5, n = 19 see XRF data) could be a limiting factor in the development of true framboids.

During thin section preparation framboids towards the margins (top-most and bottom-most) of the thin section may have been sliced through leaving partial framboids with diameters less than the complete framboid maximum diameter. When measured these would clearly represent incomplete framboid diameters; this would also be the case for those framboids measured from the Boulonnais basin (Wignall and Newton 2001) as they were recorded from polished blocks. In this investigation, no framboids were seen on unpolished blocks, however, thin sections approximately 30µm thick were analysed, ensuring that most small framboids (<6 µm) fell within the thickness of the slide.

FOSSIL PRESERVATION

Biomineral preservation

In the Bear Gulch Limestone Member orthocones and small ammonoids have undergone complete dissolution of their aragonite conchs; the presence of folds in the periostracum rather than fractures, suggests that aragonite dissolution occurred early and before compaction. In larger cephalopods carbonate and some morphological relief is still present, which may suggest that their large size made them less susceptible to dissolution, owing to their greater potential to buffer corrosive porewaters. After some dissolution the remaining aragonite composing these thicker shells would have remineralised to calcite.

Williams (1983) suspected that the cause of carbonate dissolution was the incursion of H_2S bearing pore waters generated from the surrounding black shales. However, the high carbonate abundance in the basin facies (see tables 2 and 4) would have had a high buffering capacity. Further, it seems unlikely that H_2S derived from several kilometres away could caused wholesale carbonate dissolution. The low pH conditions responsible for carbonate dissolution are more likely to have been sourced more locally, and could have been due to decay-induced changes in the porewater chemistry. H_2S, a weak acid, has been shown to be the product of sulphate reducing bacteria decaying organic tissue (Sageman *et al.* 1998). Any available Fe would normally combine with the H_2S to create FeS (Berner 1970) and later pyrite (Krauskopf and Bird 1995); thus fixing the H_2S and stopping local porewaters from becoming acidic. In the Bear Gulch Limestone Member available Fe is very low in abundance (FeO mean = 1.45 wt% sd = 0.5, n = 19; see table 4A), and so most of the H_2S produced through organic decay would not have been fixed. Experiments by Sageman *et al.* (1998) have shown that the local Eh/pH conditions immediately surrounding a decaying carcass can differ critically from those in the surrounding environment. Therefore, in the Bear Gulch Limestone Member, despite the high buffering capacity of the surrounding carbonate sediment, conditions immediately around and within a decaying organism could have caused carbonate biomineral dissolution. Furthermore, if the sediment had a high concentration of original dolomite the sediment surrounding the organism may have been less susceptible to dissolution than the calcite and aragonite biominerals, thus on lithification of the sediment a mould of the organism could have been retained.

Apatite. Fish scales and lingulid brachiopods from the Bear Gulch Limestone Member are preserved as carbonate fluorapatite ($Ca_5(PO_4,CO_3)_3F$), so called CARFAP, the most

common marine phosphate mineral. This composition was produced through diagenetic alteration of the original biomineral fluorapatite composition by substitution of $CO3_3$ into this ionic lattice. This process is common and occurs in such a way that one kind of apatite can be changed to another by slow reaction (Krauskopf and Bird 1995). For example, fossil bone undergoes a slow conversion from hydroxylapatite ($Ca_5(PO_4)_3OH$) to fluorapatite ($Ca_5(PO_4)_3F$) (Krauskopf and Bird 1995).

Preservation of non-mineralized tissues

Post-mortem, an organism's non-mineralized tissues are usually destroyed rapidly by a number of processes including scavenging, metabolism by bacteria and autolysis. It is because these processes are ordinarily so ubiquitous that the term "exceptional preservation" is applied to the fossilization of non-mineralized tissues. Rapid burial, and inhospitable bottom waters, such as anoxia or hypersalinity, may protect carcasses from macroscavengers, but autolysis and bacterial decomposition will continue. However, the morphology of non-mineralized tissues may be captured when they are rapidly mineralized before they have decayed away. Several minerals have been reported to do this; apatite (Müller and Walossek 1985; Martill 1988, 1990; Briggs *et al.* 1993, Wilby 1993), pyrite (Stürmer 1970; Cisne 1973; Conway-Morris 1986; Briggs *et al.* 1991; 1996; Gabbott *et al.* 2004), clays (Gabbott 1998; Orr *et al.* 1998; Gabbott *et al.* 2001), silica (Voigt 1988) and carbonate (Wuttke 1983). Phosphatization has the highest fidelity of soft tissue reproduction and can reproduce information to a cellular level (Martill 1990). Allison and Briggs (1991), after collating information from a wealth of conservation Lagerstätten reported four broad preservational styles of non-mineralized tissues: tissue imprints, carbonized refractory tissues, carbonized volatile soft tissues, and mineralized tissues. Non-mineralized tissues represented in the Bear Gulch Limestone Member show all four of these preservational styles. More recalcitrant organic molecules such as chitin (shrimp cuticle, polychaete setae and scolecodont jaws) have been mineralized by apatite or have been carbonized, whereas labile tissues were mineralized by either apatite, and in rare cases calcite, (such as polychaete gut tracts and polychaete bodies) or are preserved as tissue imprints or organic films (polychaete worms, ferrodiscus of *T. wellsi* and the eye and the putative heart or liver of the fish specimen ROM-29784).

Phosphate mineralization

The setae of Recent polychaete worms (Briggs and Kear 1993) and the exoskeletons of shrimp (Briggs and Kear 1994; Baas *et al.* 1995) are chitinous. In the Bear Gulch

Limestone Member setae and shrimp cuticles have been replaced by apatite, which has retained the gross morphology of the original chitinous structures. Phosphatization of soft tissues is well recorded throughout the fossil record, occurring in a variety of depositional settings and taxa (Müller and Walossek 1985; Martill 1990, Wilby 1993). Non-mineralized shrimp tissues have been successfully phosphatized under laboratory conditions (Briggs and Kear 1994; Sageman *et al.* 1998). These experiments have elucidated the Eh/pH conditions required for rapid soft-tissue phosphatization to occur. However, despite such advances the source of the ions, especially P, required for phosphatization is still uncertain. Calcium and phosphorus may be derived from non-mineralized tissues themselves. Phosphorus is relatively abundant in the non-mineralized tissues of most organisms (see Vinogradov 1953). Internal sources of P for phosphatization may include body fluids, adenosine tri-phosphate (ATP) and the contents of guts (Wilby 1993). Schultze (1989) suggested that fish soft-tissues from the Cordillera de Domeyko (Jurassic, Chile) were phosphatised and that the P for this was supplied from the fish body fluids. Although blood and other body fluids are supersaturated with respect to apatite it does not precipitate owing to nucleation inhibitors and kinetic barriers (Lehninger 1982). After death precipitation barriers would fail, but it has been postulated that they may persist post-mortem for a considerable length of time (Wilby 1993). Eventually, however, body fluids may represent a potential source of phosphorous for soft-tissue mineralization. Shrimp from the Bear Gulch Limestone Member do not preserve phosphatised muscle tissue and this suggests that these tissues decayed before they could be rapidly mineralized. The microbial decay of muscle tissue, which would be rich in ATP, could lead to the release of phosphate into the local environment, leading to an increase in the P concentration. The increased concentration of P may then be available for phosphatization of the more recalcitrant exoskeleton. Decay experiments on crustaceans (Briggs and Kear 1994; and Hof and Briggs 1997) suggest that some decay is required to promote mineralization, and that the amount of phosphate in the cuticle increases with decay although the abundance of calcium remains similar (Briggs and Kear 1994). Briggs and Kear (1994) showed that partial phosphatization of non-mineralised tissue was possible when the source of P was the organism itself, indeed as much as 80% of the phosphate came from the decaying shrimp (Briggs and Kear 1994). For example, in their decay experiments, the worm *Nereis* did not become phosphatised, whereas the shrimp *Crangon crangon* and the prawn *Palaemon* sp. did show phosphatization of the cuticle and muscles (Briggs and Kear 1993). This difference may be attributed to the higher original concentration of P in the shrimp compared with the worm as no sediment was used in the experiments. Anaerobic decay of organic matter can also cause the release of volatile fatty acids and CO_2 which if unable to escape can build up (Parkes and Senior

1988) and lead to a drop in pH from approximately 8 to between 6 and 7 (Briggs and Kear 1993). Subsequently, with an increased concentration of P and a lower pH, kinetic factors could be overcome and phosphatization would be more likely to be activated because a lowering of the pH generally increases the stability of apatite relative to $CaCO_3$ (Nathan and Sass 1981).

Fossilized fish from the Santana Formation (Lower Cretaceous, Brazil) have phosphatised muscle tissue preserved in very fine detail and this is thought to be associated to a build up of P in the surrounding sediment (Martill 1988). However, it is unlikely that the Bear Gulch Limestone Member had much P available for phosphatization of non-mineralized tissues. Ca^{2+} is the fifth most abundant element in seawater ($\approx 4.1 \times 10^5$ µg/l), whereas phosphorus is a biolimiting element and seldom exceeds 90 µg/l (Mason and Moore 1982). Seawater is supersaturated with apatite (Dietz *et al.* 1942), but kinetic factors prevent it from precipitating authigenically (Atlas 1975). Therefore, post-mortem phosphatization of non-mineralized tissues must involve a process that elevates the concentration of dissolved phosphorus ($H_2PO_4^-$, HPO_4^{2-}, PO_4^{3-}) in the proximity of the decaying non-mineralized tissues, and overcomes the kinetic barriers that at low ambient seawater temperature would ordinarily render authigenesis extremely slow (Mason and Moore 1982). P is usually returned to the water column. However, under oxic conditions P is adsorbed and precipitated with ferric iron oxides, but, on removal of oxygen and subsequent reduction of Fe, P is liberated to solution (Ingall *et al.* 1993). Phosphorus chelated onto iron hydroxides within the sediment (Wilby 1993), or fixed to microbial mats (Wilby *et al.* 1996), represents a source of elevated P concentration for soft tissue phosphatization. In the Bear Gulch Limestone Member there are low levels of both clay and iron (see table 4A); XRF data reveals that the maximum FeO is 1.45 wt%, much lower than the value for PAAS. In addition, microbial mats cannot be invoked to temporarily fix P (cf. Wilby *et al.* 1996) in the Bear Gulch Limestone Member. Although there are strands of mineralized 'hyphae' in the sediment and running across some fossils from the basin facies (Text-fig. 3A-B), which may represent the remains of microbial mats, there is no evidence of extensive broken laminae in the sediments, which are characteristic of sediments that contained microbial mats (see Gall *et al.* 1985; Bernier *et al.* 1991). Therefore, neither adequate clays nor microbial mats for chelation and trapping of P occurred in the Bear Gulch Limestone Member. I conclude that P must have been dominantly sourced internally.

There are conflicting views on the length of time required for phosphatization of non-mineralized tissues. Based on observations of the rate of gill decomposition of modern fish in seawater, Martill and Harper (1990), suggested that mineralization in gills of fish from the Romualdo Member of the Santana Formation (Cretaceous, Brazil) was

extremely rapid, occurring between 1 to 2 hours post-mortem. Wilby (1993) suggested that phosphatization of skeletal fish muscle from the Crato Formation (Cretaceous, Brazil) occurred within 55 hours after death. However, in both the Santana Formation and the Crato Formation the source of P was thought to be external and already highly concentrated (Wilby 1993). Briggs and Kear (1994), based on experimental phosphatization of shrimp, suggested that a time lapse of two weeks was necessary between death and mineralization, in order to permit microbes to release P from the shrimp's cuticle into the surrounding water. In the shrimp from Bear Gulch Limestone Member it is clear that some initial decay has occurred because no muscles have been preserved and fossils are found preserved in two dimensions. This initial decay may have been a prerequisite to cuticle phosphatization; firstly, to reduce the pH and secondly to release sufficient P for phosphatization. Apatite precipitation is extremely pH and supersaturation sensitive (Nancollas 1982), and thus the most heavily mineralised zone of non-mineralized tissue should represent the area that provided the most favourable environment for its precipitation. Phosphatization of non-mineralized tissues in the Burgess Shale (Middle Cambrian, Canada) is restricted to particular taxa, and even to particular organs (Briggs and Whittington 1985). In *Leanchoilia* from the Burgess Shale phosphatization is limited to the midgut and possibly the excretory organs on the third podomere of its great appendages (Burton and Whittington 1983, Butterfield 2002). This specificity of mineralization implies that the source of phosphorus was internal and that the absence of any Santana-type preservation of muscle argues against a significant source of external phosphate (Butterfield 2002). The presence of phosphatised gut tracts of polychaetes from the Bear Gulch Limestone Member (Text-fig. 9) implies that the majority of phosphate was from an internal source, and perhaps related to the prey it had consumed. Furthermore, the gut of the organism would have contained bacteria, which may have mediated the mineralization process by overcoming nucleation barriers. Unfortunately, the textures seen in the polychaete gut, setae, shrimp cuticles and polychaete gut from the Bear Gulch Limestone Member provided no clues as to the process of mineralization.

Calcite mineralization

Whilst many polychaetes from the Bear Gulch Limestone Member have only retained an imprint of their soft tissue and the trace of their gut, two polychaete worms studied were composed entirely of crystals of calcium carbonate (Text-fig. 8A-C). In these specimens, $CaCO_3$ crystals define both the body of the polychaete and their scolecodonts and show a sharp margin with the adjacent sediment (Text-fig. 8A-C). This indicates that the fossil

was the focus for mineral growth. In experiments on shrimp, calcite crystals formed more consistently and extensively when the pH was above the dissociation constant for carbonic acid (pK_1 = 6.38), below this $CaPO_4$ precipitated (Sageman *et al.* 1998). The Bear Gulch Limestone Member polychaetes are 30mm long and it is possible that the mass of tissue was insufficient to release an adequate amount of acidic biproducts during decay to sustain any significant fall in pH and initiate apatite formation, thus $CaCO_3$ precipitated instead.

Tissue imprints

Polychaete worms from the Bear Gulch Limestone Member are frequently found as tissue imprints (see *Symmetroprion* n. sp., chapter 2), where none of the original fossil material remains, but where the fossil morphology is recorded as an imprint in the sediment. Imprints are likely to result from the consolidation of the surrounding fine-grained sediment prior to the complete decay of the body of the polychaete. The polychaete must have been rapidly buried, but presumably conditions, especially Eh/pH, were not conducive towards soft part mineralization.

Carbonized refractory versus carbonized volatile tissue

There is no clear distinction between which tissue types should be classed as refractory and which as volatile. Organic carbon occurs in sediments in a variety of complex molecules in association with oxygen, nitrogen, hydrogen and phosphorus (Allison 1990). These various molecules decay at different rates according to molecular configuration and chemical formulae (Allison 1990). On decay of an organism all organic material will be affected by many variable factors such as the supply of oxygen and other electron donors; environmental factors such as pH, sediment geochemistry, rate of burial, temperature; and the nature of the organic carbon (see Allison 1988b; 1990; Allison and Briggs 1991). Forms of organic material which are most amenable to decay, such as soft parts of most animals, are known as volatiles and those that exhibit a degree of decay resistance are known as refractories (Allison 1990). In normal marine conditions it is usual that those tissues with an originally high mechanical strength survive. Whereas, only in conservation Lagerstätte, where one or more of the variable factors may be abnormal, do tissues with a low mechanical strength, that would otherwise decay rapidly, survive. For the examples below I have made the distinction between the tissue types based upon their decay resistance and occurrence in the fossil record. Those that I have considered as carbonized refractory tissues (scleroprotein) are often found outside conservation

Lagerstätten whereas the carbonized volatile tissues (eyes and internal organs of fish) considered below are almost exclusively found in conservation Lagerstätten.

Carbonized refractory tissues

Scolecodonts of polychaetes are relatively decay resistant; they are commonly the only remains of a polychaete to be found (see Eriksson 2000). Modern polychaete jaw apparatuses are composed of scleroprotein (Voss-Foucart *et al.* 1973). In the Bear Gulch Limestone Member scolecodonts are composed of carbon. Based on decay experiments Briggs *et al.* (1995) suggested that some organic material can be decay resistant and eventually be replaced by other organic matter. For example, graptolites are thought to have a periderm originally composed of unmineralized scleroprotein (Crowther 1981; Underwood 1992) but remains are often composed of carbon (Briggs *et al.* 1995). *Rhabdopleura* periderm is assumed to be similarly decay resistant to graptolite periderm (Briggs *et al.* 1995). Decay experiments on *Rhabdopleura*'s proteinaceous periderm found that the periderm survived for at least ten weeks under anoxic conditions (Briggs *et al.* 1995). Briggs *et al.* (1995) suggested (based on Curie-point-gas-chromatography and Curie-point-gas-chromatography-mass spectrometry of graptolite and *Rhabdopleura* periderm) that graptolite periderm underwent incorporation and replacement by components derived probably from algal cell walls, which may have led to the formation of resistant biomacromolecules of a kerogen-like composition. Therefore, the scolecodonts composed of carbon in the Bear Gulch Limestone Member may have been preserved by the slow replacement of the original material, by organic components that then formed resistant biomacromolecules in a similar manner to that suggested by Briggs *et al.* (1995) for graptolite periderm. Alternatively, the scolecodonts from the Bear Gulch Limestone Member may not have undergone chemical replacement over time and the carbon may represent the chemical residue of the original resistant scleroprotein. However, further analysis would be required using techniques employed by Briggs *et al.* (1995) to determine whether the scolecodonts have undergone chemical replacement or alteration of the original scleroprotein.

Carbonized volatile tissues

Bear Gulch Limestone Member fish preserve non-mineralized volatile soft tissues including gut tracts and well-vascularized abdominal organs such as the liver, spleen and gonads, as well as major venous sinuses such as orbital, gonadal and pelvic (Grogan and Lund 1997; 2002). The liver, spleen and gonads are preserved as black coloured areas

and the livers occasionally as bituminous layers of measurable thickness (Grogan and Lund 2002). However, previously, no chemical analyses of these areas have been carried out.

Fish analysed in this investigation revealed elevated levels of carbon, coincident with the position of the eyes and probable heart or liver, relative to the surrounding sediment. These areas look, at least superficially, very similar to the 'black-coloured areas' representing various fish organs described by Grogan and Lund (1997; 2002). There was also a clay mineral coating the carbon film.

Organic preservation of non-mineralizing animals is rare. However, preservation of non-mineralized tissues as carbonized organic films has been recognised in some Burgess Shale fossils (Butterfield 1990), in fossils from the Waukesha Dolomite (Wisconsin, USA) of Silurian age (Mikulic *et al.* 1985), in a graptolite of Silurian age (Loydell *et al.* 2004), in the Upper Carboniferous Castlecomer Fauna of southeastern Ireland (Orr *et al.* 2002), the Pennsylvanian Francis Creek Shale (Thompson 1979) and the Eocene Green River Shale (Bradley 1931).

Preservation of organic carbon in the Burgess Shale has been thoroughly investigated (Butterfield 1990, 1995; Orr *et al.* 1998). Here, so called Burgess Shale-type preservation of originally non-mineralized arthropod cuticles occurs as carbon compressions (Butterfield 1990). However, Orr *et al.* (1998) showed that Burgess Shale-type preservation also involved clay mineralization of more labile tissues. Butterfield (1990) suggested that the inhibition of organic biodegradation in the fossils was due to pervasive clay-organic interactions, so that decay and autolytic enzyme destruction was terminated (Butterfield 1990, 1995). Clays with their potentially enormous surface area have a high adsorption potential and this was thought to aid in preservation of organic carbon in the Burgess Shale (Butterfield 1990). Butterfield (1990, 1995) noted that although the original clay mineralogy of the Burgess Shale is now difficult to determine, owing to diagenesis, it may have included an abundance of expandable and/or high cation exchange capacity clays, such as those in the montmorillonite-smectite group, and particularly nontronite (Fe-rich smectite) (Butterfield 1990 p. 279). The presence of these clays was important as they could have had the capacity to adsorb carbon compounds onto the clay mineral surfaces and within the smectite interlayer (Kennedy *et al.* 2002). However, the presence of these clays in the Burgess Shale sediment has since been questioned by Powell (2003). XRF data of the Bear Gulch Limestone Member reveals a maximum Fe0 at 2.4 wt% (mean = 1.44 wt%, sd = 0.5, n = 19), whereas FeO in the Burgess Shale is 2.74 wt% (Walcott Quarry 1), 3.87 wt% (Walcott Quarry 2), 7.17 wt% (Raymond Quarry) 5.56 wt% (Tuzoia Beds) (Powell 2003). The low Fe content in the Burgess Shale led Powell (2003) to suggest that there were no significant Fe-rich phases

e.g. nontronite or other Fe-rich smectites present in the rock prior to metamorphism. The total FeO in the Bear Gulch Limestone Member is, in turn, lower than analyses from the Burgess Shale, which would imply that no Fe-rich smectites were present in the Bear Gulch Limestone Member beds, so adsorption of enzymes and bacteria onto their surfaces cannot have been important.

Butterfield (1990) stated that high levels of decay inhibition are associated with high clay to organic-carbon ratios and that the Burgess Shale has a low total organic carbon of <0.13%. Towe (1996) and Powell (2003) both argued that the initial depositional values of total organic carbon in the Burgess Shale were a lot higher (>1.5%; Powell 2003). Williams (1983) showed that the Bear Gulch Limestone Member basin facies has low levels of total organic carbon (T.O.C. 0.52%). XRD analysis of the Bear Gulch Limestone Member revealed that there is some illite/mica, smectite and kaolinite present in the basin facies sediment. However, the maximum abundance of clays was only 9% of the sediment (mean = 5.05, sd = 2.25, n = 19) (see table 2). Therefore, with a low clay and low total organic carbon composition in the sediment it is unlikely that the model proposed by Butterfield (1990) of incomplete recycling of organic carbon involving a high clay to organic ratio is applicable in the Bear Gulch Limestone Member.

Butterfield's model (1990) mainly accounts for external cuticular carbon preservation (Butterfield 2002), where the cuticle would have been in direct contact with the sediment. Carbon preservation is also found in at least *Ottoia*, *Canadia* and the gut of *Eldonia* from the Burgess shale (Butterfield 1995), where internal cavities were thought to have been permeated with fine-grained clays. The Bear Gulch Limestone Member has acuticular tissues preserved as carbon films, e.g. eyes of fish, and some internal tissues. For clay to halt biodegradation of internal tissues it would have to be forcibly injected into the body cavities or grow authigenically, but evidence of this has not seen in the Bear Gulch Limestone Member fossils.

Petrovich (2001) presented a model that claimed that preservation in the Burgess Shale and several other conservation Lagerstätten could be attributed to decay inhibition as a result of adsorption of free Fe^{2+} ions onto structural biopolymers derived from Fe (III) reduction. Again this is problematic when applied to the Bear Gulch Limestone Member because there is no indication of initial Fe^{2+} concentrations in the water column and there is no significant amount of Fe associated with the Bear Gulch Limestone Member fossils. Indeed, the addition of $FeCl_2$ or $FeSO_4$ during decay experiments on shrimp, did not result in any reduction in decay (Briggs 2003). XRD analysis of the Bear Gulch Limestone Member basin facies sediments revealed that the low percentage of Fe in the sediment is now contained within ankerite (maximum 7%), or in pyrite (up to 1% in bed 10b) (see table 2). Although the Bear Gulch Limestone Member sediments had a low Fe content and low

clay content carbon preservation still occurred. The low Fe content implies that Petrovich's (2001) model for organic carbon preservation cannot be applied to account for organic preservation in fossils in the Bear Gulch Limestone Member.

Where organic carbon is preserved in specimens from the Bear Gulch Limestone Member, they are often coated with, or associated with, a fine film of clays. Clays replacing soft tissues have been noted from fossils from the Burgess Shale and the Ordovician Soom Shale (Towe 1996; Gabbott *et al.* 1998; Orr *et al.* 1998). The clays seen on the Bear Gulch Limestone Member fossils may have formed authigenically in the same manner as outlined by Gabbott (1998) and Orr *et al.* (1998), but this is very difficult to assess. Gabbott *et al.* (1998) showed that the clays replacing soft tissues in the Soom Shale had a distinctive texture, compared with those in the sediment. In the Bear Gulch Limestone Member the texture of the clay coating on the fossils was not dissimilar to the texture of the surrounding sediment, which was also Si and Al rich. Any further compositional differences could not be tested due to the very thin nature of the sediment coating the fossils. It is highly possible that the clay rich layer may simply represent a very thin clay rich lamination on the fossil, which was not directly involved in fossil preservation.

The preserved eye of the fish (specimen ROM-29784) may be attributed to the original presence of the pigment eumelanin, an insoluble polymer (Cheun 2004) whose complex bonds may have made it relatively resistant to bacterial decay (Viohl 1990). Subsequent degradation and transformation of the original complex molecule may lead to the preservation of the tissue as condensed insoluble organic matter (Allison and Briggs 1991). Allison (1988) recorded the presence of a preserved ink sac in a Jurassic cephalopod; originally this would have been composed of the molecule melanin (Allison and Briggs 1991). Melanin pigments are also present within internal organs of modern fish (Rocha, Monteiro and Pereira 1994; Meseguer, Lopezruiz and Esteban 1994), but whether the concentration of such pigments is sufficient to render fossilised impressions of organs is not known.

Unknown original composition

Taphonomy can be useful in interpreting enigmatic organisms because it can provide clues to their original composition. For example, based on the interpretation of the mode of preservation of the original histology Butterfield (2003) suggested that putative lobopods in the Sirius Passet biota and putative deuterostomes in the Chengiang biota were in fact arthropods. Although the Bear Gulch Limestone Member fossils show a complex taphonomic history, it can be seen that for some original tissue compositions a

fossil composition may be predicted. Thus, it may be possible to suggest the original composition of fossil enigmatic organisms preserved in the Bear Gulch Limestone Member from their fossil compositions and this may help to constrain their taxonomic affinities.

The enigmatic square objects are preserved as amorphous carbon films or as impressions in the sediment (Text-fig. 11A-B). It is possible that these enigmatic fossils were originally wholly organic. However, in the Bear Gulch Limestone Member the starfish *Lepidastella* Welch 1984 which should have had calcitic hardparts is also found preserved as either amorphous carbon films or impressions in the sediment. Therefore, it is also possible that the square objects may have had a carbonate biomineral component. However, it is considered unlikely that the square objects had an apatitic biomineral component as this mineral has survived dissolution in other fossil taxa in the Bear Gulch Limestone Member.

The distinctive, so-called ferrodiscus structure of *T. wellsi* (Text-fig. 12a-b) has a taphonomy that is similar to that of the fish eye and heart or liver investigated herein. All are composed of amorphous carbon films and are surrounded by elevated Ca and P abundances. This taphonomy was not observed in any of the other Bear Gulch Limestone Member tissues investigated and suggests that the ferrodiscus was perhaps an eye or other major organ within *T. wellsi*.

SUMMARY AND CONCLUSION

There are no published examples of mass kill horizons in the Bear Gulch Limestone Member that would represent instantaneous critical changes in the environment. Immediately post-mortem pelagic organisms would have sunk at varying rates to the seabed. There is no evidence to suggest any significant lateral transport prior to deposition on the seabed, although disarticulation does not always result from transport if the organism is freshly dead (Allison 1986). There is a lack of alignment of fossils indicating that there was an absence of strong currents in the Bear Gulch bay. Water column anoxia, with intermittent times of an oxic water column, is evident from the framboid size distribution in the sediment and offers an explanation for the limited macrobiological activity on the sea floor. However, at times when the bottom was oxygenated, carcasses would have been susceptible to scavenging by benthic organisms. Articulated skeletons and the remarkable preservation of non-mineralized tissue further suggests that at times there was little macrobiological activity on the floor of the basin; and this is supported by the lack of macro-bioturbation. Consequently, there would have been a higher preservation potential of organisms during times of anoxia. Episodic events of

rapid burial are evident from archaeostomatopods with folded raptorial thoracopods underneath their carapace (c.f. Hof and Briggs 1997), the presence of preserved fully articulated fish, and buried arborescent sponge communities (Lund *et al.* 1993). The substrate was probably not soupy as few fossils lie at an angle to bedding.

Fossils from the Bear Gulch Limestone Member demonstrate preservation of original biominerals, where apatite remains, but is chemically altered, and carbonate phases are variously preserved, either occurring as altered carbonate, or as impressions. Organic biomolecules are preserved as impressions, mineral replacements, or as carbon.

H_2S produced by organic decay caused the pH surrounding the decaying organism to decrease, leading in some instances, to calcite dissolution. Burial of a decaying organism caused a slower diffusion of decay gases into the water column leading to a lower pH immediately around the organism. The low Fe concentrations allowed H_2S to build up around the decaying carcasses, further reducing the pH and therefore favouring apatite rather than carbonate precipitation (Briggs and Kear 1994; Sagemann *et al.* 1998). In comparison with the detailed muscle tissues preserved in apatite in the Santana Formation, where there may already have been an external source of P in the sediment, enabling very rapid mineralization, muscle tissue in the Bear Gulch Limestone Member is extremely rare (Lund *et al.* 1993). Most of the phosphate required for apatite mineralization was probably derived from an internal source and thus phosphatization only occurred in taxa with phosphate rich organic tissues; therefore, some decay was a prerequisite for phosphatization to occur.

It is possible to speculate that the most rapidly decayed tissues have been lost and consequently, it is probable that most organisms present in the Bear Gulch Bay living community that were entirely composed of labile, easily decayed tissues, such as jellyfish and ophioroids, are absent from the preserved community.

Labile internal and external tissues from the Bear Gulch Limestone Member show carbon preservation. The low Fe and clay content of the sediment means that models proposed for carbon preservation in the Burgess Shale by Butterfield (1990) and Petrovich (2001) are not applicable to preservation in the Bear Gulch Limestone Member. Therefore, in the Bear Gulch Limestone Member an alternative pathway for carbon preservation must have occurred.

CONCLUSIONS

Conservation Lagerstätten provide more data on the diversity of ancient communities than the normal fossil record (Briggs 2003). The Bear Gulch Limestone Member of central Montana, USA, is a conservation Lagerstätte and contains exceptionally preserved vertebrate and invertebrate fossils.

Several taxa from the Bear Gulch Limestone Member have been investigated in this thesis and our knowledge of the taxonomy, morphology, palaeoecology and evolutionary relationships of these fossil groups has increased.

Large 0coiled cephalopods (>70mm in diameter) from the Bear Gulch Limestone Member are encrusted with epibionts: *Sphenothallus*, bryozoans, 'microconchids', orbiculoid brachiopods. However, smaller cephalopods (<50mm in diameter) do not have epibionts. *Sphenothallus* displays holoperipheral cover and a preferred growth orientation forwards of, and towards the apertures of two of the coiled cephalopods. This indicates that the epibionts attached to the cephalopod whilst it was alive and swimming in the water column.

That *Sphenothallus* attached primarily to live coiled cephalopods in the Bear Gulch Limestone Member may indicate that *Sphenothallus* had a planktonic larval stage. Specimens of *Sphenothallus* had a film between their longitudinal thickenings and the film, which displays previously unknown millimetre scale annulations, was sometimes encrusted by other sphenothallid basal attachment discs. The presence of the basal attachment discs on the film implies that this film was originally quite rigid and inflexible, so as to be able to withstand such a large number of epibionts attaching to it.

Complete jaw apparatuses of two eunicid polychaete worms were described. *Symmetroprion* n. sp. is of labidognath type and is distinguished from members of Polychaetaspidae, Paulinitidae, Ramphoprionidae and Kielanoprionidae by the presence of a leobasal plate and a high degree of symmetry in the jaw apparatus. Although the family Conjungaspidae has a basal and laeobasal plate the morphology of these elements together with the morphology of the carriers was very different from that of *Symmetroprion* n. sp. This is the first record of a member of the genus from the Carboniferous and the first assemblage of a member of the Symmetrioprionidae found together with the remains of its body. Articulated fossil polychaete jaws found in their preserved bodies are extremely rare, supplying a second aspect in the identification of extinct polychaetes, and providing further morphological characters to compare with extant polychaetes.

Brochosogenys reidiae was distinguished from *B. bipunctus* because the MI elements do not have the prominent second denticles. *B. reidiae* also does not have

small secondary denticles along the falcal arch that are characteristic of *B. siciliensis*. This is the first record of this species from the Bear Gulch Limestone Member and only the second articulated assemblage of *B. reidiae* reported from the Carboniferous.

The first cycloid *Halicyne montanensis* was also described from the Bear Gulch Limestone Member (Appendix 8). The pattern of the segments in its posterior thorax reinforces analogous similarities between crabs and cycloids suggested by Schram *et al.* (1997).

The presence of a member of the genus *Halicyne* in Bear Gulch supports the Late Paleozoic chronofaunal continuum described by Schram (1981) and furthers our understanding of the habitat in which they lived.

The remarkable preservation of non-mineralized tissues and the many articulated skeletons in the Bear Gulch Limestone Member indicate that at times there was little macrobiological activity on the floor of the basin. Periodic events of rapid burial occurred, aiding fossil formation by excluding macroscavengers. Evidence of small pyrite framboids (<5μm) indicates that water column anoxia occurred, but the presence of some large framboids (>7μm) suggests that intermittently an oxic water column existed.

Fossils from the Bear Gulch Limestone Member demonstrate preservation of original biominerals, where apatite remains, but is chemically altered, and carbonate phases are variously preserved. The carbonate phases either occur as altered carbonate, or as impressions. Non-mineralized tissues are preserved as impressions, permineralized replacements in apatite or calcite, or preserved as carbon residues or films.

Most of the phosphate required for apatite permineralization was probably derived from an internal source, because there was limited P in the surrounding sediment and thus phosphatization only occurred in taxa with phosphate rich organic tissues. Therefore, some decay, to release P from tissues, must have been a prerequisite for phosphatization to occur. This investigation corroborates the idea of a calcium carbonate-calcium phosphate switch (Allison 1988b) and decay experiments by Briggs and Kear (1994), which indicated that the main control on whether calcium phosphate or calcium carbonate precipitated was decay-induced pH.

Labile internal and external tissues are preserved as carbon. The low clay and Fe content of the sediment means that models proposed for carbon preservation in the Burgess Shale by Butterfield (1990) and Petrovich (2001) are not applicable for the Bear Gulch Limestone Member fauna. Consequently, in the Bear Gulch Limestone Member an alternative pathway for carbon preservation must have occurred. It is possible that within certain organs, bacteria did not break down recalcitrant macromolecules, such as melanin, and subsequently, though time, these altered to stable carbon residues that mimic the position of original organs.

FUTURE WORK

The research described in this thesis has opened up several lines of further enquiry. To date the lateral extent of the Bear Gulch Limestone Member and its relationship to the surrounding Heath Shale Formation is not well understood. A geological map of the Bear Gulch Limestone Member and surrounding locations has not been published. Progress in this area has been hindered by poor outcrop exposure, lack of permission to access the area from landowners and the presence of military installations. It is possible that in future some of these circumstances may change and allow more work on the relationship between the Bear Gulch Limestone Member and the Heath Shale to be carried out.

This investigation centred on the basin facies of the Bear Gulch Limestone Member. Ideally a study of sediment mineralogy and fossil geochemistry should be carried out in the shelf and marginal facies of the Bear Gulch Limestone Member in order to determine whether there is any relationship between fossil distribution, preservation and sedimentology across the basin. Comparable taphonomic studies with other carbonate conservation Lagerstätten such as the Solnhofen Limestone, of Germany, which has similar styles of fossil preservation (e.g. apatite in fish, polychaetes, crustaceans and squid (Wilby *et al.* 1995), calcite crystal bundles in crustaceans (Briggs and Wilby, 1996) and carbon in cephalopod ink sacs (Viohl, 1990), would be useful to determine the geochemical disparities or similarities between these sites.

To date, little work has been done on the distribution of the fauna across the basin. It was an initial aim of this thesis to gain an understanding of the distribution of the fauna using fieldwork and field notes compiled by Grogan and Lund (fossil locality information is not given in this thesis in order to protect the site). However, this was not possible because in previous excavations not all fossils found were retained or recorded. A further problem was the lack of information indicating what horizon the fossils were found at. Without knowing whether the fossil came from the top or bottom of a section it is impossible to detect a facies change or a real distribution at a specific time horizon. Therefore, it is hoped that detailed locational, and bed by bed, fossil collection will be carried out in the Bear Gulch Limestone Member in the future so that a comprehensive faunal distribution analyses across the basin can be undertaken.

Many more specimens of polychaete fossils, with their scolecodonts, from the Bear Gulch Limestone Member exist in museum collections, which have not yet been described. Scolecodont systematics and the phylogeny of polychaetes are both in need of further research. The ability to combine scolecodont systematics with the morphology of the body of the fossil polychaete will enhance our knowledge of the characteristics of

the families of fossil polychaetes and will aid in establishing their relationship with modern polychaetes.

The Bear Gulch Limestone Member is well known for its well preserved fish fauna. The fish are thought to display the preserved remains of internal organs and vascular systems (Horner and Lund 1985; Grogan and Lund 1995, 1997) but this requires further investigation in order to elucidate the factors that control decay inhibition and preservation. Although analyses of the eye of two fish, and an internal organ (heart or liver) of one fossil fish have been carried out herein, showing them to be composed of carbon, a more detailed investigation into the preservation of these internal structures, particularly those present in large fish fossils, should be carried out. A detailed chemical analysis, perhaps by gas chromatography-mass spectrometry analysis may aid in understanding the processes of preservation and highlight disparities in the mode of preservation of different internal organs.

Underlying the Bear Gulch Limestone Member is the stratigraphically older Becket Limestone Member, also a limestone lens. The formation of the Becket Limestone Member was thought to be similar to the formation of the Bear Gulch Limestone Member (Williams 1983); therefore, it is possible that the Becket Limestone Member is also a conservation Lagerstätte. However, thus far the Becket Limestone Member has received little attention. If the Becket Limestone Member contains exceptionally well preserved fossils then a comparison between its fauna and the Bear Gulch Limestone Member would determine whether any changes in palaeoecology occurred between the two Members and may lend further credence to the suggestion of a Carboniferous faunal continuum (Schram 1979). If the Becket Limestone Member does not contain exceptionally preserved fossils then a mineralogical and sedimentological comparison between it and the Bear Gulch Limestone Member may lead to a better understanding of why the Bear Gulch Limestone Member contains exceptionally well-preserved fossils.

REFERENCES

ALLISON, P. A. 1986. Soft-bodied animals in the fossil record; the role of decay and fragmentation during transport. Geology, 14:979-981.

ALLISON, P. A. 1988. Soft-bodied squids from the Jurassic Oxford Clay. Lethaia, 21:403-410.

ALLISON, P. A. 1988b. Konservat- Lagerstätten: cause and classification. Palaeobiology, 14:331-344

ALLISON, P. A. 1990. Decay processes. *In* D. E. G. Briggs and P. R. Crowther (eds.), Palaeobiology a synthesis. Blackwell scientific publications, 583p.

ALLISON, P. A., AND D. E. G. BRIGGS. 1991. Taphonomy of non-mineralized tissues, p. 560. *In* P. A. Allison and D. E. G. Briggs (eds.), Taphonomy: releasing the data locked in the fossil record. Plenum Press, New York and London.

ATLAS, E. L. 1975. Phosphate Equilibria in sea water and interstitial waters, PhD thesis Oregon State University, USA.

BAAS, M., D. E. G. BRIGGS, J. D. H. V. HEEMST, A. J. KEAR, AND J. W. D. LEEUW. 1995. Selective preservation of chitin during the decay of shrimp. Geochemica et Cosmochimica Acta, 59:945-951.

BABCOCK, L. E., AND R. M. FELDMAN. 1986. The Phylum Conulariida, p. 135-147. *In* A. Hoffman and M. H. Nitecki (eds.), Problematic Fossil Taxa. Oxford University Press.

BAIRD, G. C., C. E. BRETT, AND R. C. FREY. 1989. "Hitchhiking" epizoans on orthoconic cephalopods preliminary review of the evidence and its implications. Senckenbergiana Lethaea, 69:439.

BARTHEL, K. W., N. H. M. SWINBURNE, AND S. CONWAY MORRIS. 1990. Solnhofen: A study in Mesozoic palaeontology. Cambridge University Press.

BERGMAN, C. F. 1989. Silurian paulinitid polychaetes from Gotland. Fossils and Strata, 25:1-128.

BERGMAN, C. F. 1995. *Symmetroprion spatiosus* (Hinde), a jawed polychaete showing preference for reef environments in the Silurian of Gotland. GFF, 117:143-150.

BERNER, R. A. 1970. Sedimentary pyrite formation. American Journal of Science, 268: 1—23.

BERNIER, P., C. GAILLARD, J. C. GALL, G. BARALE, J. P.BOURSEAU, E. BUFFETAUT, AND S. WENZ. 1991. Morphogenetic impact of microbial mats on surface structures of Kimmeridgian micritic limestones (Cerin, France). Sedimentology, 38:127-136.

BEUS, S. S. 1980. Devonian serpulid bioherms in Arizona. Journal of Palaeontology, 54:1125-1128.

BODENBENDER, B. E., M. A. WILSON, AND T. J. PALMER. 1989. Paleoecology of *Sphenothallus* on an Upper Ordovician hardground. Lethaia, 22:217-225.

BOTTJER, D. J. 1981. Palaeoecological implications of antifouling adaptations in shelled molluscs. Geographical Society of America Abstracts with programs, 13:413-414.

BOTTJER, D. J., W. ETTER, J. W. HAGADORN, AND C. M. TANG. 2002. Exceptional Fossil Preservation. Columbia University Press, New York, 403p.

BRADLEY, W. H. 1931. Origin and Microfossils of the Oil Shale of the Green River Formation of Colorado and Utah: U. S. Geological Survey Professional Paper 168.

BRENCHLEY, G. A. 1979. Post mortem transport and population longevity recorded in scolecodont death assemblages. Palaeogeography, palaeoclimatology, palaeoecology, 28:297-314.

BRIGGS, D.E.G. 2003 The role of decay and mineralization in the preservation of soft-bodied fossils. Annual Review of Earth and Planetary Sciences 31, 275-301.

BRIGGS, D. E. G., S. H. BOTTRELL, AND R. RAISWELL. 1991. Pyritization of soft-bodied fossils: Beecher's Trilobite Bed, Upper Ordovician, New York State. Geology, 19:1221-1224.

BRIGGS, D. E. G., AND A. J. KEAR. 1993. Decay and preservation of polychaetes - taphonomic thresholds in soft-bodied organisms. Paleobiology, 19:107-135.

BRIGGS, D. E. G., AND A. J. KEAR. 1994. Decay and mineralisation of shrimps. Palaios, 9:431-456.

BRIGGS, D. E. G., A. J. KEAR, D. M. MARTILL, AND P. R. WILBY. 1993. Phosphatization of soft-tissue in experiments and fossils. Journal of the Geological Society of London, 150:1035-1038.

BRIGGS, D. E. G., R. RAISWELL, S. H. BOTTRELL, D. HATFIELD, AND C. BARTELS. 1996. Controls on the pyritization of exceptionally preserved fossils: an analysis of the Lower Devonian Hunsrück Slate of Germany. American Journal of Science, 296:633-663.

BRIGGS, D. E. G., AND H. B. WHITTINGTON. 1985. Terror of the trilobites. Natural History, 94:34-39.

BURCHETTE, T. P., AND R. RIDING. 1977. Attached vermiform gastropods in Carboniferous marginal marine stromatolites and biostromes. Lethaia, 10:17-28.

BURTON, D. L., AND H. B. WHITTINGTON. 1983. *Emeraldella* and *Leanchoilia*, two arthropods from the Burgess Shale, British Columbia. Philosophical Transactions of the Royal Society London Series B-Biolological Science, 300:553-585.

BUTTERFIELD, N. J. 1990. Organic preservation of non-mineralising organisms and the taphonomy of the Burgess Shale. Paleobiology, 16:272-286.

BUTTERFIELD, N. J. 1995. Secular distribution of Burgess-Shale-type preservation. Lethaia, 28:1-13.

BUTTERFIELD, N. J. 2002. Leanchoilia guts and the interpretation of three dimensional structures in Burgess Shale-type fossils. Paleobiology, 28:155-171.

BUTTERFIELD, N. J. 2003. Exceptional fossil preservation and the Cambrian explosion. Integrative and Comparative Biology, 43:166-177.

CHAMBERLAIN, J. A. J., P. D. WARD, AND J. S. WEAVER. 1981. Postmortem ascent of *Nautilus* shells: implications for cephalopod paleo-biogeography. Paleobiology, 7:494-509.

CHEUN, W. L. 2004. The Chemical Structure of Melanin. *Pigment Cell Research* 17:422-423.

CHIA, F. S. AND KOSS, R. 1994. Asteroidea. In: Microscopic Anatomy of Invertebrates, volume 14: Harrison, F. W. & Chia, F. S. eds, Echinodermata. pp. 169-245, Wiley- Liss, New York.

CHOI, D. K. 1990. *Sphenothallus* (Vermes) from the Tremadocian Dumugol Formation, Korea. Journal of Paleontology, 64:403-408.

CISNE, J. L. 1973. Anatomy of *Triarthrus* and the relationships of the Trilobita. Fossils Strata, 4:45-64.

CLARK, N. D. L. 1989. A study of a Namurian crustacean-bearing shale from the western Midland Valley of Scotland. Unpublished Ph.D. dissertation, University of Glasgow, 341p.

CLARKSON, E. N. K. 1998. Invertebrate palaeontology and evolution. Blackwell Sci., London, 452p.

COLBATH, G. K. 1986a. Jaw mineralogy in eunicean polychaetes (Annelida). Micropalaeontology, 32:186-189.

COLBATH, G. K. 1986b. Taphonomic implications of polychaete jaws recovered from gut contents of queen triggerfish. Lethaia, 19:339-342.

COLBATH, G. K. 1987a. Evidence for shedding maxillary jaws in eunicid polychaetes. Journal of Natural History, 21:443-447.

COLBATH, G. K. 1987b. An articulated polychaete jaw apparatus from the Carboniferous Kittanning Formation, western Pennsylvania, U.S.A. Paläontologische Zeitschrift, 61:81-86.

CONWAY MORRIS, S. 1986. The community structure of the Middle Cambrian Phyllopod bed (Burgess Shale). Palaeontology, 29:423-467.

CONWAY MORRIS, S. 1990. *Typhloesus wellsi* (Melton and Scott, 1973), a bizarre metazoan from the Carboniferous of Montana, USA. Philosophical Transactions of the Royal Society of London B, 327:595-624.

CORRADINI, D., AND R. OLIVIERI. 1974. *Langeites siciliensis* n. sp., a polychaete jaw apparatus from the Permo-Carboniferous of northwestern Sicily. *Bollettino Società Paleontologica Italiana*, 13:156-163. Modena.

COX, R. S. 1986. Preliminary report on the age and palynology of the Bear Gulch Limestone (Mississippian, Montana). Journal of Paleontology, 60:952-956.

CROWTHER, P.R. 1981. The fine structure of graptolite periderm. – Special Papers in Palaeontology 26: 1-119.

DALES, R. P. 1962. The polychaete stomodeum and the interrelationships of the families of Polychaeta. Proceedings of the Geological Society London, 139:398-428.

DALES, R. P. 1963. Annelids. Hutchinson University Library, London.

DEER, W. A., R. A. HOWIE, AND J. ZUSSMAN. 1995. An introduction to the rock forming minerals. Longman Scientific and Technical, 696p.

DI CANZIO, J. 1985. Ecomorphology of the Osteichthyes from the Bear Gulch Limestone. C.r. IX Congr. Int. Strat. Geol. Carbonifère, 5:501-512.

DIETZ, R. S., K. O. EMERY, AND F. P. SHEPARD. 1942. Phosphorite deposits on the sea floor off southern California. Bulletin of the Geological Society of America, 53:815-847.

DONOVAN, S. K. 1989. Taphonomic significance of the encrustation of the dead shell of Recent *Spirula spirula* (Linne) (Cephalopoda: Coleoidea) by *Lepas anatifera* Linne (Cirripedia:Thoracia). Journal of Palaeontology, 63:698-702.

DONOVAN, S. K., AND S. BAKER. 2003. Post-Palaeozoic nautiloids. Geology Today, 19:181.

EHLERS, E. 1864-68. Die Borstenwurmer, nach systematischen und anatomischen Untersuchungen dargestellt (Annelida, Chaetopoda) 1/2. Leipzig, 748p.

EICHWALD, E. 1854. Die Grauwackenschichten von Liev- und Esthland. Bulletin de la Societe Imperiale des Naturalistes de Moscou, 27:1-111.

ERIKSSON, M. 2000. Early Palaeozoic jawed polychaetes with focus on polychaetaspids and ramphoprionids from the Silurian of Gotland, Sweden, Lund Publications in Geology. 151:1-19.

ERIKSSON, M., AND C. F. BERGMAN. 1998. Scolecodont systematics exemplified by the polychaete *Hadoprion cervicornis* (Hinde, 1879). Journal of Paleontology, 72:477-485.

ERIKSSON, M., AND M. ELFMAN. 2000. Enrichment of metals in the jaws of fossil and extant polychaetes - distribution and function. Lethaia, 33:75-81.

FACTOR, D., AND R. FELDMANN. 1985. Systematics and palaeoecology of malacostracan arthropods in the Bear Gulch Limestone (Namurian) of Central Montana. Annals of Carnegie Museum, 54:319-356.

FAUCHALD, K. 1992. A review of the Genus Eunice (Polychaeta:Eunicidae) based upon type material. Smithsonian Contribution to Zoology, 523:1-422.

FAUCHALD, K., W. STURMER, AND E. L. YOCHELSON. 1986. Sphenothallus "Vermes" in the Early Devonian Hunsrück Slate, West Germany, 77:583-588

FAUVEL, P. 1919. Annélides Polychaetes de la Guyane Française. Bulletin du Museum National D'histoire Natureille, Paris, 25:472-479.

FAUVEL, P. 1953. Annelida Polychaeta, p. 507. *In* S. Sewell (ed.), The fauna of India, including Pakistan, Ceylon, Burma and Malaya. Volume I-XII. Allahabad.

FELDMAN, H. R., R. LUND, C. G. MAPLES, AND A. W. ARCHER. 1994. Origin of the Bear Gulch Beds (Namurian, Montana, USA). Geobiology M. S., 16:283-291.

FRAAIJE, R. H. B., F. R. SCHRAM AND R. VONK. 2003. *Maastrichtiocaris rostratus* new genus and species, the first Cretaceous cycloid. Journal of Paleontology, 77: 386-388.

GABBOTT, S. E. 1998. Taphonomy of the Ordovician Soom Shale Lagerstätte: An example of soft tissue preservation in clay minerals. Palaeontology, 41:631-667.

GABBOTT, S. E. 1999. Orthoconic cephalopods and associated fauna from the late Ordovician Soom Shale Lagerstätte, South Africa. Palaeontology, 42:123-148.

GABBOTT, S. E., R. J. ALDRIDGE, AND J. N. THERON. 1998. Chitinozoan chains and cocoons from the Upper Ordovician Soom Shale Lagerstätte, South Africa; implications for affinity. Journal of the Geological Society of London, 155:447-452.

GABBOTT, S. E., M. J. NORRY, R. J. ALDRIDGE, AND J. N. THERON. 2001. Preservation of fossils in clay minerals; a unique example from the Upper Ordovician Soom Shale, South Africa. Proceedings of the Yorkshire Geological Society, 53:237-244.

GABBOTT, S. E., Hou X-G, Norry, M. J., Siveter, D. J. 2004. Preservation of Early Cambrian animals of the Chengjiang biota. Geology, 32: 901-904

GALL, J.-C. 1971. Faunes et paysages du grès à Volzia du nord des Vosges. Essai Paléoécologique sur le Buntsandstein Supérieur. Mémoires du Service de la Carte Géologique d'Alsace et de Lorraine, 34:1-318

GALL, J. C., P. BERNIER, C. GAILLARD, G. BARALE, J. P. BOURSEAU, E. BUFFETAUT, AND S. WENZ. 1985. Development of an algal film and its effect on sedimentation and taphonomy in lithographic limestones - the case of the cerin site (Upper Kimmeridgian, Southern French Jura). Compte Rendus de l academie des sciences serie II, 301:547.

GLAESSNER, M. F. 1969. Cycloidea, p. 567-570. *In* R.C. Moore (ed.), Treatise on Invertebrate Paleontology, Part R, Arthropoda 4, Volume 2. Geological Society of America and University of Kansas Press, Lawrence

GROGAN, E. D., AND R. LUND. 1995. Pigment patterns, soft anatomy and relationships of Bear Gulch Chondrichthyes., p. 145-146. *In* S. W. H. Lelièvre, A. Blieck & R. Cloutier, (eds.), Premiers Vertébrés et Vertébrés Inférieurs. Geobios, M.S.Volume 19.

GROGAN, E. D., AND R. LUND. 1997. Soft tissue pigments of the Upper Mississippian chondrenchelyid, *Harpagofututor volsellorhinus* (Chondrichthyes, Holocephali) from the Bear Gulch Limestone, Montana, USA. Journal of Paleontology, 71:337-342.

GROGAN, E. D., AND R. LUND. 2002. The geological and biological environment of the Bear Gulch Limestone (Mississippian of Montana, USA) and a model for its deposition. Geodiversitas, 24:295-315.

HALL, J. 1847. Paleontology of New-York. Volume 1. Containing descriptions of the organic remains of the Lower Division of the New-York system (equivalent to the Lower Silurian rocks of Europe). C. Van Benthuysen, Albany, 338p.

HAMADA, T. 1964. Notes on the Drifted Nautilus in Thailand, p. 255–278, Contributions to the Geology and Palaeontology of Southeast Asia, XXI. Tokyo University of Science Papers Coll. Gen. Education.Volume 14.

HARRIS, W. L. 1972. Upper Mississippian-Pennsylvanian stratigraphy of central Montana. Unpublished Ph.D. Thesis. University of Montana, Missoula. 89pp.

HARTMAN, O. 1954. Polychaetous Annelids. Part V Eunicea. Allen Hancock Pacific Expeditions, 10:1-200.

HELFMAN, G. S., B. B. COLLETTE, AND D. E. FACEY. 1997. The Diversity of Fishes. Blackwell Science, Inc., 528p.

HEMLEBEN, C. 1977. Autochthone und allochthone Sedimentanteile in den Solnhofener Plattenkalken. N. Jb. Geol. Paläont., Mh, 9:257-271.

HEMLEBEN, C., AND N. H. M. SWINBURNE. 1991. Cyclical deposition of the Plattenkalk Facies, p. 572-591. *In* G. Einsele, W. Ricken, and A. Seilacher (eds.), Cycles and Events in Stratigraphy. Springer-Verlag, Berlin.

HEPTONSTALL, W. B. 1970. Buoyancy control in ammonoids. Lethaia, 3:317-328.

HINDE, G. J. 1882. On annelid remains from the Silurian strata of the Isle of Gotland. Bihang till Kungliga Vetenskapsakademiens Handlingar, 7:3-28.

HINDE, G. J. 1896. On the jaw-apparatus of an annelid (*Eunicites reidiae* sp.nov.) from the Lower Carboniferous of Halkin Mountain, Flintshire. The Quarterly Journal of the Geological Society London, 52:438-450.

HINTS, O. 1999. Two new polychaete families from the Upper Ordovician of Estonia. Palaeontology, 42:897-906.

HOF, C. H. J., AND D. E. G. BRIGGS. 1997. Decay and mineralization of mantis shrimps (Stomatopoda: Crustacea) - A key to their fossil record. Palaios, 12:420-438.

HORNER, J. R., AND R. LUND. 1985. Biotic distribution and diversity in the Bear Gulch Limestone of central Montana. Compte Rendu, Neuvième Congrès International de Stratigraphie et de Géologie du Carbonifère, 5:437-442.

HUBERT, J. F., P. T. PANISH, AND K. S. PROSTAK. 1996. Chemistry, microstructure, petrology, and diagenetic model of Jurassic dinosaur bones, Dinosaur National Monument, Utah. Journal of Sedimentary Research, 66:531-547.

IMAJIMA, M. 1977. A new polychaete family, Hartmaniellidae, from Japan, p. 171-184. *In* D. J. Reish and K. Fauchald (eds.), Essays on Polychaetous Annelids in memory of Dr. Olga Hartman.Volume 11. Bulletin of the National Science Museum, Tokyo, A, (Zoology).

INGALL, E. D., R. M. BUSTIN, AND P. V. CAPPELLEN. 1993. Influence of water column anoxia on the burial and preservation of carbon and phosphorus in marine shales. Geochemica et Cosmochimica Acta, 54:373-386.

JENNER, R. A., C. H. J. HOF, AND F. R. SCHRAM. 1998. Palaeo- and archaeostomatopods (Hoplocarida, Crustacea) from the Bear Gulch Limestone, Mississippian (Namurian), of central Montana. Contributions to Zoology, 67:155-185.

KAUFFMAN, E. G. 1978. Benthic environments and paleoecology of the Posidonienschiefer (Toarcian). Neues Jahrbuch für Geologie und Paläontologie, Abhandlungen, 157:18-36.

KAUFFMAN, E. G. 1981. Ecological reappraisal of the German Posidonienschiefer (Toarcian) and the Stagnant Basin Model, p. 311-381 (623). *In* J. Gray, A. J. Boucot, and W. B. N. Berry (eds.), Communities of the past. Hitchinson Ross Publishing Company, Stroudsburg, Pennsylvania, 623pp.

KEMP, A. 2000. Geology. Probing the memory of mud. Nature, 406:951-953.

KEMP, R. A., AND C. N. TRUEMAN. 2002. Rare earth elements in Solnhofen biogenic apatite: geochemical clues to the palaeoenvironment. Sedimentary Geology, 155:109-127.

KENNEDY M. J., PEVEAR, D. R. AND HILL, R. J., 2002. Mineral Surface Control of Organic Carbon in Black Shale, *Science* 2002 295: 657-660

KIELAN-JAWOROWSKA, Z. 1966. Polychaete jaw apparatuses from the Ordovician and Silurian of Poland and a comparison with modern forms. Palaeontologica Polonica, Warsaw, 16:1-152;.

KINBERG, J. G. H. 1865. Annulata nova. Öfversigt af Kongliga Vetenskaps-Akademiens Förhandlingar, Stockholm, 22:239-258.

KIZILSHTIEN, L. J., AND L. G. MINAEVA. 1972. Origin of the framboidal pyrite. Doklady akademii nauk SSSR, 206:1187-1189.

KOSACZ, R., AND Z. SAWLOWICZ. 1983. Framboidal pyrite from the copper deposit on the Fore-Sudetic monocline, Poland. Rudy Metale, 8:292-297.

KOZLOWSKI, R. 1956. Sur quelques appareils masticateurs des annelides polychetes Ordoviciens. Acta Palaeontologica Polonica, 1:1-102.

KRAUSKOPF, K. B., AND D. K. BIRD. 1995. Introduction to Geochemistry (3rd Ed.), 647p.

LANDMAN, N. H., AND R. DAVIS. 1988. Preserved jaw and crop in an orthoconic nautilid cephalopod from the Bear Gulch Limestone (Mississippian, Montana, USA), p. 102-107. *In* D. L. Wolberg (ed.), New Mexico Bureau of Mines and Mineral Resources Special Volume.

LANDMAN, N. H., W. B. SAUNDERS, J. E. WINSTON, AND P. J. HARRIES. 1987. Incidence and kinds of epizoans on the shells of live *Nautilus*, p. 163-177. *In* W. B. Saunders and N. H. Landman (eds.), *Nautilus*- the biology and palaeobiology of a fossil. Plenum Press, New York.

LANGE, F. W. 1947. Annelidos poliques dos folhelhos devonianos do Parana. Arquivos do Museu Paranaense, 6:161-230.

LEHNINGER, A. L. 1982. Principles of biochemistry. Worth Publishers, New York, 1011p.

LICHTENEGGER, H. L., T. SCHOBERL, M. BARTL, H. WAITE, AND G. D. STUCKY. 2002. High abrasion resistance with sparse mineralization : copper biomineral in worm jaws. Science, 298:389-392.

LIEBIG, K. 1998. Fossil Microorganisms from the Eocene Messel Oil Shale of Southern Hesse, Germany. Kaupia, 7:1-96.

LINDSTRÖM, M. 1974. The conodont apparatus as a food gathering mechanism. Palaeontology, 17:729-744.

LOVE, L. G. 1967. Early diagenetic iron sulfides in Recent sediments of the Wash (England). Sedimentology, 9:327-352.

LOWNEY, K. A. 1985. Palaeonisciformes from the Bear Gulch Limestone. C.r. IX Congr. Int. Strat. Geol. Carbonifère, 5:513-522.

LOYDELL D.K., P. J. ORR AND S. KEARNS 2004. Preservation of soft tissues in Silurian graptolites from Latvia. Palaeontology, 47:503-513.

LUND, R. 1974. *Stethacanthus altonensis* (Elasmobranchii) from the Bear Gulch Limestone of Montana. Annals of the Carnegie Museum, 45:161-178.

LUND, R. 1977a. New information on the evolution of the bradyodont chondrichthyes. Fieldiana, Geology, 33:521-539.

LUND, R. 1977b. A new petalodont (Chondrichthyes, Bradyodonti) from the upper Mississippian of Montana. Annals of the Carnegie Museum, 46:129-155.

LUND, R. 1977c. *Echinochimaera meltoni*, new genus and species (Chimaeriformes), from the Mississippian of Montana. Annals of the Carnegie Museum, 46:195-221.

LUND, R. 1980. Viviparity and intrauterine feeding in a new holocephalan fish from the Lower Carboniferous of Montana. Science, Washington, 209:697-699.

LUND, R. 1982. *Harpagofututor volsellorhinus* new genus and species (Chondrichthyes, Chondrenchelyiformes) from the Namurian Bear Gulch Limestone, *Chondrenchelys problematica* Traquair (Visean), and their sexual dimorphism. Journal of Paleontology, 56:938-958.

LUND, R. 1983. On a dentition of *Polyrhizodus* (Chondrichthyes, Petalodontiformes) from the Namurian Bear Gulch Limestone of Montana. Journal of Vertebrate Paleontology, 3:1-6.

LUND, R. 1984. On the spines of the Stethacanthidae (Chondrichthyes) with a description of a new genus from the Mississippian Bear Gulch Limestone. Geobios, 17:281-295.

LUND, R. 1985a. The morphology of *Falcatus falcatus* (St John and Worthen) a Mississippian stethacanthid chondrichthyan from the Bear Gulch Limestone of Montana. Journal of Vertebrate Paleontology, 5:1-19.

LUND, R. 1985b. Stethacanthid elasmobranch remains from the Bear Gulch Limestone (Namurian E2b) of Montana. Am. Mus. Novit., 2828:1-24.

LUND, R. 1986a. On *Damocles serratus*, nov. gen. et sp. (Elasmobranchii: Cladodontida) from the Upper Mississippian Bear Gulch Limestone of Montana. Journal of Vertebrate Paleontology, 6:12-19.

LUND, R. 1986b. The diversity and relationships of the Holocephali. Indo-Pacific Fish Biology : Proceedings of the Second International Conference on Indo-Pacific Fishes, Tokyo : Ichthyological Society of Japan:97-106.

LUND, R. 1988. New information on *Squatinactis caudispinatus* (Chondrichthyes, Cladodontida) from the Chesterian Bear Gulch Limestone of Montana. Journal of Vertebrate Paleontology, 8:340-342.

LUND, R. 1989. New Petalodonts (Chondrichthyes) from the Upper Mississippian Bear Gulch Limestone (Namurian E_2b) of Montana. Journal of Vertebrate Paleontology, 9:350-368.

LUND, R., H. FELDMANN, W. L. LUND, AND C. G. MAPLES. 1993. The depositional environment of the Bear Gulch Limestone, Fergus County, Montana. Montana Geological Society Guidebook- energy and mineral resources of Central Montana:87-96.

LUND, R., AND W. LUND. 1984. New genera and species of coelacanths from the Bear Gulch Limestone (Lower Carboniferous) of Montana (U.S.A). Geobios, 17:237-244.

LUND, R., W. LUND, AND G. A. KLEIN. 1985. Coelacanth feeding mechanisms and ecology of the Bear Gulch coelacanths. C.r. IX Congr. Int. Strat. Geol. Carbonifere, 5:492-500.

LUND, R., AND W. G. MELTON. 1982. A new actinopterygian fish from the Mississippian Bear Gulch Limestone of Montana. Palaeontology, 25:485-498.

LUND, R., AND C. POPLIN. 1997. The rhadinichthyids (paleoniscoid actinopterygians) from the Bear Gulch Limestone of Montana. Journal of Vertebrate, Paleontology, 17:466-486.

LUND, R., AND C. POPLIN. 1999. Fish diversity of the Bear Gulch Limestone, Namurian, Lower Carboniferous of Montana, USA. Geobios, 32:285-295.

LUND, R., AND C. POPLIN. 2002. Cladistic analysis of the relationships of the Tarrasiids (Lower Carboniferous Actinopterygians). Journal of Vertebrate Paleontology, 22:480-486.

LUND, R., AND R. ZANGERL. 1974. *Squatinactis caudispinatus*, a new elasmobranch from the Upper Mississippian of Montana. Annals of the Carnegie Museum, 45:43-55.

LUTZ-GARIHAN, A. B. 1979. Brachiopods from the Upper Mississippian Bear Gulch Limestone of Montana. Palaeontology, Palaeoecology, Palaeogeography, 5:457-467.

LUTZ-GARIHAN, A. B. 1985. Brachiopods from the Upper Mississippian Bear Gulch Limestone of Montana. C.r. IX Congr. Int. Strat. Geol. Carbonifere, 5:457-467.

MAEDA, H., AND A. SEILACHER. 1996. Ammonoid taphonomy, p. 544-573. *In* L. N. H., K. Tanabe, and R. A. Davies (eds.), Ammonoid Palaeobiology.Volume 13. Plenum Press, New York and London.

MALLORY, W. W. 1972. Regional synthesis of the Pennsylvanian system. Rocky Mountain Association of Geologists, Denver, 111-127p.

MAPES, R. S. 1987. Upper Palaeozoic cephalopod mandibles: frequency of occurrence, modes of preservation and paleoecological implications. Journal of Paleontology, 61:521-538.

MARTILL, D. M. 1987. Prokaryote mats replacing soft tissues in Mesozoic marine reptiles. Modern Geology, 11:265-269

MARTILL, D. M. 1988. Preservation of fish in the Cretaceous Santana Formation of Brazil. Palaeontology, 31:1-18.

MARTILL, D. M. 1990. Macromolecular resolution of fossilized muscle tissue from an elopomorph fish. Nature, 346:171-172.

MARTILL, D. M. 1993. Soupy Substrates: A Medium for the Exceptional Preservation of Ichthyosaurs of the Posidonia Shale (Lower Jurassic) of Germany. Kaupia – Darmstädter Beiträge zur Naturgeschichte, 2:77-97.

MARTILL, D. M., AND L. HARPER. 1990. An application of critical-point drying to the comparison of modern and fossilized soft-tissues of fishes. Palaeontology, 33:423-428.

MASON, B., AND C. B. MOORE. 1982. Principles of Geochemistry. (4th Ed.). John Wiley, New York, 344p.

MASON, C., AND E. L. YOCHELSON. 1985. Some tubular fossils (*Sphenothallus*:"Vermes") from the Middle and Late Paleozoic of the United States. Journal of Paleontology, 59:85-95.

MASSALONGO. 1855. Monographia delle nereidi fossili del Monte Bolca., Verona.

MAUGHAN, E. K. 1984. Paleogeographic setting of Pennsylvanian Tyler Formation and relation to underlying Mississippian rocks in Montana and North Dakota. Bull. Am. Ass. Petrol. Geol. 68:178-195.

MAYR, F. X. 1967. Paläobiologie und Stratinomie der Plattenkalke der Altmühlalb. Erlanger Geologische Abhandlungen, 67:1-40.

McROBERTS, C. A., AND G. D. STANLEY. 1989. A unique bivalve-algae life assemblage from the Bear Gulch Limestone (Upper Mississippian) of Central Montana. Journal of Paleontology, 63:578-581.

MELTON, W. G. 1969. A new dorypterid fish from Central Montana:. Northwest Science, 43:196-286.

MELTON, W. G. 1971. The Bear Gulch fauna from Central Montana. Proceedings of the North American Paleontological Convention, 1969:1202-1207.

MELTON, W. G. J. 1972. The Bear Gulch Limestone and the first conodont-bearing animals, Montana Geological Society Annual Field Conference. 65-68.

MELTON, W. G. J., AND H. SCOTT. 1973. Conodont bearing animals from the Bear Gulch Limestone, Montana. Geological Society of America Special Paper, 141:31-65.

MERKT, J. 1966. Uber Austern und Serpeln als Epoken auf Ammonitengehausen. N. Jb. Geol. Pälaont. Abh, 125:467-479.

MESEGUER J., LOPEZRUIZ A. AND ESTEBAN M.A. 1994. Melanomacrophages of the seawater teleosts, Sea Bass (*Dicentrarchus-Labrax*) and Gilthead Seabream (*Sparus-aurata*) – Morphology, form and possible function. Cell and tissue research, 277:1.

MEYER, H. VON, 1847. *Halicyne* und *Litogaster*, zwei Crustaceen genera aus dem Muschelkalke Würtemsberg's. Paläontographica, 1:134-140.

MIERZEJEWSKA, G., AND P. MIERZEJEWSKA. 1974. The ultrastructure of some fossil invertebrate skeletons. Annals of the Medical Sections of the Polish Academy of Sciences, 19:133-135.

MIKULIC, D. G., D. E. G. BRIGGS, AND K. J. KLUESSENDORF, 1985. A new exceptionally preserved biota from the lower Silurian of Wisconsin, USA. Philosophical Transactions of the Royal Society London Series B-Biolological Science, 311: 75.

MULLER, K. J., AND D. WALOSSEK. 1985. A remarkable arthropod fauna from the Upper Cambrian 'Orsten' of Sweden. Transactions of the Geological Society, London, 151:195-207.

MUNDT, P. A. 1956. The Tyler and Alaska Bench Formations. Billings Geological Society Guide Book, 7th Annual Field Conference:46-51.

NANCOLLAS, G. H. 1982. Phase transformation during precipitation of calcium salts., p. 77-79. *In* G. H. Nancollas (ed.), Biological Mineralization and Demineralization. Springer-Verlag.

NATHAN, Y., AND E. SASS. 1981. Stability relations of apatites and calcium carbonates. Chemical Geology, 34:103-111.

NEAL, M. L. AND J. T. HANNIBAL. 2000. Paleoecology and taxonomic implications of *Sphenothallus* and *Sphenothallus*-like specimens from Ohio and areas adjacent to Ohio. Journal of Paleontology, 74:369-380.

NORBY , R. D. 1976. Conodont apparatuses from Chesterian (Mississippian) strata of Montana and Illinois. Ph.D. thesis, University of Illinois at Urbana-Champaign.

NORRY, M. J., A. C. DUNHAM, AND J. D. HUDSON. 1994. Mineralogy and element fractionation during mudrock sedimentation. Journal of the Geological Society, London, 151:195-207.

ORENSANZ, J. M. 1990. The eunicemorph polychaete annelids from Antarctic and subantarctic seas. Biology of the Antartic seas XXI, Antarctic Reasearch Series, 52:1-183.

ORR, P. J., D. E. G. BRIGGS, AND S. L. KEARNS. 1998. Cambrian Burgess Shale Animals Replicated in Clay Minerals. Science, 281:1173-1175.

ORR, P. J., S. L. KEARNS, AND D. E. G. BRIGGS. 2002. Backscatter electron imaging of fossils exceptionally preserved as organic compressions. Palaios, 17:110-117.

PAPUNEN, H. 1966. Framboidal texture of the pyritic layer found in a peat bog in SE Finland. Bulletin of Comm. Geol. Finland, 222:117-125.

PARK, M.-H., AND F. FÜRSICH. 2001. Cyclic nature of lamination in the Tithonian Solnhofen Plattenkalk of southern Germany and its palaeoclimatic implications. International Journal of Earth Sciences, 90:847 - 854.

PARKES, R. J., AND E. SENIOR. 1988. Multistate chemostats and other models for studying anoxic ecosystems. P.51-71. *In* J. W. T. Wimpenny (ed.), Handbook of

laboratory model systems for microbial ecosystems, Volume 1. CRC Press, Boca Raton, Florida.

PAXTON, H. 1980. Jaw growth and replacement in Polychaeta. Journal of Natural History, 14:543-546.

PETROVICH, R. 2001. Mechanisms of fossilization of the soft-bodied and lightly armoured faunas of the Burgess shale and of some other classical localities. American Journal of Science, 301:683-726.

PHILLIPS, J. 1835. Illustration of the Geology of Yorkshire, 2nd edition. John Murray, London. i-xii, 184p., 23 plates, 1 map.

PICKERING, K. T., N. G. MARSH, AND B. DICKIE. 1993. Data report: inorganic major, trace and rare earth element analyses of the muds and mudstones from Site 808. Proceedings of the Ocean drilling Program, Scientific Results, 131.

POPLIN, C., AND R. LUND. 2000. Two new deep-bodied actinopterygians from Bear Gulch, (Montana, USA, Lower Carboniferous). Journal of Vertebrate Paleontology, 20:428-449.

POPLIN, C., AND R. LUND. 2002. Two Carboniferous fine-eyed palaeoniscoid (Pisces, Actinopterygii) from Bear Gulch (USA). Journal of Paleontology, 76:10144-11028.

POTTER, P. E., J. B. MAYNARD, AND W. A. PRYOR. 1980. Sedimentology of Shale. Springer-Verlag New York-Heidelberg-Berlin, 306p.

POWELL, W. 2003. Greenschist-facies metamorphism of the Burgess Shale and its implications for models of the fossil formation and preservation. Canadian Journal of Earth Science, 40:13-25.

PROTHERO, D. R. 1990. Interpreting the Stratigraphic Record. W.H. Freeman, New York, 410p.

PURNELL, M. A. 1993. The *Kladognathus* apparatus (Conodonta, Carboniferous): homologies with ozarkodinids, and the prioniodinid bauplan. Journal of Palaeontology, 67:875-882.

PURNELL M. A., 2003. Casting, replication and anaglyph stereo imaging of microscopic detail in fossils, with examples from conodonts and other jawless vertebrates. Palaeontologia Electronic, 6 Issue 2.

PUURA, I., AND J. NEMLIHER. 2001. Apatite varieties in recent and fossil linguloid brachiopod shells, 441p. *In* C. H. C. Brunton, L. R. M. Cocks, and S. L. Long (eds.), Brachiopods past and present. Taylor and Francis, London.

REED, S. J. B. 1993. Electron microprobe analysis. Cambridge University Press, 326p.

RHODES, F. H. T. 1973. Conodont Research: Programs, progress and prioritories. Geological Society of America Special Paper, 141:277-286.

RICHARDSON, E. S. 1969. The Conodont Animal. Earth Sciences, 6:256-257.

RIDING, R. 2000. Microbial carbonates: the geological record of calcified bacterial-algal mats and biofilms. Sedimentology, 47:179-214.

RIGBY, J. K. 1979. The Sponge fauna from the Mississippian Heath Formation of Central Montana. Palaeontology, Palaeoecology, Palaeogeography, 5:443-456.

RIGBY, J. K. 1985. The Sponge fauna from the Mississippian Heath Formation of Central Montana. Compte Rendu, Neuvième Congrès International de Stratigraphie et de Géologie du Carbonifère, 5:443-456.

ROCHA E., MONTEIRO R. A. F. AND PEREIRA C. A. 1994. The liver of the brown trout, *Salmo-trutta fario* – a light and electron microscope study. Journal of Anatomy. 185: 241-249

ROUSE, G. W., AND F. PLEIJEL. 2001. Polychaetes. Oxford University Press, 353p.

RUEDEMANN, R. H. 1896a. Note on the discovery of a sessile Conularia. American Geologist, Article 1.

RUEDEMANN, R. H. 1896b. Note on the discovery of a sessile Conularia. American Geologist, 18:65-71.

SAGEMANN, J., S. J. BALE, D. E. G. BRIGGS, AND R. J. PARKES. 1998. Controls on the formation of autigenic minerals in association with decaying organic matter: An experimental approach. Geochemica et Cosmochimica Acta, 63:1083-1095.

SALTZMAN M. R. 2003. Late Paleozoic ice age: Oceanic gateway or $pCO(_2)$? Geology, 31:151-154

SAUNDERS, W. B., AND C. SPINOSA. 1979. *Nautilus* movement and distribution in Palau, Western Caroline Islands. Science, 204:1199–1201.

SAWLOWICZ, Z. 1992. Primary sulfide mineralization in Cu-Fe-S zones of Kupferschiefer, Poland. Transactions of the Institution of Mining and Metallurgy Section B-Applied Earth Science, 101:B1-B8.

SAWLOWICZ, Z. 1993. Pyrite framboids and their development: a new conceptual mechanism. Geologische Rundschau, 82:148-159.

SCHAFHÄUTL, K. E. 1863. Süd-Bayerns Lethaea Geognostica. Der Kressenberg und die südlich von ihm gelegenen Hochalpen. Leopold Voss, Leipzig. i-xvi, 487p., 98 plates.

SCHIEBER, J., D. KRINSLEY, AND L. RICIPUTI. 2000. Diagenetic origin of quartz silt in mudstones and implications for silica cycling. Nature, 406:981-985.

SCHMARDA, L. K. 1861. Neue Wirbellose Thiere beobachtet und gesammelt auf einer Reise um die Erdr 1853 bis 1857. Wilhelm Engelmann, Leipzig, pt 2: 1-164, pl. 1-22.

SCHMID-RÖHL, A., AND H.-J. RÖHL. 2003. Overgrowth on ammonite conchs: environmental implications for the Lower Toarcian Posidonia Shale. Palaeontology, 46:339-352.

SCHMIDT, AND TEICHMÜLLER. 1958. Neue Funde von *Sphenothallus* auf dem westeuropäischen Festland, insbesondere in Belgien, und ergänzende Beobachtungen zur Gattung *Sphenothallus*. Association pour l'étude de la paléontologie et de la stratigraphie houillères, 33:34 + 36 pls., maps.

SCHRAM, F. R. 1979a. The Mazon Creek biotas in the context of a Carboniferous faunal continuum. In: M.H. Nitecki (ed.), Mazon Creek Fossils: 159-190 Academic Press, New York.

SCHRAM, F. R. 1979b. Limulines of the Mississippian Bear Gulch Limestone of Central Montana, USA. Transactions of the San Diego society of Natural History, 19:67-74.

SCHRAM, F. R. 1979c. Worms of the Mississippian Bear Gulch Limestone of central Montana, USA. Transactions of the San Diego society of Natural History, 19:107-120.

SCHRAM, F. R. 1981. Late Palaeozoic crustacean communities. Journal of Paleontology, 55:126-137.

SCHRAM, F. R. 1985. The Bear Gulch crustaceans and their bearing on Late Paleozoic diversity and Permo-Triassic evolution of Malacostraca. Compte Rendu, IX Congrès International de Stratigraphie et de Géologie du Carbonifère, 5: 468-472

SCHRAM, F. R., AND J. R. HORNER. 1978. Crustacea of the Mississippian Bear Gulch Limestone of Central Montana. Journal of Paleontology, 52:394-406.

SCHRAM, J. M., AND F. R. SCHRAM. 1979. Joanellia lundi sp. Nov. (Crustacea: Malacostraca) from the Mississippian Heath Shale of Central Montana. Transactions of the San Diego Society of Natural History, 19:53-56.

SCHRAM, F. R., R. VONK AND C. H. J. HOF. 1997. Mazon Creek Cycloidea. Journal of Paleontology, 71: 261-284

SCHULTZE, H.-P. 1989. Three-dimensional muscle preservation in Jurassic fishes of Chile. Revista Geologica de Chile, 16:183-215.

SCHWAB, K. W. 1966. Microstructure of some fossil and Recent scolecodonts. Palaeontology, 40:416-423.

SCOTT, H. W. 1973. New Conodontochordata from the Bear Gulch Limestone (Namurian, Montana). Michigan State University Publications. Museum of Paleontology, 81-100.

SEILACHER, A. 1960. Epizoans as a key to ammonoid ecology. Journal of Paleontology, 34:189-193.

SEILACHER, A., AND F. WESTPHAL. 1971. Fossil Lagerstätten, Sedimentology of parts of Central Europe. International Sedimentology Congress Guidebook, 327-335.

SHEPARD, W. 1993. Upper Mississippian Biostratigraphy and Lithostratigraphy of Central Montana, p. 27-36, Guidebook: Energy & Mineral Resources of Central Montana. Montana Geological Society.

STOTZKY, G. 1980. Surface interactions between clay minerals and microbes, viruses and soluble organics, and the probable importance of these interactions to the ecology of microbes in soil., p. 231-249. *In* J. M. L. Berkeley R. C. W., J. Melling, P.R. Rutter, B. Vincent (eds.), Microbial Adhesion to Surfaces. Ellis Horwood Ltd., Chichester.

STÜRMER, W. 1970. Soft parts of cephalopods and trilobites: some surprising results of x-ray examination of Devonian Slates. Science, 170:1300-1302.

SUITS, N. S. AND R. T. WILKIN. 1998. Pyrite formation in the water column and sediments of a meromictic lake. Geology, 26:1099-1102.

SZANIAWSKI, H. 1968. Three new polychaete jaw apparatuses from the Upper Permian of Poland. Palaeontologica Polonica, 13:255-281.

SZANIAWSKI, H. 1974. Some Mesozoic scolecodonts congeneric with recent forms. Acta Palaeontologica Polonica, 19:179-199.

SZANIAWSKI, H. 1996. Scolecodonts. *In* J. Jansonius and D. C. McGregor (eds.), Palynology: principles and applications. Volume 1. American Association of Stratigraphic Palynologists Foundation. pp. 337-354

SZANIAWSKI, H., AND M. IMAJIMA. 1996. Hartmaniellidae-living fossils among polychaetes. Acta Palaeontologica Polonica, 41:111-125.

TARNEY, J. T., AND N. G. MARSH. 1991. Major and trace element geochemistry of holes CY-1 and CY-4: implications for petrogenetic models. p. 133-176. *In* I. J. Gibson, J. Malpas, P. T. Robinson, and C. Xenophontos (eds.), Cyprus crustal study project: initial report, Holes CY-1 and 1a.Volume 19-20. Paper of the Geological Survey of Canada.

TAYLOR, S. R., AND S. M. McLENNAN. 1985. The Continental Crust: its Composition and Evolution. Blackwell Scientific Publications. Geoscience texts, 312p.

THOMPSON, I. 1979. Errant polychaetes (Annelida) from the Pennsylvanian Essex Fauna of Northern Illinois. Palaeontographica A., 163:169-199.

TORSVIK T. H. AND L. R. M. COCKS. 2004. Earth geography from 400 to 250 Ma: a palaeomagnetic, faunal and facies review. Journal of the Geological Society. 161: 555-572.

TOWE, K. M. 1996. Fossil preservation in the Burgess Shale. Lethaia, 29:107-108.

UNDERWOOD, C.J. 1992. The preservation and deformation of graptolites. Palaios, 7:178-186.

VAN ITEN, H., R. S. COX, AND R. H. MAPES. 1992. New data on the morphology of *Sphenothallus*-Hall - implications for its affinities. Lethaia, 25:135-144.

VAN ITEN, H., J. A. FITZKE, AND R. S. COX. 1996. Problematical fossil Cnidarians from the Upper Ordovician of the North Central USA. Palaeontology, 34:1037-1064.

VAN ITEN, H., J. A. FITZKE, AND R. S. COX. 1996. Problematical fossil cnidarians from the upper Ordovician of the north-central USA. Palaeontology, 39:1037-1064.

VAN ITEN, H., M.-Y. ZHU, AND D. COLLINS. 2002. First report of *Sphenothallus* Hall, 1847 in the Middle Cambrian. Journal of Paleontology, 76:902-905.

VAN OOSTEN, J. 1957. The skin and scales. Physiol Fish. 1:207-244.

VINOGRADOV, A. P. 1953. The elementary chemical composition of marine organisms. Memoirs, Sears Foundation for Marine Research II, New Haven. 647p.

VOIGT, E. 1988. Preservation of soft tissues in the Eocene lignite of the Geiseltal near Halle/S. Courier Forschungsinstitut Senckenberg, 107:325-343.

VOSS-FOUCART, M. S., M. T. FOZE-VIGNAUX, AND C. JEUNIAUX. 1973. Systematic characters of some annelid Polychaetes at the level of the chemical composition of the jaws. Biochemical Systematics and Ecology, 1:119-122.

WAHL, M., AND O. MARK. 1999. The predominantly facultative nature of epibiosis: experimental and observational evidence. Marine Ecology Progress Series, 187:59-66.

WATABE, N., AND C.-M. PAN. 1984. Phosphatic shell formation in atremate brachiopods. American Zoologist, 24:977-985.

WEEDON, M. J. 1990. Shell structure and affinity of veriform gastropods. Lethaia, 23:297-309.

WELCH, J. R. 1984. The Asteroid, *Lepidastella montanensis* n. sp., from the Upper Mississippian Bear Gulch Limestone of Montana. Journal of Paleontology, 58:843-851.

WIGNALL, P. B., AND M. J. SIMMS. 1990. Pseudoplankon. Palaeontology, 33:359-378.

WIGNALL, P. B., AND R. J. NEWTON. 2001. Black shales on the basin margin: a model based on examples from the Upper Jurassic of the Boulonnais, northern France. Sedimentary Geology, 144:335-356.

WILBY, P. R. 1993. The mechanisms and timing of mineralization of fossil phosphatized soft tissues. Unpublished Ph.D. thesis, Open University, 2 volumes, 429p.

WILBY, P. R., D. E. G. BRIGGS AND G. VIOHL. 1995. Controls on the phosphatization of soft tissues in plattenkalks. 2nd International Symposium on Lithographic Limestones, Cuenca, Spain, July1995, Extended abstracts. Universidad Autonoma de Madrid, 165-166.

WILBY, P. R., D. E. G. BRIGGS, P. BERNIER, AND C. GAILLARD. 1996. Role of microbial mats in the fossilization of soft tissue. Geology, 24:787-790.

WILKIN, R. T., H. L. BARNES, AND S. L. BRANTLEY. 1996. The size distribution of framboidal pyrite in modern sediments: An indicator of redox conditions. Geochimica et Cosmochimica Acta, 60:3897-3912.

WILLIAMS, L. A. 1981. The Sedimentational History of the Bear Gulch Limestone (Carboniferous, central Montana) an explanation of "How Them Fish Swam Between Them Rocks". PhD thesis, Princeton University, Princeton, 251p.

WILLIAMS, L. A. 1983. Deposition of the Bear Gulch Limestone: A Carboniferous Plattenkalk from Central Montana. Sedimentology, 30:843-860.

WILLIAMS, L. A., AND C. E. REIMERS. 1983. Role of bacterial mats in oxygen-deficient basins and coastal upwelling regimes: A preliminary report. Geology, 11:267-269.

WILSON, R. M., J. C. ELLIOTT, AND S. E. P. DOWKER. 1999. Rietveld refinement of the crystallographic structure of human dental enamel apatites. American Mineralogist, 84:1406-1414.

WITZKE, B. J. 1990. Paleoclimatic constraints for Paleozoic paleolatitudes of Laurentia and Euramerica. Geological Society Memoir, no. 12. London: Geological Society, London. P 57-73.

WUTTKE, M. 1983. Weichteil-Erhaltung durch lithifizierte Microorganismen bei mittelozanen Vertebraten aus den Olschiefern der Grube Messel bei Darmstadt. Senckenberg Lethaea, 64:509-527.

ZIDEK, J. 1980. *Acanthodes lundi*, new species (Acanthodii) and associated coprolites, from uppermost Mississippian Heath Formation of central Montana. Annals of the Carnegie Museum, 49:49-78.

APPENDICES

Sedimentary log from the Bear Gulch Lst. Mbr. with fossils found between beds indicated

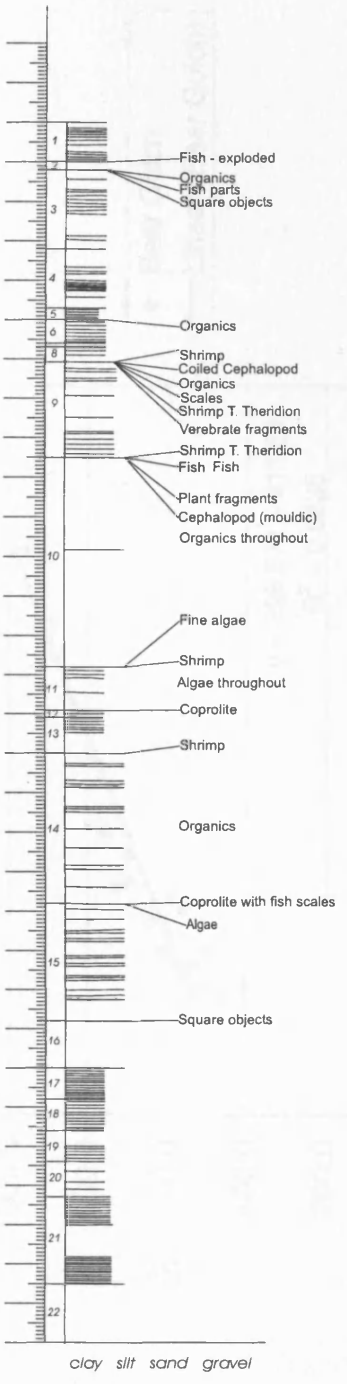

Thin sections

Bed no.

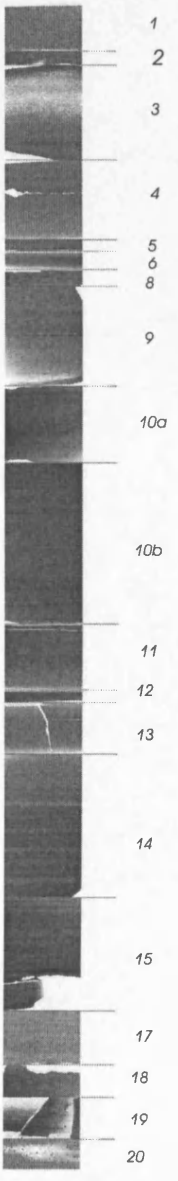

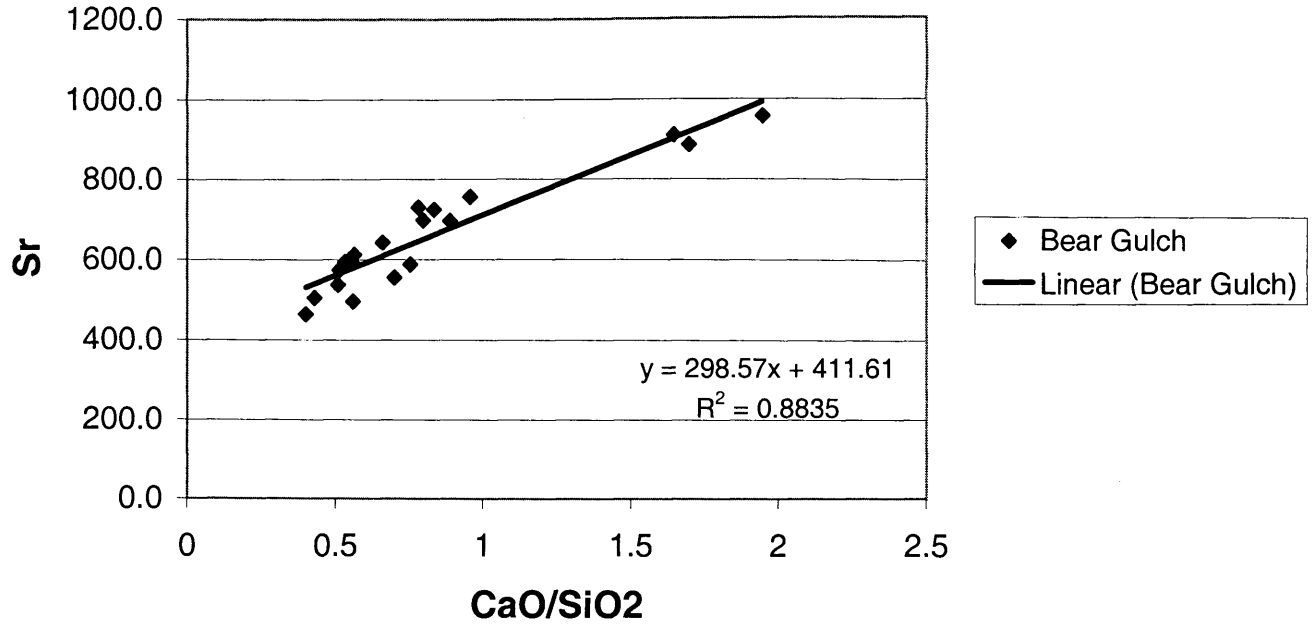

Appendix 2. A plot of Sr2+ against CaO rendered a good fit to the regression line (R2 = 0.9354) and has a positive correlation coefficient (r) of 0.97 that indicates an almost perfect relationship between the data, and reflects calcite's ability to incorporate strontium into its ionic structure.

Bed number	1	2	3	4	5	6	8	9	10a	10b	11	12	13	14	15	17	18	19	20
Bed size (mm)	10	2	20	15	3	6	5	24	24	30	11	2	9	38	30	12	8	8	8
Kaolinite	0	0	0	0	0	0	0	0	0	0	1	0	0	0	0	0	0	0	0
Illite/Mica	5	4	5	6	6	6	6	4	4	2	4	6	5	2	3	5	4	4	5
Na Smectite	0	0	3	0	0	0	0	0	0	0	1	1	0	0	0	0	0	4	0
Apatite	1	1	1	1	1	1	1	1	1	1	1	1	1	0	1	1	1	1	1
Albite	2	1	1	2	2	2	2	1	1	1	1	1	2	1	1	1	1	1	1
Kfeldspar	1	1	1	1	1	1	1	1	1	1	2	1	1	1	1	1	1	1	1
Calcite	42	50	40	37	38	33	33	50	49	66	38	37	35	70	67	48	53	43	43
Dolomite	8	7	6	8	8	8	7	6	7	4	9	10	11	3	3	7	6	7	10
Pyrite	0	0	0	0	0	0	0	0	0	1	0	0	0	0	0	0	0	0	0
Ankerite	4	4	5	4	4	5	5	4	3	1	4	4	4	2	3	4	4	7	7
Quartz	37	31	38	41	40	44	45	33	34	22	39	38	41	19	21	33	30	32	32

Appendix 3. A summary of XRD data from the Bear Gulch Limestone Member basin facies of 19 beds, recorded in sequence, and the size of the bed in mm. Beds >30mm (Flinz) are shaded.

Sample: BGDI01

University of Leicester Geological Services XRD Analysis

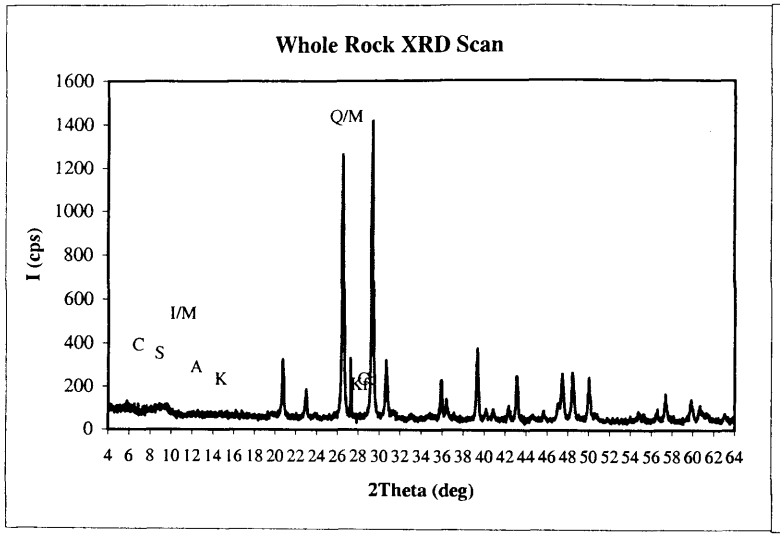

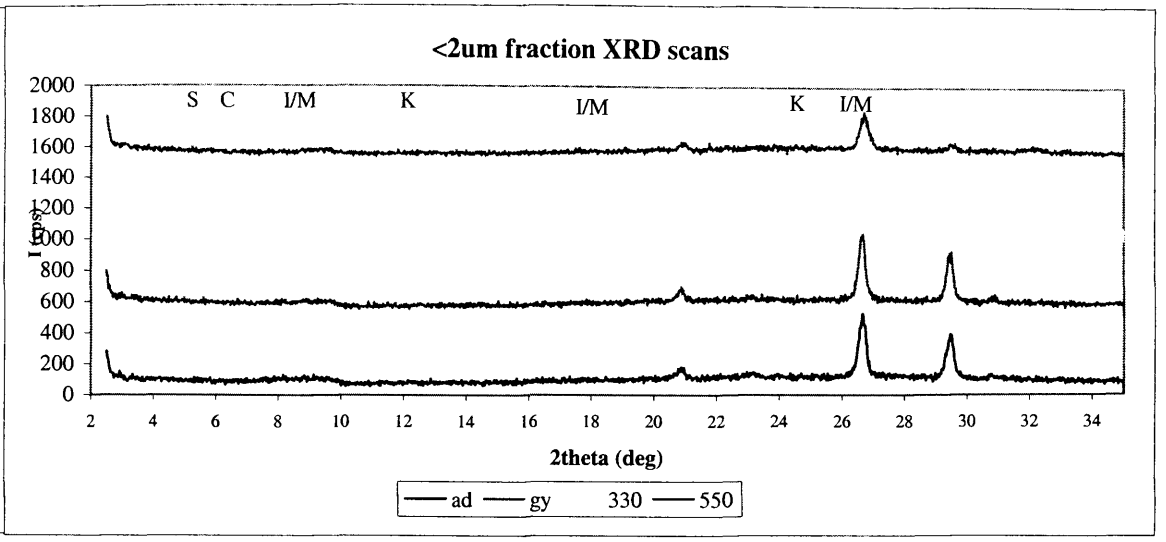

Mineral	%	Code
Illite/Mica	5	I/M
Apatite	1	Ap
Albite	2	NaF
Kfeldspar	1	Kf
Calcite	42	Cc
Dolomite	8	D
Ankerite	4	Ak
Quartz	37	Q

Mineral	Proportion of <2um fraction	Code
Illite/Mica	100	I/M

Weight of <2um fraction: **17** %

Amorphous Content: **0** %

Interlayering:

I/S	None
C/S	None

Sample: BGDI 02

University of Leicester Geological Services XRD Analysis

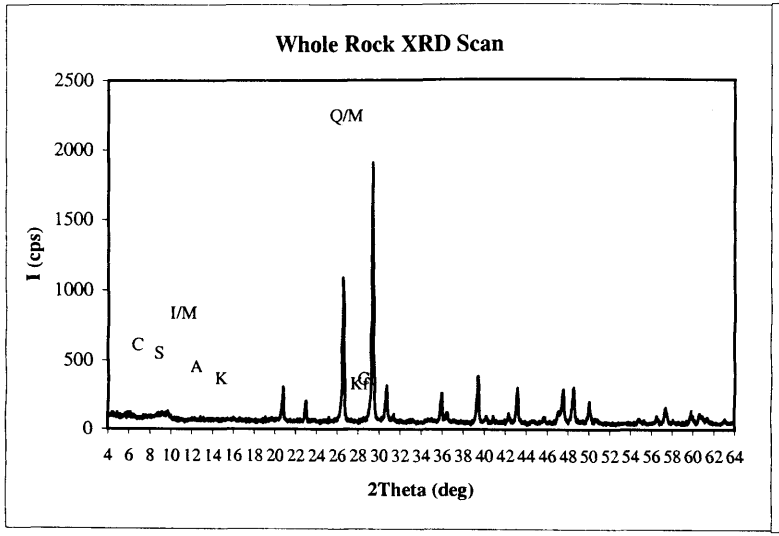

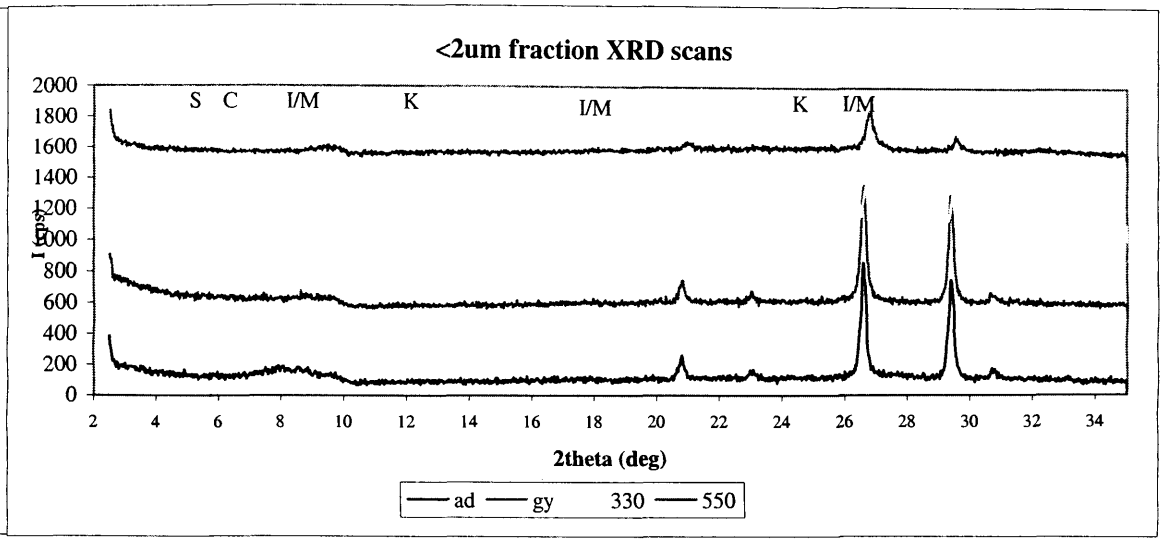

Mineral	%	Code
Illite/Mica	4	I/M
Apatite	1	Ap
Albite	1	NaF
Kfeldspar	1	Kf
Calcite	50	Cc
Dolomite	7	D
Ankerite	4	Ak
Quartz	31	Q

Amorphous Content: **0** %

Mineral	Proportion of <2um fraction	Code
Illite/Mica	100	I/M

Weight of <2um fraction: **17** %

Interlayering: I/S None
C/S None

Sample: BGDI 03

University of Leicester Geological Services XRD Analysis

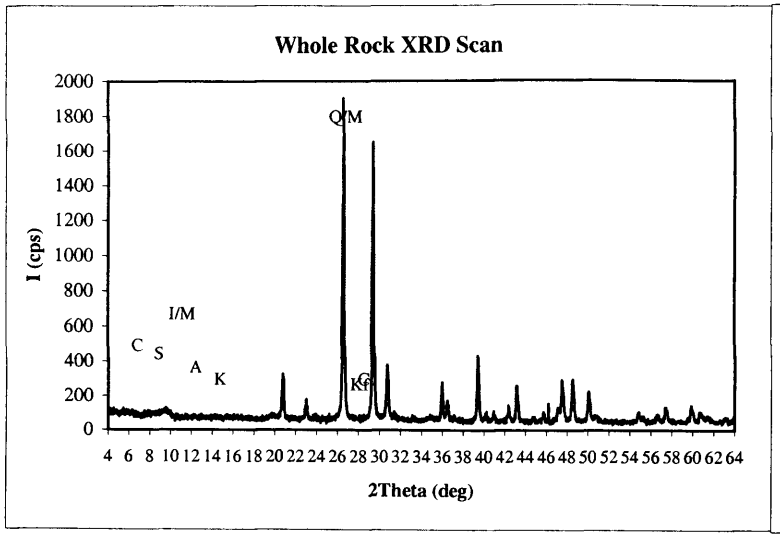

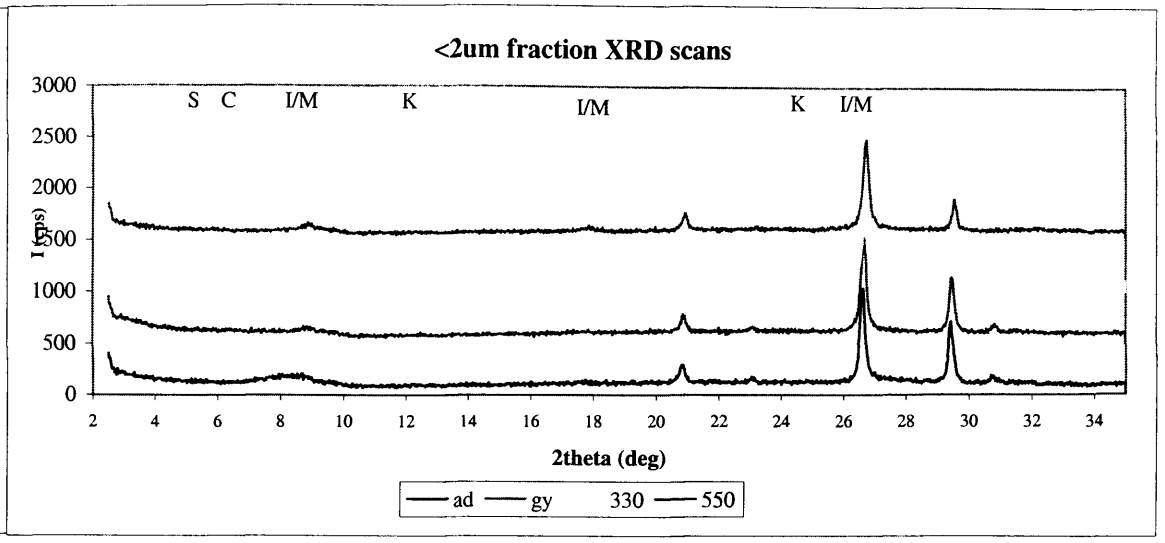

Mineral	%	Code
Illite/Mica	5	I/M
Na Smectite	3	S
Apatite	1	Ap
Albite	1	NaF
Kfeldspar	1	Kf
Calcite	40	Cc
Dolomite	6	D
Ankerite	5	Ak
Quartz	38	Q

Amorphous Content: **0** **%**

Mineral	Proportion of <2um fraction	Code
Illite/Mica	66	I/M
Smectite	34	S

Weight of <2um fraction: **16** **%**

Interlayering:	I/S	None
	C/S	None

Sample: BGDI 04

University of Leicester Geological Services XRD Analysis

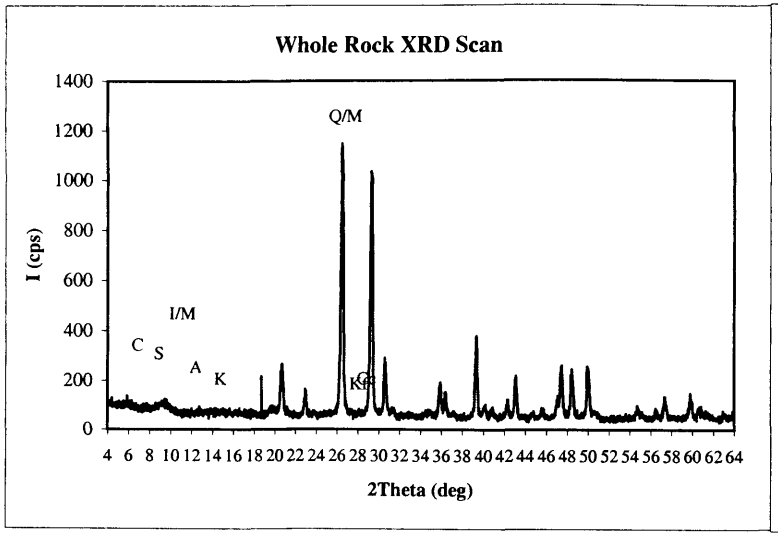

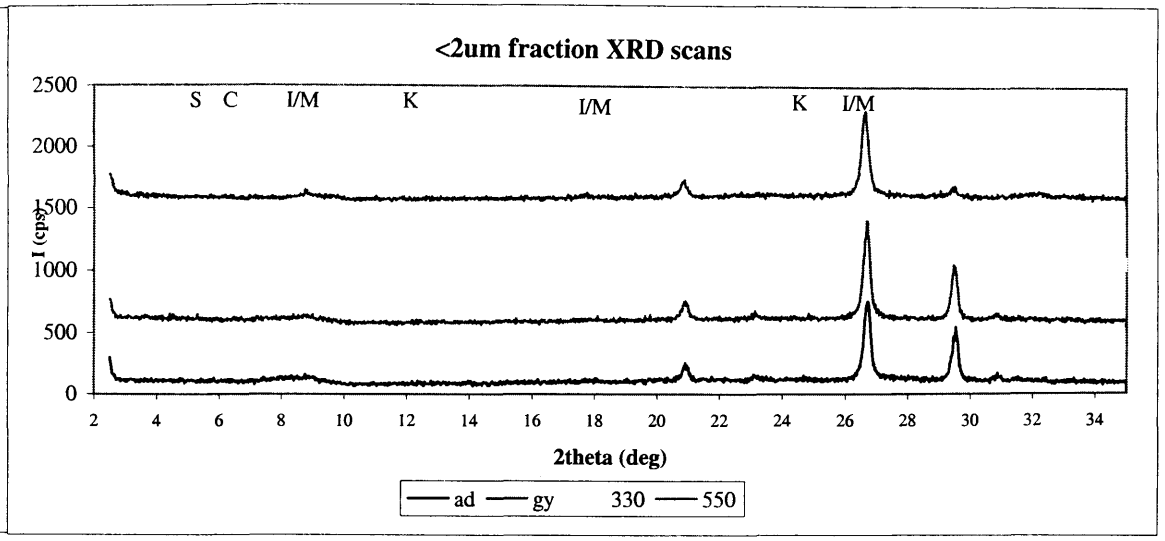

Mineral	%	Code
Illite/Mica	6	I/M
Apatite	1	Ap
Albite	2	NaF
Kfeldspar	1	Kf
Calcite	37	Cc
Dolomite	8	D
Ankerite	4	Ak
Quartz	41	Q

Amorphous Content: **0** **%**

Mineral	Proportion of <2um fraction	Code
Illite/Mica	100	I/M

Weight of <2um fraction: **21** **%**

Interlayering:	I/S	None
	C/S	None

Sample: BGDI 05

University of Leicester Geological Services XRD Analysis

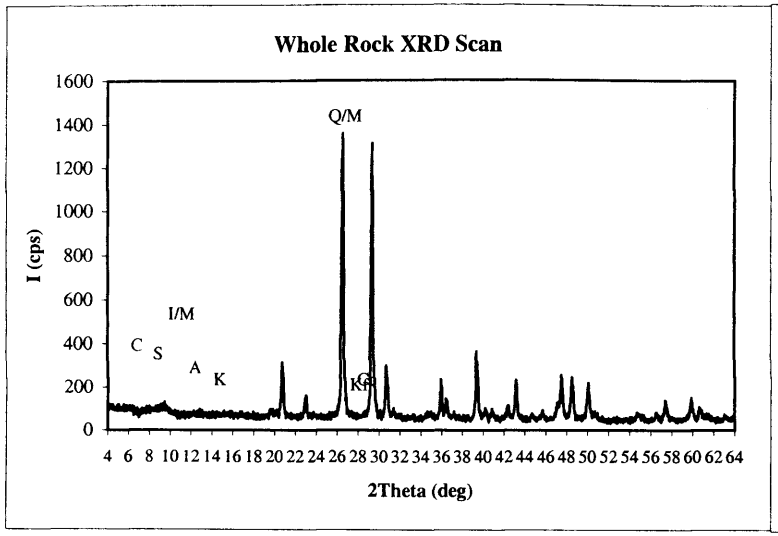

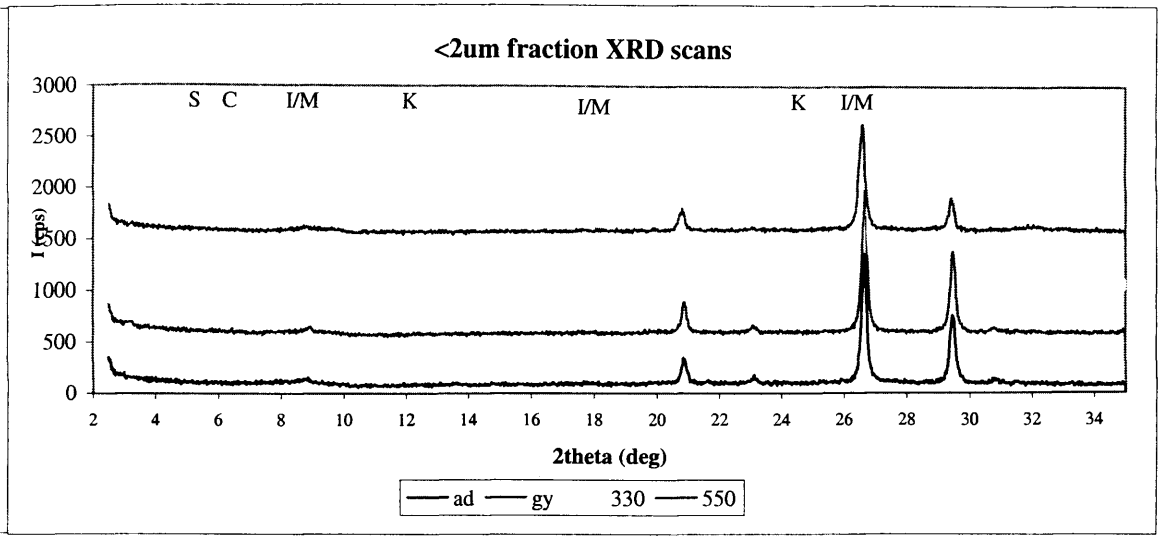

Mineral	%	Code
Illite/Mica	6	I/M
Apatite	1	Ap
Albite	2	NaF
Kfeldspar	1	Kf
Calcite	38	Cc
Dolomite	8	D
Ankerite	4	Ak
Quartz	40	Q

Amorphous Content: **0** **%**

Mineral	Proportion of <2um fraction	Code
Illite/Mica	100	I/M

Weight of <2um fraction: **27** **%**

Interlayering:	I/S	None
	C/S	None

Sample: BGDI 06

University of Leicester Geological Services XRD Analysis

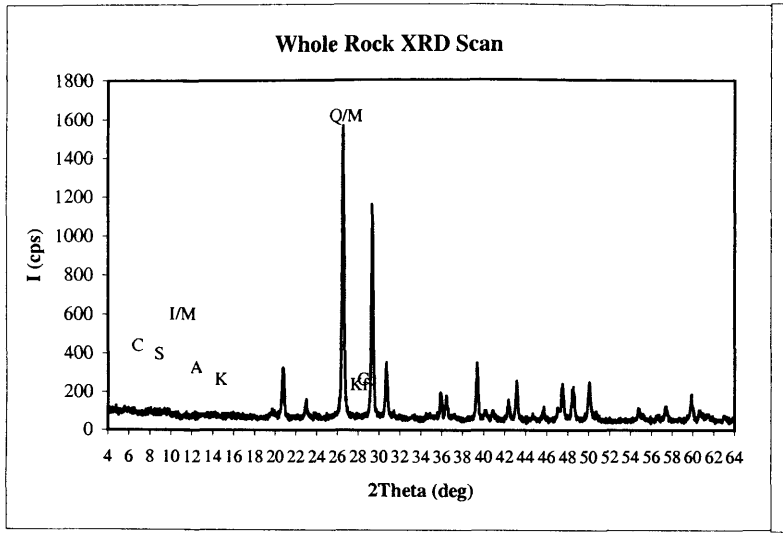

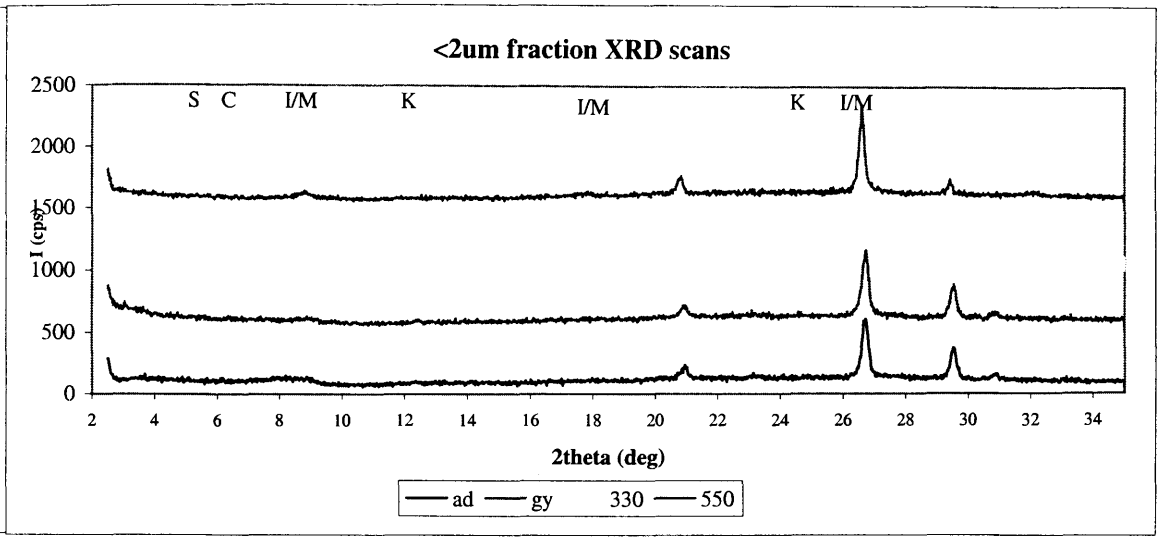

Mineral	%	Code
Illite/Mica	6	I/M
Apatite	1	Ap
Albite	2	NaF
Kfeldspar	1	Kf
Calcite	33	Cc
Dolomite	8	D
Ankerite	5	Ak
Quartz	44	Q

Amorphous Content: **0** %

Mineral	Proportion of <2um fraction	Code
Kaolinite	15	K
Illite/Mica	85	I/M

Weight of <2um fraction: **21** %

Interlayering: I/S None
C/S None

Sample: BGDI 08

University of Leicester Geological Services XRD Analysis

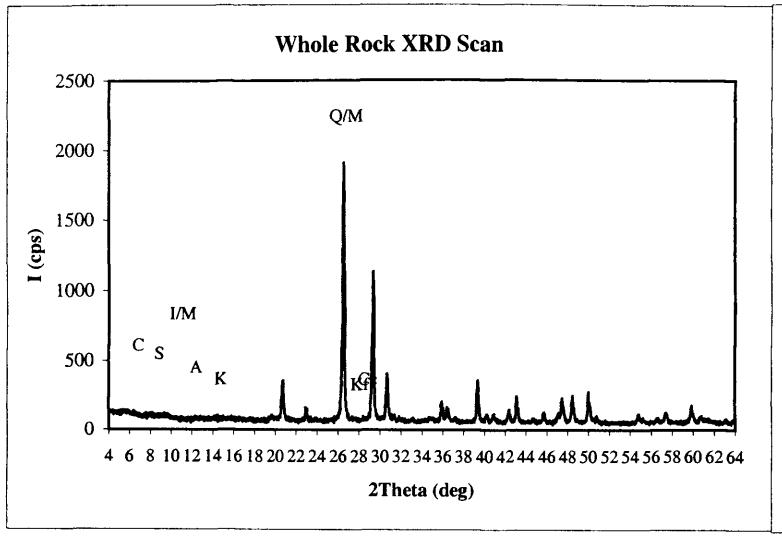

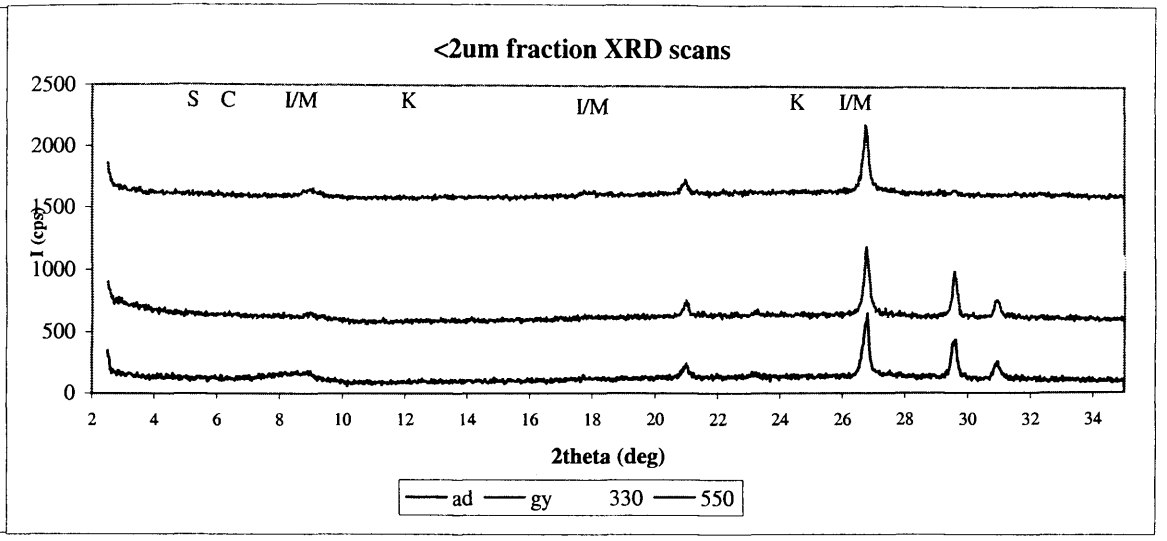

Mineral	%	Code
Illite/Mica	6	I/M
Apatite	1	Ap
Albite	2	NaF
Kfeldspar	1	Kf
Calcite	33	Cc
Dolomite	7	D
Ankerite	5	Ak
Quartz	45	Q

Amorphous Content: **0** %

Mineral	Proportion of <2um fraction	Code
Illite/Mica	100	I/M

Weight of <2um fraction: **21** %

Interlayering:

I/S	None
C/S	None

Sample: BGDI 09

University of Leicester Geological Services XRD Analysis

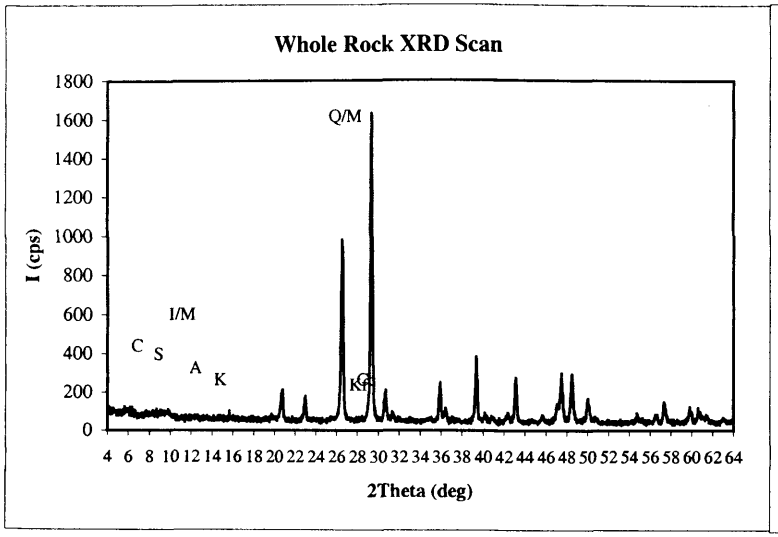

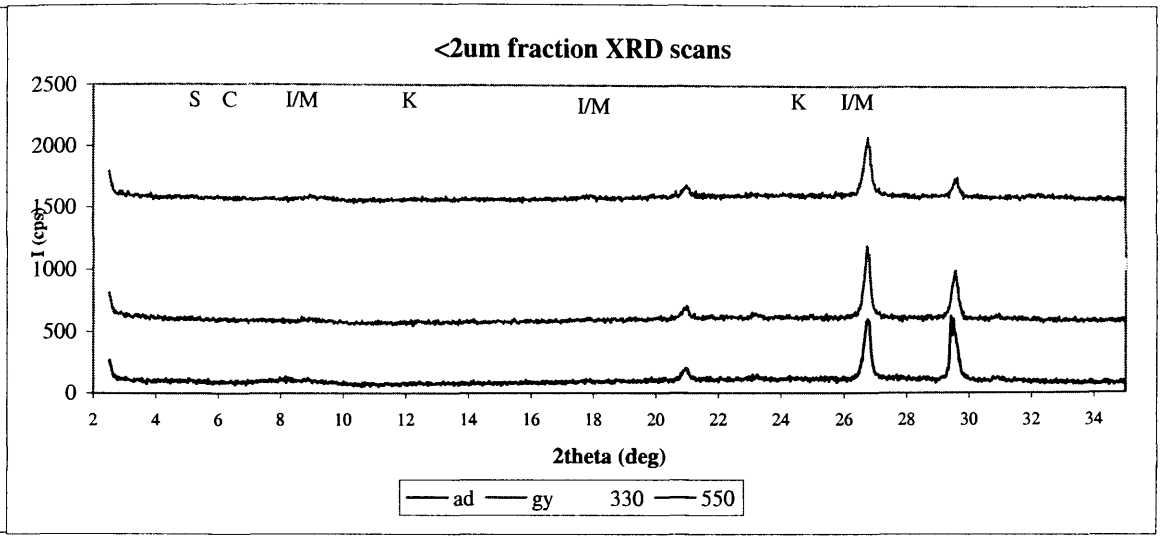

Mineral	%	Code
Illite/Mica	4	I/M
Apatite	1	Ap
Albite	1	NaF
Kfeldspar	1	Kf
Calcite	50	Cc
Dolomite	6	D
Ankerite	4	Ak
Quartz	33	Q

Amorphous Content: **0** %

Mineral	Proportion of <2um fraction	Code
Illite/Mica	100	I/M

Weight of <2um fraction: **16** %

Interlayering:		
	I/S	None
	C/S	None

Sample: BGDI 10A

University of Leicester Geological Services XRD Analysis

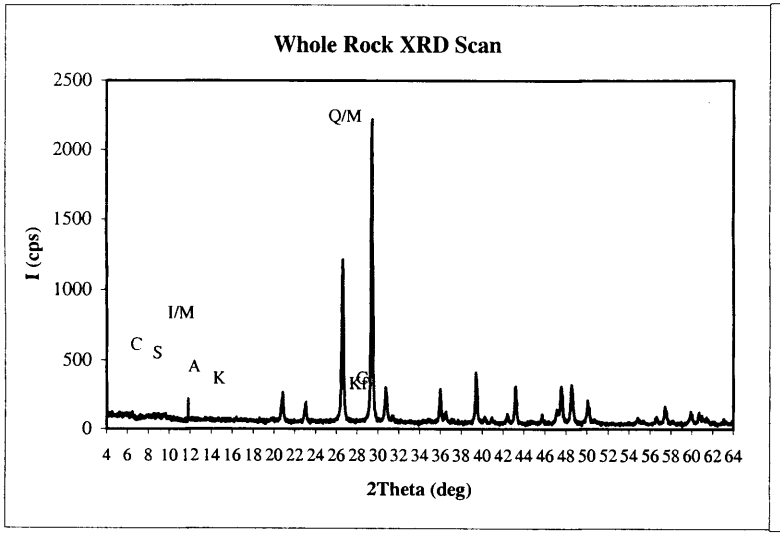

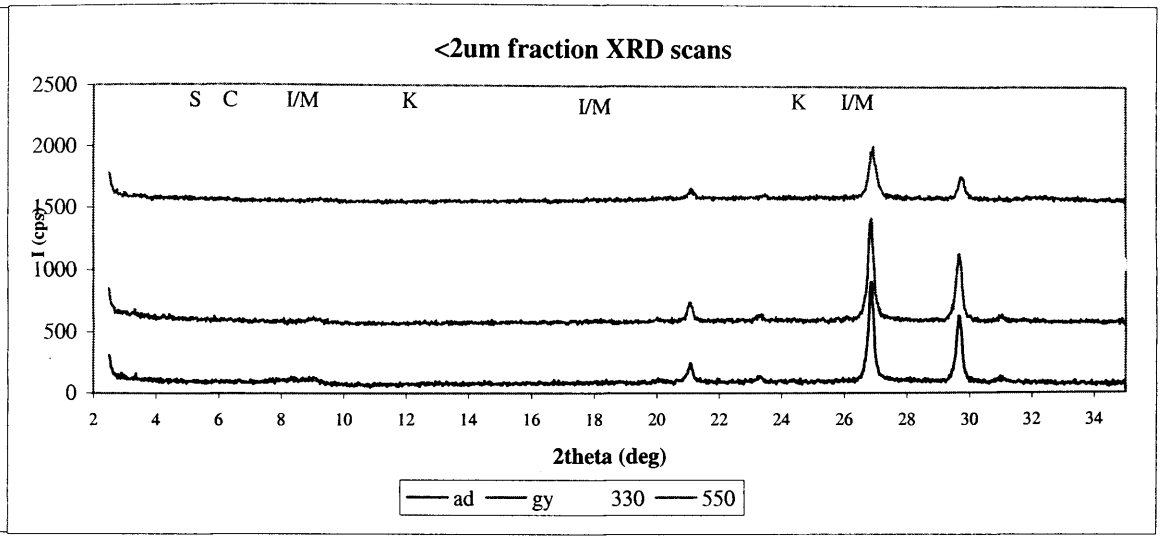

Mineral	%	Code
Illite/Mica	4	I/M
Apatite	1	Ap
Albite	1	NaF
Kfeldspar	1	Kf
Calcite	49	Cc
Dolomite	7	D
Ankerite	3	Ak
Quartz	34	Q

Mineral	Proportion of <2um fraction	Code
Illite/Mica	100	I/M

Weight of <2um fraction: **11** **%**

Amorphous Content: **0** **%**

Interlayering:

	I/S	None
	C/S	None

Sample: BGDI 10B

University of Leicester Geological Services XRD Analysis

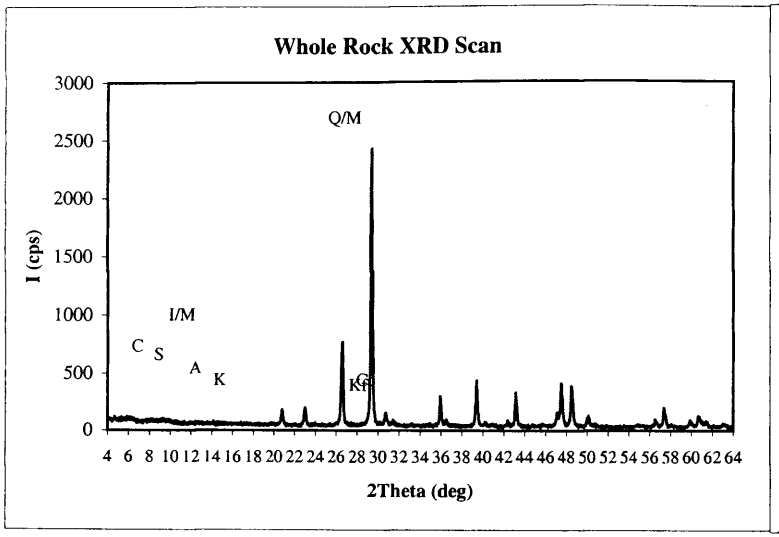

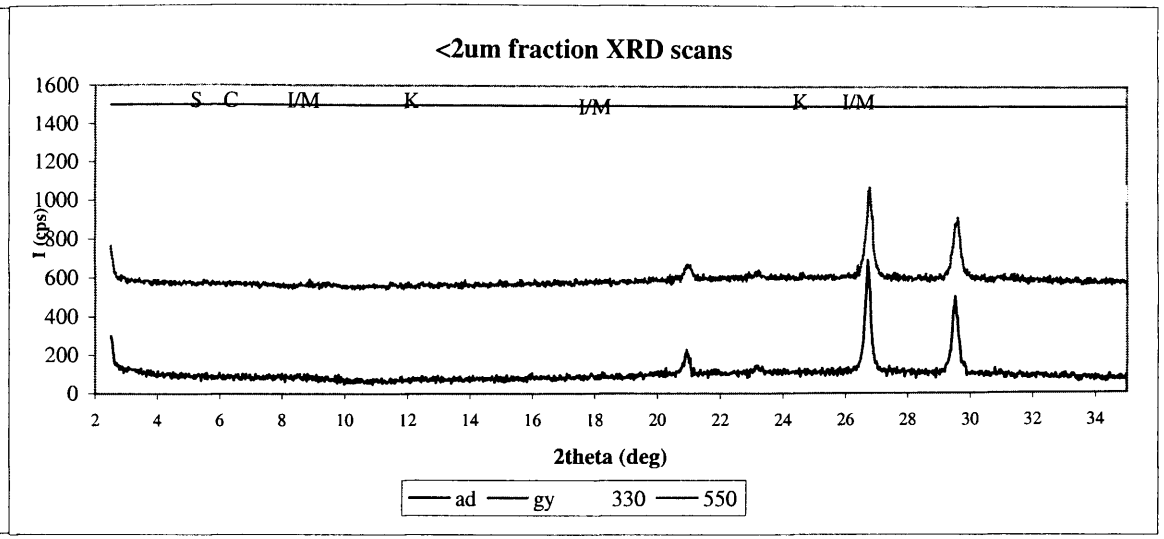

Mineral	%	Code
Illite/Mica	2	I/M
Apatite	1	Ap
Albite	1	NaF
Kfeldspar	1	Kf
Calcite	66	Cc
Dolomite	4	D
Pyrite	1	Py
Ankerite	1	Ak
Quartz	22	Q

Amorphous Content: **0** %

Mineral	Proportion of <2um fraction	Code
Illite/Mica	100	I/M

Weight of <2um fraction: **7** %

Interlayering:	I/S	None
	C/S	None

Sample: BGDI 11

University of Leicester Geological Services XRD Analysis

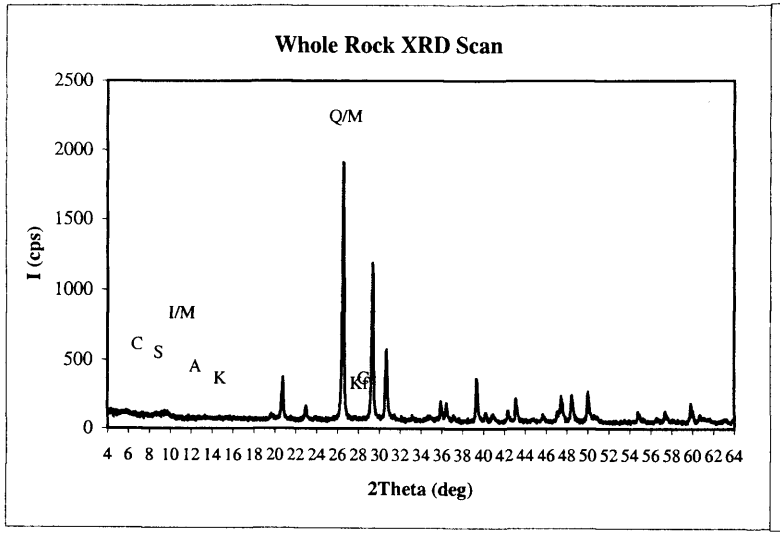

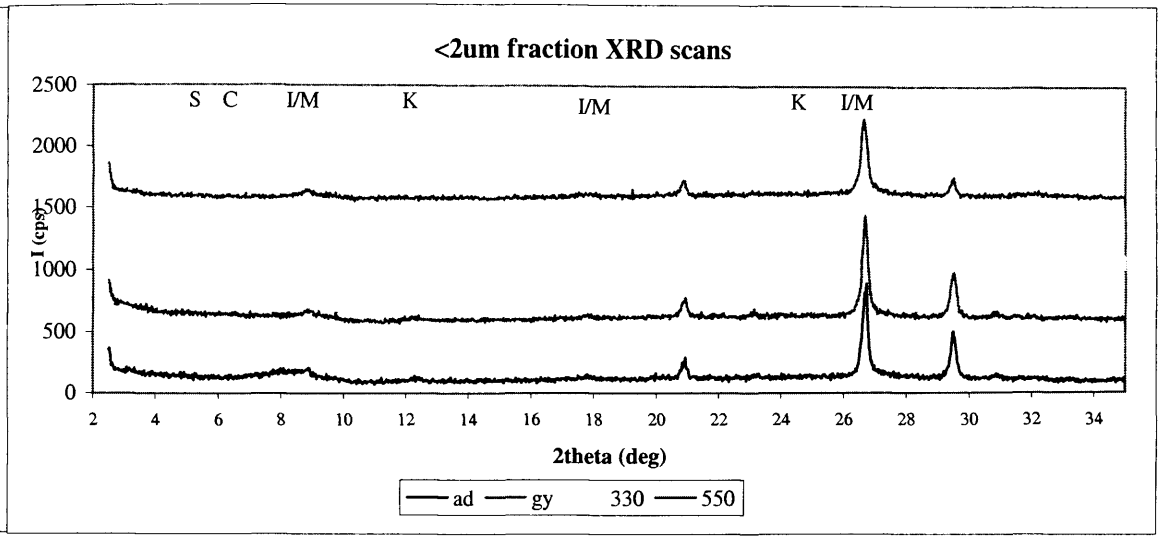

Mineral	%	Code
Kaolinite	1	K
Illite/Mica	4	I/M
Na Smectite	1	S
Apatite	1	Ap
Albite	1	NaF
Kfeldspar	2	Kf
Calcite	38	Cc
Dolomite	9	D
Ankerite	4	Ak
Quartz	39	Q

Amorphous Content: **0** **%**

Mineral	Proportion of <2um fraction	Code
Kaolinite	10	K
Illite/Mica	44	I/M
Smectite	46	S

Weight of <2um fraction: **14** **%**

Interlayering:	I/S	None
	C/S	None

Sample: BGDI 12

University of Leicester Geological Services XRD Analysis

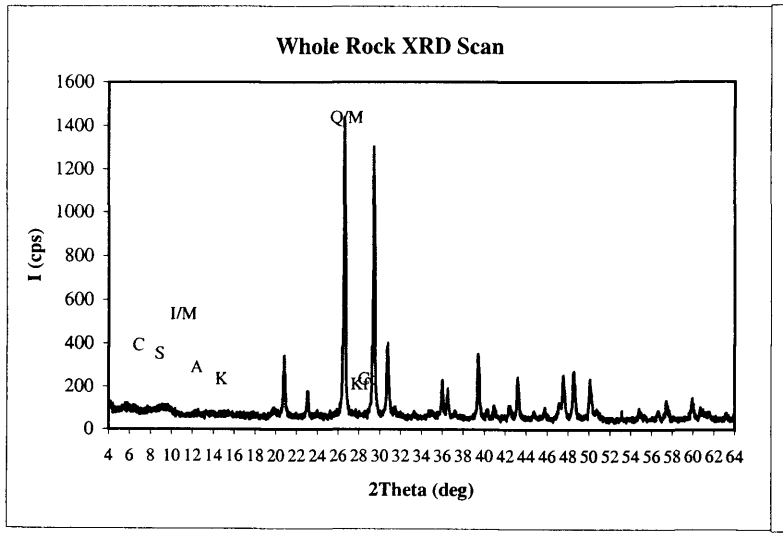

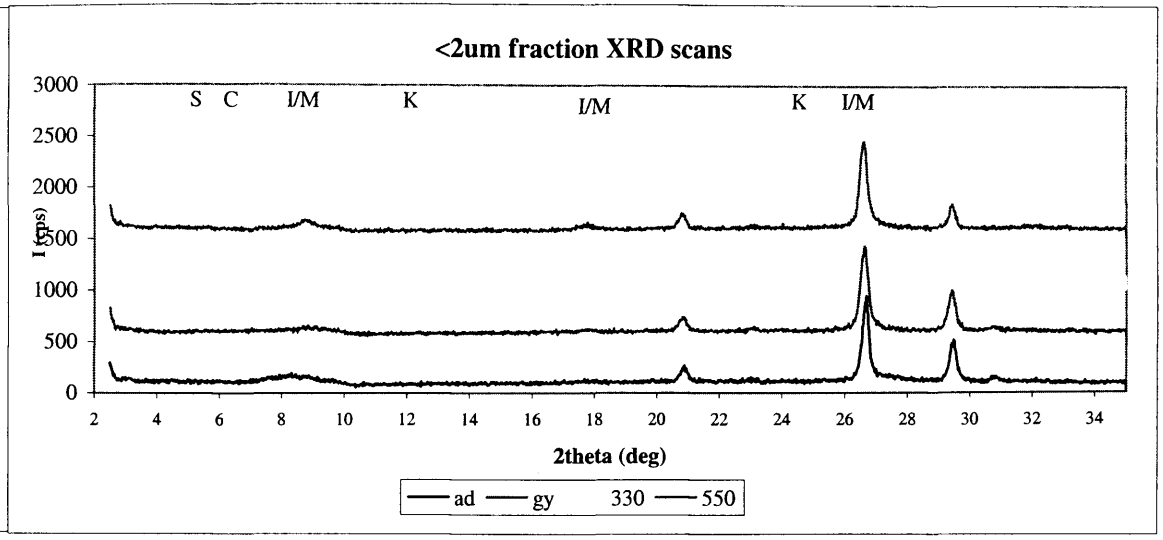

Mineral	%	Code
Illite/Mica	6	I/M
Na Smectite	1	S
Apatite	1	Ap
Albite	1	NaF
Kfeldspar	1	Kf
Calcite	37	Cc
Dolomite	10	D
Ankerite	4	Ak
Quartz	38	Q

Amorphous Content: 0 %

Mineral	Proportion of <2um fraction	Code
Illite/Mica	48	I/M
Smectite	52	S

Weight of <2um fraction: 18 %

Interlayering:		
	I/S	Yes
	C/S	None

Sample: BGDI 13

University of Leicester Geological Services XRD Analysis

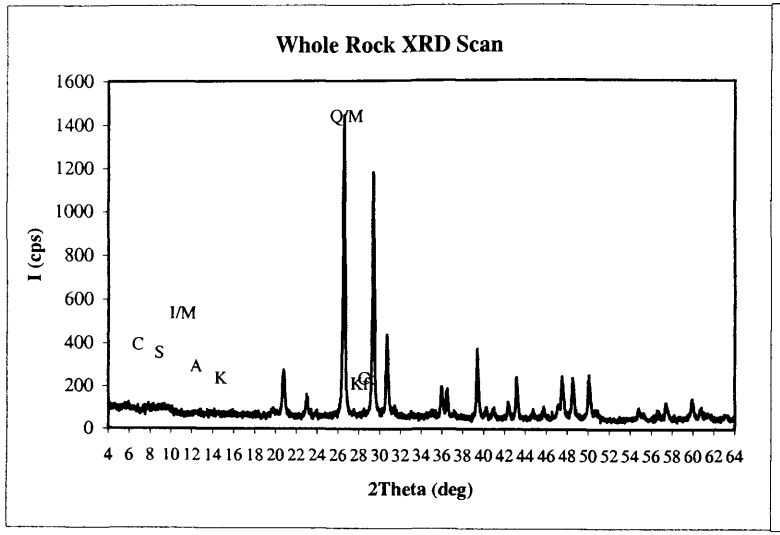

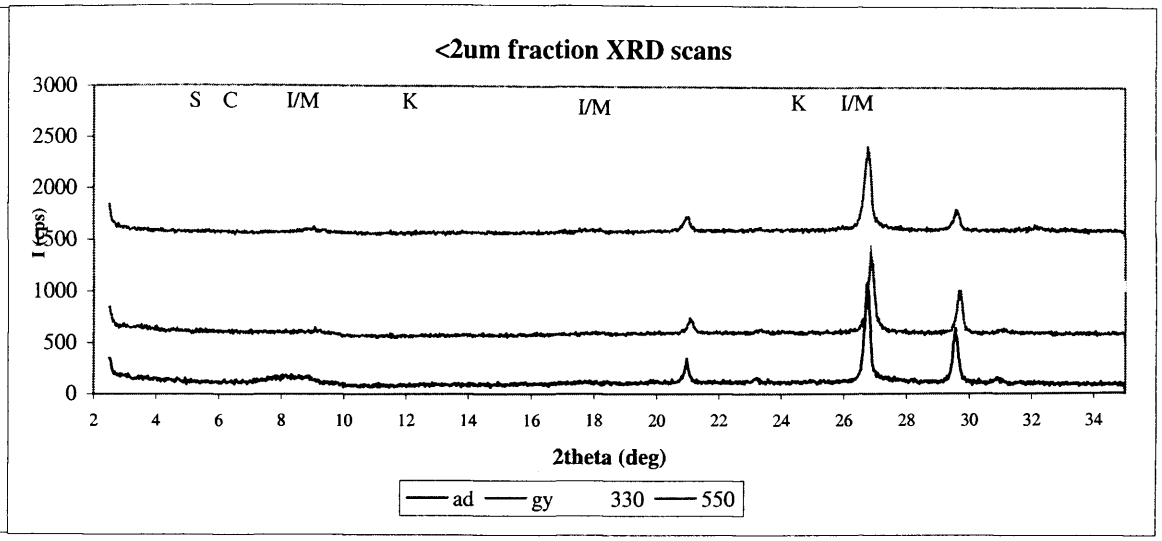

Mineral	%	Code
Illite/Mica	5	I/M
Apatite	1	Ap
Albite	2	NaF
Kfeldspar	1	Kf
Calcite	35	Cc
Dolomite	11	D
Ankerite	4	Ak
Quartz	41	Q

Amorphous Content: **0** **%**

Mineral	Proportion of <2um fraction	Code
Illite/Mica	100	I/M

Weight of <2um fraction: **18** **%**

Interlayering:	I/S	None
	C/S	None

Sample: BGDI 14

University of Leicester Geological Services XRD Analysis

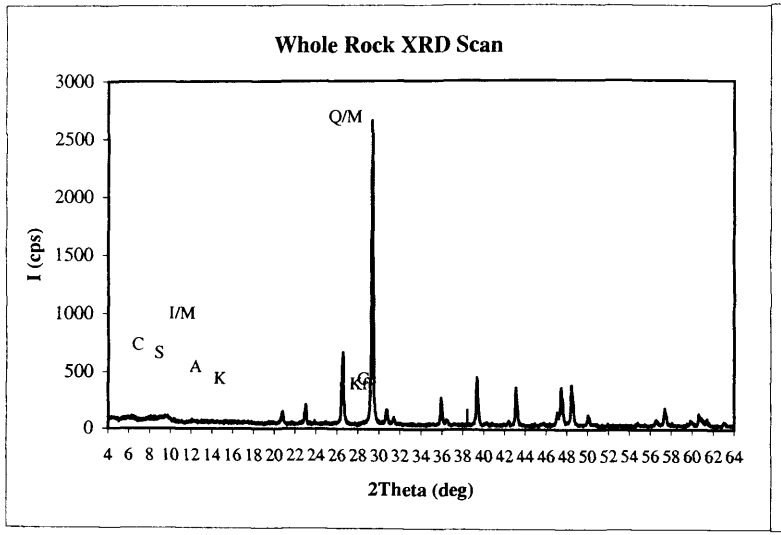

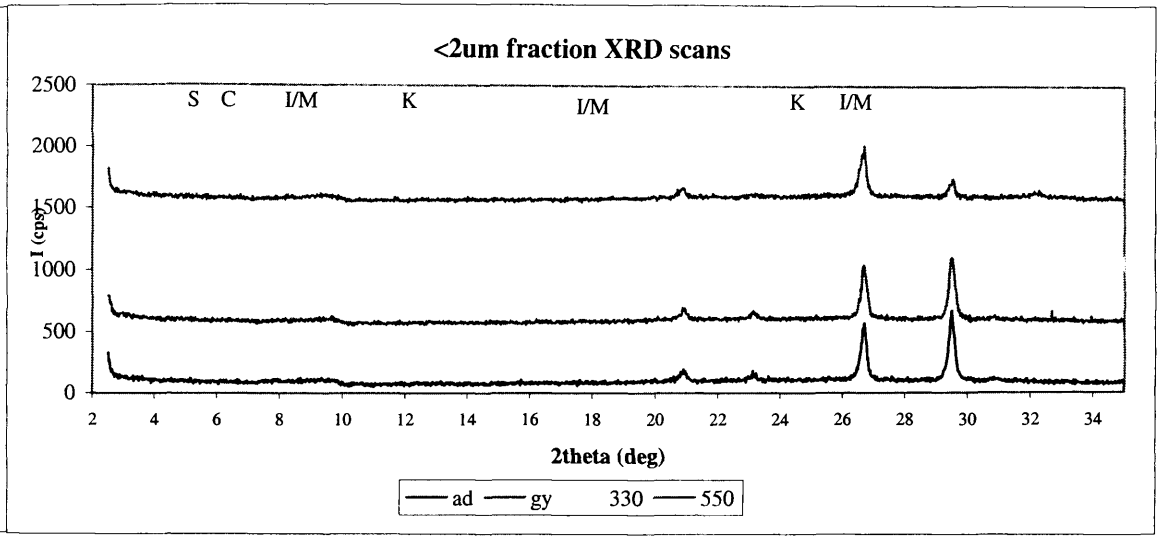

Mineral	%	Code
Illite/Mica	2	I/M
Albite	1	NaF
Kfeldspar	1	Kf
Calcite	70	Cc
Dolomite	3	D
Ankerite	2	Ak
Quartz	19	Q

Amorphous Content: **0** **%**

Mineral	Proportion of <2um fraction	Code
Illite/Mica	100	I/M

Weight of <2um fraction: **13** **%**

Interlayering:	I/S	None
	C/S	None

Sample: BGDI 15

University of Leicester Geological Services XRD Analysis

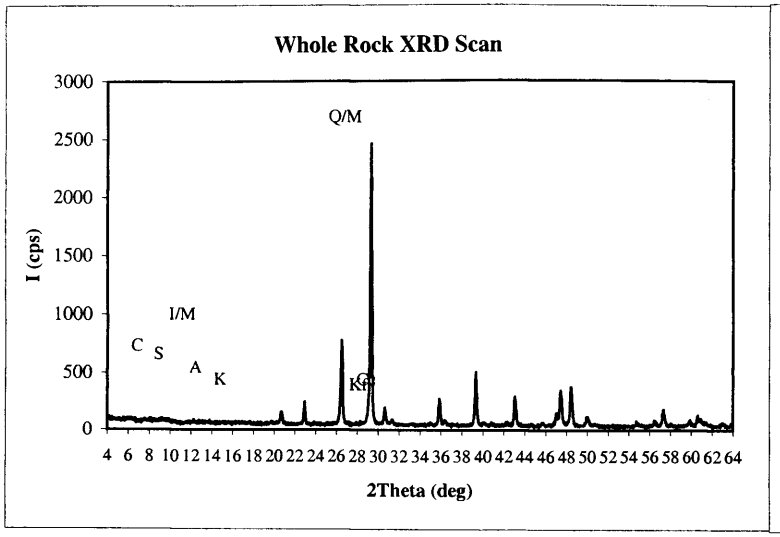

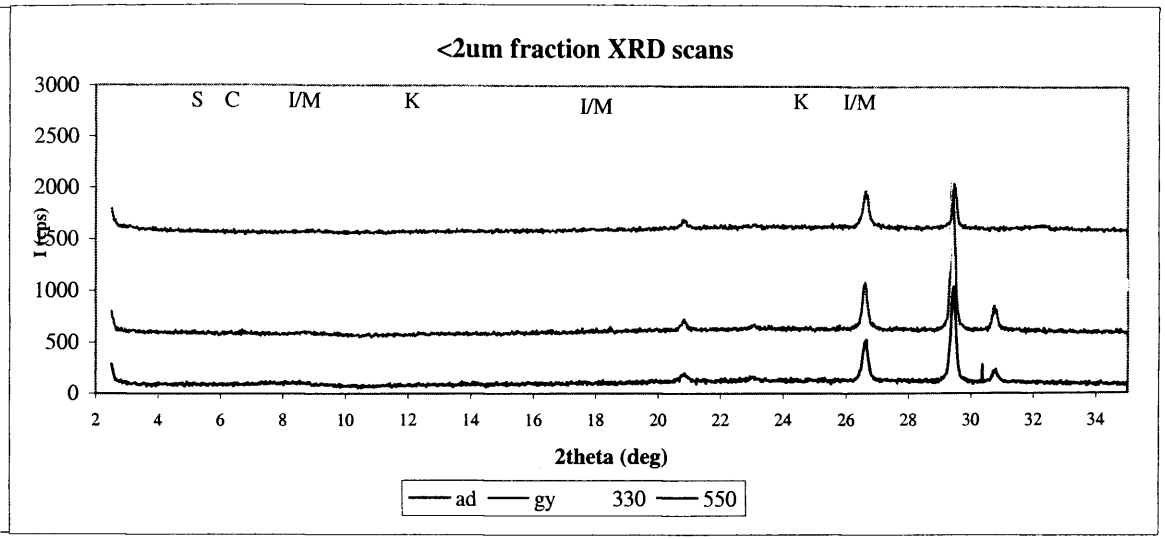

Mineral	%	Code
Illite/Mica	3	I/M
Apatite	1	Ap
Albite	1	NaF
Kfeldspar	1	Kf
Calcite	67	Cc
Dolomite	3	D
Ankerite	3	Ak
Quartz	21	Q

Amorphous Content: **0** %

Mineral	Proportion of <2um fraction	Code
Illite/Mica	100	I/M

Weight of <2um fraction: **13** %

Interlayering:		
	I/S	None
	C/S	None

Sample: BGDI 17

University of Leicester Geological Services XRD Analysis

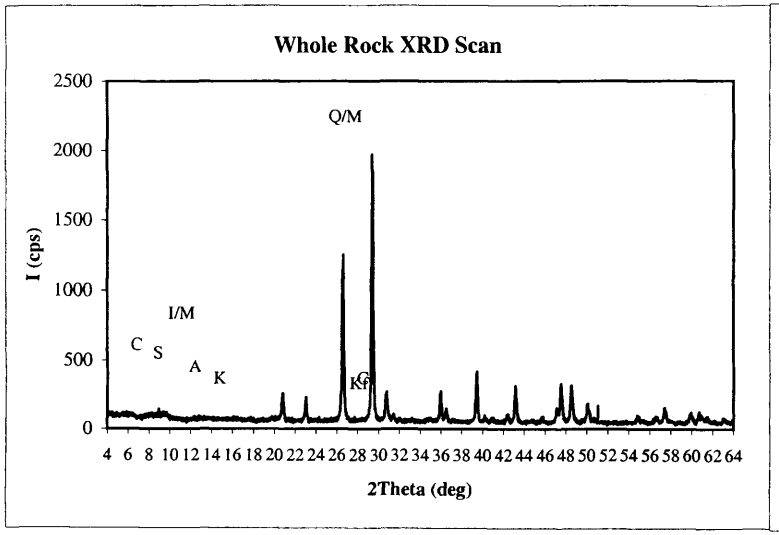

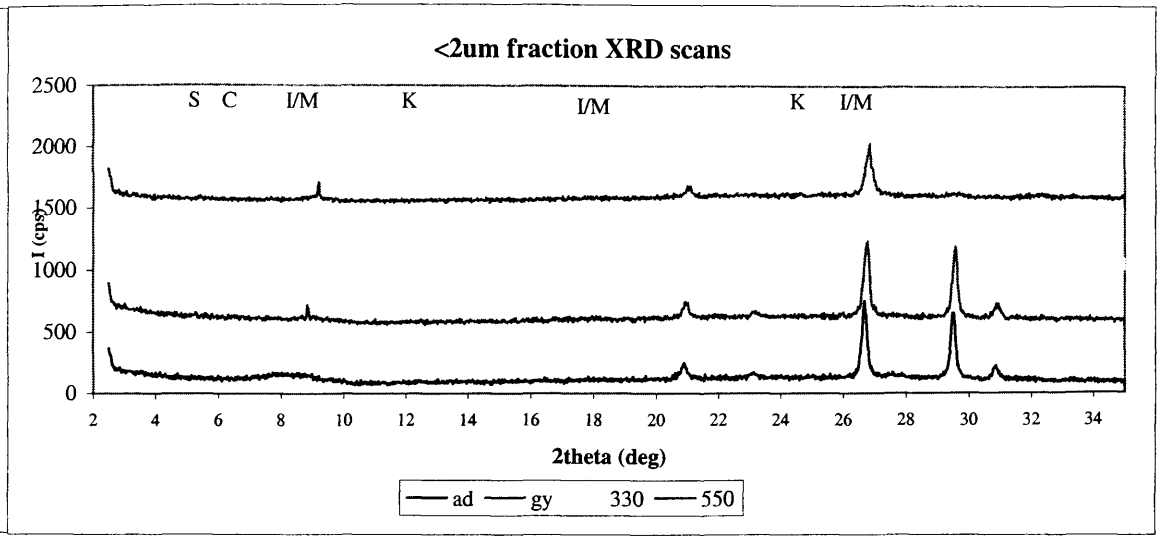

Mineral	%	Code
Illite/Mica	5	I/M
Apatite	1	Ap
Albite	1	NaF
Kfeldspar	1	Kf
Calcite	48	Cc
Dolomite	7	D
Ankerite	4	Ak
Quartz	33	Q

Amorphous Content: **0** **%**

Mineral	Proportion of <2um fraction	Code
Illite/Mica	100	I/M

Weight of <2um fraction: **18** **%**

Interlayering:	I/S	None
	C/S	None

Sample: BGDI 18

University of Leicester Geological Services XRD Analysis

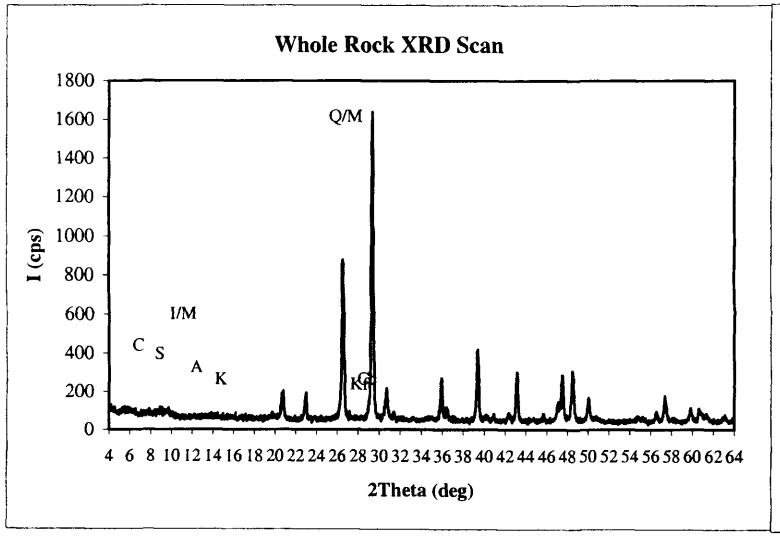

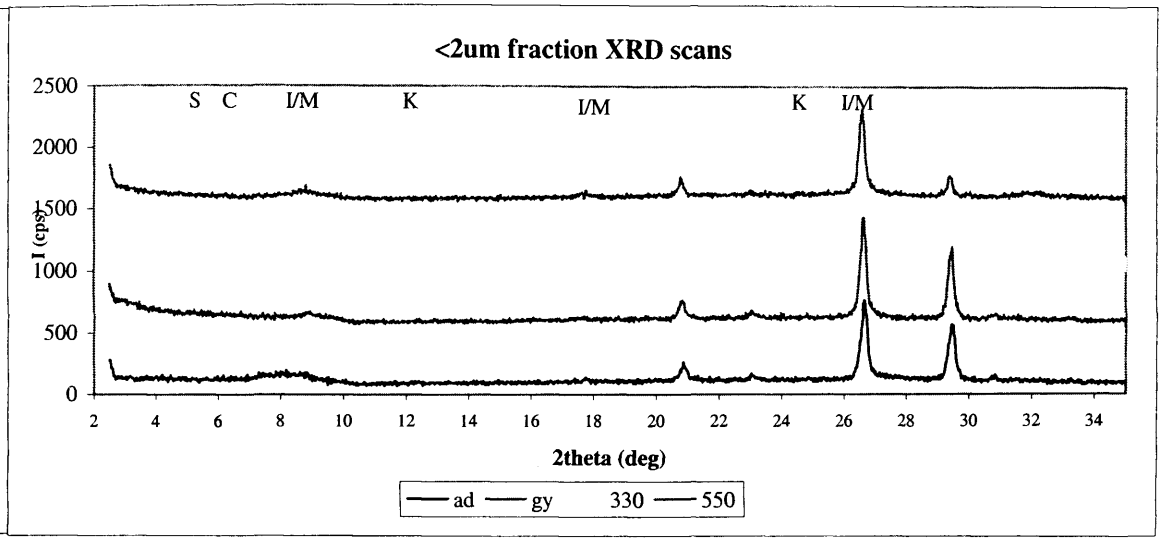

Mineral	%	Code
Illite/Mica	4	I/M
Apatite	1	Ap
Albite	1	NaF
Kfeldspar	1	Kf
Calcite	53	Cc
Dolomite	6	D
Ankerite	4	Ak
Quartz	30	Q

Amorphous Content: **0** %

Mineral	Proportion of <2um fraction	Code
Illite/Mica	100	I/M

Weight of <2um fraction: **13** %

Interlayering:		
	I/S	None
	C/S	None

Sample: BGDI 19

University of Leicester Geological Services XRD Analysis

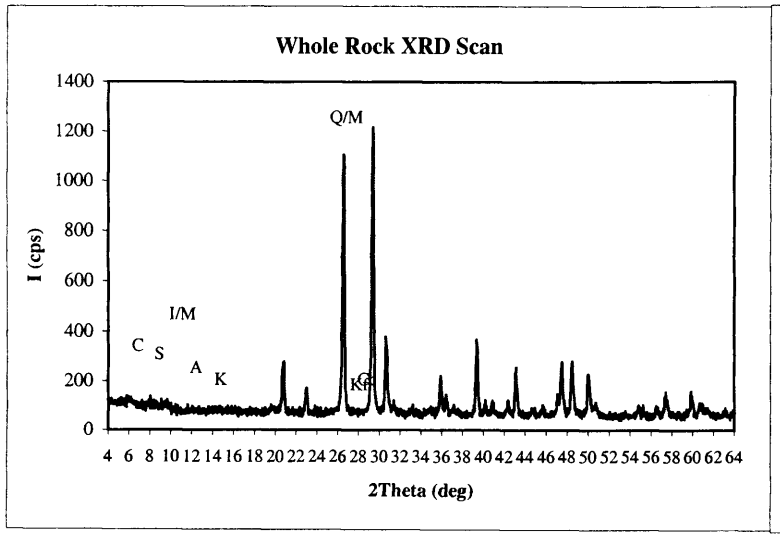

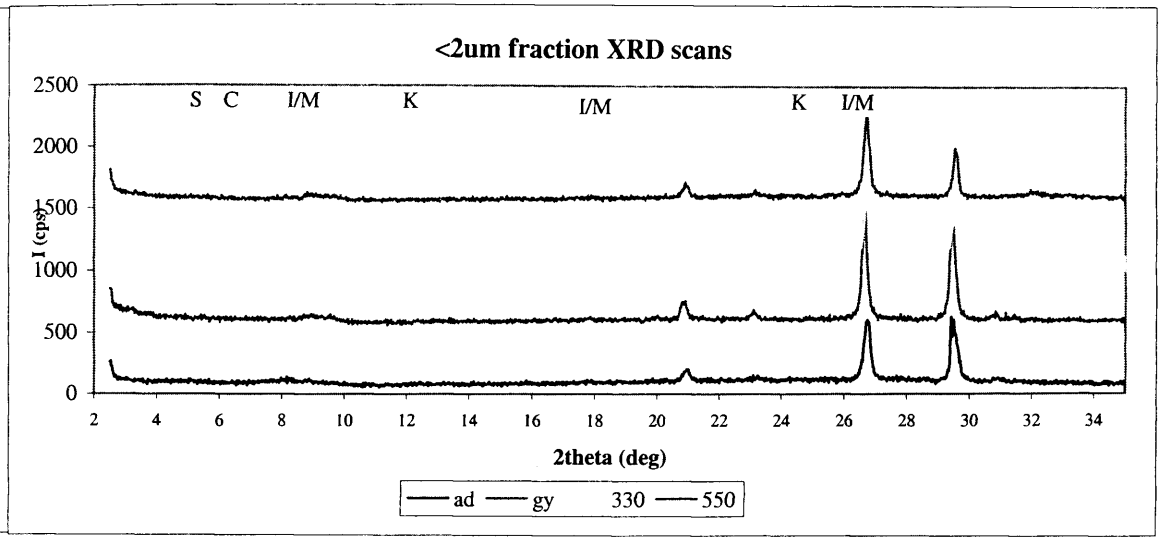

Mineral	%	Code
Illite/Mica	4	I/M
Na Smectite	4	S
Apatite	1	Ap
Albite	1	NaF
Kfeldspar	1	Kf
Calcite	43	Cc
Dolomite	7	D
Ankerite	7	Ak
Quartz	32	Q

Amorphous Content: **0** %

Mineral	Proportion of <2um fraction	Code
Illite/Mica	56	I/M
Smectite	44	S

Weight of <2um fraction: **14** %

Interlayering:		
	I/S	None
	C/S	None

Major (wt%)

	BGDI01	BGDI02	BGDI03	BGDI04	BGDI05	BGDI06	BGDI08	BGDI09	BGDI10 A	BGDI10 B	BGDI11	BGDI12	BGDI13	BGDI14	BDGI15	BGDI17	BGDI18	BGDI19	BGDI20
SiO2	40.16	33.21	42.33	44.14	43.34	47.72	48.85	35.44	36.69	23.77	43.16	41.87	44.15	20.47	23.17	35.42	32.20	36.62	35.26
TiO2	0.18	0.16	0.22	0.24	0.25	0.27	0.26	0.15	0.14	0.07	0.23	0.25	0.22	0.08	0.09	0.17	0.14	0.21	0.21
Al2O3	2.61	2.34	3.17	3.40	3.56	3.69	3.51	2.33	2.30	1.47	2.94	3.50	3.13	1.41	1.74	2.66	2.43	2.89	2.98
Fe2O3	1.61	1.63	1.82	1.69	1.61	1.85	1.98	1.35	1.14	0.73	1.73	1.62	1.63	0.70	1.01	1.67	1.49	2.70	2.56
MnO	0.03	0.03	0.03	0.03	0.03	0.03	0.03	0.03	0.03	0.03	0.03	0.03	0.03	0.02	0.03	0.03	0.03	0.04	0.04
MgO	2.46	2.24	2.53	2.45	2.50	2.62	2.48	2.05	1.98	1.05	2.90	3.05	3.03	1.06	1.21	2.25	1.98	3.28	3.45
CaO	26.49	29.51	23.85	22.60	23.05	20.48	19.50	29.56	28.65	39.05	24.12	23.33	22.43	39.80	39.27	28.22	30.79	25.62	26.59
Na2O	0.18	0.16	0.18	0.18	0.18	0.21	0.19	0.17	0.17	0.15	0.18	0.19	0.19	0.13	0.14	0.15	0.15	0.16	0.17
K2O	0.58	0.57	0.76	0.83	0.83	0.87	0.83	0.53	0.53	0.38	0.72	0.84	0.74	0.36	0.42	0.63	0.55	0.67	0.71
P2O5	0.40	0.37	0.40	0.40	0.42	0.45	0.43	0.31	0.29	0.23	0.39	0.43	0.38	0.19	0.22	0.32	0.31	0.44	0.44
SO3	0.07	0.16	0.20	0.18	0.15	0.13	0.17	0.06	0.07	0.31	0.14	0.16	0.17	0.09	0.11	0.14	0.11	0.17	0.10
LOI	26.23	28.87	24.87	23.70	23.86	22.00	21.47	28.43	27.84	32.72	23.25	24.97	24.00	34.33	33.02	27.97	29.49	26.91	27.78
Total	101.00	99.25	100.35	99.84	99.78	100.31	99.70	100.41	99.83	99.95	99.79	100.24	100.10	98.64	100.44	99.63	99.67	99.71	100.29

XRF analyses traces (ppm)

	BGDI01	BGDI02	BGDI0 3	BGDI04	BGDI05	BGDI06	BGDI08	BGDI0 9	BGDI10 A	BGDI10 B	BGDI11	BGDI1 2	BGDI13	BGDI14	BDGI15	BGDI1 7	BGDI18	BGDI19	BGDI20
Ba	34.76	17.12	38.58	50.15	37.16	51.31	42.71	22.94	25.26	6.91	40.65	53.05	43.94	16.86	10.14	24.23	11.11	52.73	34.83
Ce	6.46	6.27	12.13	12.28	19.24	20.44	9.83	1.69	10.36	3.77	6.18	15.90	9.05	1.92	5.74	12.81	7.16	16.58	22.53
Co	2.23	1.04	2.29	2.91	2.98	4.76	3.51	2.80	1.54	-1.54	1.77	1.98	2.25	1.97	-0.09	1.86	1.96	4.87	5.68
Cr	33.35	53.70	49.67	63.92	50.46	78.41	77.95	29.39	23.39	15.25	47.14	46.90	28.58	11.98	17.51	20.48	20.27	25.62	34.60
Cs	-1.78	1.70	-0.22	4.78	0.75	3.25	6.13	0.14	0.06	0.22	2.71	6.66	-1.06	6.26	0.63	-0.28	-1.67	-1.00	2.48
Cu	3.55	3.99	3.86	2.36	3.85	4.91	3.98	2.06	2.88	5.41	2.96	6.80	2.68	4.41	3.22	3.20	4.08	3.49	6.46
Ga	4.49	3.61	5.82	5.50	4.89	5.20	5.20	4.06	4.47	3.19	5.29	5.27	4.65	3.34	2.76	4.05	3.99	6.26	5.24
La	8.74	7.62	11.24	8.38	12.32	12.87	12.51	8.17	7.51	7.26	13.57	10.35	12.04	5.59	7.08	6.76	9.37	7.35	13.12
Mo	3.40	2.51	3.20	2.35	2.41	3.10	3.17	2.33	1.75	2.12	2.41	1.61	2.28	1.29	2.38	3.11	2.44	3.31	2.77
Nb	3.38	3.04	4.48	4.69	5.10	4.48	4.38	2.03	3.01	2.20	3.56	4.49	3.52	0.43	2.27	3.66	3.05	4.33	4.06
Nd	14.51	15.24	13.06	15.15	15.99	12.61	11.88	7.57	11.77	10.21	9.11	12.79	13.75	9.71	10.25	13.85	8.98	12.14	11.46
Ni	10.58	10.33	11.92	11.76	15.84	11.36	10.90	7.34	2.66	3.18	15.52	12.24	15.71	3.19	4.59	7.58	10.05	19.48	17.36
Pb	3.00	3.66	3.42	4.04	7.28	5.52	5.30	4.15	3.02	1.33	2.72	5.73	5.48	3.56	3.96	4.34	2.79	5.73	4.32
Rb	14.12	13.99	18.26	19.66	20.73	22.67	20.61	14.36	12.98	7.97	17.43	20.27	17.66	9.57	10.52	14.49	15.22	15.75	18.12
Sn	6.86	4.45	7.96	9.15	7.65	11.38	8.20	9.08	7.11	7.75	7.16	9.22	6.91	8.98	8.12	8.08	6.82	10.16	7.37
Sr	641.78	696.12	611.69	574.48	593.50	504.80	464.18	723.75	729.31	909.69	495.78	591.83	537.95	956.95	885.91	696.61	754.85	555.44	587.05
Th	4.93	3.78	6.43	7.36	5.79	4.52	7.90	2.80	7.18	3.12	5.76	7.37	5.06	2.23	1.65	5.75	5.11	5.60	3.30
U	1.96	2.86	2.18	2.47	1.99	2.39	2.69	2.23	2.05	-0.71	2.96	4.13	2.60	1.39	-0.60	2.81	0.44	2.78	1.43
V	29.12	21.46	25.87	31.70	33.28	28.24	32.10	19.34	25.94	12.64	24.69	35.17	28.33	15.03	20.88	27.60	24.54	28.73	33.38
Y	11.24	10.52	11.76	10.64	10.59	11.76	13.50	8.69	8.86	7.54	13.27	11.16	12.19	7.04	8.11	9.21	8.01	12.78	11.58
Zn	6.52	7.47	8.17	8.08	9.28	9.49	8.38	6.92	5.37	6.59	17.55	7.83	8.13	5.38	5.83	11.57	12.06	32.05	16.32
Zr	72.04	58.24	83.84	81.83	60.98	100.63	110.78	51.81	51.79	25.64	93.39	71.56	78.79	26.82	34.72	55.51	39.99	97.75	88.90

Appendix 4a. XRF analyses of 19 samples. Analyses by N. Marsh. Department of Geology University of Leicester

	SiO_2	TiO_2	Al_2O_3	Fe_2O_3	MnO	MgO	CaO	Na_2O	K_2O	P_2O_5	SO_3	Total	LOI	total+ LOI
:SiO2	100.14	0.03	0.13	0.02	0.007	0.08	0.05	0.14	0.029	0.01	0.019	100.66	0	
:WS-1	51.49	2.63	14.02	13.11	0.178	5.31	8.71	3.01	1.379	0.306	0.081	100.22	0.63	
:BH-1	68.68	0.51	14.32	5.95	0.134	2.72	3.63	4.08	0.873	0.08	0.037	101.01	2.52	
:BLANK	0.29	0.01	0.08	0.03	0.009	0.11	0.03	0.14	0.039	0.004	0.014	0.76	0	
:CaCO3	0.16	0	0.13	0.02	0.001	0.11	55.85	0.2	0.031	0.007	0.016	56.53	43.67	100.20
:MgCO3	0.14	0	0.07	0.04	0.01	23.91	0.06	0	0.036	0.003	0.023			
	0.28	0	0.14	0.08	0.02	47.82	0.12	0	0.072	0.006	0.046	48.58	51.87	100.45

Appendix 4b. Table of internal and international rock reference material from which XRF calibrations were set.

Appendix 5

QUANTATIVE EDX DATA

	Fish1	Fish2	Fish3	Fish4	Fish5	Fish6	Fish7	Mean	Sd
SiO2	0.03	0.00	0.00	0.00	0.00	0.00	0.00	0.00	0.01
Al2O3	0.11	0.13	0.10	0.08	0.00	0.14	0.02	0.08	0.05
FeO	0.00	0.17	0.00	0.15	0.04	0.00	0.07	0.06	0.07
MnO	0.00	0.00	0.00	0.04	0.00	0.00	0.00	0.01	0.02
MgO	0.08	0.09	0.00	0.10	0.01	0.21	0.19	0.10	0.08
CaO	53.18	53.10	53.21	52.80	52.92	54.26	53.87	53.33	0.53
Na2O	0.81	0.64	0.44	0.70	0.62	1.07	1.04	0.76	0.23
K2O	0.06	0.05	0.03	0.07	0.01	0.00	0.04	0.04	0.03
P2O5	36.29	36.07	36.05	36.24	35.88	37.39	37.40	36.47	0.64
SO3	2.83	3.03	3.29	3.12	3.19	1.85	1.87	2.74	0.62
F2O	6.60	6.71	6.16	6.70	7.25	5.07	5.33	6.26	0.79
Cl2O	0.00	0.01	0.08	0.00	0.07	0.01	0.18	0.05	0.06
Total	100.00	100.00	99.37	100.00	100.00	100.00	100.00		

Lingulid brachiopod

	L1	L2	L3	L4	L5	Mean	Sd
SiO2	0.00	0.00	0.00	0.21	0.00	0.04	0.09
Al2O3	0.12	0.13	0.12	0.15	0.10	0.13	0.02
FeO	0.20	0.04	0.01	0.02	0.21	0.09	0.10
MnO	0.00	0.00	0.00	0.00	0.00	0.00	0.00
MgO	0.83	0.87	0.65	0.51	0.58	0.69	0.16
CaO	52.64	52.83	52.73	52.10	52.78	52.62	0.30
Na2O	1.34	1.43	1.25	1.17	1.14	1.26	0.12
K2O	0.00	0.00	0.02	0.00	0.09	0.02	0.04
P2O5	36.15	36.15	36.80	36.50	36.21	36.36	0.28
SO3	2.18	1.94	1.99	2.45	2.07	2.13	0.20
F2O	6.47	6.58	6.43	6.89	6.75	6.62	0.19
Cl2O	0.07	0.03	0.00	0.00	0.07	0.03	0.03
Total	100.00	100.00	100.00	100.00	100.00		

Conulariid

	Con 1	Con 2	Con 3	Con 4	Con 5	Mean	Sd
SiO2	0.00	0.05	0.00	0.01	0.08	0.03	0.04
Al2O3	0.15	0.19	0.10	0.10	0.11	0.13	0.04
FeO	0.00	0.00	0.09	0.17	0.00	0.05	0.07
MnO	0.06	0.06	0.00	0.00	0.20	0.06	0.08
MgO	0.40	0.54	0.39	0.20	0.32	0.37	0.13
CaO	51.09	50.35	50.30	53.17	51.18	51.22	1.16
Na2O	1.08	1.13	1.24	0.87	0.98	1.06	0.14
K2O	0.08	0.13	0.15	0.14	0.16	0.13	0.03
P2O5	36.36	36.67	36.13	35.98	36.46	36.32	0.27
SO3	1.66	1.65	1.83	1.96	1.60	1.74	0.15
F2O	9.01	9.08	9.68	7.33	8.71	8.76	0.87
Cl2O	0.10	0.13	0.09	0.08	0.19	0.12	0.05
Total	100.00	100.00	100.00	100.00	100.00		

Shrimp

	SH 1	SH 2	SH 3	SH 4	SH 5	Mean	Sd
SiO2	0.13	0.00	0.00	0.52	0.00	0.13	0.20
Al2O3	0.30	0.25	0.17	0.18	0.20	0.22	0.05
FeO	0.00	0.09	0.09	0.05	0.00	0.05	0.04
MnO	0.00	0.00	0.00	0.00	0.00	0.00	0.00
MgO	0.29	0.33	0.24	0.43	0.31	0.32	0.06
CaO	54.72	54.34	53.71	53.51	54.50	54.16	0.47
Na2O	0.76	0.88	0.85	0.90	0.92	0.86	0.06
K2O	0.07	0.14	0.04	0.11	0.04	0.08	0.04
P2O5	34.80	34.99	34.51	34.86	35.26	34.89	0.25
SO3	2.09	2.07	1.88	1.92	1.96	1.99	0.08
F2O	6.79	6.85	6.24	7.39	6.70	6.80	0.37
Cl2O	0.04	0.06	0.02	0.11	0.11	0.07	0.04
Total	100.00	100.00	97.75	100.00	100.00		

Appendix 6. Electron microprobe analyses

Fish	1.00	2.00	3.00	4.00	5.00	6.00	7.00	8.00	9.00	10.00
SiO2	0.00	0.00	0.00	0.24	0.00	0.00	0.04	0.00	0.18	0.00
FeO	0.00	0.06	0.00	0.02	0.00	0.00	0.01	0.05	0.06	0.05
MnO	0.02	0.00	0.00	0.00	0.00	0.00	0.00	0.00	0.02	0.00
MgO	0.11	0.11	0.08	0.10	0.11	0.11	0.08	0.13	0.26	0.10
CaO	53.99	52.36	54.12	53.39	55.00	54.29	54.46	54.98	45.90	49.60
Na2O	0.77	0.79	0.73	0.81	0.80	0.79	0.83	1.19	0.76	0.59
SrO	0.38	0.34	0.51	0.37	0.47	0.45	0.37	0.54	0.40	0.45
La2O3	0.08	0.00	0.00	0.04	0.11	0.01	0.00	0.03	0.06	0.00
Ce2O3	0.07	0.00	0.07	0.03	0.14	0.07	0.04	0.00	0.00	0.00
Y2O3	0.05	0.02	0.04	0.03	0.00	0.03	0.00	0.00	0.04	0.00
P2O5	37.18	36.85	36.99	36.93	37.47	37.06	37.39	36.21	32.90	33.42
F	2.43	2.54	2.47	2.30	2.53	2.57	2.37	2.63	1.45	1.92
-O=F	1.02	1.07	1.04	0.97	1.07	1.08	1.00	1.11	0.61	0.81
Cl	0.07	0.09	0.05	0.05	0.06	0.06	0.06	0.08	0.15	0.09
-O=Cl	0.02	0.02	0.01	0.01	0.01	0.01	0.01	0.02	0.03	0.02
SO3	1.47	1.77	1.53	1.59	1.50	1.67	1.54	1.69	1.49	1.50
Total	95.59	93.84	95.55	94.92	97.10	96.01	96.16	96.39	83.02	86.90
O	10.00	10.00	10.00	10.00	10.00	10.00	10.00	10.00	10.00	10.00
Si	0.00	0.00	0.00	0.02	0.00	0.00	0.00	0.00	0.01	0.00
Fe2	0.00	0.00	0.00	0.00	0.00	0.00	0.00	0.00	0.00	0.00
Mn	0.00	0.00	0.00	0.00	0.00	0.00	0.00	0.00	0.00	0.00
Mg	0.01	0.01	0.01	0.01	0.01	0.01	0.01	0.01	0.03	0.01
Ca	4.22	4.15	4.23	4.18	4.24	4.23	4.22	4.31	4.05	4.25
Na	0.11	0.11	0.10	0.11	0.11	0.11	0.12	0.17	0.12	0.09
Sr	0.02	0.01	0.02	0.02	0.02	0.02	0.02	0.02	0.02	0.02
La	0.00	0.00	0.00	0.00	0.00	0.00	0.00	0.00	0.00	0.00
Ce	0.00	0.00	0.00	0.00	0.00	0.00	0.00	0.00	0.00	0.00
Y	0.00	0.00	0.00	0.00	0.00	0.00	0.00	0.00	0.00	0.00
P	2.29	2.31	2.29	2.28	2.28	2.28	2.29	2.24	2.29	2.26
F	0.56	0.59	0.57	0.53	0.58	0.59	0.54	0.61	0.38	0.49
Cl	0.01	0.01	0.01	0.01	0.01	0.01	0.01	0.01	0.02	0.01
S	0.08	0.10	0.08	0.09	0.08	0.09	0.08	0.09	0.09	0.09
Total	6.73	6.70	6.74	6.71	6.76	6.75	6.73	6.85	6.62	6.72
X	47.28	47.25	47.22	47.20	47.18	47.13	47.10	47.09	47.05	47.05
Y	45.54	45.53	45.46	45.48	45.43	45.40	45.37	45.35	45.34	45.35
Ca	38.57	37.40	38.66	38.14	39.29	38.78	38.90	39.27	32.79	35.43
P	16.22	16.08	16.14	16.12	16.35	16.17	16.32	15.80	14.36	14.59
Ca/P	2.38	2.33	2.40	2.37	2.40	2.40	2.38	2.49	2.28	2.43

11.00	12.00	13.00	14.00	15.00	16.00	17.00	18.00	19.00	20.00	21.00
0.00	0.00	0.00	0.00	0.00	0.00	0.00	0.00	1.39	0.00	0.00
0.00	0.04	0.04	0.02	0.00	0.03	0.02	0.63	0.18	0.07	0.00
0.04	0.00	0.03	0.00	0.00	0.00	0.02	0.05	0.01	0.00	0.00
0.05	0.36	0.10	0.07	0.08	0.08	0.14	0.05	0.20	0.23	0.04
40.73	49.28	53.18	52.05	52.04	50.50	49.72	49.97	47.98	47.88	50.96
0.35	2.80	0.94	0.54	0.75	0.77	1.23	0.48	0.48	1.80	0.48
0.09	0.14	0.33	0.25	0.20	0.25	0.07	0.08	0.08	0.09	0.07
0.00	0.06	0.00	0.10	0.02	0.00	0.00	0.06	0.11	0.04	0.04
0.00	0.04	0.04	0.04	0.01	0.15	0.11	0.03	0.00	0.03	0.00
0.04	0.04	0.00	0.02	0.00	0.00	0.04	0.10	0.07	0.05	0.02
26.55	31.72	34.02	32.50	33.35	31.93	31.38	32.03	30.86	30.87	33.28
2.36	3.10	3.09	3.03	3.35	3.58	3.01	3.28	2.79	3.23	3.17
0.99	1.31	1.30	1.28	1.41	1.51	1.27	1.38	1.18	1.36	1.34
0.01	1.42	0.04	0.02	0.03	0.03	0.35	0.03	0.04	0.13	0.03
0.00	0.32	0.01	0.01	0.01	0.01	0.08	0.01	0.01	0.03	0.01
2.42	2.58	1.98	2.48	2.27	2.30	2.51	2.59	2.43	2.62	2.50
71.63	89.96	92.48	89.84	90.68	88.09	87.25	87.97	85.42	85.65	89.25
10.00	10.00	10.00	10.00	10.00	10.00	10.00	10.00	10.00	10.00	10.00
0.00	0.00	0.00	0.00	0.00	0.00	0.00	0.00	0.11	0.00	0.00
0.00	0.00	0.00	0.00	0.00	0.00	0.00	0.04	0.01	0.01	0.00
0.00	0.00	0.00	0.00	0.00	0.00	0.00	0.00	0.00	0.00	0.00
0.01	0.04	0.01	0.01	0.01	0.01	0.02	0.01	0.02	0.03	0.00
4.28	4.29	4.39	4.42	4.39	4.43	4.37	4.34	4.23	4.29	4.33
0.07	0.44	0.14	0.08	0.11	0.12	0.20	0.08	0.08	0.29	0.07
0.00	0.01	0.01	0.01	0.01	0.01	0.00	0.00	0.00	0.00	0.00
0.00	0.00	0.00	0.00	0.00	0.00	0.00	0.00	0.00	0.00	0.00
0.00	0.00	0.00	0.00	0.00	0.00	0.00	0.00	0.00	0.00	0.00
0.00	0.00	0.00	0.00	0.00	0.00	0.00	0.00	0.00	0.00	0.00
2.20	2.18	2.22	2.18	2.22	2.21	2.18	2.20	2.15	2.19	2.23
0.73	0.80	0.75	0.76	0.83	0.93	0.78	0.84	0.73	0.85	0.80
0.00	0.20	0.00	0.00	0.00	0.00	0.05	0.00	0.00	0.02	0.00
0.18	0.16	0.11	0.15	0.13	0.14	0.15	0.16	0.15	0.16	0.15
6.74	7.13	6.89	6.86	6.88	6.93	6.93	6.84	6.76	6.97	6.79
47.05	47.09	47.12	47.15	47.20	47.22	47.24	47.27	47.27	47.29	47.23
45.27	45.29	45.33	45.34	45.36	45.38	45.37	45.37	45.41	45.44	45.26
29.09	35.20	37.99	37.18	37.17	36.07	35.52	35.69	34.27	34.20	36.40
11.59	13.84	14.84	14.18	14.55	13.93	13.70	13.98	13.47	13.47	14.52
2.51	2.54	2.56	2.62	2.55	2.59	2.59	2.55	2.54	2.54	2.51

22.00	23.00	24.00	25.00	26.00	27.00	28.00	29.00	30.00	31.00
0.00	0.00	0.00	0.00	0.00	0.00	0.00	0.00	0.00	0.00
0.00	0.00	0.08	0.03	0.01	0.03	0.00	0.03	0.03	0.02
0.00	0.04	0.00	0.00	0.00	0.00	0.00	0.00	0.00	0.00
0.06	0.05	0.06	0.59	0.03	0.05	0.04	0.06	0.09	0.03
51.68	51.99	53.44	44.33	52.75	53.08	53.93	52.74	52.13	36.54
0.60	0.53	0.46	4.44	0.48	0.43	0.44	0.42	0.83	0.45
0.11	0.10	0.09	0.15	0.11	0.11	0.11	0.12	0.14	0.04
0.00	0.02	0.00	0.00	0.00	0.18	0.00	0.01	0.03	0.04
0.00	0.00	0.00	0.12	0.00	0.07	0.01	0.00	0.19	0.11
0.08	0.06	0.05	0.02	0.04	0.02	0.05	0.05	0.05	0.03
32.57	32.85	33.84	28.54	33.36	33.29	34.03	32.98	32.58	22.87
3.27	3.51	3.55	2.31	3.70	3.38	3.57	3.19	3.11	2.27
1.38	1.48	1.49	0.97	1.56	1.42	1.50	1.35	1.31	0.96
0.05	0.03	0.04	2.08	0.02	0.02	0.03	0.03	0.06	0.03
0.01	0.01	0.01	0.47	0.00	0.01	0.01	0.01	0.01	0.01
2.42	4.40	2.47	2.88	2.53	2.47	2.40	2.45	2.49	2.02
89.45	92.09	92.56	84.05	91.46	91.72	93.08	90.73	90.39	63.50
10.00	10.00	10.00	10.00	10.00	10.00	10.00	10.00	10.00	10.00
0.00	0.00	0.00	0.00	0.00	0.00	0.00	0.00	0.00	0.00
0.00	0.00	0.01	0.00	0.00	0.00	0.00	0.00	0.00	0.00
0.00	0.00	0.00	0.00	0.00	0.00	0.00	0.00	0.00	0.00
0.01	0.01	0.01	0.08	0.00	0.01	0.00	0.01	0.01	0.01
4.42	4.28	4.42	4.15	4.43	4.43	4.44	4.44	4.41	4.39
0.09	0.08	0.07	0.75	0.07	0.07	0.06	0.06	0.13	0.10
0.00	0.00	0.00	0.01	0.00	0.00	0.01	0.01	0.01	0.00
0.00	0.00	0.00	0.00	0.00	0.01	0.00	0.00	0.00	0.00
0.00	0.00	0.00	0.00	0.00	0.00	0.00	0.00	0.01	0.00
0.00	0.00	0.00	0.00	0.00	0.00	0.00	0.00	0.00	0.00
2.20	2.13	2.21	2.11	2.21	2.20	2.21	2.19	2.18	2.17
0.82	0.85	0.87	0.64	0.92	0.83	0.87	0.79	0.78	0.81
0.01	0.00	0.01	0.31	0.00	0.00	0.00	0.00	0.01	0.01
0.14	0.25	0.14	0.19	0.15	0.14	0.14	0.14	0.15	0.17
6.87	6.76	6.86	7.30	6.88	6.86	6.87	6.85	6.89	6.85
47.18	47.14	47.09	47.03	47.08	47.13	47.17	47.20	47.23	47.23
45.26	45.26	45.27	45.23	45.19	45.19	45.17	45.21	45.22	45.14
36.92	37.13	38.17	31.67	37.68	37.92	38.52	37.67	37.24	26.10
14.21	14.34	14.77	12.46	14.56	14.53	14.85	14.39	14.22	9.98
2.60	2.59	2.58	2.54	2.59	2.61	2.59	2.62	2.62	2.62

Lingulid brachiopod

47.00	48.00	49.00	50.00	51.00	52.00	53.00	54.00	55.00	56.00	57.00
0.00	0.00	0.00	0.00	0.00	0.00	0.00	0.00	0.00	0.00	0.00
0.02	0.01	0.04	0.01	0.02	0.00	0.00	0.02	0.00	0.01	0.03
0.00	0.01	0.00	0.01	0.00	0.00	0.00	0.00	0.01	0.00	0.00
0.57	0.53	0.53	0.56	0.53	0.54	0.59	0.59	0.52	0.57	0.58
38.35	48.81	49.29	49.90	49.93	41.96	48.57	48.77	49.48	48.89	49.57
1.24	1.06	1.10	1.33	1.07	1.12	1.17	1.26	1.08	1.04	1.26
0.70	0.44	0.37	0.35	0.39	0.24	0.34	0.42	0.34	0.48	0.42
0.03	0.02	0.14	0.00	0.00	0.05	0.00	0.12	0.00	0.09	0.00
0.00	0.02	0.00	0.00	0.00	0.13	0.09	0.01	0.14	0.01	0.04
0.00	0.00	0.04	0.05	0.04	0.01	0.08	0.09	0.04	0.08	0.00
28.84	33.50	32.98	33.55	33.85	28.52	34.54	32.94	33.79	33.99	33.24
3.33	3.51	2.96	3.01	3.09	3.38	2.98	2.76	3.06	2.54	3.24
1.40	1.48	1.24	1.27	1.30	1.42	1.26	1.16	1.29	1.07	1.37
0.01	0.02	0.03	0.03	0.02	0.02	0.02	0.08	0.02	0.03	0.02
0.00	0.00	0.01	0.01	0.00	0.00	0.01	0.02	0.00	0.01	0.00
1.29	1.85	1.96	1.88	1.90	1.47	1.76	1.86	1.75	1.65	1.96
72.96	88.30	88.19	89.40	89.53	76.01	88.89	87.74	88.93	88.28	88.99
10.00	10.00	10.00	10.00	10.00	10.00	10.00	10.00	10.00	10.00	10.00
0.00	0.00	0.00	0.00	0.00	0.00	0.00	0.00	0.00	0.00	0.00
0.00	0.00	0.00	0.00	0.00	0.00	0.00	0.00	0.00	0.00	0.00
0.00	0.00	0.00	0.00	0.00	0.00	0.00	0.00	0.00	0.00	0.00
0.08	0.06	0.06	0.07	0.06	0.08	0.07	0.07	0.06	0.07	0.07
4.02	4.22	4.24	4.23	4.23	4.27	4.11	4.21	4.22	4.15	4.25
0.23	0.17	0.17	0.20	0.16	0.21	0.18	0.20	0.17	0.16	0.20
0.04	0.02	0.02	0.02	0.02	0.01	0.02	0.02	0.02	0.02	0.02
0.00	0.00	0.00	0.00	0.00	0.00	0.00	0.00	0.00	0.00	0.00
0.00	0.00	0.00	0.00	0.00	0.00	0.00	0.00	0.00	0.00	0.00
0.00	0.00	0.00	0.00	0.00	0.00	0.00	0.00	0.00	0.00	0.00
2.39	2.29	2.24	2.25	2.26	2.29	2.31	2.24	2.27	2.28	2.25
1.03	0.90	0.75	0.75	0.77	1.02	0.74	0.70	0.77	0.64	0.82
0.00	0.00	0.00	0.00	0.00	0.00	0.00	0.01	0.00	0.00	0.00
0.09	0.11	0.12	0.11	0.11	0.10	0.10	0.11	0.10	0.10	0.12
6.86	6.87	6.86	6.88	6.85	6.96	6.79	6.86	6.85	6.78	6.90
33.28	33.24	33.15	33.15	33.19	33.28	33.32	33.32	33.38	33.37	33.31
34.55	34.53	34.53	34.57	34.60	34.59	34.60	34.57	34.61	34.64	34.65
27.39	34.86	35.20	35.64	35.67	29.97	34.70	34.84	35.34	34.92	35.41
12.59	14.62	14.39	14.64	14.77	12.44	15.08	14.38	14.75	14.83	14.50
2.18	2.38	2.45	2.43	2.41	2.41	2.30	2.42	2.40	2.35	2.44

58.00	59.00	60.00	61.00	62.00	63.00	64.00	65.00	66.00	67.00	68.00
0.00	0.00	0.00	0.00	0.00	0.09	0.00	0.00	0.00	0.00	0.02
0.03	0.01	0.00	0.02	0.00	0.04	0.01	0.00	0.00	0.04	0.00
0.00	0.02	0.00	0.00	0.01	0.00	0.03	0.01	0.00	0.03	0.00
0.61	0.62	0.58	0.56	0.58	0.61	0.57	0.52	0.70	0.64	0.63
48.67	50.88	51.77	51.04	50.34	49.59	51.09	50.61	49.42	49.07	49.36
1.09	1.23	1.14	1.20	1.11	1.18	1.11	1.10	1.27	1.10	1.25
0.35	0.45	0.38	0.53	0.31	0.40	0.37	0.37	0.40	0.39	0.42
0.00	0.07	0.00	0.00	0.10	0.01	0.09	0.00	0.15	0.02	0.00
0.17	0.11	0.00	0.00	0.00	0.02	0.00	0.16	0.05	0.06	0.00
0.03	0.00	0.02	0.00	0.05	0.05	0.00	0.00	0.01	0.03	0.07
33.18	33.28	32.70	34.65	33.90	32.35	34.48	34.34	33.08	33.74	32.71
2.77	3.31	3.05	2.72	2.81	2.80	3.10	3.23	2.96	2.97	2.95
1.17	1.39	1.29	1.14	1.18	1.18	1.31	1.36	1.25	1.25	1.24
0.02	0.01	0.02	0.01	0.04	0.01	0.01	0.01	0.01	0.01	0.01
0.00	0.00	0.01	0.00	0.01	0.00	0.00	0.00	0.00	0.00	0.00
1.82	1.76	1.73	1.78	1.70	1.86	1.63	1.72	1.75	1.84	1.77
87.56	90.35	90.10	91.36	89.74	87.82	91.19	90.70	88.54	88.68	87.94
10.00	10.00	10.00	10.00	10.00	10.00	10.00	10.00	10.00	10.00	10.00
0.00	0.00	0.00	0.00	0.00	0.01	0.00	0.00	0.00	0.00	0.00
0.00	0.00	0.00	0.00	0.00	0.00	0.00	0.00	0.00	0.00	0.00
0.00	0.00	0.00	0.00	0.00	0.00	0.00	0.00	0.00	0.00	0.00
0.07	0.07	0.07	0.06	0.07	0.07	0.07	0.06	0.08	0.08	0.08
4.19	4.32	4.40	4.21	4.24	4.29	4.25	4.24	4.24	4.18	4.27
0.17	0.19	0.18	0.18	0.17	0.18	0.17	0.17	0.20	0.17	0.19
0.02	0.02	0.02	0.02	0.01	0.02	0.02	0.02	0.02	0.02	0.02
0.00	0.00	0.00	0.00	0.00	0.00	0.00	0.00	0.00	0.00	0.00
0.00	0.00	0.00	0.00	0.00	0.00	0.00	0.00	0.00	0.00	0.00
0.00	0.00	0.00	0.00	0.00	0.00	0.00	0.00	0.00	0.00	0.00
2.26	2.23	2.20	2.26	2.26	2.21	2.27	2.27	2.24	2.27	2.23
0.71	0.83	0.77	0.66	0.70	0.71	0.76	0.80	0.75	0.75	0.75
0.00	0.00	0.00	0.00	0.01	0.00	0.00	0.00	0.00	0.00	0.00
0.11	0.10	0.10	0.10	0.10	0.11	0.10	0.10	0.11	0.11	0.11
6.83	6.95	6.97	6.83	6.85	6.90	6.87	6.87	6.90	6.83	6.90
33.20	33.15	33.12	33.03	32.92	32.93	33.02	33.08	33.21	33.34	33.42
34.69	34.68	34.69	34.69	34.65	34.69	34.71	34.73	34.71	34.72	34.73
34.77	36.35	36.98	36.45	35.96	35.42	36.49	36.15	35.30	35.05	35.26
14.48	14.52	14.27	15.12	14.79	14.12	15.05	14.98	14.44	14.73	14.28
2.40	2.50	2.59	2.41	2.43	2.51	2.43	2.41	2.45	2.38	2.47

69.00	70.00	71.00	72.00	73.00	74.00	75.00	76.00	77.00	78.00	79.00
0.00	0.00	0.00	0.00	0.00	0.00	0.00	0.00	0.00	0.00	0.00
0.00	0.04	0.01	0.00	0.00	0.02	0.00	0.00	0.01	0.00	0.00
0.00	0.00	0.00	0.01	0.00	0.00	0.00	0.00	0.02	0.04	0.00
0.63	0.65	0.46	0.57	0.43	0.55	0.52	0.58	0.56	0.60	0.61
49.06	49.98	50.00	49.86	48.14	50.36	48.04	51.45	50.21	51.40	51.65
1.15	1.18	1.13	1.00	0.95	1.10	1.08	1.07	1.06	1.36	1.28
0.36	0.44	0.29	0.52	0.76	0.45	0.37	0.34	0.46	0.46	0.42
0.00	0.08	0.00	0.00	0.02	0.00	0.06	0.01	0.00	0.10	0.12
0.05	0.09	0.05	0.15	0.11	0.11	0.00	0.05	0.10	0.14	0.03
0.03	0.02	0.04	0.04	0.00	0.00	0.05	0.04	0.00	0.02	0.00
33.39	33.52	32.71	34.00	33.31	33.96	33.08	33.36	33.81	33.77	34.69
3.18	3.04	3.21	2.84	2.76	3.00	3.01	2.82	2.95	3.40	3.01
1.34	1.28	1.35	1.20	1.16	1.26	1.27	1.19	1.24	1.43	1.27
0.02	0.02	0.00	0.02	0.03	0.02	0.03	0.02	0.01	0.02	0.03
0.01	0.01	0.00	0.00	0.01	0.00	0.01	0.01	0.00	0.00	0.01
1.81	1.79	2.06	1.46	1.49	1.66	1.79	1.47	1.50	1.78	1.71
88.32	89.57	88.62	89.26	86.83	89.95	86.74	90.02	89.45	91.66	92.27
10.00	10.00	10.00	10.00	10.00	10.00	10.00	10.00	10.00	10.00	10.00
0.00	0.00	0.00	0.00	0.00	0.00	0.00	0.00	0.00	0.00	0.00
0.00	0.00	0.00	0.00	0.00	0.00	0.00	0.00	0.00	0.00	0.00
0.00	0.00	0.00	0.00	0.00	0.00	0.00	0.00	0.00	0.00	0.00
0.08	0.08	0.05	0.07	0.05	0.06	0.06	0.07	0.07	0.07	0.07
4.22	4.24	4.31	4.23	4.19	4.25	4.19	4.35	4.26	4.31	4.25
0.18	0.18	0.18	0.15	0.15	0.17	0.17	0.16	0.16	0.21	0.19
0.02	0.02	0.01	0.02	0.04	0.02	0.02	0.02	0.02	0.02	0.02
0.00	0.00	0.00	0.00	0.00	0.00	0.00	0.00	0.00	0.00	0.00
0.00	0.00	0.00	0.00	0.00	0.00	0.00	0.00	0.00	0.00	0.00
0.00	0.00	0.00	0.00	0.00	0.00	0.00	0.00	0.00	0.00	0.00
2.27	2.25	2.23	2.28	2.29	2.26	2.28	2.23	2.27	2.24	2.25
0.81	0.76	0.82	0.71	0.71	0.75	0.77	0.70	0.74	0.84	0.73
0.00	0.00	0.00	0.00	0.00	0.00	0.00	0.00	0.00	0.00	0.00
0.11	0.11	0.12	0.09	0.09	0.10	0.11	0.09	0.09	0.10	0.10
6.87	6.88	6.91	6.84	6.81	6.87	6.83	6.92	6.87	6.96	6.88
33.45	33.37	33.18	33.20	33.28	33.34	33.46	33.49	33.39	32.81	32.64
34.86	34.85	34.85	34.93	34.98	35.00	35.00	35.06	35.05	34.77	34.82
35.04	35.70	35.71	35.61	34.39	35.97	34.31	36.75	35.86	36.72	36.89
14.57	14.63	14.28	14.84	14.54	14.82	14.44	14.56	14.76	14.74	15.14
2.40	2.44	2.50	2.40	2.37	2.43	2.38	2.52	2.43	2.49	2.44

Conulariid

81.00	82.00	83.00	84.00	85.00	86.00	87.00	88.00	89.00	90.00	91.00
0.00	0.00	0.01	0.00	0.00	0.00	0.01	0.01	0.12	0.00	0.00
0.07	0.00	0.00	0.01	0.00	0.00	0.04	0.02	0.04	0.03	0.00
0.00	0.04	0.01	0.02	0.00	0.00	0.00	0.03	0.02	0.01	0.01
0.33	0.34	0.35	0.31	0.29	0.26	0.31	0.23	0.27	0.23	0.31
42.00	43.33	39.51	42.04	40.27	37.74	46.91	42.76	36.94	42.40	35.13
0.77	0.81	0.84	0.78	0.86	0.69	0.75	0.70	0.70	0.68	0.82
0.29	0.18	0.28	0.26	0.22	0.25	0.29	0.23	0.21	0.28	0.19
0.04	0.00	0.00	0.11	0.00	0.00	0.00	0.00	0.02	0.04	0.10
0.00	0.08	0.03	0.11	0.07	0.16	0.11	0.14	0.13	0.17	0.00
0.06	0.04	0.01	0.05	0.05	0.03	0.05	0.04	0.04	0.02	0.00
29.19	27.97	25.66	28.97	27.45	26.07	26.07	29.39	21.68	28.64	24.67
3.17	2.96	3.76	3.07	3.04	2.79	2.89	3.17	2.86	3.49	3.42
1.33	1.24	1.58	1.29	1.28	1.18	1.22	1.33	1.20	1.47	1.44
0.05	0.06	0.05	0.05	0.09	0.04	0.05	0.03	0.03	0.01	0.06
0.01	0.01	0.01	0.01	0.02	0.01	0.01	0.01	0.01	0.00	0.01
1.02	1.10	0.95	1.10	1.08	0.97	0.90	1.07	0.90	1.08	0.87
75.63	75.63	69.86	75.56	72.11	67.82	77.15	76.49	62.74	75.63	64.13
10.00	10.00	10.00	10.00	10.00	10.00	10.00	10.00	10.00	10.00	10.00
0.00	0.00	0.00	0.00	0.00	0.00	0.00	0.00	0.01	0.00	0.00
0.01	0.00	0.00	0.00	0.00	0.00	0.00	0.00	0.00	0.00	0.00
0.00	0.00	0.00	0.00	0.00	0.00	0.00	0.00	0.00	0.00	0.00
0.05	0.05	0.06	0.04	0.04	0.04	0.04	0.03	0.05	0.03	0.05
4.26	4.43	4.49	4.27	4.30	4.27	4.82	4.29	4.68	4.36	4.29
0.14	0.15	0.17	0.14	0.17	0.14	0.14	0.13	0.16	0.13	0.18
0.02	0.01	0.02	0.01	0.01	0.02	0.02	0.01	0.01	0.02	0.01
0.00	0.00	0.00	0.00	0.00	0.00	0.00	0.00	0.00	0.00	0.00
0.00	0.00	0.00	0.00	0.00	0.01	0.00	0.00	0.01	0.01	0.00
0.00	0.00	0.00	0.00	0.00	0.00	0.00	0.00	0.00	0.00	0.00
2.34	2.26	2.30	2.32	2.32	2.33	2.11	2.33	2.17	2.33	2.38
0.95	0.89	1.26	0.92	0.96	0.93	0.87	0.94	1.07	1.06	1.23
0.01	0.01	0.01	0.01	0.02	0.01	0.01	0.00	0.01	0.00	0.01
0.07	0.08	0.08	0.08	0.08	0.08	0.06	0.08	0.08	0.08	0.07
6.89	6.98	7.11	6.89	6.93	6.89	7.21	6.88	7.18	6.95	6.99
34.56	34.52	34.56	34.59	34.60	34.59	34.56	34.62	34.65	34.64	34.62
43.09	43.11	43.14	43.20	43.22	43.27	43.29	43.26	43.23	43.18	43.11
30.00	30.95	28.22	30.03	28.76	26.96	33.51	30.54	26.38	30.29	25.09
12.74	12.21	11.20	12.64	11.98	11.38	11.38	12.83	9.46	12.50	10.76
2.36	2.54	2.52	2.38	2.40	2.37	2.95	2.38	2.79	2.42	2.33

	Shrimp						
	36	37	38	39	40	41	42
SiO2	0.00	0.07	2.06	0.06	0.00	0.00	0.24
FeO	0.01	0.03	0.02	0.04	0.09	0.00	0.00
MnO	0.00	0.00	0.01	0.02	0.02	0.00	0.02
MgO	0.26	0.31	0.94	0.19	0.22	0.16	0.16
CaO	45.36	45.99	39.46	41.02	45.82	39.86	40.63
Na2O	0.92	0.75	0.63	0.62	0.61	0.68	0.80
SrO	0.36	0.47	0.30	0.37	0.45	0.40	0.31
La2O3	0.06	0.00	0.03	0.00	0.04	0.11	0.00
Ce2O3	0.04	0.04	0.06	0.02	0.02	0.00	0.00
Y2O3	0.02	0.04	0.04	0.03	0.00	0.00	0.00
P2O5	29.00	29.22	24.29	26.32	28.67	25.86	26.91
F	4.54	3.94	2.51	2.32	2.92	2.42	2.83
-O=F	1.91	1.66	1.06	0.98	1.23	1.02	1.19
Cl	0.04	0.04	0.04	0.02	0.05	0.04	0.02
-O=Cl	0.01	0.01	0.01	0.01	0.01	0.01	0.01
SO3	1.48	1.54	1.74	1.59	1.47	1.78	1.62
Total	80.17	80.76	71.06	71.65	79.16	70.28	72.34
O	10.000	10.000	10.000	10.000	10.000	10.000	10.000
Si	0.000	0.006	0.206	0.006	0.000	0.000	0.024
Fe2	0.001	0.002	0.002	0.004	0.007	0.000	0.000
Mn	0.000	0.000	0.001	0.002	0.002	0.000	0.001
Mg	0.036	0.042	0.141	0.029	0.030	0.024	0.024
Ca	4.514	4.480	4.228	4.357	4.473	4.324	4.296
Na	0.165	0.132	0.122	0.120	0.108	0.134	0.152
Sr	0.019	0.025	0.018	0.022	0.024	0.023	0.018
La	0.002	0.000	0.001	0.000	0.002	0.004	0.000
Ce	0.001	0.001	0.002	0.001	0.001	0.000	0.000
Y	0.001	0.002	0.002	0.002	0.000	0.000	0.000
P	2.281	2.249	2.056	2.209	2.212	2.217	2.248
F	1.335	1.132	0.794	0.728	0.841	0.776	0.884
Cl	0.006	0.006	0.006	0.004	0.007	0.007	0.004
S	0.103	0.105	0.131	0.118	0.101	0.135	0.120
Total	7.123	7.045	6.908	6.868	6.958	6.861	6.884
Ca	32.397857	32.850714	28.188571	29.298571	32.731429	28.472857	29.019286
P	12.656423	12.751125	10.600043	11.486399	12.512843	11.286085	11.741701
Ca/P	2.5597957	2.5762993	2.6592883	2.5507186	2.6158267	2.5228285	2.4714721

Typhloesus

Counts/arbitrary	Raman shift/cm^{-1}	Counts/arbitrary	Raman shift/cm^{-1}	Counts/arbitrary
146.89921	601.787924	335.569372	661.66135	520.330064
150.429335	715.272045	339.026037	703.336579	523.715419
153.958079	902.840639	342.481361	750.501052	527.099474
157.485444	1099.963775	345.935346	761.064252	530.482228
161.01143	1227.601459	349.387993	790.440977	533.863683
164.536038	1269.940111	352.839302	837.075341	537.24384
168.059268	1176.678293	356.289275	852.158652	540.622698
171.581122	1049.465394	359.737911	810.172317	544.000259
175.1016	908.653451	363.185212	804.321337	547.376524
178.620703	839.171701	366.631178	838.244485	550.751493
182.138431	846.868973	370.07581	855.882912	554.125167
185.654786	864.31935	373.519109	862.49508	557.497546
189.169768	847.39961	376.961076	885.871729	560.868632
192.683378	845.606764	380.40171	948.963782	564.238424
196.195617	792.605795	383.841014	942.145131	567.606925
199.706485	832.506876	387.278988	913.485291	570.974133
203.215983	859.208751	390.715632	892.419072	574.340051
206.724112	889.611283	394.150947	873.797429	577.704679
210.230874	923.373674	397.584934	890.943652	581.068017
213.736267	951.730456	401.017593	903.111058	584.430066
217.240294	962.440208	404.448927	865.545125	587.790827
220.742955	995.517133	407.878934	885.694718	591.150301
224.24425	984.895117	411.307616	875.696611	594.508488
227.744182	1023.529926	414.734973	858.886061	597.865389
231.242749	1065.959129	418.161007	819.572719	601.221005
234.739954	1119.850913	421.585718	787.029221	604.575336
238.235796	1120.307219	425.009106	767.822844	607.928383
241.730277	1062.962254	428.431173	696.425094	611.280147
245.223397	1016.87671	431.851919	620.886102	614.630629
248.715157	947.200904	435.271345	653.662523	617.979828
252.205558	902.007884	438.689451	656.23681	621.327747
255.694601	836.296534	442.106239	587.625939	624.674385
259.182286	842.275815	445.521709	555.606067	628.019743
262.668614	793.57934	448.935862	518.504538	631.363823
266.153586	747.356182	452.348698	467.461488	634.706624
269.637202	675.432567	455.760219	443.598262	638.048147
273.119464	646.266656	459.170424	455.978086	641.388393
276.600371	606.168712	462.579315	483.821768	644.727363
280.079926	568.096127	465.986893	507.349966	648.065058
283.558128	497.313202	469.393157	447.538261	651.401477
287.034978	500.818078	472.79811	437.697018	654.736622
290.510478	456.28771	476.201751	392.806045	658.070494
293.984627	463.215713	479.604081	372.404579	661.403093
297.457427	468.022518	483.005101	334.099526	664.73442
300.928878	446.115639	486.404812	331.916542	668.064475
304.398981	430.424135	489.803214	322.757049	671.39326
307.867737	392.380154	493.200308	326.221572	674.720774
311.335146	374.56153	496.596095	291.406906	678.047019
314.80121	393.685419	499.990576	259.716361	681.371995
318.265928	439.226232	503.383751	233.567485	684.695704
321.729303	497.747087	506.775621	224.282821	688.018145
325.191334	539.191393	510.166186	189.660843	691.339319
328.652022	571.28372	513.555448	204.523307	694.659227
332.111368	611.824151	516.943407	226.382097	697.97787

Raman shift/cm^{-1}	Counts/arbitrary	Raman shift/cm^{-1}	Counts/arbitrary	Raman shift/cm^{-1}
210.826831	701.295249	782.803711	878.574462	1089.933507
194.407622	704.611363	815.520137	881.823324	1008.84053
165.303883	707.926214	786.128185	885.070958	1059.601895
211.203791	711.239803	766.141305	888.317366	1126.851431
259.052779	714.55213	789.831667	891.562549	1159.385383
307.161766	717.863195	745.670994	894.806505	1157.392055
317.59631	721.173	712.743989	898.049238	1160.433006
279.147298	724.481546	691.05862	901.290746	1107.103498
245.020768	727.788832	659.550107	904.531032	1114.734857
288.655899	731.094859	700.024453	907.770094	1063.562334
280.582912	734.399629	676.005546	911.007935	1114.021538
297.41806	737.703141	669.718419	914.244555	1129.178782
274.094523	741.005397	712.098792	917.479953	1076.262273
284.821928	744.306398	716.201731	920.714132	1033.59442
278.701408	747.606143	768.250959	923.947092	1001.0929
234.125116	750.904634	764.578515	927.178833	1071.518058
285.408236	754.201871	756.783997	930.409355	1181.705445
380.18205	757.497855	785.98167	933.638661	1200.862317
423.255743	760.792586	766.470696	936.86675	1309.882856
434.024856	764.086066	798.851796	940.093622	1353.733181
455.782319	767.378295	824.31741	943.319279	1343.743954
452.173711	770.669273	829.181925	946.543722	1309.130377
472.506657	773.959002	908.621813	949.76695	1248.27084
454.608618	777.247482	881.807174	952.988964	1263.953772
482.89666	780.534713	888.787796	956.209766	1382.249449
442.35012	783.820696	914.398044	959.429356	1398.593437
426.613552	787.105433	925.508537	962.647734	1466.042789
395.236254	790.388923	1004.779891	965.864901	1473.918601
447.048396	793.671167	994.710757	969.080858	1484.807388
448.404223	796.952167	959.618287	972.295605	1465.242518
510.432339	800.231922	990.658417	975.509143	1433.359741
561.957895	803.510433	940.467091	978.721473	1444.59138
595.925207	806.787701	943.272247	981.932595	1546.536133
580.935042	810.063727	954.603558	985.14251	1560.864205
569.556211	813.338512	1009.242989	988.351219	1591.344102
556.641675	816.612055	1044.204678	991.558722	1619.050892
587.858115	819.884358	1016.453165	994.76502	1569.671835
572.155971	823.155421	931.534013	997.970113	1498.596103
626.978499	826.425245	910.079104	1001.174002	1464.841462
647.362303	829.693831	864.171634	1004.376688	1467.964014
675.559223	832.961179	854.375642	1007.578172	1518.933495
711.870345	836.22729	884.964357	1010.778453	1621.134884
702.541246	839.492164	920.646012	1013.977533	1715.386156
714.578816	842.755803	944.098004	1017.175413	1737.847215
699.502814	846.018207	941.008981	1020.372092	1728.032644
674.717447	849.279376	921.465591	1023.567572	1668.470452
662.325732	852.539312	995.100444	1026.761854	1674.336027
634.09235	855.798015	996.13215	1029.954937	1700.492788
634.291454	859.055485	1031.425482	1033.146822	1706.45274
637.242962	862.311723	1074.413416	1036.337511	1813.946551
653.435474	865.566731	1084.479768	1039.527003	1892.714793
705.499578	868.820508	1122.513743	1042.7153	2017.160637
724.174053	872.073055	1157.748339	1045.902402	2027.034604
775.901753	875.324373	1110.63297	1049.08831	2000.305654

Counts/arbitrary	Raman shift/cm^{-1}	Counts/arbitrary	Raman shift/cm^{-1}	Counts/arbitrary
1052.273024	1984.06354	1222.492235	5176.550715	1389.329572
1055.456544	2015.059641	1225.612254	5309.411039	1392.38786
1058.638873	1963.946178	1228.731114	5376.287003	1395.44502
1061.820009	2021.628436	1231.848816	5515.753663	1398.501055
1064.999954	2061.212908	1234.96536	5607.097107	1401.555963
1068.178709	2073.949325	1238.080746	5799.990381	1404.609747
1071.356274	1929.69819	1241.194976	5953.804612	1407.662406
1074.532649	1876.773522	1244.30805	6089.305864	1410.713941
1077.707836	1842.981107	1247.419969	6206.400064	1413.764352
1080.881835	1946.641184	1250.530732	6389.727279	1416.813641
1084.054646	2000.566179	1253.640342	6489.427422	1419.861808
1087.226271	2185.159634	1256.748798	6633.583591	1422.908853
1090.396709	2259.720759	1259.8561	6679.047252	1425.954776
1093.565962	2317.173298	1262.962251	6835.342487	1428.999579
1096.73403	2296.799617	1266.067249	6964.516763	1432.043263
1099.900913	2312.386311	1269.171097	7040.520536	1435.085827
1103.066613	2352.051301	1272.273794	7131.408609	1438.127272
1106.23113	2392.827741	1275.37534	7286.485677	1441.167599
1109.394465	2433.745146	1278.475738	7401.684169	1444.206808
1112.556617	2498.555673	1281.574986	7514.809323	1447.244901
1115.717589	2515.540983	1284.673087	7511.565787	1450.281877
1118.87738	2535.51829	1287.77004	7588.959063	1453.317737
1122.035991	2519.228404	1290.865845	7654.891409	1456.352481
1125.193422	2479.461047	1293.960505	7721.265702	1459.386111
1128.349675	2455.635213	1297.054018	7881.023456	1462.418627
1131.50475	2440.427274	1300.146387	8064.378295	1465.450029
1134.658648	2518.901388	1303.237611	8201.794538	1468.480319
1137.811368	2639.648081	1306.32769	8331.526768	1471.509496
1140.962913	2792.662874	1309.416627	8505.947943	1474.537561
1144.113282	2973.252347	1312.50442	8637.187965	1477.564514
1147.262475	3145.411921	1315.591071	8781.37096	1480.590357
1150.410495	3182.449995	1318.676581	9005.837205	1483.61509
1153.557341	3191.246765	1321.76095	9236.219281	1486.638713
1156.703013	3217.279916	1324.844178	9447.917968	1489.661228
1159.847513	3301.016487	1327.926266	9563.422083	1492.682634
1162.990842	3418.712279	1331.007215	9722.756793	1495.702932
1166.132999	3446.44911	1334.087025	9932.491398	1498.722122
1169.273985	3571.925294	1337.165698	9940.373636	1501.740206
1172.413801	3630.599287	1340.243232	10165.5943	1504.757184
1175.552448	3728.088609	1343.31963	10330.43179	1507.773057
1178.689926	3732.458484	1346.394892	10405.70556	1510.787824
1181.826236	3763.120499	1349.469018	10386.43744	1513.801487
1184.961378	3862.359224	1352.542008	10303.89944	1516.814046
1188.095353	4046.769149	1355.613865	10383.28924	1519.825502
1191.228162	4102.359733	1358.684587	10474.4521	1522.835855
1194.359805	4235.132442	1361.754176	10404.81631	1525.845105
1197.490283	4265.325031	1364.822632	10573.27532	1528.853255
1200.619597	4351.756054	1367.889956	10617.79229	1531.860303
1203.747746	4348.802549	1370.956148	10503.36942	1534.866251
1206.874732	4451.449903	1374.02121	10386.62086	1537.871099
1210.000556	4572.418219	1377.085141	10177.63839	1540.874847
1213.125217	4780.133143	1380.147942	10072.74596	1543.877497
1216.248717	4940.496592	1383.209614	9940.110626	1546.879048
1219.371056	5092.382678	1386.270157	9730.322655	1549.879502

Raman shift/cm^{-1}	Counts/arbitrary	Raman shift/cm^{-1}	Counts/arbitrary	Raman shift/cm^{-1}
9546.199771	1552.878859	8708.452897	1713.230441	800.171672
9387.988079	1555.87712	9174.555813	1716.170316	523.702604
9160.979069	1558.874284	9668.073562	1719.109124	506.592373
9057.687602	1561.870353	10089.30988	1722.046866	575.533911
8793.349557	1564.865327	10500.01307	1724.983544	645.676813
8537.362228	1567.859207	10960.11906	1727.919157	670.384981
8357.637086	1570.851993	11407.22411	1730.853706	581.627249
8163.088739	1573.843686	11880.5599	1733.787192	433.078267
7923.734035	1576.834287	12262.52454	1736.719614	271.513712
7676.406959	1579.823795	12568.49958	1739.650975	189.746598
7532.496326	1582.812212	12766.91124	1742.581273	128.255243
7296.500965	1585.799538	12896.32609	1745.51051	88.349948
7108.677457	1588.785774	13077.88762	1748.438687	213.056472
6920.953979	1591.77092	13284.90717	1751.365803	267.738585
6854.833255	1594.754977	13394.67411	1754.29186	240.870845
6746.007153	1597.737945	13517.53301	1757.216858	241.618854
6586.46403	1600.719825	13432.72204	1760.140797	539.037572
6392.70043	1603.700617	13267.22978	1763.063678	672.08466
6362.206056	1606.680323	12956.66283	1765.985501	660.385174
6121.267568	1609.658942	12572.54315	1768.906268	667.242343
6012.288732	1612.636475	12125.04485	1771.825978	664.081002
5943.958282	1615.612923	11482.74845	1774.744632	686.17567
5867.125666	1618.588286	10749.60762	1777.662231	563.435229
5744.783871	1621.562565	9924.551941	1780.578775	600.806777
5638.980751	1624.53576	9090.63366	1783.494265	751.179217
5519.962059	1627.507872	8184.174731	1786.4087	644.362079
5513.124203	1630.478901	7351.311747	1789.322083	586.144617
5453.197644	1633.448848	6572.68984	1792.234413	515.353513
5342.19741	1636.417714	5822.001571	1795.145691	468.595313
5234.64713	1639.3855	5127.749431	1798.055917	467.814168
5170.72537	1642.352204	4430.697694	1800.965092	490.450985
5085.937641	1645.317829	3827.259702	1803.873217	619.957152
5073.612585	1648.282375	3389.999348	1806.780291	718.55998
5109.955759	1651.245842	3023.243393	1809.686316	791.843889
5163.83723	1654.208231	2744.570275	1812.591292	859.286028
5279.138907	1657.169542	2415.63338	1815.49522	703.387168
5225.221366	1660.129776	2226.519969	1818.398099	545.516959
5148.758573	1663.088934	2188.750942	1821.299932	583.175008
5138.47589	1666.047016	1853.984969	1824.200717	615.233124
5126.799292	1669.004022	1655.741913	1827.100456	691.819158
5130.733703	1671.959953	1492.029524	1829.999149	762.282478
5266.243115	1674.914811	1425.125763	1832.896797	843.082196
5450.1611	1677.868594	1228.609272	1835.793401	894.364302
5748.240723	1680.821304	1053.211232	1838.68896	695.182681
5896.031563	1683.772942	1128.418629	1841.583475	580.942099
6086.844248	1686.723507	1238.132325	1844.476947	605.740623
6183.280288	1689.673001	1109.840248	1847.369377	463.296416
6413.160154	1692.621424	1059.124324	1850.260764	305.76821
6657.117075	1695.568777	1060.489633	1853.15111	214.936376
6992.397228	1698.515059	1216.833959	1856.040415	295.258929
7361.577043	1701.460272	1158.149543	1858.928679	408.835016
7680.597575	1704.404416	1132.569065	1861.815903	447.130616
7973.454797	1707.347492	1075.093858	1864.702088	419.596143
8329.444185	1710.2895	1025.722295	1867.587234	444.452632

Counts/arbitrary	Raman shift/cm^{-1}
1870.471341	395.911805
1873.35441	308.494245
1876.236442	312.557228
1879.117437	411.918591
1881.997396	367.240972
1884.876319	449.046562
1887.754207	438.053987
1890.631059	465.436035
1893.506878	526.284402
1896.381663	621.121054
1899.255414	610.921851
1902.128133	561.927669
1904.99982	391.282744
1907.870475	419.142888
1910.740098	384.267204
1913.608692	319.701567
1916.476255	465.651294
1919.342788	623.597924
1922.208292	829.132849
1925.072768	950.684449
1927.936216	1024.656787
1930.798636	1089.47909
1933.660029	988.144834
1936.520396	903.455272
1939.379737	917.449176
1942.238052	981.766148
1945.095342	1052.318395
1947.951608	1198.485281
1950.80685	1422.172373
1953.661068	1484.387197
1956.514264	1457.060434
1959.366437	1491.786017
1962.217588	1362.301852
1965.067718	1418.039165
1967.916827	1319.595866
1970.764915	1369.178953
1973.611984	1455.875236
1976.458033	1503.913074
1979.303064	1457.818838
1982.147076	1524.333964
1984.990071	1630.578364
1987.832048	1721.215151
1990.673008	1551.46563
1993.512953	1321.346243
1996.351881	1073.33324

Polychaete jaw

Counts/arbitrary	Raman shift/cm^{-1}	Counts/arbitrary	Raman shift/cm^{-1}
503.38	112.32	684.70	268.43
506.78	105.05	688.02	272.47
510.17	121.20	691.34	286.95
513.56	96.06	694.66	304.82
516.94	91.34	697.98	300.55
520.33	79.67	701.30	301.40
523.72	90.96	704.61	280.49
527.10	111.18	707.93	268.16
530.48	150.53	711.24	308.55
533.86	153.28	714.55	254.08
537.24	153.20	717.86	270.68
540.62	126.49	721.17	274.79
544.00	130.76	724.48	245.71
547.38	111.87	727.79	274.41
550.75	96.08	731.09	253.47
554.13	107.44	734.40	285.01
557.50	134.38	737.70	310.59
560.87	149.88	741.01	251.66
564.24	144.08	744.31	284.81
567.61	162.45	747.61	270.89
570.97	203.91	750.90	252.21
574.34	197.09	754.20	239.93
577.70	177.63	757.50	192.78
581.07	176.23	760.79	207.43
584.43	185.77	764.09	204.55
587.79	164.98	767.38	195.91
591.15	139.20	770.67	255.53
594.51	135.44	773.96	264.97
597.87	151.48	777.25	288.35
601.22	152.75	780.53	273.98
604.58	160.21	783.82	268.63
607.93	174.01	787.11	267.61
611.28	219.80	790.39	274.22
614.63	257.48	793.67	297.93
617.98	263.97	796.95	315.89
621.33	263.12	800.23	293.26
624.67	246.93	803.51	309.37
628.02	244.90	806.79	265.76
631.36	233.31	810.06	233.58
634.71	228.33	813.34	203.71
638.05	247.22	816.61	182.12
641.39	269.21	819.88	175.78
644.73	233.35	823.16	142.56
648.07	239.94	826.43	116.47
651.40	223.79	829.69	152.11
654.74	248.81	832.96	158.48
658.07	256.92	836.23	166.81
661.40	273.23	839.49	189.49
664.73	279.96	842.76	180.95
668.06	263.99	846.02	161.45
671.39	249.26	849.28	133.48
674.72	255.94	852.54	92.99
678.05	239.81	855.80	121.39
681.37	239.41	859.06	128.18

Counts/arbitrary	Raman shift/cm^{-1}	Counts/arbitrary	Raman shift/cm^{-1}
862.31	151.09	1036.34	122.70
865.57	189.66	1039.53	72.00
868.82	195.91	1042.72	38.85
872.07	153.91	1045.90	66.65
875.32	109.93	1049.09	115.49
878.57	64.12	1052.27	150.72
881.82	75.14	1055.46	179.77
885.07	55.97	1058.64	175.09
888.32	115.51	1061.82	213.48
891.56	156.06	1065.00	207.89
894.81	141.24	1068.18	176.03
898.05	121.62	1071.36	184.79
901.29	93.15	1074.53	215.15
904.53	48.69	1077.71	220.47
907.77	28.46	1080.88	253.52
911.01	-18.13	1084.05	298.84
914.24	-15.09	1087.23	356.93
917.48	-42.51	1090.40	360.40
920.71	-15.62	1093.57	322.19
923.95	14.26	1096.73	356.54
927.18	33.45	1099.90	367.01
930.41	50.04	1103.07	403.19
933.64	90.87	1106.23	449.87
936.87	83.31	1109.39	514.20
940.09	82.03	1112.56	551.26
943.32	89.90	1115.72	537.47
946.54	133.09	1118.88	478.58
949.77	94.55	1122.04	498.06
952.99	89.00	1125.19	499.91
956.21	73.31	1128.35	564.74
959.43	29.56	1131.50	584.89
962.65	40.18	1134.66	643.45
965.86	45.02	1137.81	693.89
969.08	60.75	1140.96	734.92
972.30	73.33	1144.11	778.89
975.51	78.40	1147.26	845.50
978.72	115.46	1150.41	894.89
981.93	110.97	1153.56	966.01
985.14	78.70	1156.70	981.95
988.35	99.69	1159.85	1004.79
991.56	54.27	1162.99	1019.80
994.77	64.95	1166.13	1060.47
997.97	101.28	1169.27	1122.38
1001.17	109.65	1172.41	1172.85
1004.38	106.01	1175.55	1212.35
1007.58	125.83	1178.69	1218.73
1010.78	102.97	1181.83	1224.87
1013.98	70.69	1184.96	1236.46
1017.18	52.58	1188.10	1256.36
1020.37	120.27	1191.23	1322.26
1023.57	192.86	1194.36	1404.06
1026.76	185.55	1197.49	1447.61
1029.95	186.50	1200.62	1470.14
1033.15	165.89	1203.75	1452.42

Counts/arbitrary	Raman shift/cm^{-1}	Counts/arbitrary	Raman shift/cm^{-1}
1206.87	1489.72	1374.02	4309.31
1210.00	1501.99	1377.09	4271.53
1213.13	1565.26	1380.15	4181.42
1216.25	1657.63	1383.21	4098.26
1219.37	1779.52	1386.27	4024.66
1222.49	1835.53	1389.33	3967.80
1225.61	1892.66	1392.39	3862.22
1228.73	1972.40	1395.45	3890.64
1231.85	2033.34	1398.50	3852.13
1234.97	2013.61	1401.56	3829.24
1238.08	2047.13	1404.61	3742.73
1241.19	2055.92	1407.66	3630.73
1244.31	2089.87	1410.71	3508.83
1247.42	2132.06	1413.76	3387.03
1250.53	2233.46	1416.81	3256.55
1253.64	2358.68	1419.86	3156.36
1256.75	2455.03	1422.91	3104.02
1259.86	2479.81	1425.95	3111.57
1262.96	2527.61	1429.00	3060.75
1266.07	2523.65	1432.04	3004.33
1269.17	2557.32	1435.09	2982.90
1272.27	2585.05	1438.13	2981.64
1275.38	2661.51	1441.17	2931.68
1278.48	2750.60	1444.21	2798.38
1281.57	2798.87	1447.24	2814.08
1284.67	2830.68	1450.28	2748.04
1287.77	2867.43	1453.32	2647.66
1290.87	2868.11	1456.35	2560.75
1293.96	2891.54	1459.39	2503.89
1297.05	2900.57	1462.42	2477.94
1300.15	2963.49	1465.45	2456.41
1303.24	3095.89	1468.48	2367.32
1306.33	3143.48	1471.51	2397.82
1309.42	3215.60	1474.54	2356.13
1312.50	3293.00	1477.56	2327.05
1315.59	3337.36	1480.59	2317.05
1318.68	3403.19	1483.62	2245.61
1321.76	3496.54	1486.64	2232.72
1324.84	3582.34	1489.66	2227.20
1327.93	3724.24	1492.68	2237.30
1331.01	3831.96	1495.70	2255.53
1334.09	3909.33	1498.72	2290.94
1337.17	3982.80	1501.74	2368.53
1340.24	4033.07	1504.76	2457.29
1343.32	4096.07	1507.77	2443.82
1346.39	4145.01	1510.79	2496.65
1349.47	4111.04	1513.80	2530.22
1352.54	4129.12	1516.81	2600.02
1355.61	4174.10	1519.83	2621.35
1358.68	4198.15	1522.84	2610.97
1361.75	4240.35	1525.85	2716.64
1364.82	4305.40	1528.85	2775.93
1367.89	4313.54	1531.86	2774.42
1370.96	4345.12	1534.87	2868.44

Counts/arbitrary	Raman shift/cm^{-1}	Counts/arbitrary	Raman shift/cm^{-1}
1537.87	2981.44	1698.52	446.86
1540.87	3119.50	1701.46	375.13
1543.88	3240.95	1704.40	323.53
1546.88	3334.60	1707.35	312.50
1549.88	3561.81	1710.29	370.93
1552.88	3667.50	1713.23	372.69
1555.88	3745.45	1716.17	353.49
1558.87	3916.76	1719.11	298.43
1561.87	4053.66	1722.05	278.65
1564.87	4171.23	1724.98	208.79
1567.86	4276.50	1727.92	179.29
1570.85	4358.33	1730.85	169.41
1573.84	4498.89	1733.79	181.67
1576.83	4522.65	1736.72	147.11
1579.82	4564.07	1739.65	112.52
1582.81	4650.73	1742.58	139.99
1585.80	4744.61	1745.51	189.95
1588.79	4835.07	1748.44	190.81
1591.77	4889.67	1751.37	219.24
1594.75	4878.47	1754.29	232.10
1597.74	4883.93	1757.22	238.63
1600.72	4806.79	1760.14	237.57
1603.70	4693.12	1763.06	238.48
1606.68	4566.78	1765.99	268.78
1609.66	4489.81	1768.91	314.18
1612.64	4331.75	1771.83	302.99
1615.61	4114.75	1774.74	321.78
1618.59	3919.68	1777.66	312.64
1621.56	3623.55	1780.58	294.66
1624.54	3310.81	1783.49	295.33
1627.51	2997.95	1786.41	309.28
1630.48	2747.80	1789.32	304.71
1633.45	2501.02	1792.23	302.59
1636.42	2278.05	1795.15	225.61
1639.39	2078.09	1798.06	146.02
1642.35	1897.76	1800.97	85.16
1645.32	1698.13	1803.87	78.72
1648.28	1548.52	1806.78	120.65
1651.25	1409.76	1809.69	224.98
1654.21	1357.47	1812.59	260.50
1657.17	1239.25	1815.50	309.08
1660.13	1187.55	1818.40	309.42
1663.09	1069.00	1821.30	283.95
1666.05	918.34	1824.20	261.95
1669.00	860.09	1827.10	249.65
1671.96	769.79	1830.00	280.44
1674.91	679.64	1832.90	334.69
1677.87	688.19	1835.79	347.28
1680.82	671.83	1838.69	363.88
1683.77	677.83	1841.58	372.35
1686.72	677.09	1844.48	438.75
1689.67	657.23	1847.37	389.25
1692.62	633.74	1850.26	355.84
1695.57	543.68	1853.15	379.82

Counts/arbitrary	Raman shift/cm^{-1}
1856.04	359.23
1858.93	403.60
1861.82	356.24
1864.70	363.05
1867.59	391.18
1870.47	370.13
1873.35	318.28
1876.24	319.26
1879.12	334.71
1882.00	346.89
1884.88	342.82
1887.75	350.09
1890.63	333.99
1893.51	337.48
1896.38	313.15
1899.26	353.82
1902.13	386.09
1905.00	358.90
1907.87	352.37
1910.74	386.70
1913.61	319.89
1916.48	257.04
1919.34	284.46
1922.21	310.75
1925.07	333.39
1927.94	374.73
1930.80	410.13
1933.66	506.88
1936.52	426.38
1939.38	370.66
1942.24	368.81
1945.10	315.14
1947.95	326.33
1950.81	329.92
1953.66	341.57
1956.51	422.03
1959.37	414.80
1962.22	448.59
1965.07	440.25
1967.92	364.29
1970.76	313.50
1973.61	267.15
1976.46	182.23
1979.30	196.23
1982.15	176.79
1984.99	253.33
1987.83	283.47
1990.67	273.01
1993.51	255.71
1996.35	258.43

CYCLOIDEA OF THE MISSISSIPPIAN BEAR GULCH LIMESTONE OF CENTRAL MONTANA

FREDERICK R. SCHRAM[1], ARJAN C. BOERE[1] AND NATALIE THOMAS[2]

[1]Zoological Museum, University of Amsterdam, Maurtiskade 57, 1092 AD Amsterdam, Netherlands, <schram@science.uva.nl.>, and [2]Dept of Geology, University of Leicester, Leicester LE1 7RH, UK.

ABSTRACT. A new species of cycloid crustacean, *Halicyne montanaensis*, is described from the uppermost Mississippian locality at Bear Gulch, in central Montana. Although the species is a rare component of the fauna and the specimens at hand are not well preserved, the material does allow comparison to other species in the genus. The addition of *Halicyne montanaensis* with the species list of the Bear Gulch fauna strengthens similarities to other Carboniferous Konservat-Lagerstätten in Europe and North America and reinforces ideas about a persistent near-shore marine chronofauna in this time period.

INTRODUCTION

The strata of the Bear Gulch Limestone deposits are part of the Big Snowy Group dated as Late Mississippian, Chesterian in age (Cox, 1986; Jenner et al., 1998) just

below the Mississippian-Pennsylvanian boundary. The Bear Gulch fossils are noted for their generally high quality of preservation (Melton, 1971) and suggest an anoxic environment and rapid burial of the organisms, though this would seem to be contradicted by the presence of a large array of burrowing and benthic fishes. The history of deposition has been reconstructed in great detail (Feldman *et al.*, 1994; Williams, 1983; Cox, 1986); it represents a bay at latitude approximately 10°N in an arid, monsoonal climate comparable to the present-day Sahel. Depending on the prevailing winds and circulation, the bay appears to have developed seasonally an anoxic bottom layer associated with high rates of cyclic deposition. This would explain the extraordinary preservation, the presence of those problematic bottom-dwelling fishes and other benthos, and the peculiar, regularly alternating size and coloring of the sediments.

The first cycloid described was under the name *Agnostus radialis* (Phillips, 1835). From that time on, the higher taxonomic placement of cycloids has shifted from group to group with numerous conflicting suggestions as to their affinity (for an overview, see Schram *et al.*, 1997). It appears that the cycloids belong within the crustaceans and most likely within the class Maxillopoda. They were quite diverse in the Paleozoic (see the reviews in Clark, 1989; Schram *et al.*, 1997; Brambilla *et al.*, 2002) and are now known to have survived through the close of the Cretaceous (Fraaije *et al.*, 2003). The most recent cladistic analysis places the cycloids near the Copepoda (Schram *et al.*, 1997).

There is a moderate degree of diversity in shapes and numbers of taxa within the group. Three distinct morphotypes are now recognized within the genus *Cyclus* alone and, in addition, *Halicyne* shows yet another different morphology. However, some of these divergences in shape may be a result of taphonomy, since the vaulted,

convex specimens are in general found in limestones, while the flattened specimens are mainly found in shales (Schram *et al.*, 1997). Nevertheless, there are a number of distinct characters that unite the cycloids, e.g., the shield-like carapace fused to all thoracic segments, uniramous antennae, large sub-chelate maxillae and maxillipeds, posterior thoracopods as robust uniramous walking limbs, and a short 1- or 2-segment abdomen.

Cycloids are found in Austria, Belgium, Bosnia, France, Germany, Ireland, Italy, Russia, Netherlands, the U.K ., central Asia, and the U.S.A. (Glaessner, 1969; Schram *et al.*, 1997) and are mainly associated with marine to brackish environments. Cycloids frequently co-occur with plant material. Schram *et al.* (1997) suggested cycloids might have had an herbivorous or scavenging life style, i.e., that they perhaps occupied a niche equivalent to modern crabs (Brachyura).

MATERIALS AND METHODS

This study is based on only 6 specimens: five collected in the 1970s near Beckett, Montana, U.S.A. (Natural History Museum of Los Angeles County, Invertebrate Paleontology locality 15424), and one specimen (CM-45816) from the collections of the Carnegie Museum of Natural History. The specimens were examined with a variety of light microscopic techniques using various lighting strategies in both a dry state and submerged under water. Digitized photographs and camera lucida drawings were made under these varying conditions.

SYSTEMATICS

Maxillopoda Dahl, 1956

Cycloidea Glaessner, 1928

Cyclidae Packard, 1885

Halicyne von Meyer, 1838

Halicyne montanaensis new species

DIAGNOSIS. Carapace round to oval in outline, slightly vaulted in cross section. Surface papillose, marginal shelf distinctly thickened with a smooth to slightly irregular edge. Carapace excavated posteriorly. Distinct optic notches with large, stalked, compound eyes. Rostral plate broadly fused with carapace and anteriorly truncated. Anterior-most part of carapace bearing rounded knobs or bosses. Terminal segments of all geniculate claws moderate in size and relatively narrow, penultimate segments wide.

HOLOTYPE. LACMIP 7310 (Fig. 1.1,2)

MATERIAL EXAMINED. LACMIP 7310, 7311, 7312, 7313, 7314, CM 45816

DESCRIPTION. The carapace shield is round to oval in outline ranging from 10.8 to approximately 25 mm in length, with a distinct thickened marginal shelf (LACMIP 7310a, Fig. 1.1,2; LACMIP 7313, Fig. 3.2; CM 45816, Fig. 1.3,4) and distinct cross-sectional vaulting (LACMIP 7310a, LACMIP 7313) characteristic of the genus. The edge of the carapace shelf is smooth (CM 45816) to irregular (LACMIP 7310) in outline. The surface of the carapace is distinctly papillated (LACMIP 7311a, Fig. 1.5,6; LACMIP 7313, Fig. 3.2), the mid-anterior surface especially so (CM 45816) where the patterning consists of almost rhombohedral knobs or bosses. The center of the carapace shield displays two faint ridges running

anterior-posteriorly and delineating a v-shaped area (LACMIP 7310). The carapace shield covers virtually the entire body (Fig. 1.1-4) and includes an anterior extension or rostral plate that is truncated and covers the cephalon proper (LACMIP 7310a, LACMIP 7313, CM 45816). The carapace directly over the optical notches is slightly raised; between these areas is a semi-oblong elevated area just posterior to the rostral plate (CM 45816). The anteriormost rostral aspect of the carapace has an irregular margin.

Optical notches (Fig. 1.3,4) are located just anterior to either end of the marginal shelf, (CM 45816; LACMIP 7310). Within these notches are stalked compound eyes that are exceptionally well preserved, with up to 45 hexagonal to rounded ommatidia visible (CM 45816; Fig. 3.5).

Both pairs of antennae are very poorly preserved. One set may be partly visible on the anterior lateral left side of specimen LACMIP 7313 protruding from where the edge of the rostrum and carapace would have been (Figs. 3.2, 4.2). These seem to consist of the peduncular segments and the proximal portions of the flagella. The holotype, LACMIP 7310 also shows a slight trace of antennae (Figs. 1.1, 2.1.

Anteriorly, there is a pair of large uniramous second maxillae (Fig. 1.1-4) extending antero-laterally from the frontal portions of the head. Also, at least one set of rather broad maxillipeds is present. Both these limbs bear serrate armature along the anterior margins of the dactylus and propodus (LACMIP 7310b, CM 45816). It is not entirely clear if the seconnd set of thoracopods were developed as maxillipeds as well. The segmentation of the cephalic appendages is obscured, but the cuticle of these limbs seems to be finely papillated (LACMIP 7313, Fig. 3.2). The flexion of the dactyl of the maxillae and maxilliped back onto the serrate anterior edge of the propodus probably facilitated grasping.

The uniramous thoracic limbs 2 through 6 (LACMIP 7310a, LACMIP 7310b, Fig. 1.2; LACMIP 7314, Fig. 3.1) are robust, short and terminally pointed, with the narrow dactyls generally directed anteriad, especially on thoracopods 2 and 3. The penultimate segments are relatively thick (LACMIP 7310). Little is discernable concerning the more proximal segments of these limbs. Only on the right hand side of LACMIP 7310, where part of the carapace is missing, can one see parts of the thoracic tergites and proximal segments of the thoracopods (Figs. 2.1, 2.2), which appear to be less robust, yet longer than either of the two distal segments. These thoracopods were probably used for walking or pushing along the substrate.

The major feature in common among all the specimens is the fan-shaped pattern of the posterior thoracic segments, clearly evident on LACMIP 7311a (Fig. 1.5), LACMIP 7312a (Fig. 3.3,4), and LACMIP 7313. LACMIP 7311 shows only a small part of the posterior end of the animal, while the anterior half was not well preserved. More anteriorly, the trunk shows traces of segmentation that is either chevron shaped, with the lateral aspect directed anteriorly (LACMIP 7313, Fig. 2.3) or parallel, laterally-directed segmentation (LACMIP 7310a; LACMIP 7312, Fig. 4.3). What one actually sees in all these instances are the endophragmal partitions between the segments themselves.

A large sub-triangular area is visible (Fig. 2.2) on the central aspect of the trunk (LACMIP 7310a, CM-45816), which corresponds to the v-shaped area of the carapace and probably marks where the carapace was attached to the underlying segments. The gut or digestive tract (Figs. 3.1, 4.1) is preserved in only one specimen as a dark, irregularly shaped cast (LACMIP-7314).

There is a short, apparently 2-segment abdomen (LACMIP 7311a, Figs. 1.5, 2.3; LACMIP 7314, Figs. 3.1, 4.1), exposed because of the posterior notch of the

carapace. Only one specimen (LACMIP 7311b) displays distinct caudal rami (Figs. 1.6, 2.4). These rami appear to be uniramous, long (up to 5 mm), thin, blade-like, and attached to the posterior-most abdominal segment.

REMARKS. Most specimens at hand are of relatively poor quality. Only the holotype specimen is fairly complete. Specimens LACMIP 7310, 7311, 7312, and CM 45816 comprise both parts and counterparts.

One can note differences among the specimens, e.g., in quality or amount of organic material preserved, and these are undoubtedly due to taphonomy, which probably also explains the variation visible in the differential coloring of the surrounding rock matrix and the degree of preservation of associated plant material (LACMIP 7312) (Fig. 3.3).

A reconstruction of *Halicyne montanaensis* is offered in Figure 5.

DISCUSSION

Currently, five species are easily recognized in *Halicyne*, and most of the characteristic features for the genus are clearly present in the specimens in this study including the round to oval shape, the marginal shelf and the papillated surface of the carapace, the distinct optical notches, and the truncated anterior part of the rostral plate. [The affinities of a sixth species, *H. plana* (Müller, 1955) is uncertain, the described material consisted only of poorly preserved carapace shields.] The large maxillipeds, which also are found in *H. max* Schram, Vonk and Hof, 1997 and *H. gondwanae* Brambilla et al., 2002, are preserved in other species of the genus such as *H. ornata* Gall and Grauvogel, 1967, *H. agnota* (von Meyer, 1847), or the enigmatic genus *Carcinaspides* (Schafhäutl, 1863). The elevated pattern of bosses on the dorsal surface of the carapace, including the anterior-most bosses or knobs, is similar to

those in *H. ornata* and *H. agnota* from the Triassic Muschelkalk. Although it is not certain whether the edge of the marginal shelf is smooth or irregular, there is no indication of a regularly sculpted margin as seen in *H. max.* The postero-median edge of the carapace, which is rounded in *H. max* but pointed in *H. ornata* and *H. agnota*, though obscured in most of the specimens at hand possesses a posterior notch. There is a small abdomen or telson with two caudal rami, bearing some resemblance to the posterior part of *H. gondwanae* (Bambilla et al., 2002).

The stout, robust thoracopods on *H. montanaensis* are quite different from the limbs of *H. max*, which are longer and thinner. The thoracopods of *H. montanaensis* resemble the robust, supposedly biramous limbs of *H. ornata*, but there is no indication of any biramous limbs on the Bear Gulch species. The presence or absence of biramous limbs has been both important and controversial in discussions of the affinity of the cycloids (Glaessner, 1969, Schram et al., 1997), but there is no indication of exopods in *H. max* or *H. gondwanae,* nor in the specimens under study here. In addition, the orientation of the limbs with respect to the trunk differs. In *H. max* they are concentrated in the anterior portion of the thorax, while in the specimens here they are positioned more evenly along the trunk. The strongest resemblance of *H, montanaensis* seems to be to *H. ornata* as reconstructed by Gall and Grauvogel (1967) and Gall (1971) and *H. gondwanae.*

The radial lamellae or radiating grooves observed in *H. max* and *H. ornata* are not preserved on *H. montanaensis.* Schram et al. (1997) referred to these structures as a possible diagnostic feature to help distinguish between *Halicyne* and other cycloid genera. It is conceivable that the specific taphonomic conditions at the Bear Gulch locality were unsuited to preserve these particular soft tissues.

Little is known about segmentation patterns in cycloids, except some clues from the position of the proximal-most segments of the limbs (Schram et al., 1997). The distinctly fan-shaped segmentation seen in these specimens, e.g., LACMIP 7311 (Fig. 1.5), might be a general character of the genus (or even the family) that was not recognized previously. Re-investigation of the specimens described in Schram et. al. (1997) showed that this feature is present in *Cyclus americanus*, but it was not explicitly recognized or mentioned. This pattern is probably convergent to the segmentation seen in crabs (Brachyura), where the strongly reduced abdomen causes the laterally oriented, parallel pattern of the endophragmal structures to be disrupted in the posterior part of the thorax. In crabs, the solid ventral endophragms between the segments like those seen in LACMIP 7311 (Fig. 1.5) are used for attachment of the extrinsic musculature of the legs.

Based on the fauna of malacostracan crustaceans, e.g., a characteristic diversity of hoplocaridans and primitive eumalacostracans, the Bear Gulch biota was recognized by Schram (1985) and Briggs and Gall (1990) as part of a spatio-temporally extended, marine, near-shore, faunal continuum. The biota found in Bear Gulch shows strong similarities to both the biota of the Glencartholm deposits of Scotland (Viséan age) and the Essex biota of the Middle-Pennsylvanian Mazon Creek deposits (Illinois, USA). These similarities are also reflected in other taxa, including polychaete worms and other invertebrates (Schram, 1979) and suggest that the chronofauna had existed virtually unchanged for millions of years. Note, however, that chronofaunas (Olson, 1966) did not remain completely unchanged, especially at the species level, but rather only at higher taxonomic levels. Species did evolve, became extinct, and were replaced, but the general higher taxonomic composition and particular combination of feeding types remained stable (Schram, 1981; Briggs and

Gall, 1990.). The crustaceans of the Bear Gulch Konservat-Lagerstätte have long figured as among the most interesting assemblages in the Carboniferous (Schram and Horner, 1978; Factor and Feldmann, 1985; Schram, 1985; Jenner *et al.*, 1998). We can now add the Cycloidea to the faunal list of the crustaceans of Bear Gulch, although cycloids at Bear Gulch remain very rare.

In conclusion, the specimens at hand provide support for two hypotheses about the Cycloidea. First, the pattern of the segments in the posterior thorax reinforces analogous similarities between crabs and cycloids proposed by Schram et al., 1997). Second, the presence of a member of the genus *Halicyne* in Bear Gulch supports the Late Paleozoic chronofaunal continuum described by Schram (1981).

ACKNOWLEDGMENTS

We would like to thank our colleagues at the Natural History Museum of Los Angeles County section for Invertebrate Paleontology for making available most of the specimens, and the Carnegie Museum (in particular Albert Koller) for loan of the other specimen. Special thanks to Jan van Arkel of the University of Amsterdam for help with photography, Profs. Rod Feldmann and Derek Briggs offered constructive suggestions for improving an early version of the manuscript.

LITERATURE CITED

Brambilla, S., A. Garassino, G. Pasini, and G. Teruzzi. 2002. Studies on Permo-Trias of Madagascar. 6. First record of Cycloidea from the Lower Triassic (Olenekian) of Ambilobé region (NW Madagascar). *Atti della Societá Italiana*

di Scienze Naturali e del Museo Civico di Storia Naturale de Milano 143: 105-115.

Briggs, D.E.G., and J.-C. Gall. 1990. The continuum in soft-bodied biotas from transitional environments: a quantitative comparison of Triassic and Carboniferous Konservat-Lagerstätten. *Paleobiology* 16: 204-218.

Clark, N. D. L. 1989. *A study of a Namurian crustacean-bearing shale from the western Midland Valley of Scotland.* Unpublished Ph.D. dissertation, University of Glasgow, 341 p.

Cox, R.S. 1986. Preliminary report on the age and palynology of the Bear Gulch Limestone (Mississippian, Montana). *Journal of Paleontology* 60: 925-956.

Dahl, E. 1956. Some crustacean relationships. In *Bertil Hangström, zoological papers in honour of his sixty-fifth birthday, November 20, 1956*, ed. K.G. Wingstrand, 138-147. Lund, Sweden: Zoological Institute.

Factor, D., and R. M. Feldmann. 1985. Systematics and paleoecology of malacostracan arthropods in the Bear Gulch Limestone (Namurian) of Central Montana. *Annals of Carnegie Museum* 54: 319-356.

Feldman, H., R. Lund, C. Maples, and A. Archer. 1994. Origin of the Bear Gulch beds (Namurian, Montana, USA). *Geobios* 19: 283-291.

Fraaije, R. H. B., F. R. Schram and R. Vonk. 2003. *Maastrichtiocaris rostratus* new genus and species, the first cretaceous cycloid. *Journal of Paleontology* 77: 386-388.

Gall, J.-C. 1971. Faunes et paysages du grès à Volzia du nord des Vosges. Essai Paléoécologique sur le Buntsandstein Supérieur. *Mémoires du Service de la Carte Géologique d'Alsace et de Lorraine* 34:1-318.

Gall, J.-C., and L. Grauvogel. 1967. Faune du Buntsandstein II. Les Halicynés. *Annales de Paléontologie* 53: 1-14, plates A-G.

Glaessner, M. F. 1928. Zur Frage der ältesten fossilen Krabben. *Centralblatt für Minerologie, Geologie und Paläontologie Stuutgart* (B)6: 388-398.

Glaessner, M. F. 1969. Cycloidea. In *Treatise on Invertebrate Paleontology, Part R, Arthropoda 4, Volume 2,* ed. R.C. Moore, 567-570. Lawrence: Geological Society of America and University of Kansas Press.

Jenner, R. A., C. H. J. Hof, and F. R. Schram. 1998. Paleo- and archaeostomatopods (Hoplocarida: Crustacea) from the Bear Gulch Limestone, Mississippian (Namurian), of central Montana. *Contributions to Zoology* 67: 155-185.

Melton, W. G. 1971. The Bear Gulch fauna from Central Montana. *Proceedings of the North American Paleontological Convention* 1969:1202-1207.

Meyer, H. von, 1847. *Halicyne* und *Litogaster*, zwei Crustaceen genera aus dem Muschelkalke Würtemsberg's. *Paläontographica* 1: 134-140.

Müller, A. H. 1955. Über einem Neufund von *Halicyne plana* und die systematische Stellung von *Halicyne* (Crustacea?). *Paläontologische Zeitschrift* 29: 131-135.

Olson, E.C. 1966. Community evolution and the origin of mammals. *Ecology* 47: 291-302.

Packard, A.S. 1885. Types of Carboniferous Xiphosura new to North America. *American Naturalist* 19: 291-294.

Phillips, J. 1835. *Illustration of the Geology of Yorkshire*, 2nd edition. London: John Murray. i-xii, 184 p., 23 plates, 1 map.

Schafhäutl, K. E. 1863. *Süd-Bayerns Lethaea Geognostica. Der Kressenberg und die südlich von ihm gelegenen Hochalpen.* Leipzig: Voss. i-xvi, 487p., 98 plates.

Schram, F. R. 1979. The Mazon Creek biotas in the context of a Carboniferous faunal continuum. In *Mazon Creek Fossils*, ed. M.H. Nitecki, 159-190. New York: Academic Press.

Schram, F. R. 1981. Late Paleozoic Crustacean Communities. *Journal of Paleontology* 55: 126-137.

Schram, F. R. 1985. The Bear Gulch crustaceans and their bearing on Late Paleozoic diversity and Permo-Triassic evolution of Malacostraca. *Compte Rendu, IX Congrès International de Stratigraphie et de Géologie du Carbonifère* 5: 468-472.

Schram, F. R. and J. Horner. 1978. Crustacea of the Mississippian Bear Gulch Limestone of Central Montana. *Journal of Paleontology* 52: 394-406.

Schram, F. R., R. Vonk and C. H. J. Hof. 1997. Mazon Creek Cycloidea. *Journal of Paleontology* 71: 261-284.

von Meyer, H. 1838. Mitteilungen an Professor Bronn gerichtet. *Neues Jahrbuch für Mineralogie, Geologie und Paläontologie*. 1838: 413-418.

Williams, L. A. 1983. Deposition of the Bear Gulch Limestone: a Carboniferous Plattenkalk from Central Montana. *Sedimentology* 30: 843-860.

Figure captions

Figure 1 *Halicyne montanaensis* n. sp. *1, 2,* LACMIP 7310 part and counterpart (holotype), under direct light, showing vaulted trunk, thoracic appendages, segmentation and rostral plate, ×5 (see Figs. 2.1, 2.2). *3, 4,* CM 45816 part and counterpart, under water, showing cephalic appendages, compound eyes and rostral plate, ×4. *5, 6,* LACMIP 7311 part and counterpart, under direct light, showing part of the posterior thoracic segmentation and caudal rami, ×4.5 (see Figs. 2.3, 2.4). abd = abdomen, an = antenna fragment, ce = compound eye, cr = caudal rami, ms = marginal shelf, mx 2 = second maxilla, mxpd = maxilliped, on = optic notch, pap = papillae, pn = posterior notch, r = rostral plate, s = posterior thoracic segmentation, 2/6 = thoracic appendages..

Figure 2 Camera lucida drawings of specimens of *Halicyne montanaensis* n. sp. *1, 2,* LACMIP 7310 part and counterpart (holotype), corresponding to the photographs of Fig. 1.1,2. *3, 4,* LACMIP 7311 part and counterpart, corresponding to photographs of Fig. 1.5,6. abd = abdomen, an = antenna fragment, ce = compound eye, cr = caudal rami, ms = marginal shelf, mx 2 = second maxilla, mxpd = maxilliped, on = optic notch, pap = papillae on carapace shield, pn = posterior notch, r = rostral plate, s = posterior thoracic segmentation, 2/6 = thoracic appendages.

Figure 3 *Halicyne montanaensis* n. sp. *1,* LACMIP 7314, photographed with green filter to enhance contrast, showing thoracic appendages, abdomen and gut cast, ×6.8 (see Fig. 4.1). *2,* LACMIP 7313, under direct light, showing papillated carapace surface, fragment of marginal shelf, maxillipeds and antenna, ×9.5 (see Fig. 4.2). *3, 4,* LACMIP 7312 part and counterpart, revealing part of posterior thoracic segmentation, surrounding plant material, *3,* under direct high angle light (see Fig. 4.3), *4,* under direct low angle light, ×5.3. *5,* CM

45816, close-up of compound eye with facets, x 30. abd = abdomen, an = antenna, g= gut cast, ms= marginal shelf, mxpd = maxilliped, pap = papillae carapace surface, pl = plant material, r = rostral plate, s = posterior thoracic segmentation, 2/6 = thoracic appendages.

Figure 4 Camera lucida drawings of specimens of *Halicyne montanaensis* n. sp. *1,* LACMIP 7314, corresponding to photograph in Fig. 3.1. *2,* LACMIP 7313, corresponding to photograph in Fig. 3.2. *3,* LACMIP 7312, corresponding to photograph in Fig. 3.3. abd = abdomen, an = antenna, g= gut cast, ms= marginal shelf, mxpd = maxilliped, pap = papillae carapace surface, pl = plant material, pn = posterior notch, r = rostral plate, s = posterior thoracic segmentation, 2/6 = thoracic appendages.

Figure 5 Reconstruction of *Halicyne montanaensis*.

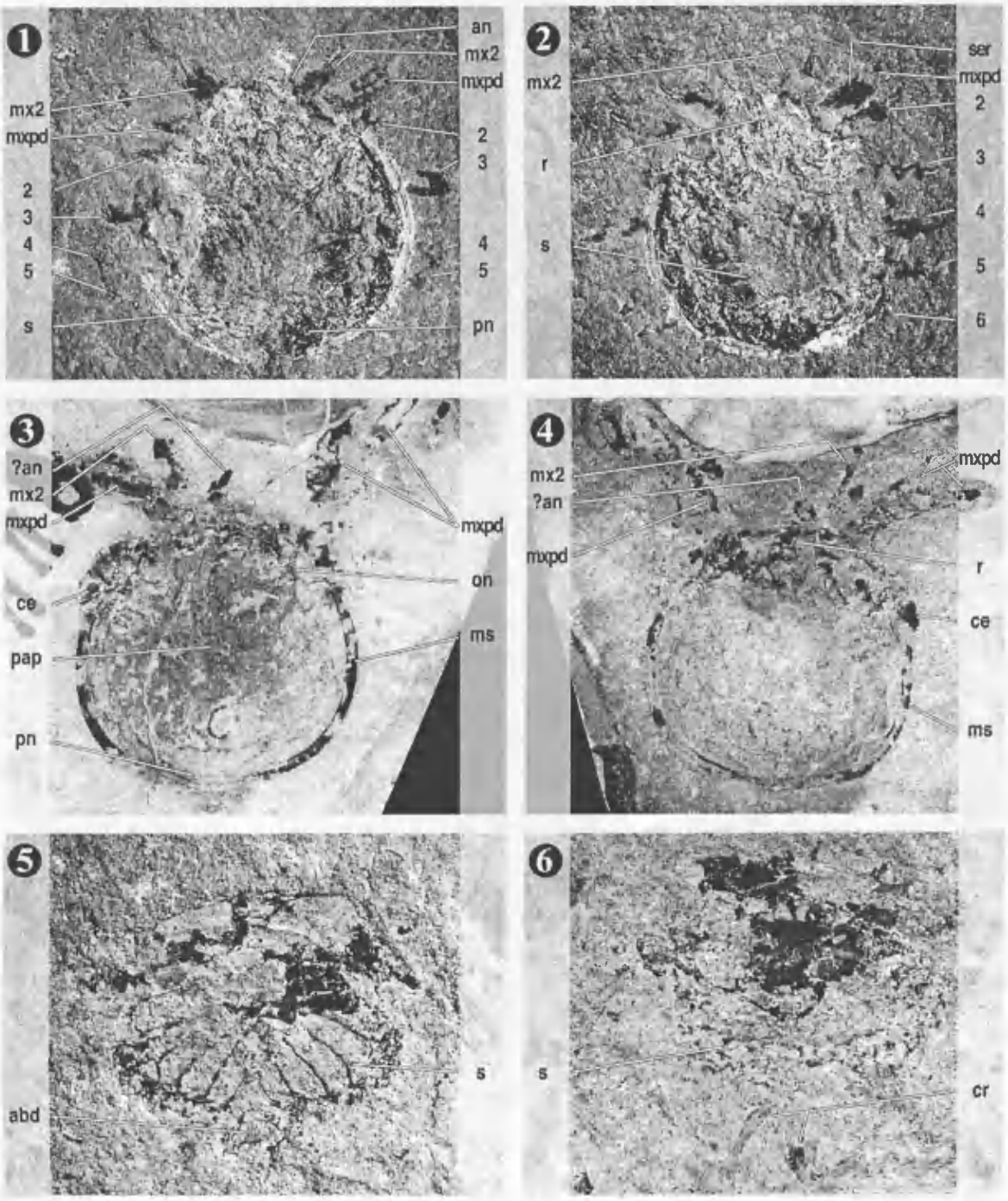
1
an
mx2
mxpd
mx2
mxpd
2
3
2
3
4
4
5
5
s
pn
2
ser
mx2
mxpd
2
r
3
4
s
5
6
3
?an
mx2
mxpd
mxpd
on
ce
ms
pap
pn
4
mx2
?an
mxpd
mxpd
r
ce
ms
5
s
abd
6
s
cr

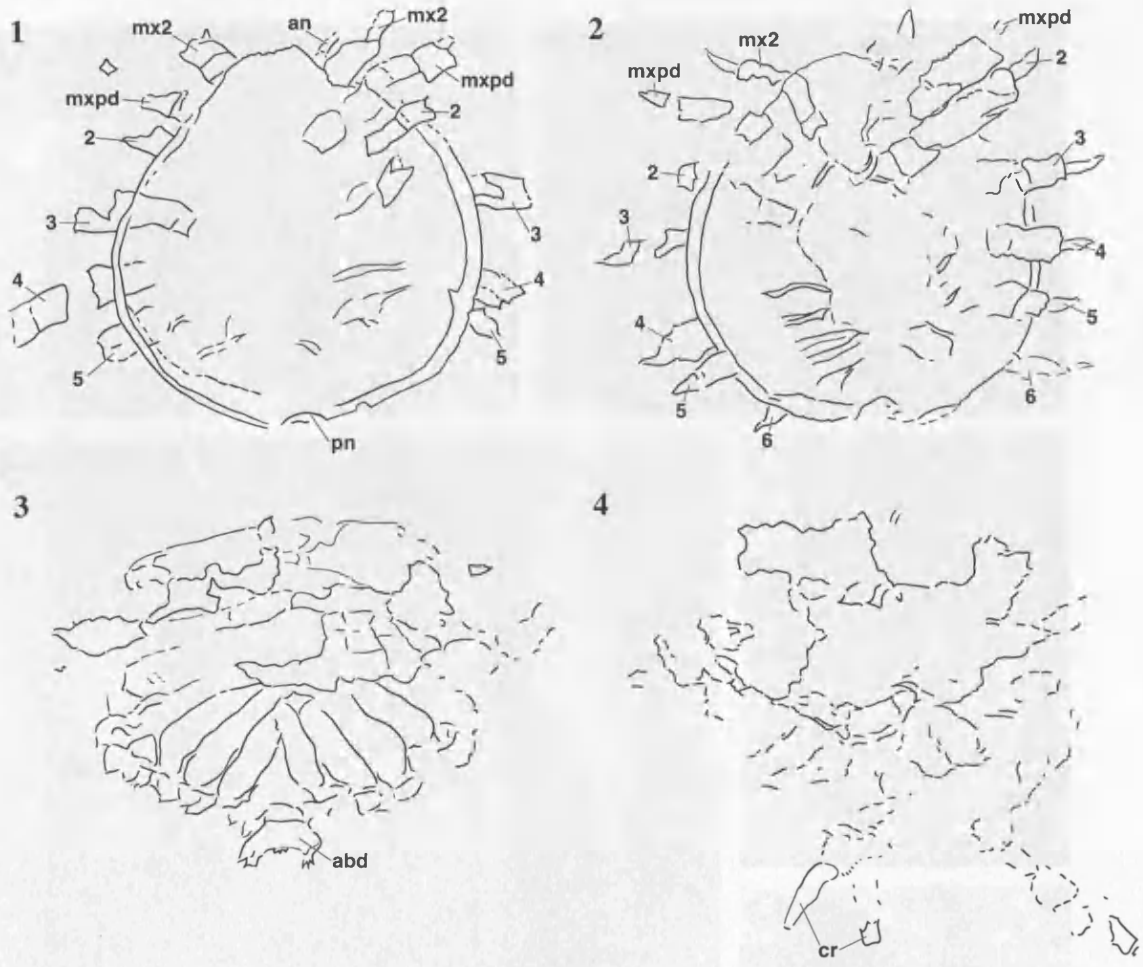
1
mx2
an
mx2
mxpd
mxpd
2
2
3
3
4
4
5
5
pn
2
mxpd
mx2
mxpd
2
3
2
3
4
4
5
5
6
6
3
abd
4
cr

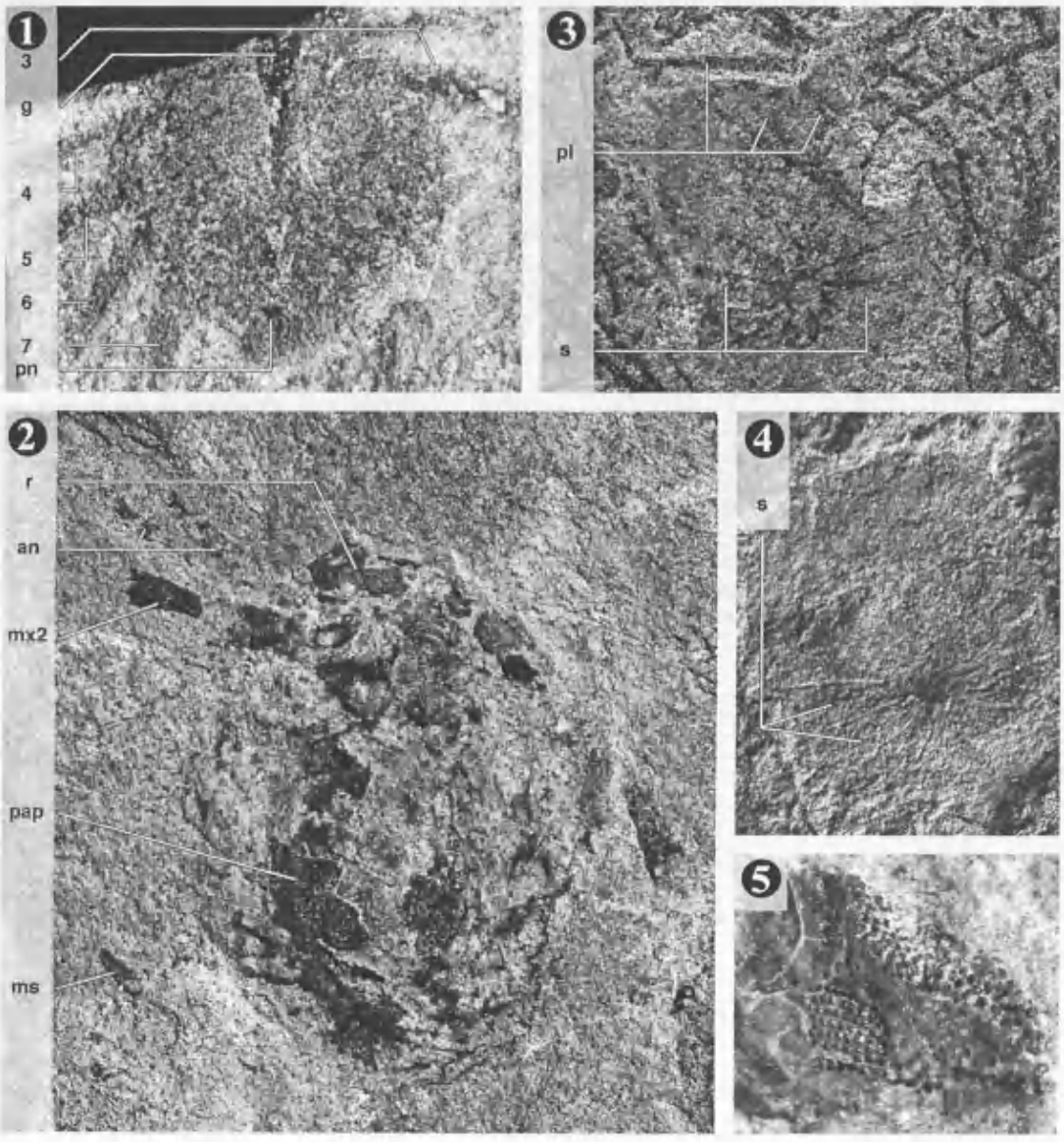
1
3
g
4
5
6
7
pn
3
pl
s
2
r
an
mx2
pap
ms
4
s
5

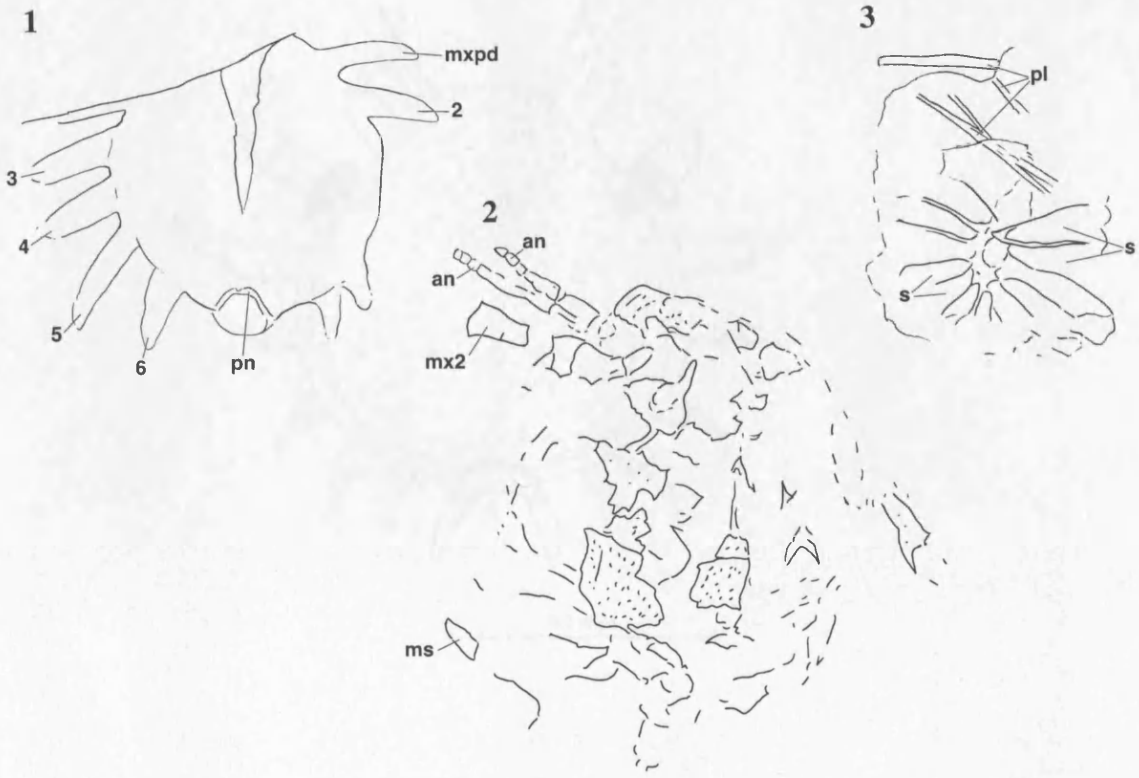
1
mxpd
2
3
4
5
6
pn
2
an
an
mx2
ms
3
pl
s
s

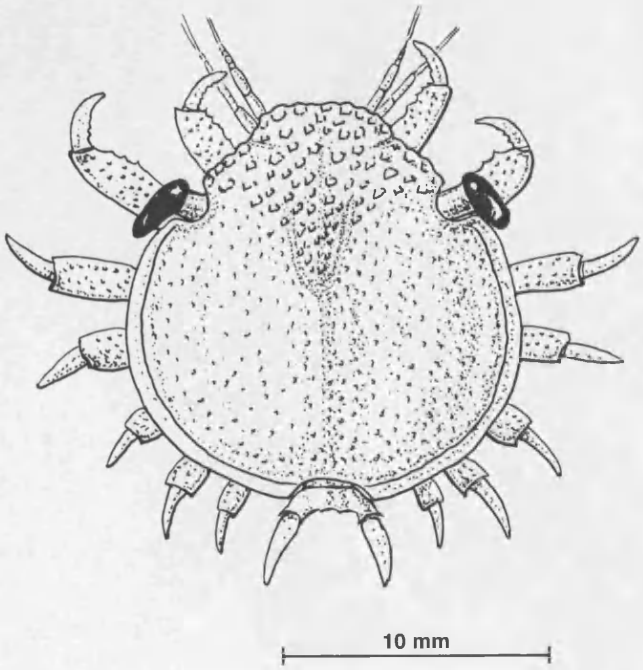
10 mm